TRANSPORTATION RESEARCH
RECORD

No. 1269

Materials and Construction

Asphalt Mix Materials and Mixtures 1990

A peer-reviewed publication of the Transportation Research Board

TRANSPORTATION RESEARCH BOARD
NATIONAL RESEARCH COUNCIL
WASHINGTON, D.C. 1990

Transportation Research Record 1269
Price: $31.00

Subscriber Category
IIIB materials and construction

Modes
1 highway transportation
4 air transportation

Subject Area
31 bituminous materials and mixes

TRB Publications Staff
Director of Publications: Nancy A. Ackerman
Senior Editor: Naomi C. Kassabian
Associate Editor: Alison G. Tobias
Assistant Editors: Luanne Crayton, Kathleen Solomon, Norman Solomon
Graphics Coordinator: Diane L. Ross
Office Manager: Phyllis D. Barber
Production Assistant: Betty L. Hawkins

Printed in the United States of America

Library of Congress Cataloging-in-Publication Data
National Research Council. Transportation Research Board.

Asphalt mix materials and mixtures 1990.
p. cm. — (Transportation research record ISSN 0361-1981 : no. 1269)
ISBN 0-309-05050-2
1. Pavements. Asphalt. 2. Asphalt—Testing. I. National Research Council (U.S.). Transportation Research Board. II. Series: Transportation research record ; 1269.
TE7.H5 no. 1269
[TE270]
388 s—dc20 90-47827
[625.8'5] CIP

Sponsorship of Transportation Research Record 1269

GROUP 2—DESIGN AND CONSTRUCTION OF TRANSPORTATION FACILITIES
Chairman: Raymond A. Forsyth, Sacramento, California

Bituminous Materials Section
Chairman: Leonard E. Wood, Purdue University

Committee on Characteristics of Bituminous Materials
Chairman: Vytautas P. Puzinauskas, The Asphalt Institute
Chris A. Bell, Bernard Brule, Joe W. Button, Brian H. Chollar, Jack N. Dybalski, Norman W. Garrick, Bobby J. Huff, John E. Huffman, Prithvi S. Kandhal, N. Paul Khosla, Robert P. Lottman, Tinh Nguyen, R. D. Pavlovich, Rowan J. Peters, J. Claine Petersen, Charles F. Potts, Lawrence E. Santucci, Peggy L. Simpson, Bernard A. Vallerga, John S. Youtcheff

Committee on Characteristics of Nonbituminous Components of Bituminous Paving Mixtures
Chairman: N. Paul Khosla, North Carolina State University
Secretary: John E. Huffman, U.S. Oil & Refining Company
Douglas M. Colwill, Ervin L. Dukatz, Jr., John J. Emery, Frank Fee, Douglas I. Hanson, Nyla M. Heath, Ilan Ishai, Prithvi S. Kandhal, Bobby D. Lagrone, Dah-Yinn Lee, Kang-Won Wayne Lee, Robert P. Lottman, Roderick W. Monroe, Frank P. Nichols, Jr., John W. H. Oliver, Roger C. Olson, G. C. Page, J. Claine Petersen, Lawrence E. Santucci, K. K. Sarin, Russell H. Schnormeier, Scott Shuler, Ronald L. Terrel, Harold H. Weber, Jr., Leonard E. Wood

Committee on Characteristics of Bituminous Paving Mixtures To Meet Structural Requirements
Chairman: Ronald L. Terrel, Terrel Research
Secretary: Robert N. Jester, Federal Highway Administration
David A. Anderson, Benjamin Colucci, David S. Decker, R. N. Doty, Jack N. Dybalski, R. G. Hicks, R. J. Holmgreen, Jr., Rudolph A. Jimenez, Ignat V. Kalcheff, N. Paul Khosla, Kang-Won Wayne Lee, Dallas N. Little, J. M. Machet, Michael S. Mamlouk, Harold R. Paul, R. D. Pavlovich, James A. Scherocman, David G. Tunnicliff, Bernard A. Vallerga, James P. Walter, Gary C. Whited, John S. Youtcheff

Geology and Properties of Earth Materials Section
Chairman: C. William Lovell, Purdue University

Committee on Frost Action
Chairman: Thomas C. Kinney, University of Alaska
Kenneth O. Anderson, Richard L. Berg, Frederick M. Boyce, Edwin J. Chamberlain, George R. Cochran, Barry J. Dempsey, Denis E. Donnelly, David C. Esch, Wilbur M. Haas, Larry K. Heinig, Ira J. Huddleston, Newton Jackson, Ronald H. Jones, Hiroshi Kubo, C. William Lovell, Joe P. Mahoney, Melvin W. Morgan, Mary Rutherford, John A. Shuster, Ted S. Vinson, Gary C. Whited, Chen Xiaobai, Qian Zhu

Frederick D. Hejl and G. P. Jayaprakash, Transportation Research Board staff

Sponsorship is indicated by a footnote at the end of each paper. The organizational units, officers, and members are as of December 31, 1989.

Transportation Research Record 1269

Contents

Foreword

This Record contains information on asphalt mix materials and on the design, testing, and evaluation of asphalt mixtures. The Record should be of interest to state and local materials and construction engineers, contractors, and materials producers.

Burr et al. focus on incomplete solvent removal from asphalt binders extracted from asphalt mixtures and the effect solvents have on the asphalt physical properties. Neither the Abson nor the Roto-vap methods adequately remove the solvent, small amounts of which cause significant decreases in viscosity. Martin et al. report on measures of asphalt aging on 16 test sections in Texas. The sections were laid in 1982–1983 at three different locations using five asphalt sources and two grades. Voids and aging were strongly correlated; asphalts showing nearly the same aging index at low voids differed several-fold at high voids. Noureldin and Wood report that the thin-film oven test can be used to identify recycling agents to be added to recycled asphalt binders. Garrick and Biskur evaluate effects of asphalt composition and physical properties on indirect tensile strength of an asphalt mix. Bishara and McReynolds present a method using ultraviolet detection for calculating the molecular size distribution of asphalt cement.

Curtis et al. discuss adsorption behavior of asphalt and of asphaltic functionalities on aggregates precoated with commercial polyamine antistripping agents. Stroup-Gardiner and Newcomb compare the benefits of dolomitic lime (Type S) and normally hydrated lime (Type N) as antistripping additives. Neither type of lime significantly influenced the temperature susceptibility of mixtures, and both significantly decreased the moisture sensitivity. Figueroa and Majidzadeh compare the performance of a manganese-treated asphalt concrete overlay to that of conventional asphalt concrete overlays. The engineering properties of asphalt concrete mixtures were not improved by treatment with a manganese-based additive. Salter and Mat investigated the effects of rubber on the behavior of asphalt mixes. On the basis of laboratory testing, adding rubber into binders generally improved the properties of binders and mixes. Lottman and Brejc develop moisture damage cutoff ratios from a prediction model, then combine them in a practical form that will provide rational specifications to control the field distresses of fatigue cracking and wheelpath rutting of AC mixtures.

Noureldin and Wood present the findings of a laboratory study in which resilient modulus and sonic pulse velocity nondestructive tests were used for characterization of hot-mix recycled asphalt paving mixtures. Franco and Lee evaluate the viability of using an air meter (normally used in determining the percent air in fresh portland cement concrete) for determining the maximum theoretical specific gravity of asphalt mixtures. Lai and Lee describe the use of a loaded wheel testing machine to evaluate the rutting characteristics of asphalt mixes. Mahboub and Little describe a rational asphalt concrete mix design and analysis methodology developed for use with the current Texas State Department of Highway and Public Transportation method of mix design. Noureldin and McDaniel evaluate the suitability of a steel slag and natural sand combination for use in bituminous pavement surface layers on high-volume, high-speed, and heavy-load highways. Greenstein et al. present preliminary conclusions of specification modifications adopted by the Peruvian road authorities to reduce thermal cracking in asphalt pavements at high altitudes. Rogge et al. determine the correlation of conventional and modified binder properties with important hot-mix properties. Coetzee and Connor investigate the applicability of typical asphalt concrete fatigue relationships to the pavement design process in Alaska. Almudaiheem reports that modified sand mixes, composed of dune sand and crusher waste dust, have great potential for use in low- and medium-volume roads in Saudi Arabia. Addition of the crusher dust to the sand significantly improved the stability, split tensile strength, and resilient modulus of the mix.

Solvent Removal from Asphalt

B. L. BURR, R. R. DAVISON, C. J. GLOVER, AND J. A. BULLIN

Asphalt recoveries by the Abson and Roto-vap methods were performed at various temperatures and for several asphalt viscosities. Solvent (trichloroethylene, TCE) concentrations after recovery were measured by gel permeation chromatography. Asphalt viscosities and residual solvent concentrations during solvent removal were determined for tank, oven-aged, and solvent-exposed asphalt to evaluate the effectiveness of the procedures and operating parameters. Small amounts of solvent cause significant decreases in viscosity, and present recovery methods do not remove solvent adequately. In general, recovery rates increase strongly with temperature in both methods. High viscosities and larger asphalt samples hinder solvent removal rates in the Abson method. Asphalt hardens significantly on extended exposure to TCE at both 200°F and 80°F. This hardening also occurs during solvent removal processes, but removal at a reduced temperature through use of a vacuum in the early stages can inhibit it.

To obtain asphalt properties that are representative of the binder in situ properties, procedures must be effective in removing the binders from the aggregate without changing or aging the asphalts. The solvents used for the extraction must be adequately removed from the asphalt binder, so as not to distort the physical properties of the binder that are subsequently measured. Problems have been reported with all aspects of the asphalt extraction and recovery process, including incomplete asphalt extraction, solvent hardening of the extracted material, loss of volatiles during recovery, and incomplete solvent removal. Incomplete solvent removal, which seems a simple problem but which has flawed many studies involving extracted asphalt, is emphasized. Typical residual concentrations of solvent can significantly distort the physical properties of asphalt.

HISTORY

Extraction and recovery of asphalt have been practiced in some form since the turn of the century. In 1903, as discussed by Abson (*1*), Dow extracted with carbon disulfide (CS_2) and recovered using simple distillation. In 1927, Bateman and Delp (*2*) centrifuge-extracted with CS_2 and removed the solvent by vacuum distillation. Soxhlet-type reflux extractions using CS_2 were common in this period. Several other methods were developed through 1930, but none gained lasting acceptance (*1*,*3*).

Typically today, solvent is removed after extraction by the Abson method introduced in 1933 or by rotary evaporation. These two methods share equal popularity. The literature shows six instances of rotary evaporation and eight of the Abson since the mid-1970s. Before that time, the Abson method dominated.

The Abson method involves recovering benzene-extracted asphalt at 300°F to 325°F with the aid of bubbling carbon dioxide (CO_2). Abson tested seven asphalts ranging in penetration from 175 to 26. After being mixed with benzene, the asphalts were recovered to within 3 percent of original penetrations. The method was designated ASTM D1856 and is still the recommended method (*1*). Rotary evaporation methods became common in the mid-1970s. ASTM is considering a standard method for recovery using this apparatus.

Through the years, several solvents have been used for extracting asphalt. CS_2 was commonly used initially, but it was phased out because of its high volatility and flammability. Benzene became its primary replacement after Abson's method appeared. In the 1950s and 1960s, chlorinated solvents became popular. The most common were trichloroethylene (TCE), 1,1,1-trichloroethane, and methylene chloride. In 1960, Abson tested several of these and found TCE to be as effective as benzene (*4*). Adding about 10 percent ethanol or methanol to benzene removed more asphalt from the aggregate (*5*). This practice has become quite popular among many researchers. Because benzene has been proven carcinogenic, its use has been phased out, and TCE has been the primary replacement.

Although Abson (*1*) showed that solvent can be completely removed using his method, many researchers have had problems caused by residual solvent that often they do not even realize.

For example, in 1963, Lottman et al. (*6*) modified the extraction-recovery procedure because he was experiencing excess hardening (probably because of solvent aging). He replaced the CO_2 distribution coil with a smaller one. This change lowered the hardening to 2 percent on test samples. However, when studying hot-mix samples he discovered viscosities lower than the originals, or negative hardening, during the mix process. In the discussion of Lottman's paper, Rostler suggested that negative hardening was probably caused by residual solvent in the sample.

A classic example of how incomplete solvent removal can ruin a massive research project was given by Carey and Paul (*7*) in a study of factors affecting asphalt in the extraction-recovery process. The project's goals were to study the effect of time in TCE for aged and unaged asphalts, the effect of reduced asphalt concentration during recovery, intra- and interoperator variations, the effect of solvent during primary distillation, and the effect of fines in aggregate mix on recovered asphalt properties. Carey and Paul performed Abson recoveries after 54 similar AC–30 samples and 54 artificially aged samples had spent different lengths of time in TCE. Using ANOVA, a statistical package, they concluded that the time in a solvent before recovery directly affected viscosity. This

Department of Chemical Engineering and Texas Transportation Institute, Texas A&M University, College Station, Tex. 77843–3122.

result had been shown by other researchers. However, 22 of the 54 AC–30 samples had lower viscosities after solvent aging and recovery. The aged samples (30,000 to 200,000 poise) softened 40 out of 54 times.

Cary and Paul noted this softening but gave no explanation for it (*7*). Residual solvent may have caused softening and added enough scatter to the data that the variables of interest had negligible effects in comparison. This effect probably masked most of the effects of solvent aging also. Larger asphalt samples had lower viscosities following recovery, indicating incomplete solvent removal.

In 1983, the Pacific Coast Users Group tested the Abson, Roto-vap, and two other recovery methods (*8*). On four different asphalts having viscosities from 4,000 to 50,000 poise, they found that no method outperformed the others. The Abson method had the lowest reproducibility rating and failed to remove the solvent adequately from two of the four asphalts tested. Consequently, the residues' viscosities were about 75 percent of the original. The other methods caused excessive hardening on the other two asphalts tested. Viscosity increases were as high as 50 percent.

Other authors have noticed or had data that indicated the presence of solvent removal problems. Roberts and Gotolski (*9*), Sandvig and Kovalt (*10*), and Gietz and Lamb (*11*) noted viscosities on recovered road samples that sometimes decreased with time on the road. This effect may actually occur, but decreasing viscosities are probably caused by an extraction-recovery problem. Noureldin and Manke (*12*) reported work in which recovered asphalt had been hardened by the recovery process. They lowered the Abson time and temperature and almost certainly compensated for solvent hardening by leaving residual solvent in the asphalt.

The problem of incomplete solvent removal is not as simple as it sounds. First, direct verification of solvent removal is rarely performed. Usually, an asphalt of known properties is mixed with solvent, recovered, and tested again. The deviations from original properties indicate the effectiveness of the recovery for that asphalt, which is assumed to be the same for similar asphalts. Petersen et al. (*13*) mention using infrared to detect solvent in asphalt. In 1936, Bussow (*14*) used odor and loss of heating as criteria for residual solvent concentration. Secondly, the mechanism of solvent evaporation may not be well understood. In a discussion of a paper by Hagen et al. (*15*), Petersen states, "When dealing with low concentrations of solvents left in residues, boiling point is no longer a major factor and diffusion and molecular associations between asphalt and solvent become controlling factors for solvent removal."

EXPERIMENTAL PROCEDURES

In order to determine the effectiveness of the existing recovery methods, examine the procedures' responses to changes in process variables, and establish new conditions that would guarantee complete solvent removal, a method of directly analyzing solvent concentrations in asphalts had to be found. TCE was chosen because of its common use. Recoveries were performed using the Abson and Roto-vap methods at various temperatures and asphalt sample sizes, on a wide range of asphalt viscosities. An in situ sampling method was developed so that samples could be taken at several different times during a recovery. To show the effect of solvent, the viscosities of solvent-contaminated asphalts were compared to their original viscosities in terms of a hardening index (ratio of the viscosity of recovered asphalt to that of the original asphalt).

The general procedure was to dissolve the asphaltic material in TCE and recover either by the Abson or Roto-vap method. Sample size, temperature, and asphalt viscosity were varied. During the recoveries, small samples of asphalt were withdrawn and analyzed for solvent content, so that the solvent concentration versus time for each set of conditions could be determined.

The tendency of solvent to harden asphalt was also studied. The asphalt-solvent solution was allowed to stand for different lengths of time before recovery at room temperature and at 200°F. A few Roto-vap recoveries were made under vacuum to achieve a low recovery temperature and less hardening.

Three asphalt viscosities were used. A 2,000-poise tank asphalt was used and was hardened to 20,000 and 200,000 poise. Recovery conditions were 325°F, 340°F, and 380°F with the Abson procedure; 280°F, 280°F at reduced pressure; and 325°F, 350°F with the Roto-vap method. Sample sizes were 50, 75, and 100 g for the Abson method and 50 g for the Roto-vap.

Most data were for 50-g samples. Although contrary to the Abson specification of 70 to 100 g, an inconsistency exists in the Abson specification. The equipment for extraction by the specified Method A of ASTM D2172 will generally allow a sample size of about 1 kg. With most mixes, this sample size yields only 50 to 60 g of asphalt. In general, as shown later, larger sample sizes only aggravate the deficiencies of the standard Abson procedure.

TCE Analysis by Gel Permeation Chromatography

The residual concentration of TCE during solvent removal can be measured easily by gel permeation chromatography (GPC). An earlier study of extracted pavements indicated that TCE elutes as a single peak with no interference from other materials of small molecular size in the sample. A distinct peak of small molecular size appeared on the chromatograms. No such peak had been seen on tank or oven-aged samples.

The GPC analyses were performed on an IBM Model LC-9533 high-pressure liquid chromatograph. A 100-μL sample [7 weight-percent asphalt in tetrahydrofuran (THF)] was injected into the carrier solvent flowing at 1 mL/min through two Polymer Laboratories (PL) columns in series containing PL gel material of 500-Å (Column 1) and 50-Å (Column 2) pore sizes. The details are described by Donaldson et al. (*16*).

Standard blends of TCE in THF were made for calibration of the solvent analysis. Dilutions in THF equivalent to those that occur in GPC analysis of 5, 2, 1, 0.5, 0.1, and 0.05 weight-percent TCE in asphalt were analyzed by GPC; the relative peak areas related linearly to the TCE concentrations with an r^2 value of 0.997. Analyses of TCE in asphalt samples were performed similarly. Solvent concentrations were determined using the calibration. Residual solvent concentrations in recovered asphalt ranged from 0 to 2.5 percent.

Asphalt Viscosity

Asphalt viscosities, measured according to ASTM D2171, were obtained at 140°F in Cannon-Manning viscometers. All samples were melted and mixed well before viscosity measurement, because asphalt tends to stratify during cooling. Samples taken near the top while cool and hard tended to have much higher TCE concentrations because of this stratification.

Fourier Transform Infrared Analysis

A Nicolet Fourier transform infrared (FT-IR) spectrometer was used to analyze the functional chemistry of samples. Some of the hot mixes left a mysterious oily film on the flask sides after recovery. This film was run on the FT-IR because of the small sample size required. An attenuated total reflectance method worked well (*17*). The samples were applied as thin films onto a special zinc selenide prism.

Sampling

An in situ sampling technique was devised. It was first thought that asphalt could be drawn into a 1-mL disposable pipette during the recovery. The asphalt would then solidify and could be stored until time for GPC sample preparation. However, the asphalt had to be melted and drained into a scintillation vial. During this process, solvent was apparently lost. Consequently, this method yielded solvent concentrations that were low and imprecise. To remedy this, 8-in. pieces of ⅛-in.-ID Nalgene autoclavable tubing were substituted for the glass pipettes. After sampling, these tubes were cut lengthwise at room temperature to allow easy removal of the asphalt for GPC sample preparation. This method seemed to be more precise than any alternative.

Materials

The asphalts were derived mainly from locally sampled Exxon AC-20. Hardened samples were produced by bubbling oxygen into 450°F Exxon AC-20 for from 3 to 8 hr. The two 300-g samples of hardened asphalt had viscosities of 20,000 and 200,000 poise. After each recovery, the asphalt was remixed with solvent for use in another recovery experiment. The small changes in properties caused by reusing material were insignificant in their effect. Recovery data on several extracted hot mixes were also taken. The recovery solvent, TCE, was recycled after each run. No serious changes in the asphalt's or solvent's properties were detected.

Abson Method

The Abson method (ASTM D-1856-79) removes solvent by distillation with the aid of a CO_2 purge. About 150 mL of a concentrated solution of asphalt and solvent, containing 50 to 100 g of asphalt, are charged to a 250-mL widemouth, round-bottom flask. The flask is electrically heated. The liquid boils and is condensed and collected in a receiving flask. The CO_2 flow is set at 100 mL/min once the temperature reaches 275°F. When the temperature is 315°F, the flow is increased to 900 mL/min. The temperature is then maintained between 320°F and 330°F for 15 min, or 5 min after the last drop has fallen, whichever is longer. In this study, the last drop had fallen within 10 min in every case but one, and that was only a few seconds over. In the case of material having a penetration less than 30, the method specifies 20 to 22 min. Therefore, the Abson time would be 15 min for all but the 200,000-poise material, and 20 to 22 min for these runs.

Instructions set forth in ASTM D1856 were adhered to strictly except for varying sample size, time, and temperature to study these parameters. The CO_2 flow was accurately metered using a Gilmont R–012 flow meter. A variac and heating mantle supplied heat to the flask of asphalt and solvent. Temperature control was found to be difficult from the beginning. Because of a lag in the response of the asphalt temperatures to heater action, significant excursions outside the specified limits were difficult to avoid. Consequently, an analysis of the heater system with respect to temperature control was performed to obtain the sequence of heater settings that would give good control at 320°F, 340°F, or 380°F, as required. Manual control of the variac using these setting profiles made temperature control easier and more accurate.

Roto-vap Method

The Roto-vap method, which uses a rotary evaporator to mix the solution and a vacuum and vent gas to vaporize and sweep away solvent, has a distinct advantage over the Abson method in that there is no need for a primary distillation of the solution down to 150 mL before proceeding with the recovery. Large volumes of solution can be handled in this apparatus. Recoveries were run on mixtures of 100 mL of TCE and 50 g of asphalt to save time and solvent.

No formally approved Roto-vap recovery procedure is available, but a tentative ASTM method and another used by the Pacific Coast User's Group (*9*) appeared identical and well studied. These methods formed the basis for the procedure.

Initially, the oil bath is heated to 280°F. A 1,000-mL round-bottom flask containing 150 mL of concentrated solution is attached to the Roto-vap. CO_2 is metered at 500 mL/min through a tube that touches the solution's surface. The flask rotates at 45 rpm in the oil bath. When the bulk of the solvent has been distilled, a 600-mm (Hg) vacuum is applied and the CO_2 flow is increased to 600 mL/min. These conditions are held for 15 min. In an alternate method studied, no vacuum is applied, but the CO_2 flow is increased to 900 mL/min.

Asphalt sampling was similar to that for the Abson method. The 1,000-mL flask was modified with the addition of a 24/40 ground-glass fitting approximately 45 degrees from the flask's neck. The connection was closed with a ground-glass cap. During the recovery, the flask rotation was stopped, the cap was removed, the Nalgene sample tube was inserted into the hole, and the sample was pulled using a pipetter. Immediately afterward, the cap was replaced and rotation resumed. This process took approximately 20 sec to perform when there was no vacuum and about 35 sec if a vacuum was used.

RESULTS AND DISCUSSION

Extraction and Solvent Removal Effects on Viscosity

Figure 1 shows the viscosity relative to initial viscosity (the hardening index) of asphalt during solvent removal processes for three situations. The tank (AC–20) and oven-aged (rolling thin-film oven test, RTFOT) asphalts were well dissolved in TCE at room temperature, and solvent removal was initiated within 1 hr. The refluxed sample was a mixture of approximately 25 weight-percent tank asphalt (AC–20) in TCE that was refluxed for 4 hr at 200°F before initiating solvent removal. This reflux procedure simulated the conditions of hot extraction methods such as ASTM D2172, Method B.

These data indicated several effects of the extraction and recovery procedures on asphalt viscosity. The first factor was the considerable softening of asphalt by even small amounts of residual solvent. Even 0.5 percent of residual solvent can produce viscosities that are 50 percent low. Second, there are different degrees of residual hardening on reaching zero-solvent concentration for different asphalts and situations. The tank asphalts typically harden 5 to 10 percent above their original values. This effect probably results from a loss of volatile components during recovery. The RTFOT samples return to their original viscosities, because their volatiles were removed in the oven-aging test. Asphalts exposed to hot reflux (simulating a reflux extraction procedure) may exhibit a 20 to 40 percent increase of viscosity, indicating significant solvent hardening beyond that attributable to volatiles lost.

Figure 2 shows that the solvent-hardening phenomenon also occurs at room temperature after extended exposure times. A series of Roto-vap solvent removals (asphalt recoveries) were conducted for mixtures of 7 weight-percent asphalt in TCE. Before recovery, however, the mixtures were allowed to incubate at room temperature for the times shown in Figure 2. For short room-temperature incubation times, hardening caused by volatiles loss and solvent aging in the hot-recovery Roto-vap method was from 14 to 18 percent. For extended times, hardening was in excess of 40 percent. For comparison, a sample was recovered immediately after dissolution using a vacuum to obtain a reduced solution temperature of approximately 100°F. This short, room-temperature exposure produced about 10 percent hardening, close to that caused by volatiles loss only.

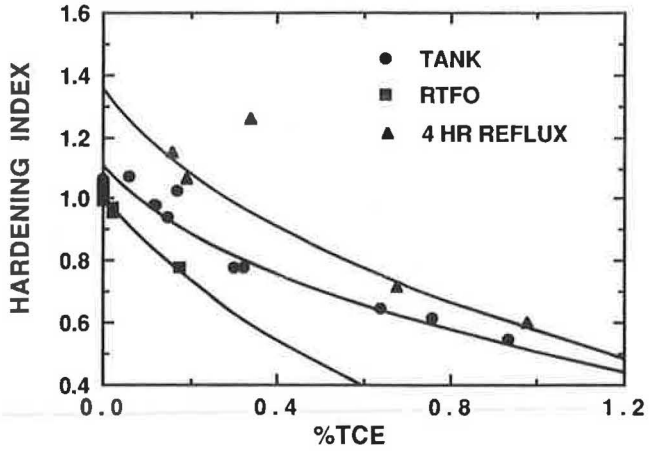

FIGURE 1 Removal of solvent and resulting changes in asphalt viscosity. The tank and oven-aged asphalts were dissolved in solvent and immediately recovered with no incubation time in the solvent.

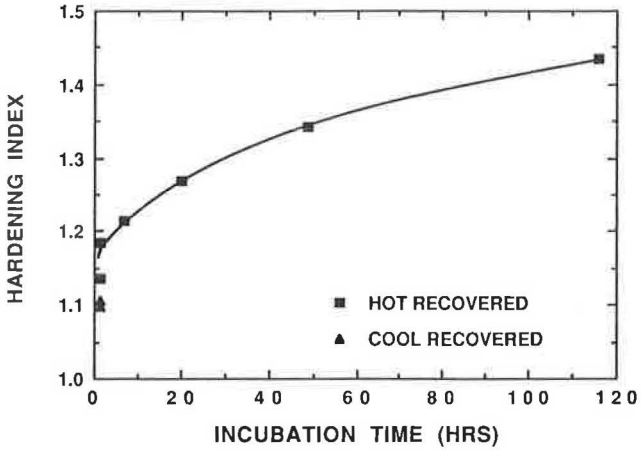

FIGURE 2 Hardening of asphalt in TCE at room temperature for extended periods of incubation time prior to hot recovery. Also shown is the aging during a cool recovery process with short incubation time.

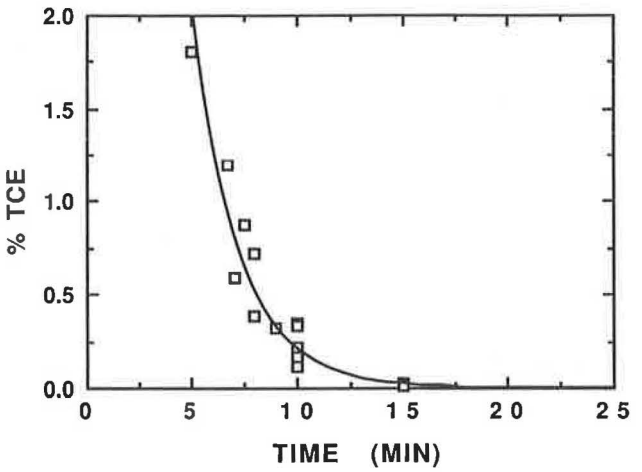

FIGURE 3 Residual solvent concentration versus Abson recovery time for a tank (AC–20) asphalt.

Abson Solvent Removal Method

Several recoveries at strict Abson conditions consistently resulted in significant TCE presence after the time required by the method. The experiments also showed the reproducibility of the Abson recovery and sampling methods used (Figure 3). Approximately 0.19 percent of the TCE remained in the asphalt after the Abson time on recoveries of 2,000-poise asphalt. From Figure 1, this value implies about a 10 percent decrease in viscosity. If the recovery procedure is calibrated with no TCE analysis technique and using tank asphalts, inadequate operating parameters are established

because tank asphalts show no viscosity decrease even though their residual TCE levels are about 0.1 to 0.2 percent, because the presence of solvent is offset by a loss of volatiles.

Recovery temperature and asphalt viscosity noticeably affect the Abson method's ability to remove TCE. Figures 4–6 show the TCE concentration profiles for recoveries of 2,000-, 20,000-, and 200,000-poise asphalts each at 325°F, 340°F, and 380°F. Figures 7–9 show the same data for each asphalt grade. These data show, without fail, that removal is achieved sooner for lower-viscosity and higher-temperature material. The poor removal at high viscosities at 325°F illustrates the need to modify the existing conditions. The viscosity of the 20,000-poise material was lowered nearly 30 percent at completion of the prescribed method.

Changes in recovery temperature and asphalt viscosity should affect the method's performance. As the solvent is removed, the solution behaves like a pure molten asphalt. The high viscosities of these materials lower the mobility of the solvent, because of increased diffusion resistance. This resistance slows the solvent in reaching the liquid-vapor interface where evaporation occurs. So, although equilibrium may be maintained

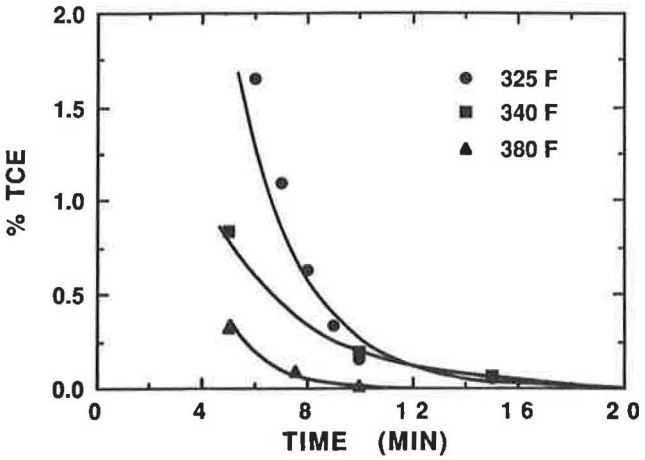

FIGURE 4 Residual solvent concentrations versus Abson recovery time at three temperatures for a tank (AC–20) asphalt.

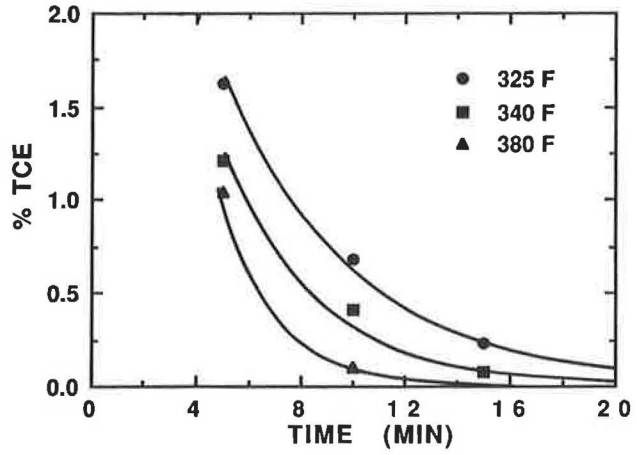

FIGURE 5 Residual solvent concentrations versus Abson recovery time at three temperatures for a 20,000-poise asphalt.

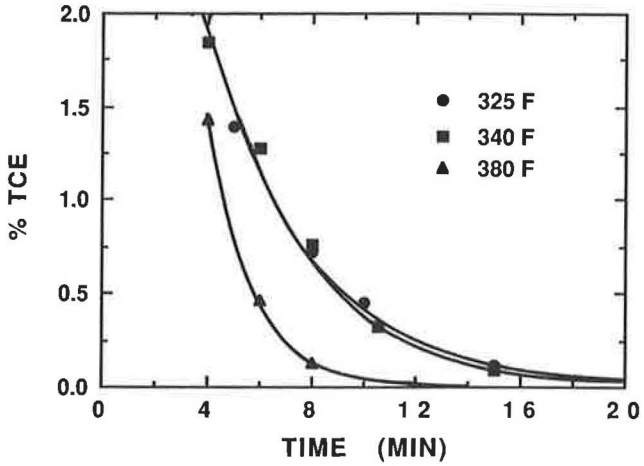

FIGURE 6 Residual solvent concentrations versus Abson recovery time at three temperatures for a 200,000-poise asphalt.

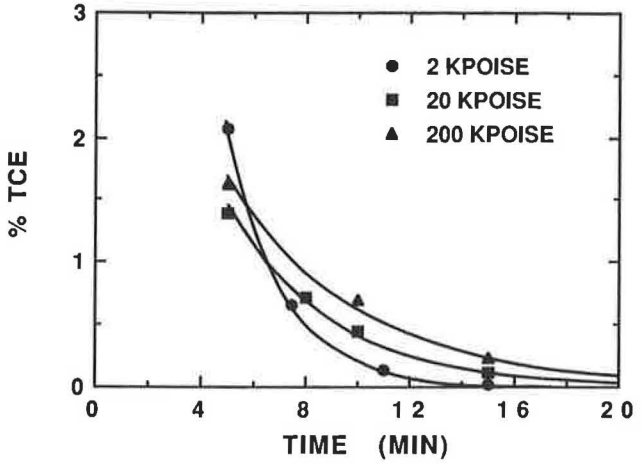

FIGURE 7 Residual solvent concentrations versus Abson recovery time for three asphalt viscosities at 325°F.

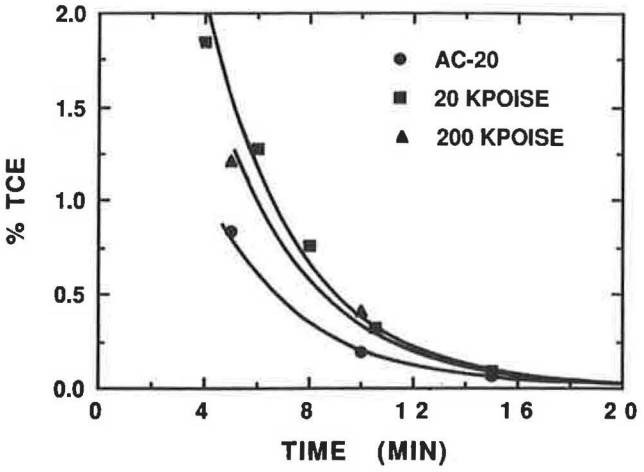

FIGURE 8 Residual solvent concentrations versus Abson recovery time for three asphalt viscosities at 340°F.

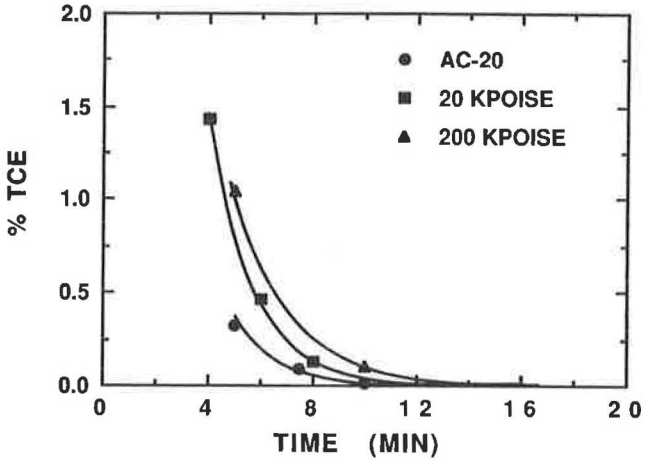

FIGURE 9 Residual solvent concentrations versus Abson recovery time for three asphalt viscosities at 380°F.

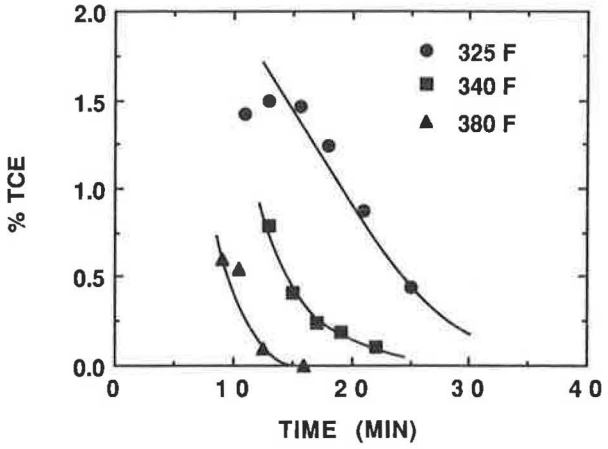

FIGURE 11 Residual solvent concentrations versus Abson recovery time at three temperatures for a 100-g sample of 200,000-poise asphalt.

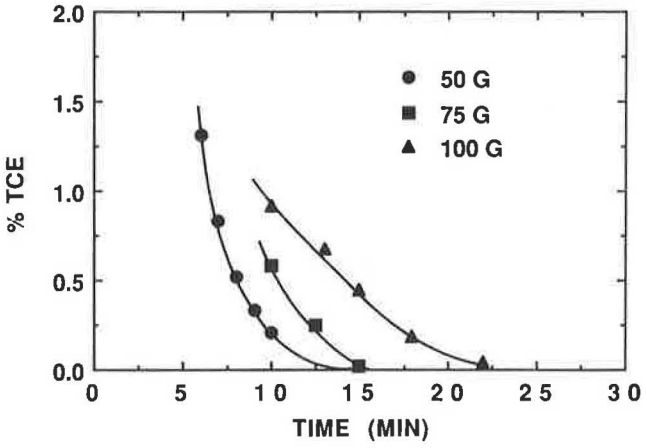

FIGURE 10 Residual solvent concentrations versus Abson recovery time for three sample sizes for 2,000-poise asphalt at 325°F.

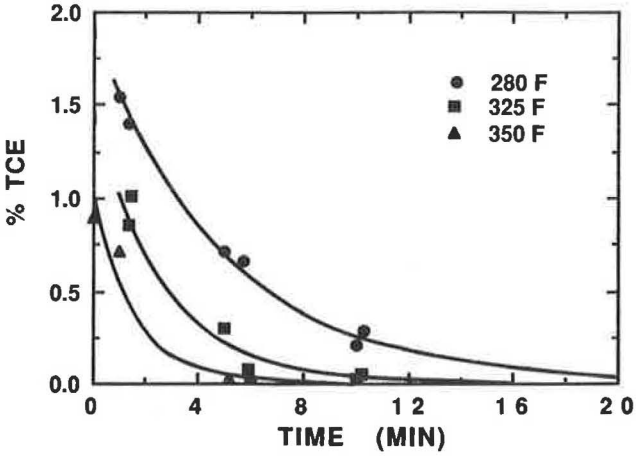

FIGURE 12 Residual solvent concentrations versus Roto-vap recovery time at three temperatures for an AC–20 asphalt.

at the asphalt surface, significant quantities of solvent remain in the bulk asphalt, its removal rate being limited by diffusion. Furthermore, higher-viscosity asphalts have lower diffusion rates, resulting in increased difficulty in removing solvent. Also, the higher asphalt viscosities reduce the mixing effectiveness of the CO_2 purge.

Figure 10 shows that increasing sample size detrimentally affects solvent removal. The Abson procedure (ASTM D1856-79), while allowing recovered asphalt quantities greater or less than the specified 75 to 100 g, states that this may affect the properties of the recovered material, in which case, 75 to 100 g should be recovered. This specification would appear to be incorrect. Figure 11 shows how poorly the Abson procedure removes solvent at higher sample sizes (except at 380°F).

Roto-vap Solvent Removal Method

Figures 12–14 show Roto-vap method residual solvent profiles for the AC–20, 20,000-poise, and 200,000-poise materials, respectively, at three removal temperatures. Zero time is that of the last-observed drop from the solvent condenser. Unless otherwise indicated, the Roto-vap method used was that without vacuum (i.e., with a CO_2 purge only). The profiles show pronounced temperature dependence, but, surprisingly, no discernible viscosity dependence. Also, the use of a gas purge alone seems to be as effective as that with a vacuum at 280°F (Figures 11 and 12). In most cases, the 280°F recoveries, vacuum or gas purged, left significant solvent residues after the method's suggested time of 15 min past the last sign of condensation. However, the 325°F and 350°F runs showed complete removal after 15 min.

The Roto-vap method appears to be less reproducible than the Abson method. Two separate recoveries of 20-kpoise asphalt at 325°F gave drastically different solvent removal profiles, one having complete removal in less than 2 min. This difference may have been caused by the difficulty in determining when the last sign of condensate disappears, though other factors are likely to contribute.

The use of a vacuum during the initial recovery seems to reduce solvent hardening. Two AC–20 recoveries were performed using a high vacuum, so that the boiling temperature

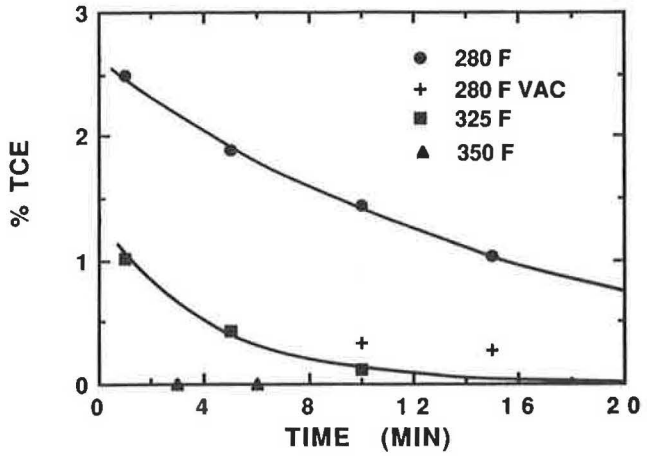

FIGURE 13 Residual solvent concentrations versus Roto-vap recovery time at three temperatures for a 20,000-poise (aged) asphalt.

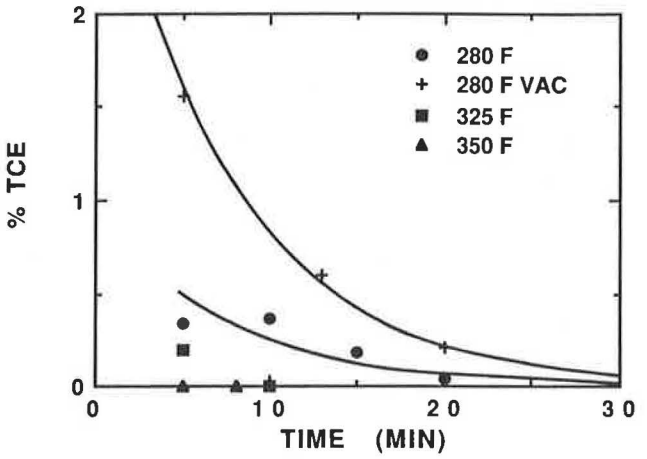

FIGURE 14 Residual solvent concentration versus Roto-vap recovery time at three temperatures for a 200,000-poise (aged) asphalt.

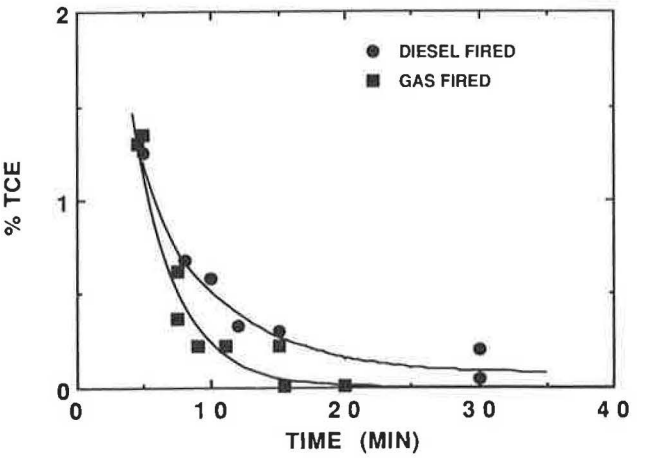

FIGURE 15 Residual solvent concentration versus Abson recovery time for two hot-mix extractions.

was less than 100°F. Two others were run using no vacuum, and boiling points were about 200°F. Figure 2 shows that the vacuum-recovered asphalts hardened about 10 percent, which is barely above the hardening typically caused by volatiles loss. The hot-recovered samples hardened about 16 percent.

Hot-Mix Recoveries and Volatiles Loss

Several extracted hot mixes were recovered (Abson method) and found to behave somewhat differently than tank or oven-aged material. Figure 15 shows a solvent removal comparison between diesel- and gas-fired plants. Hot mixes from batch and natural gas-fired plants showed normal solvent removal behavior when conducted at 320°F. However, diesel-fired drum plant mixes, even though recovered at 340°F for 30 min, contained significant levels of material eluting where TCE does on the GPC.

The diesel-fueled mixes were also different, in that they evolved a long-lasting fog and deposited an oily residue on the recovery flask's surfaces. These asphalts were all mixed at drum plants fired by diesel or fuel oil. Infrared analyses of the oily film showed it to be composed of highly oxidized hydrocarbons of small molecular weight (Figures 16a and 16b), possibly from partially oxidized fuel oil. Other asphalts mixed at batch or natural gas-fired plants did not exhibit this phenomenon.

The presence of this unusual and slightly volatile material may have given a false indication of residual solvent concentration and may account for the excessive solvent removal times of these hot mixes. A hot mix containing this material was extracted with THF in a sequence of cold, batch extractions using an amount of solvent that gave an overall concentration suitable for direct GPC analysis. Because no solvent removal was performed, all the volatile impurities remained in solution and were detected on the GPC. Several new peaks and valleys appeared near the TCE elution time, leaving open the possibility that the apparent TCE peak in the hot-mix recoveries was caused by residual oxidized fuel oil. Although the relative amount of this material in the asphalt was not determined, its significance to highway performance and to relating measured chemical properties to performance is potentially great and bears further study.

SUMMARY

The volatiles loss from virgin or unaged tank asphalts during solvent removal can produce 7 to 10 percent hardening of the original asphalt viscosity. RTFOT asphalts do not exhibit this hardening, apparently because of the loss of volatiles during the aging.

The same asphalts show hardening of from 10 to 40 percent (including that caused by volatiles loss) on contact with TCE and subsequent solvent removal. Short times and moderate temperatures for incubation of the asphalt with solvent produce little hardening; extended times at elevated temperatures (such as during reflux solvent extraction) can produce significant hardening.

Experiments were also conducted on the Abson and Roto-vap solvent removal methods for the purpose of evaluating their effectiveness in removing solvents. The Abson method, taken to its standard recovery time, can leave enough solvent

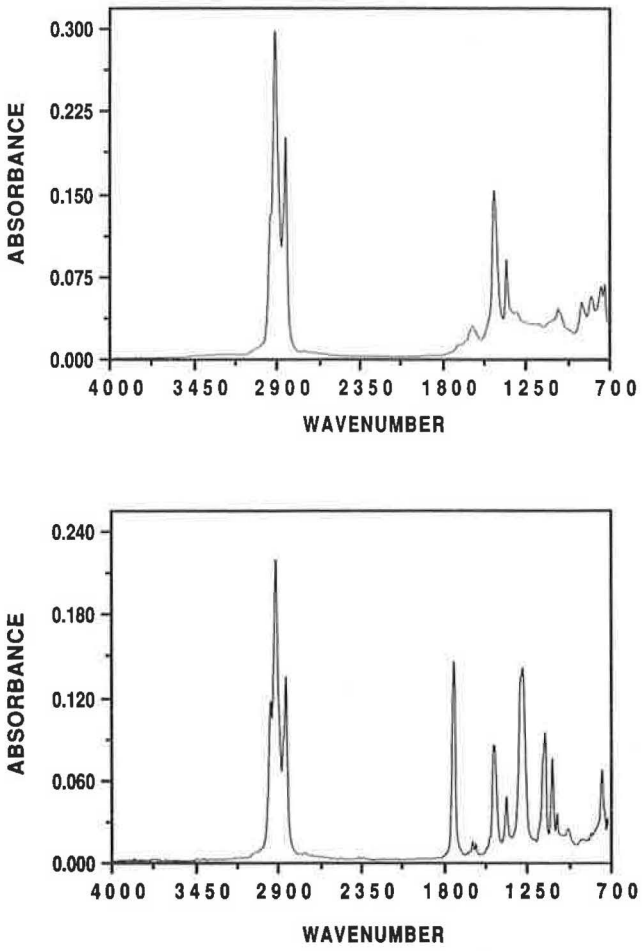

FIGURE 16 FT-IR spectra for the recovered hot-mix asphalt (top); for the volatile material recovered from the diesel-fired hot mix (bottom).

to produce significant softening, especially for larger quantities of recovered material and for hardened asphalts such as those obtained from aged pavement cores. Increasing the temperature of the solvent removal and the recovery time can reduce this residual solvent concentration, although the previously mentioned solvent-hardening effects must be considered. The Roto-vap method appears to be less consistent and less reproducible than the Abson method, but it may have some advantages for solvent removal.

For the Abson procedure at 325°F, a minimum recovery time (after the last drop) for 50-g samples is about 25 min. For 100-g samples, 380°F will remove the solvent within 20 min. For the Roto-vap procedure, 15 min past the last drop was adequate at 325°F.

A complicating factor in hot-mix and pavement core recoveries appears to be the possibility of fuel contamination from the hot-mix plant. Evidence of such contamination was found in some drum hot mixes, but the extent and significance of this possible contamination has yet to be determined.

ACKNOWLEDGMENTS

Support for this work by the Texas State Department of Highways and Public Transportation, in cooperation with the U.S. Department of Transportation, FHWA, and by the Strategic Highway Research Program is gratefully acknowledged. The technical contributions of Joe Button of the Texas Transportation Institute also are greatly appreciated.

REFERENCES

1. G. Abson. Method and Apparatus for the Recovery of Asphalt. *Proc. ASTM*, Vol. II, 1933, pp. 704–714.
2. J. H. Bateman and C. Delp. "The Recovery and Examination of the Asphalt in Asphaltic Paving Mixtures," *Proc. ASTM*, Vol. II, 1927, pp. 465–479.
3. D. C. Broome. *The Testing of Bituminous Mixtures*, 2nd ed. Edward Arnold and Co., London, 1949.
4. G. Abson and C. Burton. The Use of Chlorinated Solvents in the Abson Recovery Method. *Proc., Association of Asphalt Paving Technologists*, Vol. 29, St. Paul, Minn., 1960, pp. 246–252.
5. R. N. Traxler. Changes in Asphalt Cements During Preparation, Laying and Service of Bituminous Pavements. *Proc., Association of Asphalt Paving Technologists*, Vol. 36, St. Paul, Minn., 1967, pp. 541–561.
6. R. P. Lottman, S. K. Sonawala, and M. Al-Haboobi. Change of Asphalt Viscosity During Mixing with Hot Aggregates. *Proc., Association of Asphalt Paving Technologists*, Vol. 32, St. Paul, Minn., 1963, pp. 1–36.
7. D. E. Carey and M. R. Paul. *Evaluation of Asphalt Cement Extraction and Recovery Methods: Final Report*, FHWA/LA/82/157, 1982.
8. H. L. Davis. Progress Report: AR Grading System Subcommittee to Investigate ASTM D 1856-75, Abson Recovery Test Method. Presented at Pacific Coast User-Producer Conference, 1983.
9. J. M. Roberts and W. H. Gotolski. Paving Asphalt Properties and Pavement Durability. In *Transportation Research Record 544*, TRB, National Research Council, Washington, D.C., 1975, pp. 14–26.
10. L. D. Sandvig and J. A. Kovalt. Penetrations and Viscosity Functions in Bituminous Concrete. *Proc., Association of Asphalt Paving Technologists*, Vol. 37, St. Paul, Minn., 1968, pp. 584–621.
11. R. H. Gietz and D. R. Lamb. Age-Hardening of Asphalt Cement and Its Relationship to Lateral Cracking of Asphalts. *Proc., Association of Asphalt Paving Technologists*, Vol. 37, St. Paul, Minn., 1968, pp. 141–158.
12. M. S. Noureldin and P. G. Manke. Study of Transverse Cracking in Flexible Highway Pavements in Oklahoma. In *Transportation Research Record 695*, TRB, National Research Council, Washington, D.C., 1978, pp. 28–32.
13. J. C. Petersen, H. Plancher, E. K. Ensley, R. L. Venable, and G. Miyake. Chemistry of Asphalt-Aggregate Interactions: Relationship with Pavement Moisture-Damage Prediction Test. In *Transportation Research Record 843*, TRB, National Research Council, Washington, D.C., 1982, pp. 95–104.
14. C. Bussow. Notes on a Method of Recovering Bitumen from Paving Materials. *Proc., Association of Asphalt Paving Technologists*, Vol. 7, St. Paul, Minn., 1936, pp. 160–164.
15. A. P. Hagen, R. Jones, R. M. Hofener, B. B. Randolph, and M. P. Johnson. Characterization of Asphalt by Solubility Profiles. *Proc., Association of Asphalt Paving Technologists*, Vol. 53, St. Paul, Minn., 1984, pp. 119–137.
16. G. R. Donaldson, J. A. Bullin, R. R. Davison, C. J. Glover, and M. W. Hlavinka. The Use of Toluene as a Carrier Solvent for Gel-Permeation Chromatography Analyses of Asphalt. *Journal of Liquid Chromatography*, Vol. 11, 1988, pp. 749–765.
17. J. Fahrenfort. Attenuated Total Reflection: A New Principle for the Production of Useful Infra-red Reflection Spectra of Organic Compounds. *Spectrochimica Acta*, Vol. 17, 1961, pp. 698–709.

Publication of this paper sponsored by Committee on Characteristics of Bituminous Materials.

Asphalt Aging in Texas Roads and Test Sections

K. L. MARTIN, R. R. DAVISON, C. J. GLOVER, AND J. A. BULLIN

In 1982–1983, test sections were laid at three Texas locations using five asphalt sources and two grades. Not all combinations were used at all locations and two roads failed early, but results are reported on 16 sections. These roads were cored in 1984, 1985, and 1987. Viscosities, penetrations, voids, gel permeation chromatography (GPC), and Fourier transform infrared (FT-IR) analyses were run. Voids and aging are strongly correlated whether the aging is measured by a viscosity aging index, growth in carbonyl peak, or GPC. Although GPC, carbonyl peak, and sulfoxide generally increase with age, sulfoxide and other aging indexes are poorly correlated. Growth in sulfoxide correlates weakly with sulfur content. In general, the number of voids reveals large ranges in asphalt performance. Asphalts showing nearly the same aging index at low numbers of voids might differ several-fold at high numbers of voids. When comparison was possible, higher viscosity grades resulted in greater aging. Results also were obtained for several south Texas highways, ranging in age from 5 to 19 years. Although original tank asphalt, hot-mix, and early cores were not available for study, recovered asphalt properties from highway-aged cores followed trends similar to those for the test sections with respect to viscosity, penetration, FT-IR, and GPC measurements.

In 1982–1983, test sections were constructed at three locations in Texas using asphalts from five refineries. AC–10 and AC–20 grades were used in a total of 20 sections. In 1982, seven sections were placed east of Dickens, on the westbound travel lane of US-82. Seven sections were located north of Dumas on the northbound travel lane of US-287. These sections were also constructed in 1982. In 1983, six sections were installed on the northbound lane of two-lane US-96, about 25 mi south of San Augustine. These sections are referred to as the "Lufkin sections."

The aggregate used at Dickens was mined near the site. The coarse and intermediate fractions were crushed siliceous gravel, and the fines were similar material. The Dumas aggregate was an absorptive crushed limestone. The Lufkin aggregate consisted of a mixture of limestone and iron ore gravel plus field sand.

The principal objective of the latter study was to relate physical and chemical laboratory properties to field pavement performance. Some of the properties that were measured on the original asphalts are presented in Table 1 (*1*). Following construction, the Dumas and Dickens sites had high void contents. Cores were taken at Dickens and Dumas after 1 week and after 1 and 2 years, and at Lufkin after 1 week and 1 year. The voids after each period are shown in Table 1. At Dumas, the Dorchester section failed after 1 year and had to be replaced. The Exxon section was also in bad condition and had to be partially replaced. At Dickens, all the test sections began to show raveling and were fog sealed by 1985.

In 1986, a new study was begun with the objective of correlating certain chemical properties to physical properties and road performance. In connection with this objective, the test sections were recored in 1987. By this time, the Exxon and Diamond Shamrock AC–10 at Dumas had been completely replaced, and the remaining sections at Dumas had been seal coated. Only the Lufkin sections still had their original surfaces and these were all in good condition. One Lufkin section listed as Dorchester AC-20 was omitted from the study, because the asphalt source was actually believed to be Texaco. This procedure left 16 sections to be cored, as presented in Tables 2 and 3.

The study was expanded by including some old roads that were still in good condition. District 21, in the southern tip of Texas, was chosen because this area has a generally hot, dry climate significantly different from the other locations. This district, in cooperation with the Texas State Department of Highways and Public Transportation (SDHPT) in Austin and Texas A&M University, has established a data base on their roads containing pertinent information about the construction, use, and condition of these roads. Using this data base, only six roads could be found that were uncracked and at least 5 years old. A road found with slight transverse cracking was also included. These roads, cored in June 1988, are presented in Table 4.

State Highway 186 in Willacy County was sampled at two locations. At Milepost (MP) 25.8, the pavement was laid in the fall of 1982. The road showed a small amount of raveling but was otherwise in good condition. At MP 34, the pavement was laid in August 1980.

US-77 was also sampled in two locations. At MP 16 in Willacy County, the road was in good condition although it was laid in August 1982 and was a high-traffic area. In Cameron County, US-77 was sampled at MP 27, near Harlingen. This location had the highest traffic level. It was paved in August 1982 and was seal coated in 1987, possibly to solve a raveling problem.

The only other high-traffic road sampled was US-281 in Hidalgo County. This site, at MP 37.5 near McAllen, was laid in January 1979 and seal coated in May 1985. Raveling was obviously a problem with this stretch of road, because the verge of the road was covered with aggregate from the original asphalt, not from the seal coat.

Two Texas farm-to-market (FM) roads were included. In Cameron County, FM-2925 was sampled at MP 12. The asphalt there was laid in April 1983. This pavement was cracked

Department of Chemical Engineering and The Texas Transportation Institute, Texas A&M University, College Station, Tex. 77843–3122.

TABLE 1 VISCOSITIES OF VIRGIN ASPHALTS AND CORE VOIDS

	Viscosity (Poise)		% Voids		
	140°F	275°F	1 week	1 year	2 years
Dickens					
D.S. AC-10	1220	4.51	16.0	14.3	9.1
D.S. AC-20	2175	7.15	13.4	10.0	12.7
McM AC-20	2523	4.64	15.6	9.9	14.0
EXX AC-20	2576	3.55	14.8	9.9	13.6
Dorch AC-20	2151	4.53	11.7	14.1	13.0
Cos AC-10	1264	2.55	14.4	14.5	10.6
Cos AC-20	1515	2.87	15.0	10.5	12.3
Dumas					
D.S. AC-10	958	4.65	20.4	7.2	2.1
D.S. AC-20	2155	6.39	13.9	11.6	9.2
McM AC-10	961	3.63	12.2	13.7	10.5
EXX AC-10	1388	3.06	16.5	15.4	
Dorch AC-10	1030	3.21	12.6	12.2	8.6
Cos AC-10	1038	2.48	20.4	13.8	7.3
Cos AC-20	2354	3.17	17.1	10.5	10.2
Lufkin					
D.S. AC-20	1728	5.05	8.6	2.6	
McM AC-10	932	3.63	4.8	6.2	
EXX AC-20	1811	3.19	6.6	3.0	
Dorch AC-10	1040	2.88	3.2	4.2	
Dorch AC-20	1913	3.96	7.4	2.2	
Cos AC-20	1858	2.83	6.5	3.2	

Diamond Shamrock (D.S.) McMillan (McM) Exxon (EXX)
Dorchester (Dorch) Cosden (Cos)

TABLE 2 PHYSICAL PROPERTIES OF TEST SECTION 1987 CORES AND EXTRACTED ASPHALT

	Percent Voids	Viscosity		Penetration at 77°F (0.1 cm)	Percent Asphalt
		140°F (Kilopoise)	275°F (Poise)		
Dickens					
McM AC-20	8.0	159	23.1	16	6.2
Dorch AC-20	13.0	222	22.4	10	4.6
EXX AC-20	9.0	900	70.7	12	5.1
D.S. AC-20	12.0	260	34.2	18.5	---
D.S. AC-10	9.0	48.9	17.9	25	5.3
Cos AC-20	11.0	376	26.4	10.5	4.0
Cos AC-10	12.0	342	18.2	11.5	5.6
Dumas					
McM AC-10	5.5	13.3	9.2	38	5.5
D.S. AC-20	8.1	32.5	18.9	27.5	5.9
Cos AC-10	9.5	23.4	26.7	18	5.9
Cos Ac-20	8.5	55.6	11.7	15.5	5.9
Lufkin					
McM AC-10	2.4	4.8	6.5	39	6.6
Cos AC-20	1.8	5.4	5.7	22	6.9
D.S. AC-20	2.1	9.1	11.2	30	6.5
EXX AC-20	2.5	3.9	5.8	40.5	7.7
Dorch AC-10	2.1	2.4	4.6	38.5	5.6

McMillan (McM) Dorchester (Dorch) Exxon (EXX)
Diamond Shamrock (D.S.) Cosden (Cos)

TABLE 3 PARAMETERS USED IN AGING CORRELATIONS

	Carbonyl Peak Height	Sulfoxide Peak Height	Percent LMS	Aging Index 140°F	Aging Index 275°F
Dickens					
McM AC-20	34	23	33.6	63	5.0
Dorch AC-20	29	18	25.4	103	4.9
EXX AC-20	37	20.5	38.8	350	19.9
D.S. AC-20	35.5	13.5	53.9	119	4.8
D.S. AC-10	29.5	16.25	46.0	40	4.0
Cos AC-20	32	18	26.8	247	9.2
Cos AC-10	31	22	30.1	271	7.1
Dumas					
McM AC-10	15.5	30	24.4	13.8	2.5
D.S. AC-20	25	22.25	45.9	15.0	3.0
Cos AC-10	17	29	19.6	22.5	10.7
Cos AC-20	20.5	25	23.2	20.5	3.7
Lufkin					
McM AC-10	10	13	33.7	10	1.8
Cos AC-20	8.5	32.25	18.5	8.5	2.0
D.S. AC-20	22	10.25	45.0	22	2.2
EXX AC-20	8	25.75	23.5	8	1.8
Dorch AC-10	5	19	23.5	5	1.6

McMillan (McM) Dorchester (Dorch) Exxon (EXX)
Diamond Shamrock (D.S.) Cosden (Cos)

TABLE 4 DATA FOR SOUTH TEXAS ROADS

Highway	Carbonyl Peak Height	Sulfoxide Peak Height	% LMS	Viscosity 140°F (kpoise)	Viscosity 275°F (poise)	Penetration (0.1 cm)	Age (yrs)
FM 2925	23.5	26.75	26.4	67.8	15.4	14	5
US 77/27[a]	10.75	33	25	27.5	12.3	23.5	5+1[b]
US 77/16[a]	18	28.5	24	43.3	12.5	14.5	6
SH 186/25[a]	30.75	36	30.5	130	21.0	14	6
US 281	22	28.75	26.4	22.0	8.5	22	6+3[b]
SH 186/36[a]	30.75	23	29.7	282	23.5	10	8
FM 1017	36.75	13.5	33.8	248	21.1	13	19

[a] Milepost
[b] Years Under Sealcoat

transversely about every 8 ft. The road was made up of a thin pavement over the base, and the high level of boat traffic to the Gulf of Mexico may have contributed to the cracking. The other FM road was officially listed as having a seal coat only. FM-1017 in Hidalgo County was cored at MP 7.5. This road was easily the oldest in the study, having been laid in May 1969 over what appeared to be an old gravel road. The pavement was rutted by the oil-field trucks traveling it, but it was in good condition considering its age and construction. In fact, only about 0.6 mi of the 1969 road still existed, the rest having been replaced. All of the pavements in the south Texas test sites were constructed with aggregate resembling

river gravel, which may have contributed to the raveling in many roads. These locations and those of the original test sections are shown in Figure 1.

PROCEDURES

All of the cores were extracted by a modified ASTM D2172–81, Method A, except at Lufkin, where all but the Cosden AC–20 were extracted by Method B. The procedure was changed after it was realized that Method B can change the asphalt. In both instances, ethanol was added to improve removal from the aggregate. In the Method B procedure, a 95 percent trichloroethylene, 5 percent ethanol mixture was used. For Method A, several extractions with trichloroethylene were followed by a 90 percent trichloroethylene, 10 percent ethanol mixture. The small amount of ethanol considerably enhanced removal of the remaining amounts of asphalt.

Solvent was removed either by the Abson or by the Rotovap procedures. Gel permeation chromatography (GPC) analysis of the recovered material indicated that many samples still contained solvent, and additional solvent removal was required to avoid erroneously soft asphalt. (The times specified in the standard procedures were frequently inadequate for complete solvent removal, especially from viscous core material.)

Voids and the percentage of asphalt were calculated (see Table 2). Penetrations at 77°F using ASTM D5 and viscosities at 140°F and 275°F using ASTM D2173 were run on the recovered material. These data are presented in Tables 2 and 4.

GPC chromatograms were obtained using an IBM 9533 Liquid Chromatograph controlled by an IBM 9000 computer. Two Polymer Laboratories chromatographic gel columns were used in series, a 500-Å pore size followed by a 50-Å pore size. The detector was a Waters R401 differential refractometer. Purified tetrahydrofuran (THF) was used as the solvent. Asphalt samples were made to exactly 7 percent by weight in THF and sonicated for about 3 hr. The sonicated material was then filtered through a 0.45-μm filter to remove fines. The filtered material was placed in a 1.8-mL septum-capped vial and placed in an automatic sampler. A 100-μL sampling loop was used.

Infrared spectra of the recovered material were obtained on a Nicolet 60 SX B Fourier transform infrared (FT-IR) spectrometer. All the data were obtained by a KBr pellet procedure (*2*), which, though time consuming, gives a strong, reproducible signal. In a precise manner, 0.9750 g of KBr and 0.025 g of asphalt (frozen to enhance handling) were ground together in a mortar until the mixture was homogeneous. Then 0.300 g was taken to prepare a pellet. The mixture was placed in a pellet die and 34,000 lb of force was applied for 30 sec. A blank of pure KBr was prepared at the same time by the same procedure. Before sample preparation, the KBr was heated to about 700°F for 8 hr to remove moisture.

In order to use either GPC or IR spectra to correlate properties, some simplified characteristic was desired because the spectra are complex. For GPC, the percentage of large molecular size (LMS), as suggested by Jennings (*3*), was used. Arbitrarily, the entire spectrum was taken as 20 to 35 min and the LMS interval as 20 to 25 min during elution. The LMS percentage was calculated from the areas under the curve during these intervals.

Two areas of the IR spectrum relate specifically to oxidation. One is the carbonyl peak, occurring at about a wave number of 1,700, and the other is a sulfoxide peak at a wave number of 1,030. Because these peaks both occur in areas where absorption of other entities is present, the choice of peak height is somewhat arbitrary. For the sulfoxide peak, the method recommended by Peterson (*4*) is used as shown in Figure 2. A tangent line is drawn below the peak of interest touching the low points on either side. A similar procedure was used with the carbonyl peak. The parameter was the height of each peak above this tangent line.

FIGURE 1 Location of test sections near Dickens, Dumas, and Lufkin and of highways cored in south Texas District 21.

RESULTS AND DISCUSSION

Properties of the 1987 test section cores and the extracted asphalts are presented in Table 2. Sulfoxide and carbonyl peak

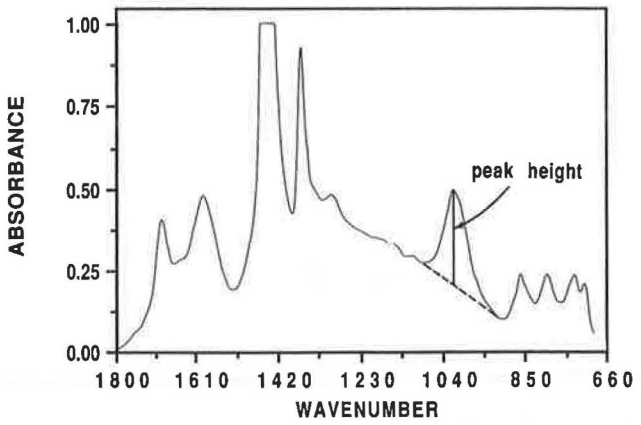

FIGURE 2 Example FT-IR spectrum showing the method of determining the sulfoxide band peak height near 1,000 cm^{-1}. The carbonyl peak height near 1,700 cm^{-1} is determined similarly.

heights from the IR analyses and LMS percentages from the GPC experiments are presented in Table 3, along with viscosity aging indexes at both 140°F and 275°F. The aging index is the ratio of the viscosity of the 1987 core extracts divided by the viscosity of the virgin asphalt from Table 1. Properties of the asphalt extracted from the south Texas cores are presented in Table 4.

Correlation of Voids and Aging

One of the surprising elements of the data in Tables 1 and 2 is the inexplicably high void level in the test sections at Dumas and Dickens, which has led to rapid aging and the early demise of three sections. For decades, high void levels have been known to shorten road life, yet they continue to be a problem, even in carefully monitored test sections.

An interesting case in point is a study of Pennsylvania test sections conducted during the 1960s and 1970s. This work, summarized by Gotolski et al. (*5*) and Roberts and Gotolski (*6*), included a variety of asphalts and aggregates. Performance was difficult to correlate with air voids because of the variability in voids from point to point, the steep variation across the road, and the effect of aggregate and gradation. Even so, it was found that: "Air voids are one, if not the greatest, factor affecting the rate of hardening of an asphalt pavement. The influence of the variable appears to be so pronounced that it completely overshadows the performance of asphalt type, aggregate type, traffic density and microclimate differences." The great effect of voids does seem incontrovertible, but the data indicate that asphalt quality becomes more critical at higher voids. One of the more interesting observations and conclusions from the Pennsylvania study, confirmed by the experience of the Texas test sections nearly 20 years later, is the following: "The pavements studied received better than average design and field control; yet these pavements were constructed with void contents as high as 13 percent. This underscores the need for more restrictive specifications and closer field control."

In Figure 3, carbonyl peak height is plotted versus percentage of voids. These are voids from 1987 cores that give better results than averaging the void data. This is probably because of variation in voids within the roadbed, so that earlier cores may not represent the cores being studied. Oxidation, as reflected in the growth of the carbonyl peak, increases rapidly with voids. The Dickens sections, which are represented by the seven highest carbonyl peaks, showed a greater response than the Dumas sections. In general, those sections constructed with the lower viscosity grade were also oxidizing less rapidly. In the three direct comparisons with the same supplier and site, Cosden at Dickens, Diamond Shamrock at Dickens, and Cosden at Dumas, this was the case. Though the Exxon at Lufkin appeared to be oxidizing no more than the other asphalts, the Exxon at Dickens was the most oxidized of all. The data are not sufficient, however, to conclude that any asphalt is more susceptible to oxidation.

In Figure 4, the aging index at 275°F is plotted versus the percentage of voids. The results are similar to those in the previous graph. The Exxon had a high aging index and a high carbonyl content. Both of the Cosdens appeared to be abnormally aged at Dickens. However, the Dumas-Cosden datum

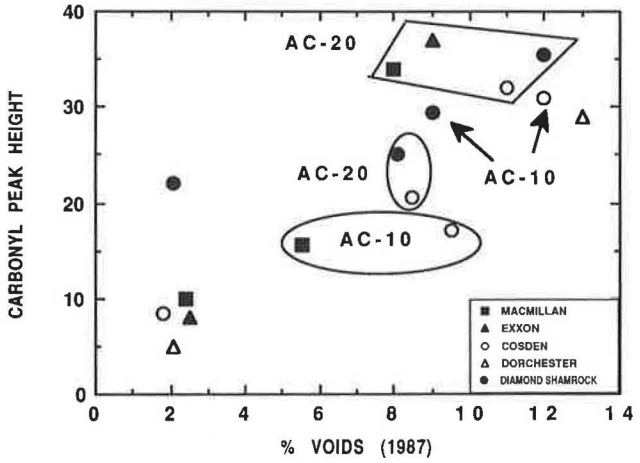

FIGURE 3 Carbonyl aging versus voids for asphalt from 1987 cores of the test sections.

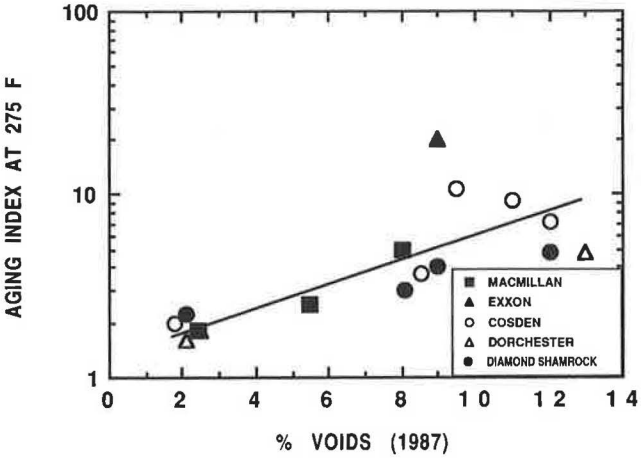

FIGURE 4 The 275°F aging index versus voids for asphalt from 1989 cores of the test sections.

at 8.5 percent voids was inconsistent with the 140°F data and with earlier cores and was probably in error. Figure 5 is a similar plot with 140°F aging indexes. Again the Exxon value was quite high, with high values for the Cosdens and perhaps for the McMillan. At Dumas, both Cosdens were near the curve. As mentioned earlier, the inherent problem in the study of voids versus aging is that roadbed variability makes it impossible to obtain an accurate voids history of the particular core being studied. So 1987 voids were used rather than average voids, no doubt accounting for much of the scatter.

Correlation of Carbonyl Content and Physical Properties

Because both the viscosity aging index and carbonyl peak height correlate with voids, they should cross-correlate. Figures 6 and 7 indicate that they do. Somewhat surprisingly, however, viscosity seems to correlate as well as the aging

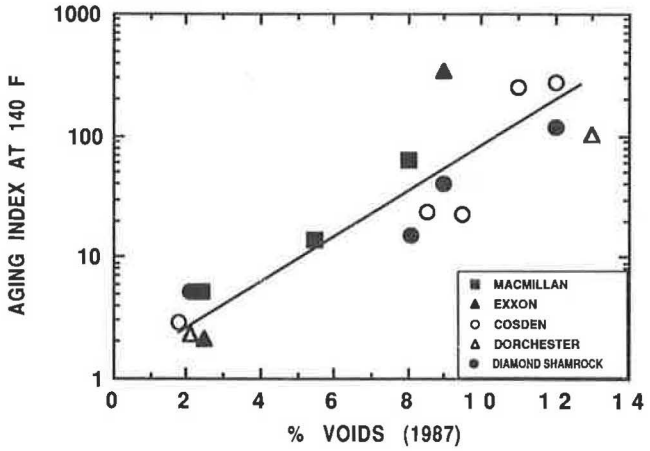

FIGURE 5 The 140°F aging index versus voids for asphalt from 1987 cores of the test sections.

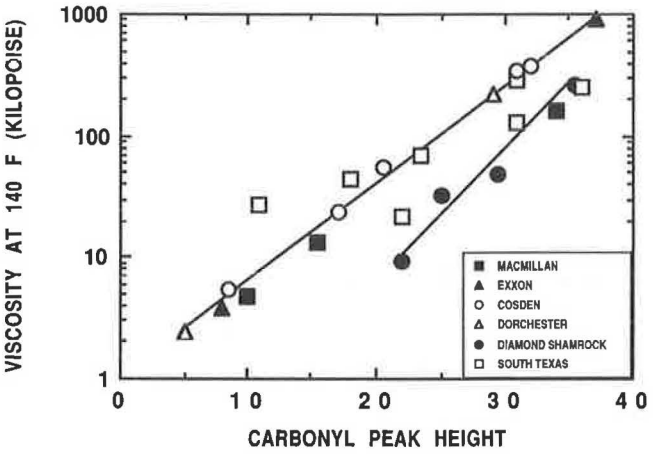

FIGURE 7 Viscosity at 140°F versus carbonyl peak height from 1987 cores of the test sections and from the south Texas highway cores.

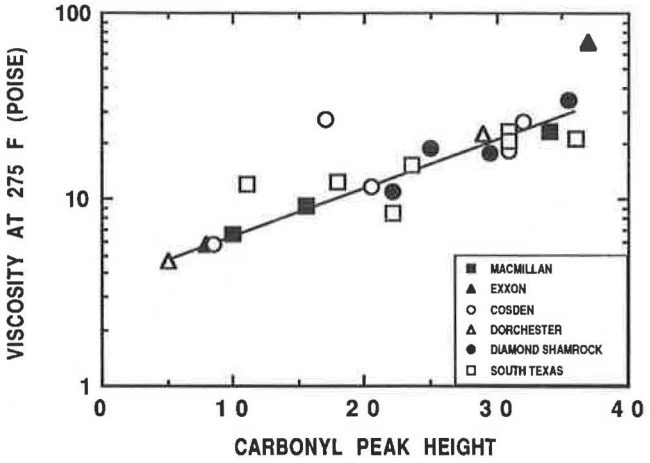

FIGURE 6 Viscosity at 275°F versus carbonyl peak height from 1987 cores of the test sections and from the south Texas highway cores.

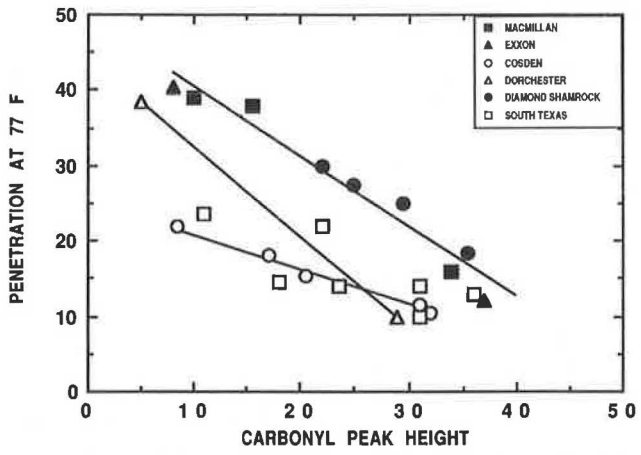

FIGURE 8 Penetration at 77°F versus carbonyl peak height from 1987 cores of the test sections and from the south Texas highway cores.

index, and this correlation allows the inclusion of the south Texas data, for which original viscosities are not available. At 275°F (see Figure 6), the Exxon Dickens value was very high. The high Cosden value is the suspect point previously discussed. Otherwise, most south Texas data fit very well.

At 140°F (see Figure 7), the Diamond Shamrock data had completely separated from the others. The Dickens Exxon was on the curve, but the plot of south Texas data had a different slope than the others. These data imply that the south Texas data in Figure 6 would also plot better with a lower slope.

In Figure 8, penetrations at 77°F are plotted versus carbonyl peak height. Individual asphalts are further separated, but Exxon and McMillan have almost merged with Diamond Shamrock, whereas Cosden has approximately joined the south Texas plot with an entirely different slope. The 19-year-old south Texas FM-1017 had only a slightly higher penetration than the 5-year-old Dickens Exxon. Several of the Dickens roads were approaching dangerously low penetrations, as was

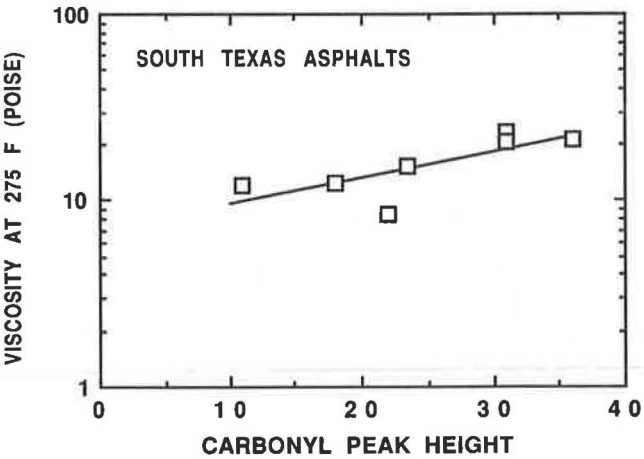

FIGURE 9 Viscosity at 275°F versus carbonyl peak height for asphalts from the south Texas highway cores.

Highway 186 at MP 36. This low penetration on Highway 186 was consistent with its high viscosity at both 140°F and 275°F.

Except for this road and Highway 281 at MP 37.5, which had abnormally high penetration and low viscosities, the south Texas roads show remarkable conformity. In Figures 9 and 10, viscosities of the south Texas roads are plotted versus carbonyl peak height at 275°F and 140°F. The 140°F correlation is particularly good, except for the two data referred to previously. All of these data tend to indicate that carbonyl peak height is a good measure of road aging for any particular asphalt with respect to both viscosity and penetration and can probably be used as an effective parameter in laboratory aging tests. However, carbonyl peak height cannot be related to road age in years, because the percentage of voids and probably other factors exert too much influence on aging. One of these other factors is almost certainly asphalt compatibility (*7*), which could account for much of the divergence of individual asphalts noted.

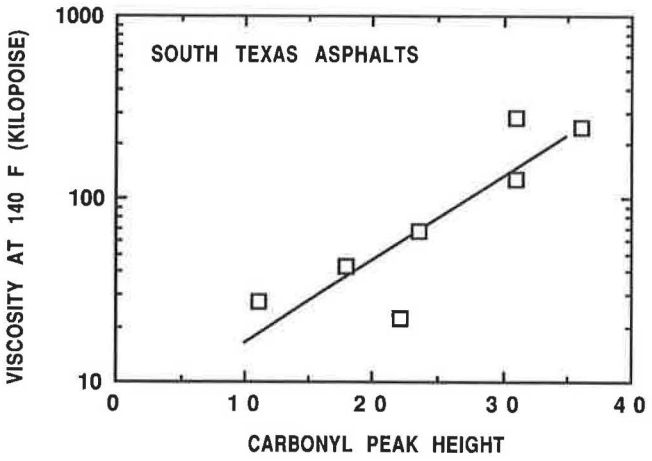

FIGURE 10 Viscosity at 140°F versus carbonyl peak height for asphalts from the south Texas highway cores.

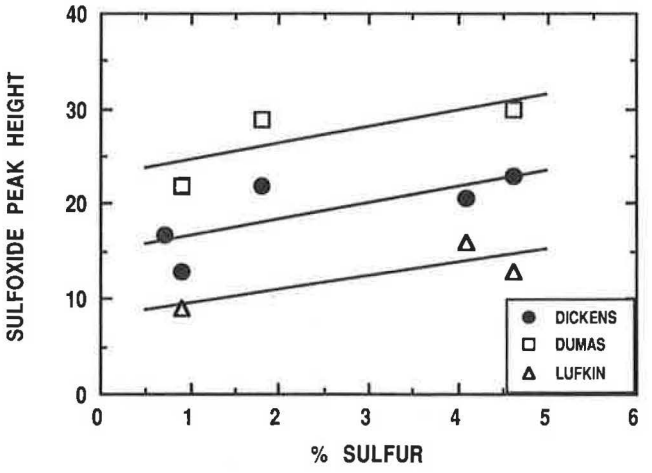

FIGURE 11 Sulfoxide peak height versus sulfur content for asphalt from 1987 cores of the test sections.

Effect of Sulfoxides

Surprisingly, the correlations so far have been made without reference to the height of the sulfoxide peak, which for some of the aged asphalts was higher than the carbonyl peak. Sulfoxide formation should be complicated by the wide variations encountered in sulfur content. Figure 11 shows sulfoxide peak height versus sulfur content for those asphalts for which data on sulfur content were available. Although a distinctly upward bias with increasing sulfur content was present overall, location had a much stronger effect. The Dickens sites had consistently higher carbonyl peaks and viscosities and generally lower penetrations, yet the Dumas asphalt had consistently higher sulfoxide peaks. These differences are even stronger when the asphalts from the same supplier are compared.

This reverse correlation between sulfoxide and carbonyl peak heights is shown in Figure 12. The scattered data at the bottom, represented by the lower curve, are from Lufkin, where both carbonyl and sulfoxide tended to be lower because of the small extent of aging. All of the other data fell reasonably well on the upper curve except for Highway 186 at MP 25, which showed a high value for both peaks. The asphalt extracted from this road fit the other correlation well, further giving evidence that sulfoxide formation has little effect on physical properties except as it affects carbonyl formation.

Apparently, there is competition between sulfoxide and carbonyl formation; because the former contributes little to hardening, it is desirable. The question remains why sulfoxide formed preferentially at Dumas. A possible answer is the aggregate, which at Dumas is an absorptive limestone and at Dickens is sandstone. Sulfoxide formation is reported to be base catalyzed (*8*).

Correlation with GPC

Figure 13 shows GPC results for Cosden AC–20 at all three locations. The progressive aging with time and the higher aging at Dickens and Dumas are clearly shown. Figure 14 shows a plot of the percentage of LMS versus carbonyl content. The correlation is not good, because the chromatograph

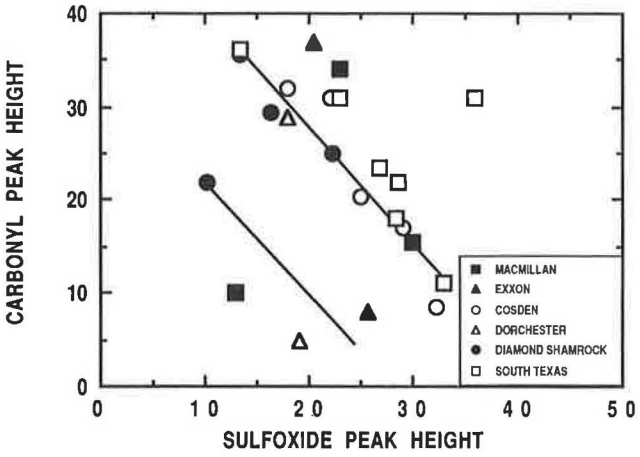

FIGURE 12 Carbonyl FT-IR peak height versus sulfoxide peak height from 1987 cores of the test sections and from the south Texas highway cores.

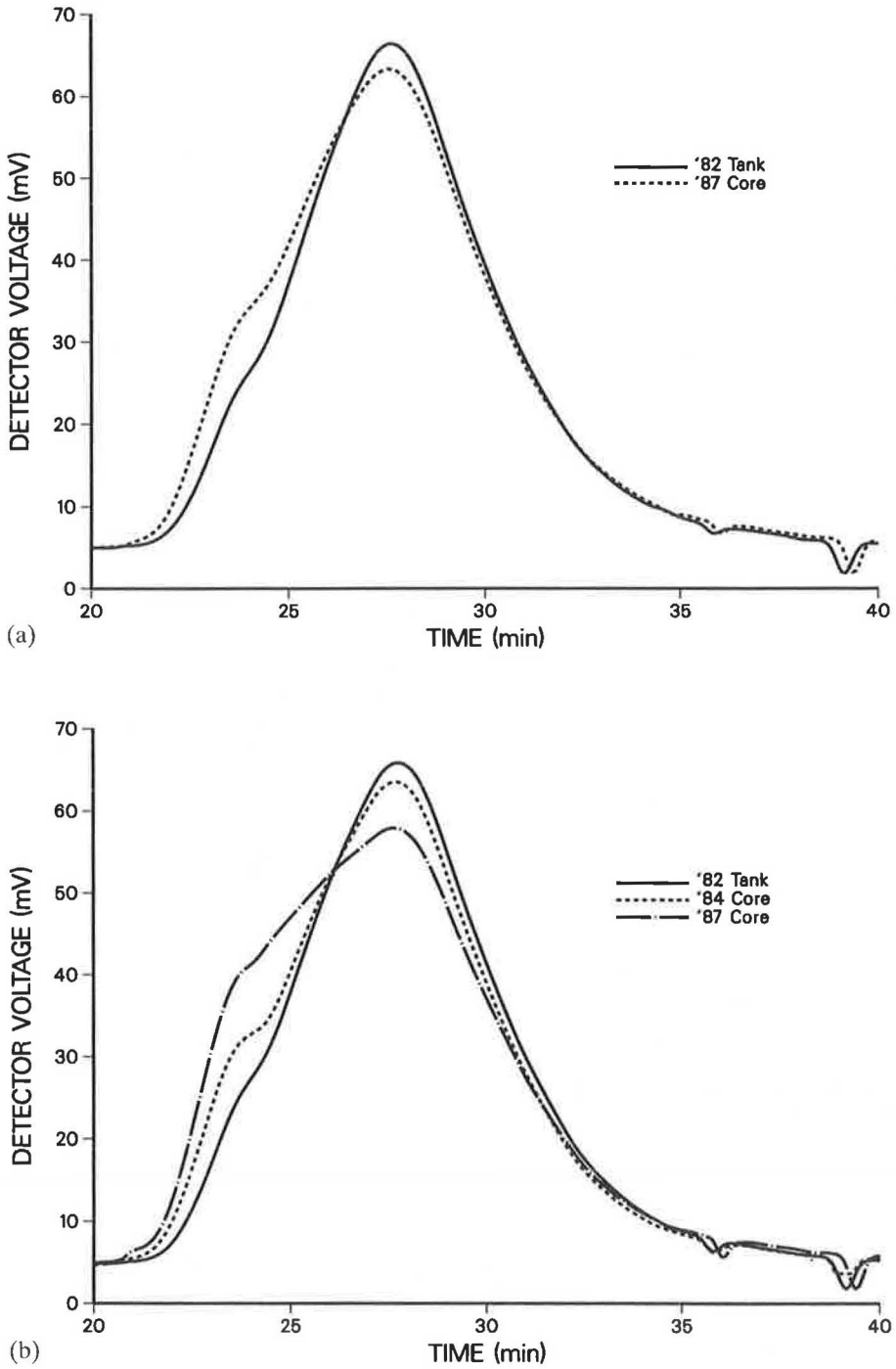

FIGURE 13 GPC chromatograms of the Cosden AC–20 asphalt as sampled before hot-mixing (tank) and as extracted and recovered from a, Lufkin, b, Dumas, and c, Dickens.
(*continued on next page*)

of each asphalt source tends to have its distinctive shape, only crudely represented in LMS. The unique shape of Diamond Shamrock chromatographs is reflected in this graph, but the scatter is disappointing, as it is for several others.

The largest and most consistent sets of data are for Cosden and south Texas. Figure 15 is a plot of the percentage of LMS versus carbonyl peak height for south Texas; except for Highway 77 at MP 16, the correlation is excellent. Figure 16 shows the GPC chromatograms for south Texas. The chromatogram for this asphalt is anomalous, having the lowest shoulder but not the lowest LMS value. In Figures 17 and 18, viscosity is plotted versus LMS percentage for the south Texas asphalts. Most of the points off the line are the same ones that did not correlate in the plot of carbonyl versus viscosity. In Figure 18, the highest and lowest points are for the same asphalts that are off the line in Figure 10. The third point represents

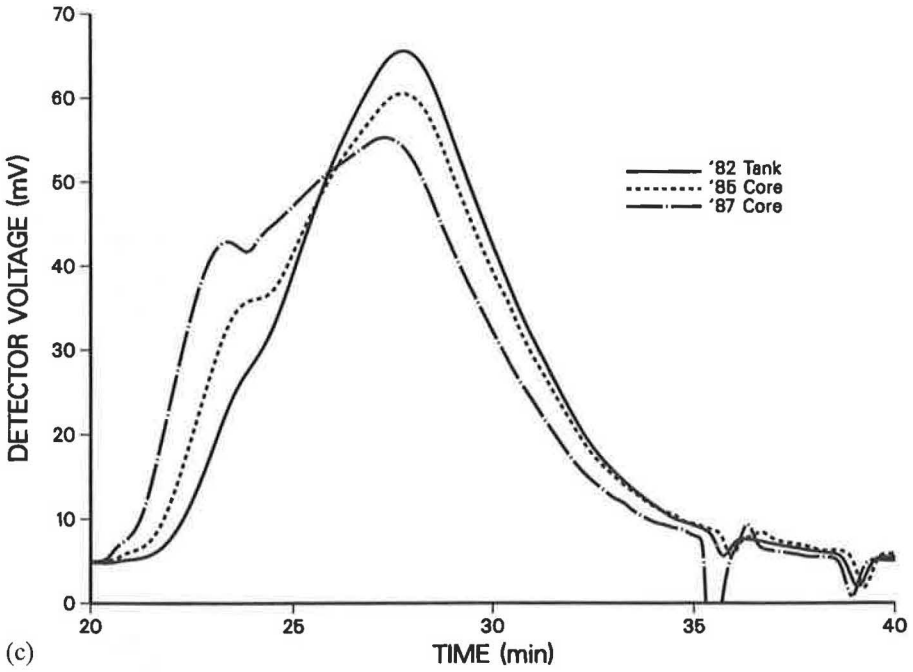

FIGURE 13 (*continued*)

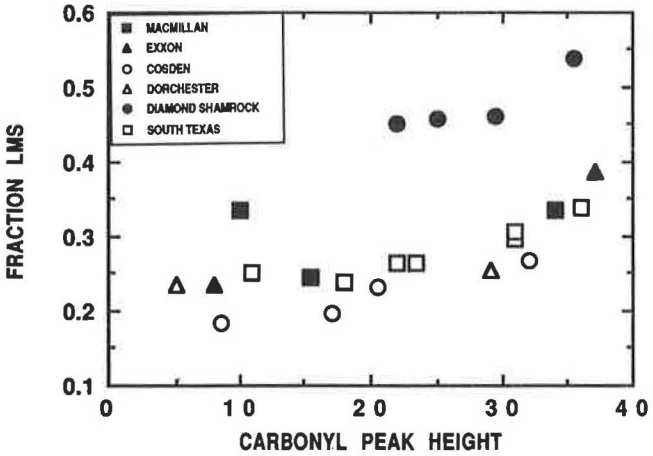

FIGURE 14 GPC chromatogram of LMS fractions versus carbonyl peak height from 1987 cores of the test sections and from the south Texas highway cores.

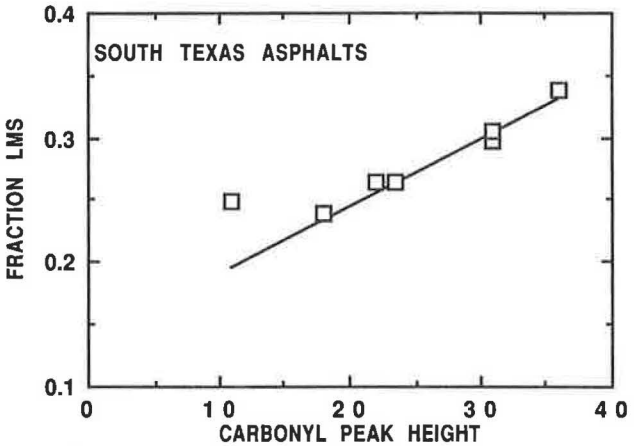

FIGURE 15 GPC chromatogram of LMS fractions versus carbonyl peak height for asphalts from the south Texas highway cores.

the asphalt that deviated from the line in Figure 15. The remaining four points form an almost perfectly straight line.

CONCLUSIONS

The extremely detrimental effect of high voids has been demonstrated again. This effect has been known for decades but seems to resist implementation. The progressive hardening of road asphalt with age will be impossible to predict apart from knowledge of the percentage of voids and perhaps knowledge of the aggregate used. Sulfoxide formation may be desirable. In this event, high-sulfur asphalts and aggregates that promote the oxidation of sulfur would be preferred. Lower viscosity grades should be used where possible.

Carbonyl formation is an excellent measure of oxidative aging and correlates with changes in physical properties. If other properties, such as compatibility, were included, the correlations would probably improve. The use of GPC to measure asphalt aging is also very useful, but GPC results are

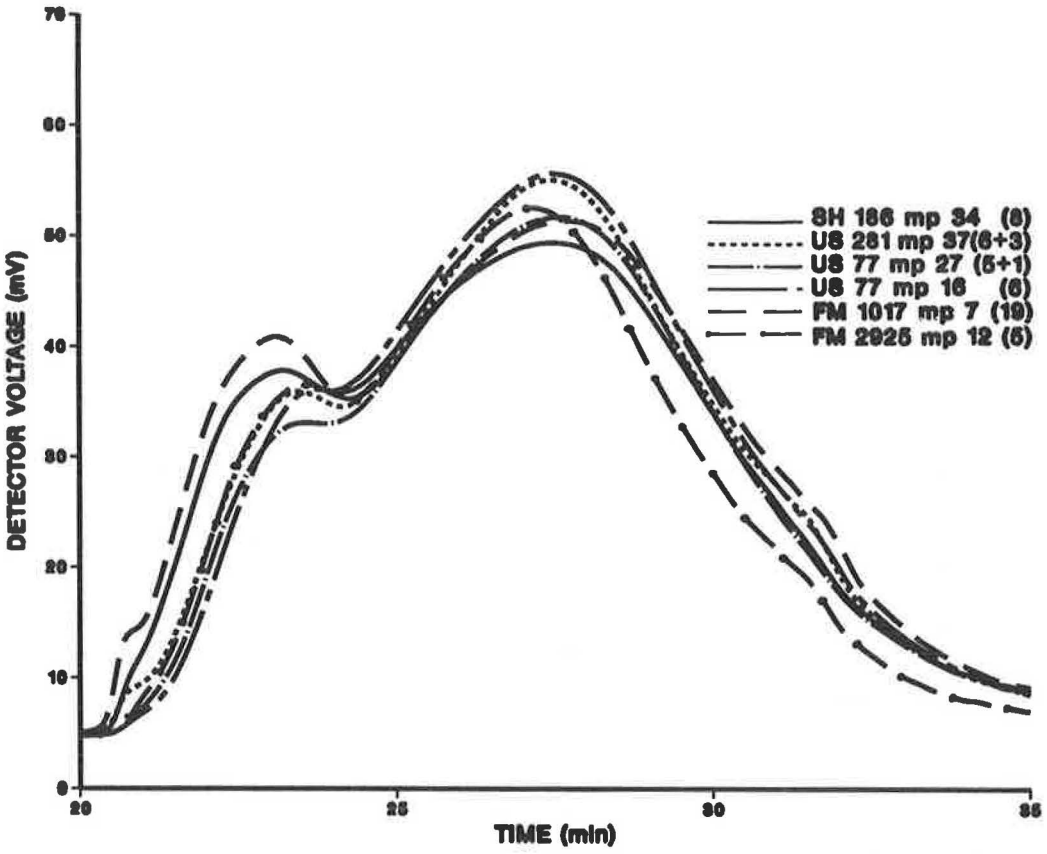

FIGURE 16 GPC chromatograms for asphalts from the south Texas highway cores.

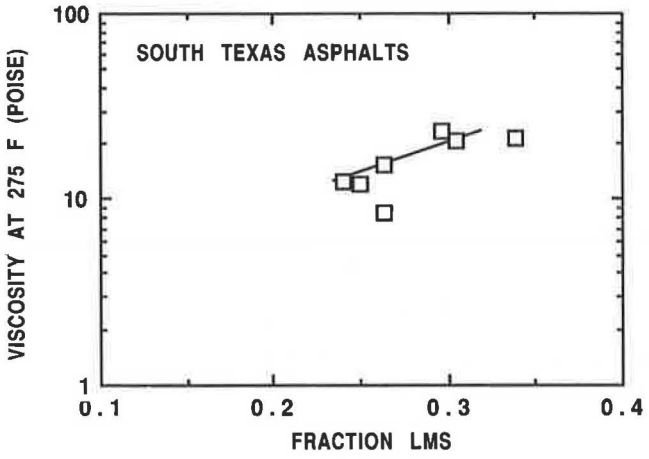

FIGURE 17 Viscosity at 275°F versus GPC LMS fractions for asphalts from the south Texas highway cores.

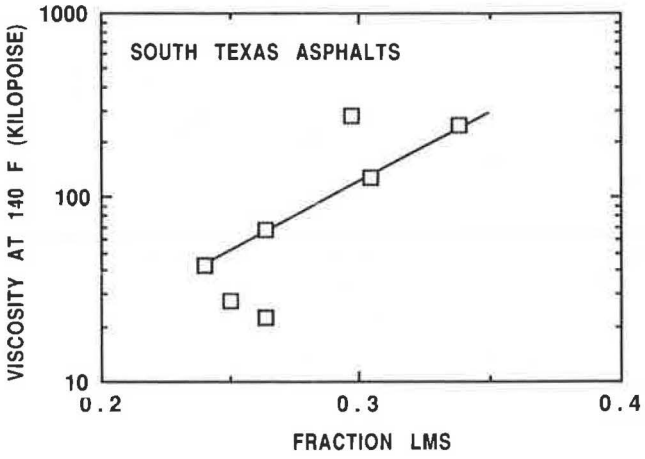

FIGURE 18 Viscosity at 140°F versus GPC LMS fractions for asphalts from the south Texas highway cores.

more difficult to correlate, because each asphalt yields a chromatogram with a distinctive shape that is dependent on the procedures used.

ACKNOWLEDGMENTS

Support for this work by the Texas State Department of Highways and Public Transportation (SDHPT), in cooperation with the U.S. Department of Transportation, FHWA, is gratefully acknowledged. Especially appreciated is the technical assistance provided by SDHPT District 21 personnel in selecting and obtaining the south Texas highway cores. Helpful discussions with Don O'Connor and Darren Hazlett of SDHPT and the technical contributions of Joan Perry and Sydney Greer are greatly appreciated.

REFERENCES

1. C. K. Adams and R. J. Holmgreen. *Asphalt Properties and Pavement Performance*. Report FHWA-TX-86/287-4. Texas Transportation Institute, College Station, 1986.
2. C. J. Glover, R. R. Davison, S. M. Ghoreishi, H. B. Jemison, and J. A. Bullin. Evaluation of Oven Simulation of Hot-Mix Aging by an FT-IR Pellet Procedure and Other Methods. In *Transportation Research Record 1228*, TRB, National Research Council, Washington, D.C., 1989, pp. 177–182.
3. P. W. Jennings, J. A. Pribanic, W. Campbell, K. R. Dawson, and R. B. Taylor. *High Pressure Liquid Chromatography as a Method of Measuring Asphalt Composition*. Report FHWA-MT–7930. State of Montana Department of Highways, 1980.
4. J. C. Petersen. Quantitative Functional Group Analysis of Asphalts Using Differential Infrared Spectrometry and Selective Chemical Reactions—Theory and Application. In *Transportation Reseach Record 1096*, TRB, National Research Council, Washington, D.C., 1986.
5. W. H. Gotolski, R. W. Smith, and J. M. Roberts. Paving Asphalt Properties. In *Highway Research Record 350*, HRB, National Research Council, Washington, D.C., 1971.
6. J. M. Roberts and W. H. Gotolski. Pavement Asphalt Properties and Pavement Durability. In *Transportation Research Record 544*, TRB, National Research Council, Washington, D.C., 1975.
7. K. H. Altgelt and O. L. Harle. The Effect of Asphaltenes on Asphalt Viscosity. *Industrial and Engineering Chemistry Product Research and Development*, Vol. 14, American Chemical Society, Washington, D.C., 1975.
8. J. March. *Advanced Organic Chemistry*. 2nd ed., McGraw-Hill, New York, 1977.

Publication of this paper sponsored by Committee on Characteristics of Bituminous Materials.

Evaluating Recycled Asphalt Binders by the Thin-Film Oven Test

A. Samy Noureldin and Leonard E. Wood

Evaluation of long-term performance and identification of nonhomogeneity, incompatibility, and hardening rate of hot-mix–recycled bituminous pavement are described. The effects of artificial laboratory aging on a virgin binder (AC–20) and three other—extracted and recovered—rejuvenated binders were determined. Laboratory aging was achieved by means of the thin-film oven test (TFOT). Analysis and evaluation of the test data revealed some important aspects of hot-mix recycling. The TFOT was identified as a potential added criterion in identifying recycling agents that tend to cause a high rate of hardening, nonhomogeneity, and noncompatibility problems in recycled binders meeting the standard specifications of a virgin binder. This identification can be obtained by visually inspecting the residues after the TFOT and classifying their consistency using penetration and viscosity tests.

During the last 15 years, recycling of asphalt pavement has become an increasingly attractive rehabilitation alternative. The decreasing supply of locally available quality aggregate in some areas, growing concern over waste disposal, geometric difficulties of successive pavement maintenances, and unstable cost of asphalt cement and fuel have made recycling an environmentally and economically attractive alternative.

Pavement recycling is a technique in which hardened, deteriorated old pavement can be processed and reused. The fundamental concept lies in softening the old binder fraction by the addition of softening agents so that the original properties of that old binder are restored (*1*).

Millions of tons of hot-mix–recycled pavements have been used in the present highway systems. Recycled-mixture designs have been prepared using the test methods and criteria historically used for conventional asphalt concrete pavements. Initial results indicate that these methods and criteria are generally acceptable. However, there is still a need for assurance that long-term aging, with a potentially higher rate of hardening, and the effects of weathering, homogeneity, and compatibility on the mechanical and structural properties of the pavement are not problems (*2*).

Data collected from previous recycling projects indicated that the rejuvenated binders in a recycled mix may have a higher rate of hardening and be more susceptible to temperature than the virgin asphalt cement used in a conventional mix (*3*). Problems caused by incompatibility were also reported when field-aged asphalts were blended with recycling agents (*4*). The type of rejuvenating agent used and the nature of the aged asphalt could have a role in these observations.

The effectiveness of a recycling agent is a function of its uniform dispersion throughout the pavement binder. This issue is important in the process of recycling, because changes in properties with time have been attributed to the fact that old binder and rejuvenating agents may not have been thoroughly mixed (*5*). Some research efforts have been conducted to establish the ability of mixing operations to produce a homogeneous mixture (*4–6*). The specifications for recycling agents proposed by the Pacific Coast User-Producer Conference (June 1980) appear to be the best currently available to select the proper type of recycling agent for a specific project. However, these specifications alone cannot adequately identify incompatibility problems. Additional tests and criteria need to be developed to identify incompatibility (*2,7,8*).

If blends of aged asphalt and recycling agents are evaluated to ensure that they meet current ASTM or AASHTO specifications for virgin asphalt cements, viscosity and penetration measurements on samples of these blends after a thin-film oven test (TFOT) can help identify potential incompatibility (*2,7,8*).

To establish the time-temperature effect that three types of recycling agents have on aged asphalt binder, the TFOT was used to identify the rate of hardening in a weathered asphalt after it was treated with the following agents: AC–2.5 (ASTM designation), AE–150 (Indiana designation), and Mobilsol-30 (a commercial type). Samples of virgin asphalt (AC–20) were used for comparison purposes. The various samples were subjected to the oven exposure for three specific periods, after which the residues were classified by means of penetration and viscosity tests.

EXPERIMENTAL DESIGN

The experimental part of this study was statistically designed in advance to investigate the effects of binder type and time of oven exposure.

1. Binder Type (*B*). This factor consisted of four levels, each representing a specific type of bituminous binder. The first type was AC–20 (typically used in Indiana for producing hot-mix bituminous pavement). The second, third, and fourth levels were the recycled asphalt pavement (RAP) restored to an AC–20 specification range using the recycling agents AC–2.5, AE–150, and Mobilsol-30, respectively.
2. Time of Oven Exposure (*T*). The four levels of this factor were the periods of time over which a specific type of binder was subjected to oven exposure in the TFOT (ASTM D1754).

A. S. Noureldin, Public Works Department, Cairo University, Cairo, Egypt. Current affiliation: Ministry of Communications, King Abdel Aziz Road, Riyadh 11178, Saudi Arabia. L. E. Wood, Department of Civil Engineering, Purdue University, West Lafeyette, Ind. 47907.

The time spans were chosen to be 0 (no oven exposure), 2, 5 (the standard time), and 10 hr.

These two factors were selected for evaluation of the performance of three specific rejuvenated binders. These binders were compared with a virgin binder (AC–20) under the same conditions of time and temperature. Rejuvenated binders with higher hardening rates and greater sensitivity to long-term weathering actions (simulated artificially by the TFOT) than a virgin binder are believed to create cracking and compatibility problems when used in the field. If so, a recycled pavement would experience a more rapid deterioration rate than a conventional virgin mix.

The following mathematical model was used to introduce the data:

$$PV = M + B_i + T_j + BT_{ij} + E_{ijk} \quad (1)$$

where

PV = penetration or viscosity response for any sample,
M = overall mean,
B_i = binder-type effect (fixed and qualitative),
T_j = time of oven exposure during the TFOT (fixed and quantitative),
BT_{ij} = interaction effect, and
E_{ijk} = experimental error (random).

Indices i, j, k run over the number of samples.

A completely randomized design with two factors each having four levels (i.e., 16 treatment combinations) was applied (*9*). Three replications were prepared for each treatment combination, so that statistical significance could be detected if it existed, making the total number of samples 48

SAMPLING PLAN AND MATERIALS

Salvaged Materials

A stockpile of representative salvaged bituminous pavement was obtained for laboratory evaluation. The material used was milled from US-52 (south of Indianapolis, Indiana) and randomly selected under the supervision of the Indiana Department of Highways. Samples were selected at random from the laboratory-created stockpile to obtain statistically representative bituminous materials.

Virgin Materials

Crushed limestone and local sand were selected to represent the coarse and fine aggregate material for virgin aggregate samples. An AC–20 from AMOCO Oil Company was chosen to produce conventional mixes. The selection was based on materials in the state of Indiana that are generally used to produce hot-mix bituminous pavements.

Three types of recycling agents were selected for use with the age-hardened salvaged bituminous binder. The agents were selected because they had been previously used in other recycling techniques and because their physical and chemical properties were known (*5,10*). The following recycling agents were used: an AC–2.5 obtained from AMOCO Oil Company; an AE–150; and Mobilsol-30, supplied by McConnaughay, Inc.

TEST RESULTS AND ANALYSIS

Salvaged Materials

Samples of RAP were randomly chosen, reduced in size, and characterized. Asphalt extraction and recovery were conducted using ASTM D2172-67, Method A, and the Abson method (ASTM D1856); respectively. The salvaged binder was characterized by means of penetration, softening point, and viscosity tests. Amount of asphalt present was determined, and the salvaged aggregate obtained from extraction was characterized by sieve analysis.

Tables 1 and 2 present the characteristics of the extracted hard asphalt and the gradation of salvaged aggregate, respectively. The values were an average of 10 samples. The Indiana specifications for No. 12 surface were also included in Table 2 for comparison purposes and for future determination of the feasibility of using salvaged aggregate in a high-quality, hot-surface mix. The amount of hardening that occurred in the old binder was not significant when compared to previous recycling projects. In addition, the sieve analysis of the salvaged aggregate indicated a gradation within the specification for No. 12 surface (Indiana Department of Transportation Specifications), except for a small margin at No. ⅜ sieve.

Recycling Agents (Rejuvenators)

Three types of recycling agents were used to restore the old binder to the AC–20 classification range. Selection of the agents was based on their previous use in recycling techniques other than hot-mix recycling. The AC–20 classification range was selected because AC–20 is widely used in producing high-quality, hot-mix paving mixtures in Indiana.

The three types used were AC–2.5 (ASTM designation), AE–150 (Indiana designation), and Mobilsol-30 (a commercial type). Table 3 presents the penetration and viscosity values of AC–20, AC–2.5, and AE–150 residue; Table 4 presents the characteristics of Mobilsol-30.

TABLE 1 CHARACTERISTICS OF EXTRACTED HARD ASPHALT

Test	Value*
Penetration, 77°F, 100 gm, 5 sec.	28
Viscosity, 140°F, Poises	20,888
Kinematic visc., 275°F, c. st	726
Softening Point, °F	137
Asphalt Content (Total wt.)	6%

*Average of 10 samples

TABLE 2 GRADATION OF SALVAGED AGGREGATE

Sieve size	3/8	#4	#8	#16	#30	#50	#100	#200
% Passing*	93	78	62	44	28	15	7.5	5
IND. spec. for #12 surface	96-100	70-80	36-66	19-50	10-38	5-26	2-17	0-8

*Average of 10 samples

TABLE 3 CHARACTERISTICS OF AC-20, AC-2.5, AND AE-150

Asphalt	Penetration	Viscosity, 140°F, Poise
AC-20	65	1890
AC-2.5	200	292
AE-150 Residue	200	270

TABLE 4 CHARACTERISTICS OF MOBILSOL-30

Percent Asphaltenes*	0
Percent Polar Compounds*	8
Percent Aromatics*	79
Percent Saturates*	13
Percent solids in Emulsified Form	66.7
Flash Point*	505
Kinematic Viscosity* at 140°F, c.st.	164

*Properties of Residue

Determination of the Amount of Rejuvenator

Asphalt Institute curves (*11*) were used to determine an initial value for the percentage of rejuvenator (AC-2.5 and AE-150) to be added to the old binder to restore the properties to an AC-20 range of classification. The curves suggest the rejuvenator percentage on the basis of its viscosity at 140°F, the old binder's viscosity at 140°F, and the required viscosity for the new rejuvenated binder at 140°F. The initial value for the percentage of Mobilsol-30 was chosen on the basis of previous recycling projects (*5,10*).

A series of extraction and recovery tests were conducted to justify these initial values. Table 5 presents the characteristics of salvaged asphalt and the three rejuvenated binders.

Preparation of Samples for TFOTs

RAP samples and the virgin aggregate were heated in an oven at 240°F for 30 min. The rejuvenators were heated in an oven at 180°F when they were used. RAP, virgin aggregate, and one of the rejuvenators were mechanically hot-mixed for 2 min. The amount and gradation of virgin aggregate were selected in such a way that the resulting binder content was 6 percent of the total weight of mix (the original binder content in the RAP) and the resulting aggregate gradation was within the Indiana specifications for No. 12 surface (typically used for producing hot-mix bituminous surface mix). The loose samples were stored in an oven for 15 hr at 140°F for curing and were directly extracted using Method A of ASTM D2172. Asphalt binders were then recovered separately using the Abson Method (ASTM D1856).

Actual field conditions were simulated by adding virgin aggregate to the RAP followed by the rejuvenator; however, Mobilsol-30 was added before the virgin aggregate. In other words, the salvaged binder was treated before the extraction and recovery process was conducted.

Results and Analysis of the TFOT

Penetration and viscosity values at 140°F were obtained on recovered, rejuvenated asphalt samples (0 hr on TFOT) and on residues after 2, 5 (the standard time), and 10 hr in the thin-film oven. Identical conditions were applied to the AC-

TABLE 5 CHARACTERISTICS OF SALVAGED ASPHALT AND REJUVENATED BINDERS

Binder	Penetration	Viscosity, 140°F*
Old Asphalt	28	20,888
40% Old Asphalt +60% AC-2.5	62	2112
45% Old Asphalt +55% AE-150 Residue	68	1994
85% Old Asphalt 15% Mobilsol-30 Residue	69	1974
AC-20 spec.	60+	1600-2400

*Average of 10 samples

Note: Mobilsol-30 characteristics are given in Table 4.

20, and its penetration and viscosity values at 140°F were obtained for comparison purposes.

Tables 6 and 7 present average penetration and viscosity values (at 140°F) of the three replications at each treatment combination (binder type and time of oven exposure). Significant differences were obtained when conducting a two-way analysis of variance (ANOVA) on the data presented in Tables 6 and 7. Increasing the time of oven exposure resulted in a significant drop in penetration and a significant increase in viscosity for all the samples (which was expected). However, these changes varied significantly, depending on the binder type. The RAP rejuvenated by the AE–150 experienced the highest hardening rate, followed by the virgin AC–20, the RAP rejuvenated by AC–2.5, and the RAP rejuvenated by the Mobilsol-30. In addition, after the TFOT on RAP samples rejuvenated by AE–150, an easily removed, brittle skin was formed on the top of the sample in the pan. This was true for all the samples of RAP modified by AE–150, even those exposed for only 2 hr in the oven.

In general, these data indicate that using AE–150 as a recycling agent for hot-mix–recycled bituminous pavements may result in incompatibility, nonhomogeneity, and a high rate of hardening problems. Test results for the AC–2.5 and the Mobilsol-30 encourage their use as recycling agents. The RAP rejuvenated by AC–2.5 or Mobilsol-30 had a hardening rate slightly slower than that of the virgin AC–20.

TABLE 6 PENETRATION VALUES OF BINDER AFTER DIFFERENT TIMES OF OVEN EXPOSURE

Binder Type	Time of Oven Exposure During TFOT			
	Zero	2 hours	5 hours	10 hours
AC-20	65	43	33	25
RAP+AC-2.5	64	48	38	29
RAP+AE-150	62	34	26	18
RAP+Msol-30	64	50	43	33

Note: Values included are average of 3 replications.

TABLE 7 VISCOSITY VALUES (AT 140°F) OF BINDERS AFTER DIFFERENT TIMES OF OVEN EXPOSURE

Binder Type	Time of Oven Exposure During TFOT			
	Zero	2 hours	5 hours	10 hours
AC-20	1890	3920	8780	25,870
RAP+AC-2.5	1980	3410	7890	15,080
RAP+AE-150	2150	9770	18,740	62,340
RAP+Mobilsol-30	2220	4680	7490	14,880

Note: Values included are averages of 3 replications.

Relationship Between the Time of Oven Exposure and Consistency of Binder

Regression analyses were conducted to establish statistical relationships between the time of oven exposure during the TFOT (0, 2.5, and 10 hr) and the consistency of binder (AC–20, RAP + AC–2.5, RAP + AE–150, or RAP + Mobilsol-30) represented by the penetration and the viscosity at 140°F. Tables 8 and 9 present the regression equations for penetration and viscosity, respectively. The symbol x was used to represent the time spent in the TFOT. The regression parameter multiplied by x can be used as an indicator for the tendency of the rejuvenated binder to have a high hardening rate and hence create short-term aging and possible incompatibility and nonhomogeneity problems.

Figures 1 and 2 show graphical representations of the statistical relationships for penetration and viscosity at 140°F versus the time of oven exposure.

SUMMARY OF RESULTS

The salvaged material was obtained from US-52, Indiana. The recycling agents applied to the salvaged material were AC–2.5, AE–150, and a commercial type (Mobilsol-30). The virgin AC–20 used for comparison purposes was obtained from

TABLE 8 REGRESSION EQUATIONS FOR THE RELATIONSHIP BETWEEN PENETRATION OF BINDER AND TIME OF OVEN EXPOSURE DURING TFOT

Binder Type	Equation	R^2
AC-20	$\text{Penetration} = \frac{100}{\sqrt{2.45+1.35x}}$	0.999
RAP+AC-2.5	$\text{Penetration} = \frac{100}{\sqrt{2.45+0.95x}}$	0.999
RAP+AE-150	$\text{Penetration} = \frac{100}{\sqrt{2.45+2.45x}}$	0.993
RAP+Mobilsol-30	$\text{Penetration} = \frac{100}{\sqrt{2.45+0.75x}}$	0.993

NOTES: "x" is the time of oven exposure during the TFOT. R^2 is the coefficient of determination.

TABLE 9 REGRESSION EQUATIONS FOR THE RELATIONSHIP BETWEEN VISCOSITY (AT 140°F) AND TIME OF OVEN EXPOSURE DURING TFOT

Binder Type	Equation	R^2
AC-20	$\text{Viscosity} = (45.4+10x)^2$	0.999
RAP+AC-2.5	$\text{Viscosity} = (45.4+9x)^2$	0.982
RAP+AE-150	$\text{Viscosity} = (45.4+22x)$	0.975
RAP+Mobilsol-30	$\text{Viscosity} = (45.4+8x)^2$	0.977

NOTES: "x" is the time of oven exposure during the TFOT. R^2 is the coefficient of determination.

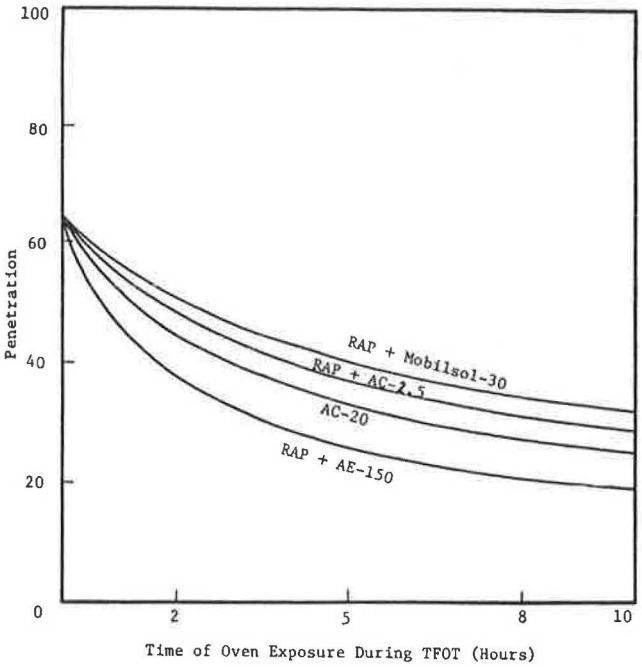

FIGURE 1 Relationship between penetration and time of oven exposure during the TFOT.

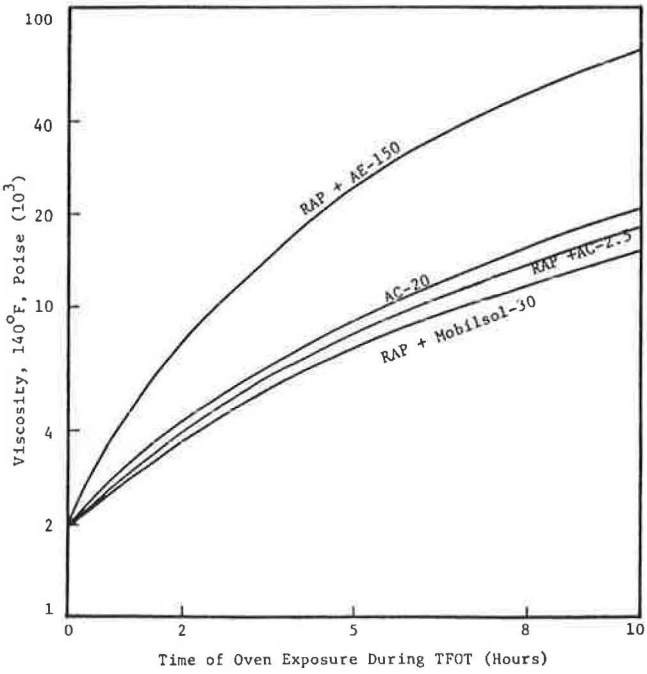

FIGURE 2 Relationship between viscosity and time of oven exposure during the TFOT.

AMOCO Oil Company. A completely randomized design was used for the design of the experiment and the analysis of data resulting from the TFOT (ASTM D1754). The analysis and evaluation of the test data revealed a number of important aspects of hot-mix–recycled bituminous pavement. However, the significant results obtained may be limited to the materials used and test conditions applied.

The main conclusions can be summarized as follows:

1. Rejuvenated binders having the same consistency as a virgin binder will probably have different long-term performances and hardening rates.
2. Having a rejuvenated binder meet the standard specifications for a virgin binder is not enough to ensure the success of a hot-mix–recycled pavement. Additional criteria and test conditions have to be developed.
3. The TFOT is suggested as a good tool to identify the rate of hardening, possible nonhomogeneity, and noncompatibility that may be expected from a rejuvenated binder in the hot-mix–recycled pavement.
4. Salvaged asphalt in the RAP may experience a high rate of hardening and create nonhomogeneity and noncompatibility problems in the hot-mix–recycled asphalt pavement if AE–150 is used as a recycling agent. However, AC–2.5 and Mobilsol-30 may not create these effects as recycling agents, and their use indicated a slightly slower hardening rate than that of the virgin AC–20.
5. When AE–150 was used for treating weathered asphalt, a brittle skin tended to form on all the TFOT residues; the skin was easily separated from the rest of the sample.
6. Careful selection and testing of a recycling agent (rejuvenator) is essential to ensure good-quality hot-mix–recycled asphalt pavement with an acceptable performance.

ACKNOWLEDGMENTS

The research described in this paper was carried out at Purdue University. The authors are grateful for the support of the Indiana Department of Highways and the U.S. Department of Transportation, FHWA.

REFERENCES

1. *Softening or Rejuvenating Agents for Recycled Bituminous Binders*. Interim Report, Texas Transportation Institute, College Station, 1980.
2. *Pavement Recycling*. Report FHWA-TS-32-224. FHWA, U.S. Department of Transportation, 1982.
3. D. I. Anderson, D. E. Peterson, M. L. Wiley, and W. B. Betenson. *Evaluation of Selected Softening Agents Used in Flexible Pavement Recycling*. Report FHWA-TS-79-204. FHWA, U.S. Department of Transportation, 1978.
4. R. L. Terrel, T. C. Lee, and J. P. Mahoney. *Mixing Efficiency of Recycled Asphalt Paving Mixtures*. Report FHWA-RD-81-174. FHWA, U.S. Department of Transportation, 1981.
5. *Effect of Added Softening Agents Upon the Behavior of Cold-Recycled Asphalt Mixtures*. Report FHWA-IN-JHRP-80-13. Indiana Department of Highways, West Lafeyette, 1980.
6. R. L. Dunning and R. L. Mendenhall. *Design of Recycled Asphalt Pavements and Selection of Modifiers*. STP 662, ASTM, Philadelphia, Pa., Nov. 1978.
7. Mang Tia. *Characterization of Cold-Recycled Asphalt Mixtures*. Report FHWA-IN-JHRP-82-5. Indiana Department of Highways, West Lafeyette, 1982.
8. T. W. Kennedy, F. L. Roberts, and J. N. Anagnos. *Mixture Design Procedure for Recycled Asphalt Pavements*. Report FHWA-TX-82-10-252-1. Texas Department of Highways and Public Transportation, Austin, 1982.

9. V. L. Anderson and R. A. McLean. *Design of Experiments: A Realistic Approach*. Marcel Dekker, New York, 1974.
10. N. P. Khosla. *Effect of Emulsified Modifiers on the Characteristics of Recycled Mixtures*. Association of Asphalt Paving Technologists, St. Paul, Minn., 1982.
11. *Asphalt Hot-Mix Recycling*. Report MS-20. The Asphalt Institute, Lexington, Ky., 1981.

Publication of this paper sponsored by Committee on Characteristics of Bituminous Materials.

Effects of Asphalt Properties on Indirect Tensile Strength

NORMAN W. GARRICK AND RAMESH R. BISKUR

The indirect tensile test on asphalt concrete mixes is a frequently used procedure for assessing likely pavement performance. Currently, the indirect tensile test is most commonly used for providing information on moisture susceptibility. However, the indirect tensile test may also be used to determine engineering properties needed for elastic and viscoelastic analyses and for evaluating thermal cracking, fatigue cracking, and potential problems with tenderness. Given the importance of this test, there appears to be a lack of information on the factors that determine indirect tensile strength (IDTS) of asphalt mixes. Consequently, the effects of asphalt composition and physical properties on IDTS values were obtained. Mixes were made with 15 different types of asphalt and with 2 different types of aggregate (traprock and gravel). Asphalt composition was characterized by gel permeation chromatographic analysis. The penetration of the thin-film oven test residue and IDTS values were strongly correlated. The IDTS values increase as penetration decreases. Asphalt composition also plays a significant role in determining the IDTS values of traprock mixes. Asphalt composition seems to account for differences of up to 55 percent in IDTS values of traprock mixes. However, the effect of asphalt composition on gravel mixes appears to be much less pronounced.

The indirect tensile test on asphalt concrete mixes is commonly used to assess moisture susceptibility. However, the indirect tensile test may also be used to determine engineering properties needed for elastic and viscoelastic analyses, and for evaluating thermal cracking and fatigue cracking (*1*). Button and his associates (*2*) have used this test as part of a system of evaluating mixes for problems with tenderness.

Little information exists about the factors that determine indirect tensile strength (IDTS) of a mix. Some reports (*3–5*) have examined how IDTS values vary with mix properties such as air void and asphalt content. But few reports concern the relationship between asphalt properties and IDTS values (*6*). The possible effects of asphalt composition have not been examined at all.

Some of these factors, mainly the effects of asphalt properties on IDTS values, are examined here. The asphalt properties considered are consistency and composition. Mixes were made with 15 different asphalts from various sources nationwide. Asphalt composition was characterized by gel permeation chromatographic (GPC) analysis.

Fifteen asphalts from six suppliers were used for this project. These asphalts are characterized in Table 1. Details of the test programs for the asphalts and the asphalt mixes are discussed in the following sections.

Department of Civil Engineering, University of Connecticut, Storrs, Conn. 06269–3037.

ASPHALT CEMENT TEST PROGRAM

The program of physical tests included viscosity (140°F) and penetration (77°F) ratings for all 15 asphalts and for residues of the asphalts after thin-film oven aging. The compositional test consisted of GPC analyses.

The GPC system included three ultrastyragel columns connected as specified in the order of 1,000, 500, and 500 Angstrom pore size. Tetrahydrofuran (THF) was used as both the solvent and the mobile phase in the system. Fifty microliters of a 0.5 percent asphalt solution was injected and allowed to flow at a rate of 1 mL/min through the columns. The detector used was a multiwavelength ultraviolet detector that was set at a wavelength of 290 nm.

GPC parameters were obtained from the GPC profiles using a modified form of a procedure that was developed at Purdue University (*7*). The procedure used in this project consisted of dividing the GPC profile into 12 equal-time segments, as opposed to the 8 unequal-time segments originally used (see Figure 1). The resulting GPC parameters, designated $X1$ to $X12$, are the percentages of total area under the curve in each segment. Molecular size can be assumed to decrease from Segment 1 to Segment 12. The GPC parameters represent the proportion of asphalt molecules of a given size. This interpretation should be applied with caution, however, because many factors affect the apparent size of an asphalt molecule (*7*).

ASPHALT CONCRETE MIX TEST PROGRAM

Eight different types of asphalt concrete (AC) mixes were made for each of the 15 asphalts. Half of the mixes were made with traprock and the other half with a river gravel. Mixes were made with two different asphalt contents (4.8 and 5.5 percent) and were compacted to two different air void contents (6 and 8 percent), resulting in a total of four types of mixes for each aggregate. Two replicates of each type of mix were tested.

The required degree of compaction was obtained by using a gyratory compactor in a constant high mode. The gradation of the mixes was the middle gradation of the Connecticut Class II mix, as follows:

Sieve Size	*Percent Passing*
½ in.	100
⅜ in.	80
#4	67
#8	52
#50	17
#200	5

Table 2 presents data on the specific gravity and absorption rate of the aggregates.

TABLE 1 ASPHALTS USED IN PROJECT

Asphalt No.	Grade	Supplier	State
NE5	AC-5	New Bituminous	Rhode Island
NE10	AC-10	New Bituminous	Rhode Island
NE20	AC-20	New Bituminous	Rhode Island
D5	AC-5	Diamond Shamrock	Texas
D10	AC-10	Diamond Shamrock	Texas
D20	AC-20	Diamond Shamrock	Texas
A5	AC-5	Ashland	Kentucky
A10	AC-10	Ashland	Kentucky
A20	AC-20	Ashland	Kentucky
E5	AC-5	Edgington	California
E20	AC-20	Edgington	California
CAG5	AC-5	Guyott	Connecticut
CAG20	AC-20	Guyott	Connecticut
CP10	AC-10	Chevron	New Jersey
CP20	AC-20	Chevron	Connecticut

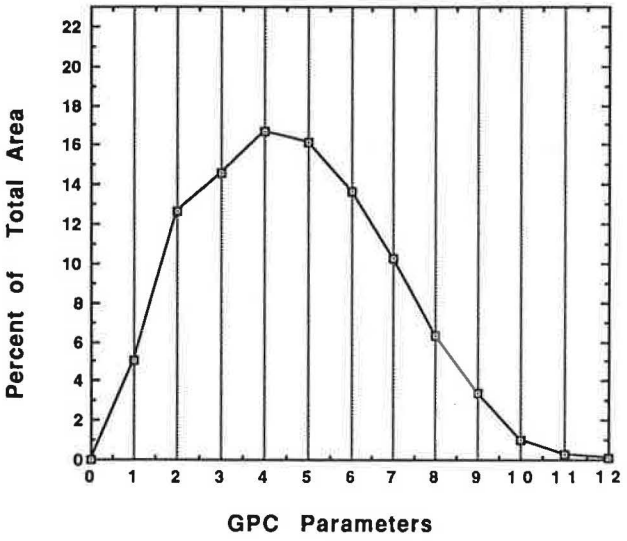

FIGURE 1 Typical GPC profile.

The IDTS value of each mix was determined at room temperature (about 75°F) using the Marshall test apparatus. The test frame for this procedure consisted of two curved loading strips, each 0.5 in. wide. The load was applied at a rate of 2 in./min, and the load at failure was recorded.

RESULTS

The results of the physical tests and the GPC analyses for the 15 asphalts are presented in Tables 3 and 4, respectively. A sample of the GPC profiles is also shown in Figure 1. Tables 5 and 6 present the indirect tensile test results for the AC mixes.

Regression analysis was used to evaluate the relationship between IDTS and the asphalt properties. The results of these analyses are used to discuss the effects of asphalt consistency and composition on IDTS in the following sections. The effects of aggregate type and of asphalt and void content are also discussed.

TABLE 2 SPECIFIC GRAVITY AND ABSORPTION OF AGGREGATES

Aggregate Type	Specific Gravity		Absorption (%)
	Bulk	Apparent	
Coarse fraction			
Trap	2.89	2.97	0.96
Gravel	2.63	2.73	1.39
Fine fraction			
Trap	2.84	3.03	2.27
Gravel	2.60	2.69	1.26

Effect of Consistency

A summary of the results of regression analyses relating IDTS values to the various measures of consistency is presented in Table 7. These results show that the penetration (at 77°F) and viscosity (at 140°F) of the original asphalt correlated with IDTS. The penetration (at 77°F) and viscosity (at 140°F) of the thin-film oven test (TFOT) residue also correlated significantly. However, the best correlation (highest r^2 value) was obtained using penetration (77°F) of the TFOT residue for all eight mix types.

From a theoretical point of view, these results are not unexpected. Because of the similarity in test temperatures, penetration at 77°F would be expected to give better correlations with tensile strength than would viscosity at 140°F. In addition, the consistency of the TFOT residue is probably closer to that of the asphalt in the mix than is the consistency of the original asphalt.

These results, though not surprising, do suggest that the relationship between asphalt and mix properties must be fully understood in terms of the characteristics of the asphalt in the mix rather than those of the original asphalt. Unfortunately, no tests were run on asphalts extracted from the mixes.

More detailed results of the regression analyses for penetration of the TFOT residue and IDTS are presented in Table 8 for the eight types of mixes. The relationship between these two variables is also shown in Figures 2–9 for each of the mixes. In all cases, the regression functions show that IDTS increases as penetration decreases. However, the slope of this relationship is significantly affected by aggregate type. The slope varied from 0.74 to 0.82 for traprock, and from 1.00 to

TABLE 3 PHYSICAL PROPERTIES OF TEST ASPHALTS

Asphalt No.	Original Asphalt		TFOT Residue	
	Penetration 0.1 dm, 77°F	Viscosity p, 140°F	Penetration 0.1dm, 77°F	Viscosity p,140°F
NE5	187	586	109	1344
NE10	110	1035	79	2155
NE20	68	1945	58	3957
D5	203	424	133	753
D10	122	896	78	1551
D20	70	2237	57	3859
A5	114	538	97	1033
A10	96	1096	58	1816
A20	74	2023	54	3837
E5	140	547	88	1107
E20	55	1711	38	3572
CAG5	177	481	126	1224
CAG20	77	2149	54	4452
CP10	117	1089	78	2947
CP20	91	1926	55	5449

TABLE 4 RESULTS OF GPC ANALYSES

Asphalt No.	X1	X2	X3	X4	X5	X6	X7	X8	X9	X10	X11	X12
N5	5.02	12.65	14.56	16.67	16.17	13.63	10.25	6.29	3.40	1.05	0.26	0.05
TN5	5.38	13.80	15.14	16.54	15.91	13.30	9.89	5.89	3.08	0.87	0.17	0.03
N10	4.18	12.62	15.26	17.68	17.15	13.94	9.70	5.53	2.82	0.86	0.19	0.03
TN10	10.92	15.97	14.95	15.61	14.84	11.92	8.20	4.65	2.20	0.63	0.11	0.01
N20	3.95	12.50	15.44	18.42	17.93	14.04	9.20	5.03	2.45	0.80	0.20	0.04
TN20	8.59	16.01	15.46	16.43	15.89	12.42	8.03	4.33	2.01	0.69	0.13	0.02
D5	5.11	14.87	19.57	21.07	17.84	11.35	5.96	2.58	1.03	0.45	0.14	0.03
TD5	5.98	16.42	20.01	20.46	17.01	10.71	5.54	2.36	0.94	0.41	0.12	0.02
D10	5.02	15.10	19.67	20.93	17.63	11.29	6.01	2.65	1.09	0.43	0.14	0.03
TD10	6.36	16.65	19.92	20.12	16.69	10.62	5.60	2.44	1.00	0.44	0.14	0.03
D20	5.44	15.38	19.63	20.63	17.35	11.19	5.98	2.66	1.11	0.45	0.15	0.03
TD20	7.01	17.38	20.25	20.19	16.24	10.00	5.30	2.22	0.89	0.38	0.12	0.03
A5	1.11	10.40	14.95	21.47	22.04	15.12	8.42	4.00	1.74	0.54	0.13	0.03
TA5	3.11	11.74	15.48	20.61	20.94	14.35	7.87	3.66	1.56	0.53	0.13	0.02
A10	2.64	10.30	14.10	19.15	20.40	15.60	9.60	4.95	2.30	0.74	0.16	0.03
TA10	3.34	11.54	14.63	18.79	19.70	14.92	9.14	4.71	2.14	0.87	0.19	0.03
A20	4.55	12.38	14.99	18.21	18.44	14.21	9.10	4.90	2.29	0.74	0.16	0.03
TA20	5.40	13.27	15.42	18.11	18.10	13.78	8.70	4.55	2.03	0.57	0.07	0.00
E5	1.00	5.84	11.90	16.20	20.41	18.64	13.80	6.71	2.66	0.69	0.13	0.02
TE5	2.28	9.25	13.74	17.57	18.81	17.01	12.43	5.85	2.25	0.68	0.12	0.02
E20	1.27	6.16	12.41	16.83	20.98	18.73	12.88	5.80	2.20	0.59	0.12	0.02
TE20	2.54	8.86	13.71	16.08	19.50	17.35	11.90	5.31	1.95	0.67	0.13	0.02
CAG5	4.22	12.32	15.11	17.87	17.44	14.06	9.64	5.48	2.77	0.86	0.19	0.03
TCAG5	5.35	13.49	15.15	17.28	16.77	13.51	9.22	5.23	2.60	1.12	0.23	0.04
CAG20	4.18	12.11	14.54	17.00	16.58	14.02	10.44	6.36	3.35	1.04	0.25	0.05
TCAG20	5.47	13.86	15.11	16.60	15.90	13.31	9.77	5.85	3.01	0.89	0.19	0.03
CP10	5.36	13.13	15.72	17.20	15.91	13.03	9.65	5.75	3.01	0.96	0.23	0.05
TCP10	9.26	15.22	15.48	15.88	14.63	12.02	8.84	5.15	2.58	0.80	0.15	0.02
CP20	4.73	12.93	15.64	17.21	16.21	13.52	9.84	5.70	2.94	0.94	0.27	0.05
TCP20	6.95	14.62	15.66	16.64	15.44	12.64	9.14	5.26	2.64	0.80	0.18	0.03

TABLE 5 IDTS OF TRAPROCK MIXES

Asphalt Number	Indirect Tensile Strength(psi) 8%Voids 4.8%AC	8%Voids 5.5%AC	6%Voids 4.8%AC	6%Voids 5.5%AC
NE5	38	37	37	39
NE10	57	62	59	58
NE20	62	62	70	69
D5	39	36	45	42
D10	55	58	66	57
D20	86	86	85	80
A5	39	33	41	33
A10	74	54	67	59
A20	77	77	87	85
E5	57	52	49	48
E20	106	99	111	108
CAG5	48	46	50	43
CAG20	58	65	67	66
CP10	46	48	50	43
CP20	75	72	78	78
Average	61	59	64	61

TABLE 6 IDTS OF GRAVEL MIXES

Asphalt Number	Indirect Tensile Strength (psi) 8%Voids 4.8%AC	8%Voids 5.5%AC	6%Voids 4.8%AC	6%Voids 5.5%AC
NE5	65	52	62	63
NE10	91	71	78	71
NE20	101	93	108	103
D5	45	39	40	38
D10	80	77	75	83
D20	136	132	142	129
A5	49	47	48	47
A10	74	76	78	83
A20	101	96	72	108
E5	57	48	61	60
E20	179	155	138	133
CAG5	45	42	42	42
CAG20	97	112	120	121
CP10	58	50	67	67
CP20	108	89	100	103
Average	86	79	82	83

TABLE 7 RESULTS OF REGRESSION ANALYSES: IDTS VERSUS ASPHALT CONSISTENCY

Mix Type	R-squared for Independent Variable: Penetration 77°F, original	Viscosity 140°F, original	Penetration 77°F, TFOT	Viscosity 140°F, TFOT
Trap 8%voids, 4.8%AC	0.69	0.60	0.78	0.50
Trap 8%voids, 5.5%AC	0.71	0.73	0.77	0.65
Trap 6%voids, 4.8%AC	0.75	0.71	0.81	0.62
Trap 6%voids, 5.5%AC	0.72	0.75	0.81	0.66
Gravel 8%voids, 4.8%AC	0.76	0.75	0.82	0.66
Gravel 8%voids, 5.5%AC	0.84	0.82	0.86	0.67
Gravel 6%voids, 4.8%AC	0.76	0.80	0.80	0.71
Gravel 6%voids, 5.5%AC	0.81	0.89	0.89	0.79

1.11 for the gravel mixes. To a smaller extent, the slope was also affected by asphalt content. Larger slope values were obtained for those mixes with the higher asphalt content (5.5 percent).

The difference in slopes means that a change in penetration will cause a much larger change in the IDTS of a gravel mix than that of a traprock mix. Because penetration of the asphalt in the mix will change with temperature, another interpretation of this result may be that mixes with different aggregates have different temperature susceptibility with respect to IDTS. If this is the case, then the temperature susceptibility of the gravel mix is greater than that of traprock mix. This hypothesis needs to be verified by tests on the mixes at different temperatures.

TABLE 8 RESULTS OF REGRESSION ANALYSES: IDTS VERSUS PENETRATION OF TFOT RESIDUE (RPEN77)

Mix Type	Regression Model	r-squared
Trap 8%voids, 4.8%AC	log(IDTS) = -0.74 * log(RPEN77) + 7.23	0.78
Trap 8%voids, 5.5%AC	log(IDTS) = -0.78 * log(RPEN77) + 7.38	0.77
Trap 6%voids, 4.8%AC	log(IDTS) = -0.76 * log(RPEN77) + 7.39	0.81
Trap 6%voids, 5.5%AC	log(IDTS) = -0.82 * log(RPEN77) + 7.57	0.81
Gravel 8%voids, 4.8%AC	log(IDTS) = -1.02 * log(RPEN77) + 8.76	0.82
Gravel 8%voids, 5.5%AC	log(IDTS) = -1.11 * log(RPEN77) + 9.02	0.86
Gravel 6%voids, 4.8%AC	log(IDTS) = -1.00 * log(RPEN77) + 8.61	0.80
Gravel 6%voids, 5.5%AC	log(IDTS) = -1.07 * log(RPEN77) + 8.92	0.89

Note: log(IDTS) is the Natural Log of Tensile Strength
log(RPEN77) is the Natural Log of TFOT Penetration

TABLE 9 RESULTS OF REGRESSION ANALYSES: IDTS VERSUS PENETRATION OF TFOT RESIDUE (RPEN77) AND GPC PARAMETERS ($X5$ AND $X12$)

Mix Type	Regression Model	r-squared
Trap 8%voids, 4.8%AC	log(IDTS) = - 0.046 * X5 - 14.37 * X12 - 0.75 * log(RPEN77) + 8.64	0.90
Trap 8%voids, 5.5%AC	log(IDTS) = - 0.096 * X5 - 17.42 * X12 - 0.83 * log(RPEN77) + 9.92	0.93
Trap 6%voids, 4.8%AC	log(IDTS) = - 0.075 * X5 - 16.55 * X12 - 0.79 * log(RPEN77) + 9.47	0.95
Trap 6%voids, 5.5%AC	log(IDTS) = - 0.089 * X5 - 16.43 * X12 - 0.86 * log(RPEN77) + 9.93	0.95
Gravel 8%voids, 4.8%AC	log(IDTS) = - 0.030 * X5 - 1.05 * log(RPEN77) + 9.41	0.84
Gravel 8%voids, 5.5%AC	log(IDTS) = - 0.024 * X5 - 1.12 * log(RPEN77) + 9.52	0.87
Gravel 6%voids, 4.8%AC	log(IDTS) = - 0.046 * X5 - 1.03 * log(RPEN77) + 9.58	0.85
Gravel 6%voids, 5.5%AC	log(IDTS) = - 0.047 * X5 - 1.11 * log(RPEN77) + 9.93	0.94

Example: Calculation of Composition Index for mix, Trap:6%voids:4.8%AC

*COMPOSITION INDEX = -0.075 * X5 -16.55 * X12*
(GPC parameters, X5 and X12, are listed in Table 4 for each asphalt)

Effect of Composition

Stepwise regression analyses were conducted to determine the best regression model that incorporated both consistency data and compositional data. The best results for the traprock mixes were obtained with a model containing (a) TFOT penetration, (b) GPC parameter $X5$, and (c) GPC parameter $X12$. The best model for the gravel mixes was the one with (a) TFOT penetration and (b) GPC parameter $X5$.

The resulting regression models (presented in Table 6) show that, in the case of the traprock mixes, the inclusion of asphalt composition (GPC parameters) significantly improved the correlation. However, the inclusion of these parameters did little to improve the prediction for the gravel mixes.

The plots in Figures 2–9, for IDT test versus penetration (at 77°F) of the TFOT residue, show some amount of scatter about the regression function. In the case of the traprock mixes, much of this scatter or deviation from the prediction line is related to differences in composition.

TABLE 10 COMPOSITION INDEXES FOR TRAPROCK MIXES

Asphalt Number	Composition Index			
	8%Voids		6%Voids	
	4.8%AC	5.5%AC	4.8%AC	5.5%AC
NE5	-1.46	-2.42	-2.04	-2.26
NE10	-1.22	-2.17	-1.78	-2.02
NE20	-1.40	-2.42	-2.01	-2.25
D5	-1.25	-2.24	-1.83	-2.08
D10	-1.24	-2.22	-1.82	-2.06
D20	-1.23	-2.19	-1.80	-2.04
A5	-1.45	-2.64	-2.15	-2.45
A10	-1.37	-2.48	-2.03	-2.31
A20	-1.28	-2.29	-1.88	-2.13
E5	-1.23	-2.31	-1.86	-2.15
E20	-1.25	-2.36	-1.90	-2.20
CAG5	-1.23	-2.20	-1.80	-2.05
CAG20	-1.48	-2.46	-2.07	-2.30
CP10	-1.45	-2.40	-2.02	-2.24
CP20	-1.46	-2.43	-2.04	-2.26
Range	-1.48 to -1.22	-2.64 to -2.17	-2.15 to -1.78	-2.45 to -2.02

TABLE 11 COMPOSITION INDEXES FOR GRAVEL MIXES

Asphalt Number	Composition Index			
	8%Voids		6%Voids	
	4.8%AC	5.5%AC	4.8%AC	5.5%AC
NE5	-0.49	-0.39	-0.74	-0.76
NE10	-0.52	-0.41	-0.79	-0.81
NE20	-0.55	-0.43	-0.83	-0.84
D5	-0.54	-0.43	-0.82	-0.84
D10	-0.54	-0.42	-0.81	-0.83
D20	-0.53	-0.41	-0.80	-0.82
A5	-0.67	-0.53	-1.01	-1.04
A10	-0.62	-0.49	-0.94	-0.96
A20	-0.56	-0.44	-0.85	-0.87
E5	-0.62	-0.49	-0.94	-0.96
E20	-0.64	-0.50	-0.97	-0.99
CAG5	-0.53	-0.42	-0.80	-0.82
CAG20	-0.50	-0.40	-0.76	-0.78
CP10	-0.48	-0.38	-0.73	-0.75
CP20	-0.49	-0.39	-0.75	-0.76
Range	-0.67 to -0.48	-0.53 to -0.38	-1.01 to -0.73	-1.04 to -0.75

In order to better illustrate the effect of composition, a composition index was calculated by considering the contribution of the GPC parameters to the regression functions in Table 9. Values of composition indices for the mixes are presented in Tables 10 and 11. In addition, the amount of deviation from the regression line in Figures 2–9 was determined for each data point. The plot of deviation versus composition index indicates the contribution of composition in determining IDTS. These plots are shown in Figures 10–17.

In general, there is a significant degree of correlation between deviation and composition index for the traprock mixes but not for the gravel mixes. This correlation confirms that asphalt composition is important in determining the IDTS of the traprock mixes.

The maximum difference in composition index for a given type of mix can also be considered to be the maximum difference (on an exponential scale) in IDTS values that is attributable to composition. For the traprock, this range in IDTS values was about 0.45 for two of the four mixes. This result means that for two asphalts of the same penetration, differences in composition would cause a maximum difference in IDTS value of about 55 percent [i.e., the IDTS value of Asphalt A was 4.00 (55 psi), the IDTS value of Asphalt B was 4.45 (87 psi)]. For the gravel mixes, the range of composition index was less than 0.29 in all four cases.

For the traprock mixes, the deviation from the line increases in a positive direction as composition index increases (Figures 10–13). In other words, the penetration model underestimates the IDTS of mixes with asphalt of relatively high values of composition index (a combination of low values for the $X5$ and $X12$ parameters). Also, the composition indexes for asphalts from the same source were not necessarily of similar magnitude.

The previously discussed results for consistency suggested the need for determining the consistency of the actual asphalt in the mix to better understand the relationship between asphalt properties and the AC mix properties. Similarly, the compositional data should be that of the actual asphalt in the mix rather than that of the original asphalt. As stated before, however, no extraction was done.

Despite the shortcomings of using compositional data for the original asphalt, the results give some indication of the effect of composition on this mix property. The same techniques could be used in studying the actual asphalts from pavements, to determine how changes in asphalt properties affect pavement properties such as IDTS. However, the compositional data might not be required if the actual consistency of the asphalt in the specimen is used in the regression. This hypothesis can only be verified by further research.

Effect of Aggregate Type, Air Voids, and Asphalt Content

Aggregate type significantly affects the relationship between penetration and IDTS value, in that the slope of the relationship is larger for gravel than for a traprock mix. In effect, the gravel mix is more susceptible to temperature changes than an equivalent traprock mix with the same asphalt.

Another important difference is that the average tensile strength (see Table 5) was higher for gravel (82 psi) than for traprock (62 psi). These averages were approximately the same for each of the four combinations of air voids and asphalt content. However, the differences between gravel and traprock were not uniform for all asphalts. For example, the IDTS value of mixes with asphalt D5 was about the same (41 psi) using either gravel or traprock; however, for asphalt NE5, the strength of the gravel mix was significantly higher (61 versus 38 psi). Many other examples of this kind of variability can be observed in Table 5.

The mix properties examined in this project were air voids (6 and 8 percent) and asphalt content (4.8 and 5.5 percent). In general, tensile strength decreased as air voids and asphalt content increased (see Table 3). The differences were small, and the amount varied from asphalt to asphalt. The differences were also smaller than have been reported in some other studies (*3*,*4*).

Like aggregate type, asphalt content also affected the slope of the relationship between IDTS value and penetration. In all cases, high-asphalt-content mixes had higher temperature susceptibility for given tensile strength.

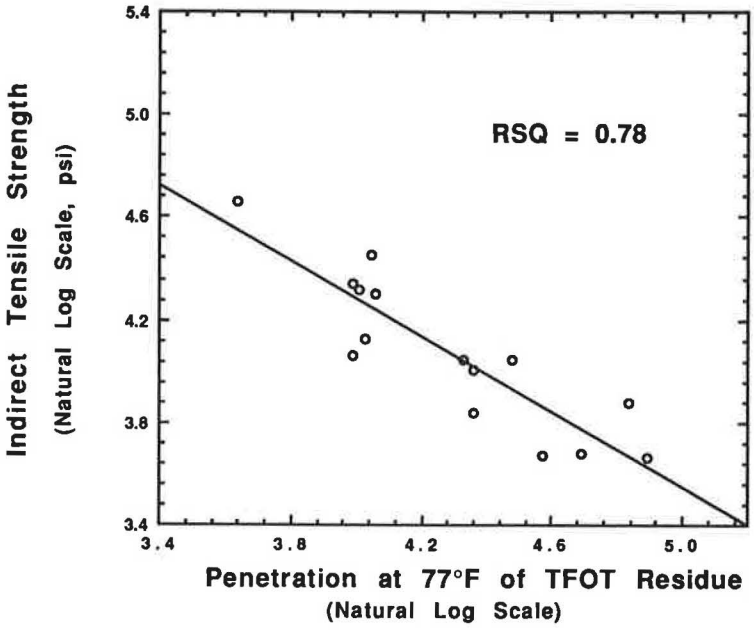

FIGURE 2 IDTS versus penetration (at 77°F) of the TFOT residue: traprock mix, 8 percent voids, 4.8 percent AC.

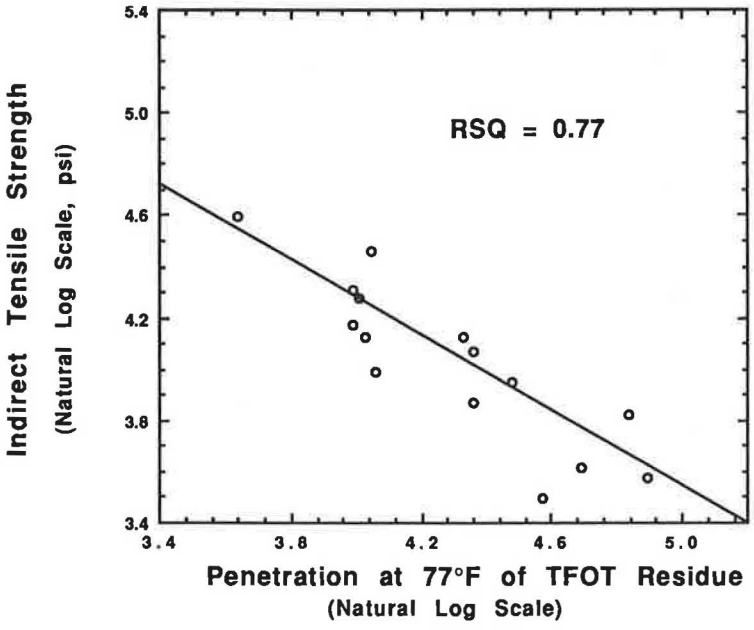

FIGURE 3 IDTS versus penetration (at 77°F) of the TFOT residue: traprock mix, 8 percent voids, 5.5 percent AC.

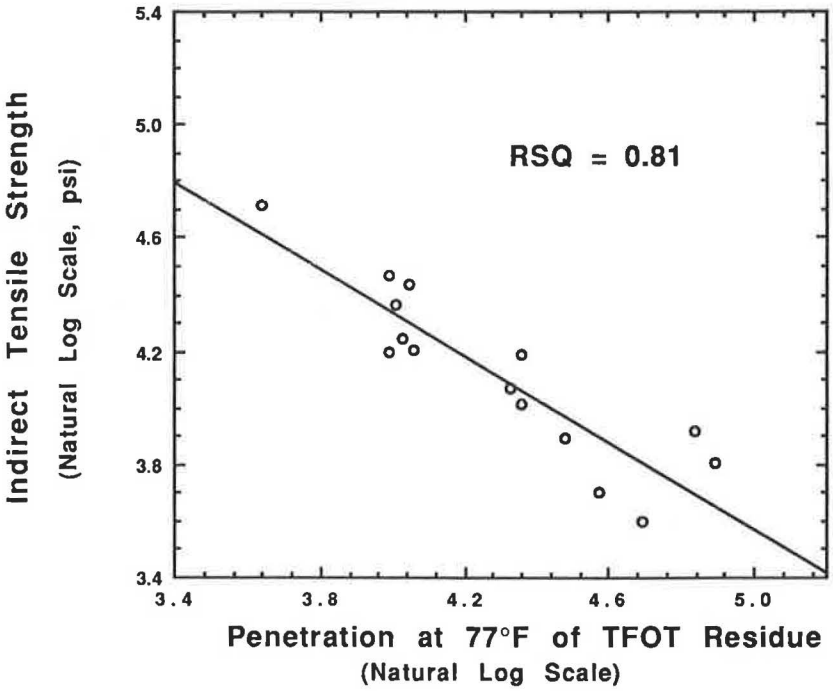

FIGURE 4 IDTS versus penetration (at 77°F) of the TFOT residue: traprock mix, 6 percent voids, 4.8 percent AC.

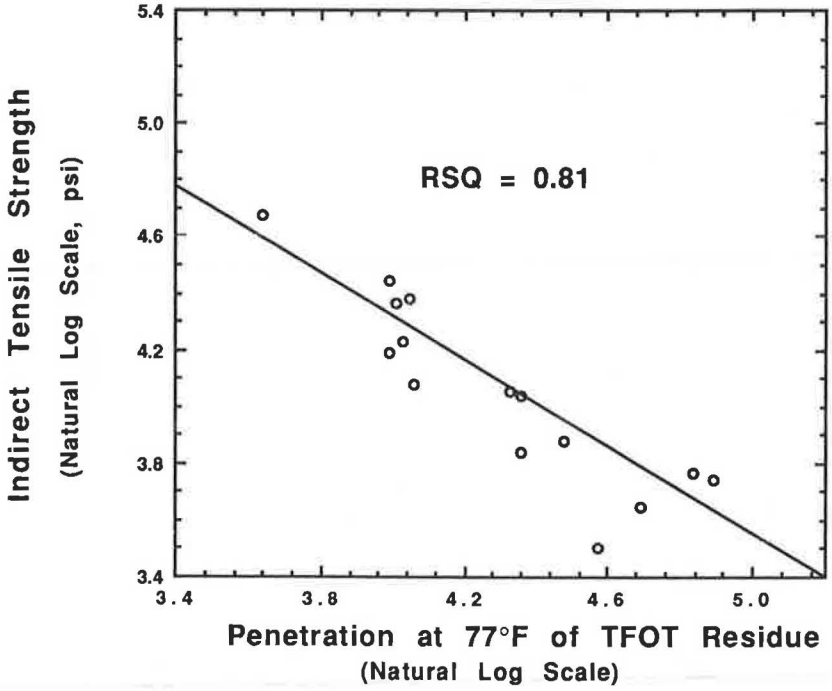

FIGURE 5 IDTS versus penetration (at 77°F) of the TFOT residue: traprock mix, 6 percent voids, 5.5 percent AC.

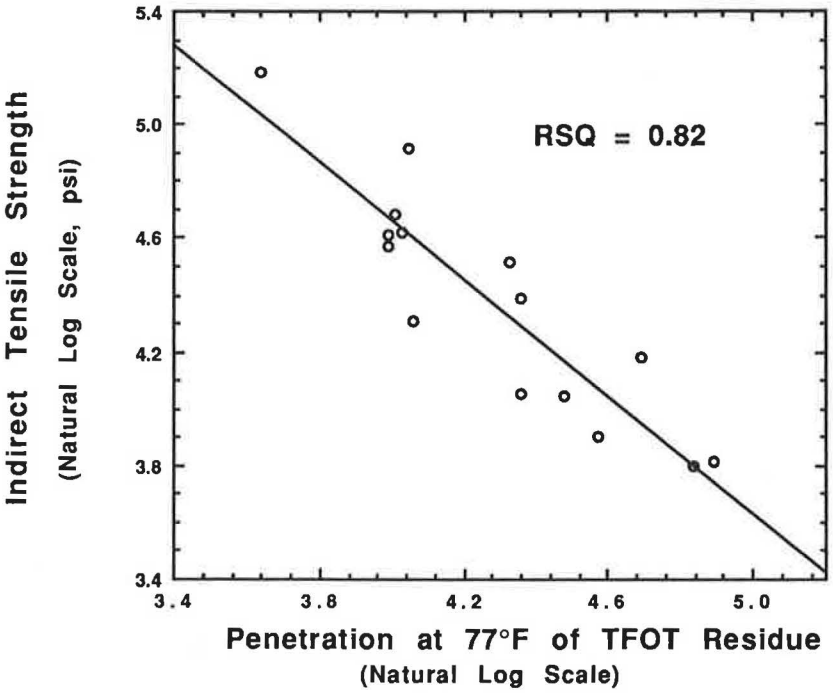

FIGURE 6 IDTS versus penetration (at 77°F) of the TFOT residue: gravel mix, 8 percent voids, 4.8 percent AC.

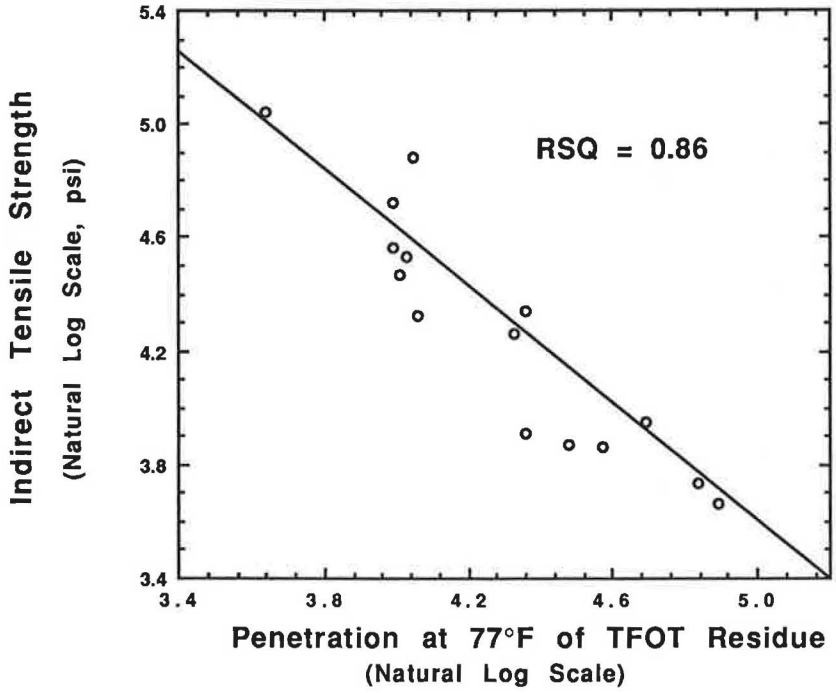

FIGURE 7 IDTS versus penetration (at 77°F) of the TFOT residue: gravel mix, 8 percent voids, 5.5 percent AC.

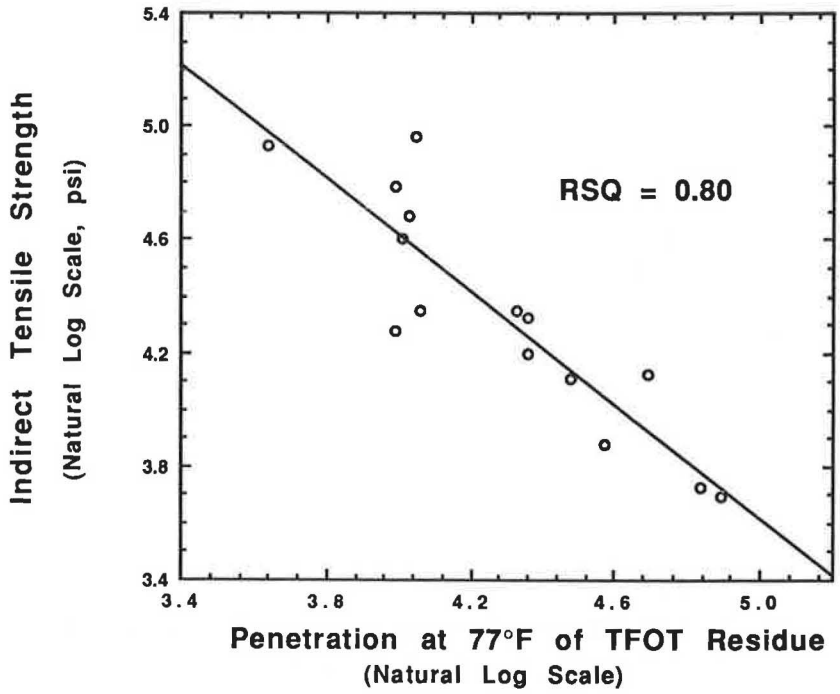

FIGURE 8 IDTS versus penetration (at 77°F) of the TFOT residue: gravel mix, 6 percent voids, 4.8 percent AC.

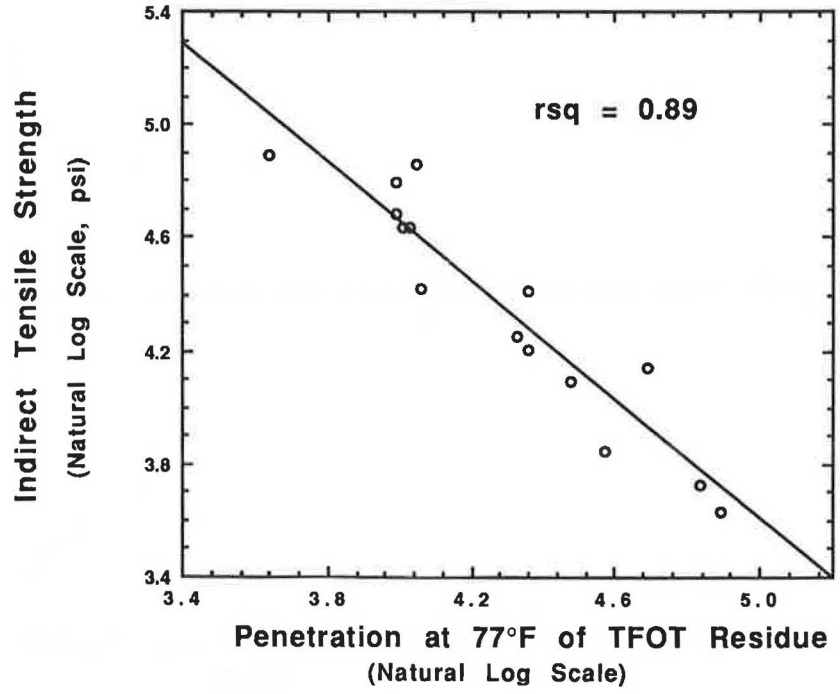

FIGURE 9 IDTS versus penetration (at 77°F) of the TFOT residue: gravel mix, 6 percent voids, 5.5 percent AC.

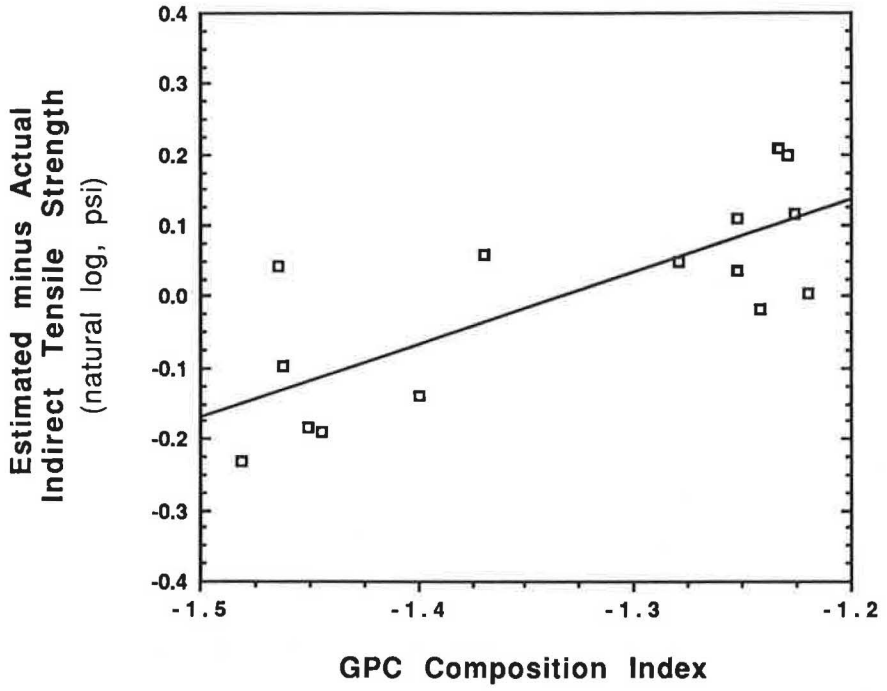

FIGURE 10 Effect of composition on IDTS: traprock mix, 8 percent voids, 4.8 percent AC.

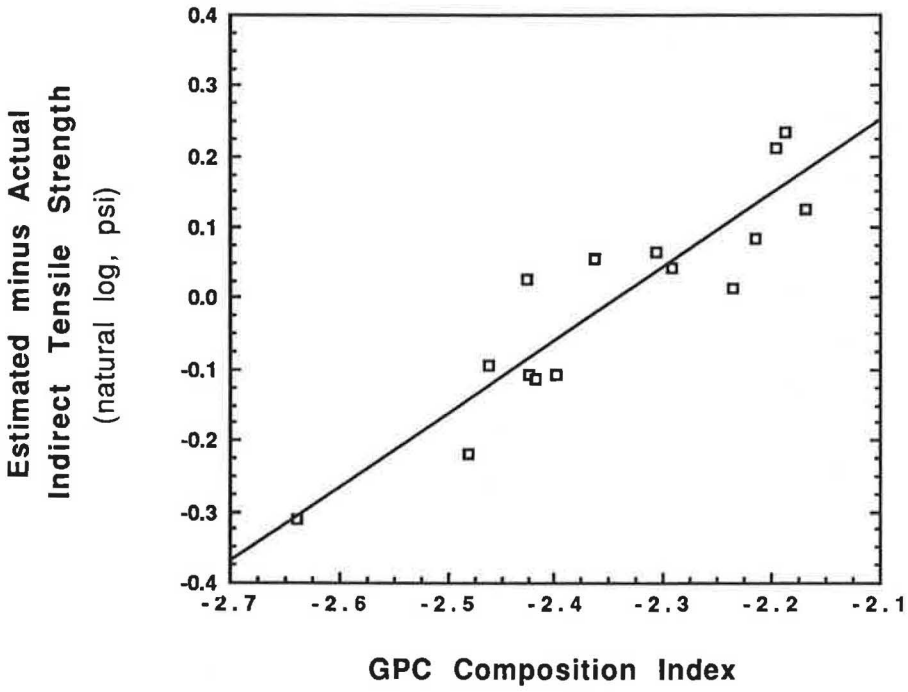

FIGURE 11 Effect of composition on IDTS: traprock mix, 8 percent voids, 5.5 percent AC.

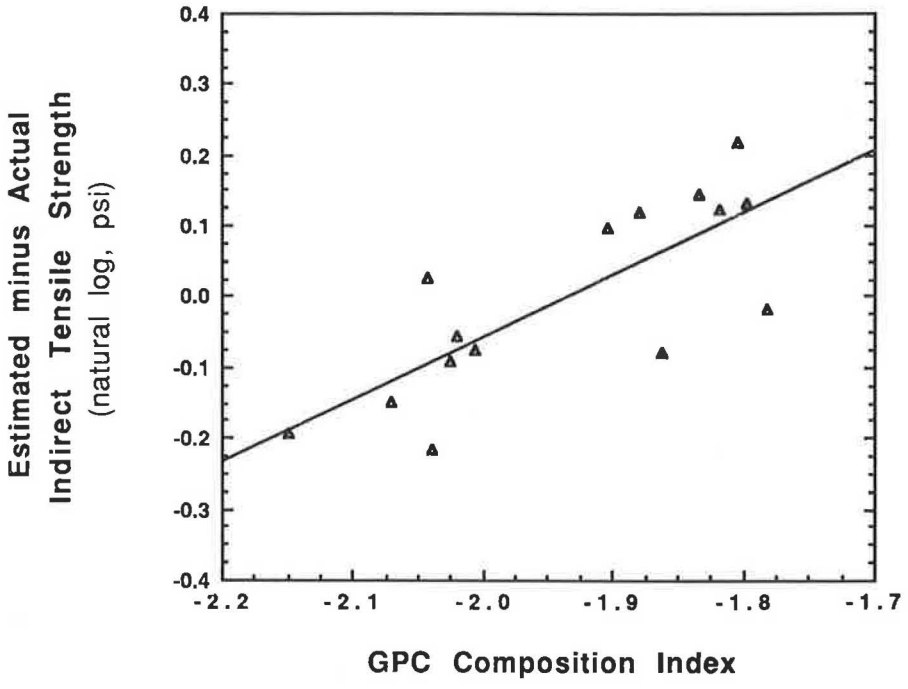

FIGURE 12 Effect of composition on IDTS: traprock mix, 6 percent voids, 4.8 percent AC.

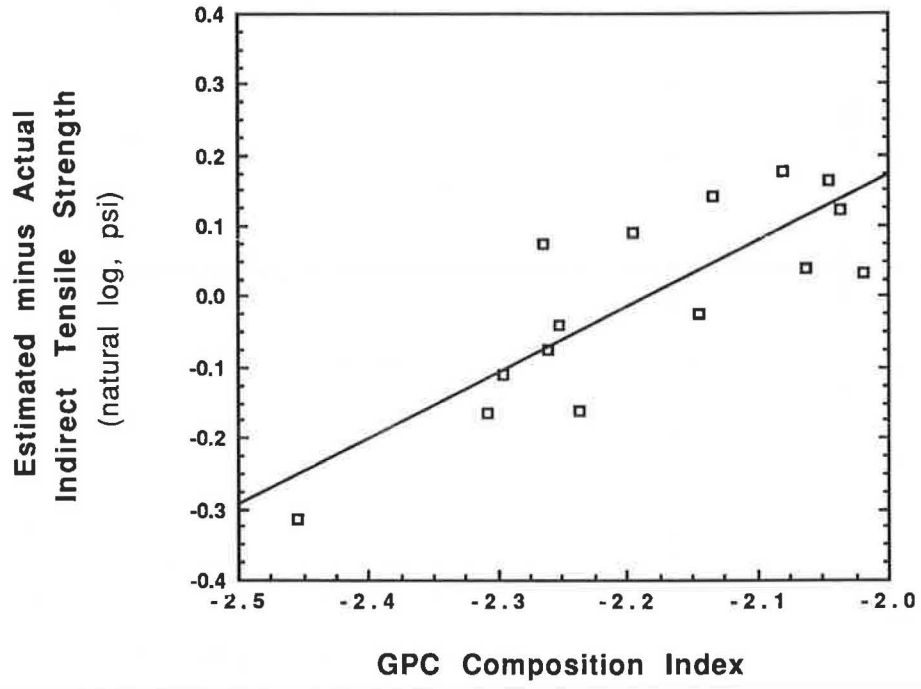

FIGURE 13 Effect of composition on IDTS: traprock mix, 6 percent voids, 5.5 percent AC.

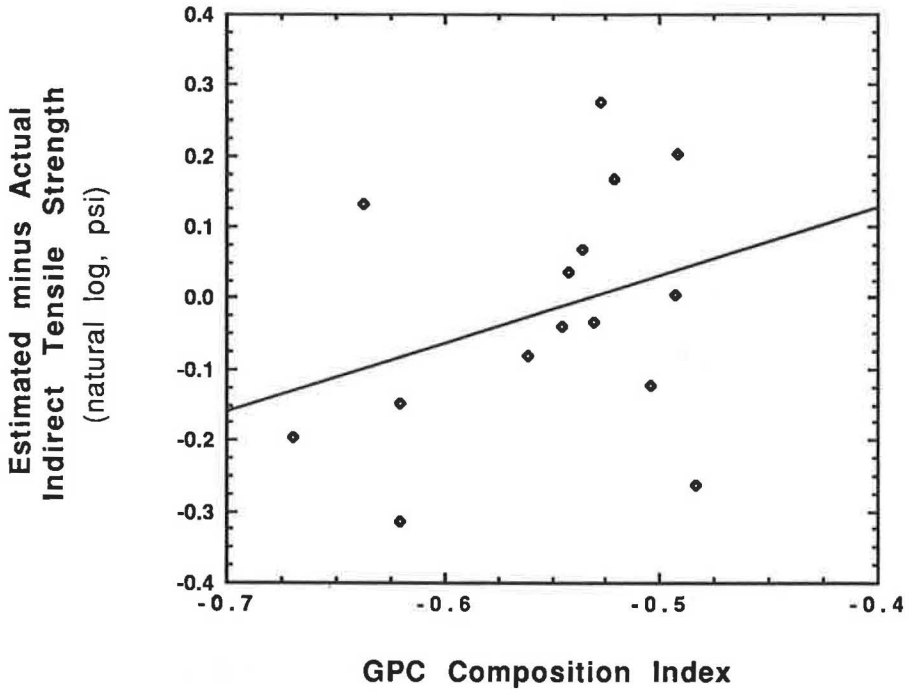

FIGURE 14 Effect of composition on IDTS: gravel mix, 8 percent voids, 4.8 percent AC.

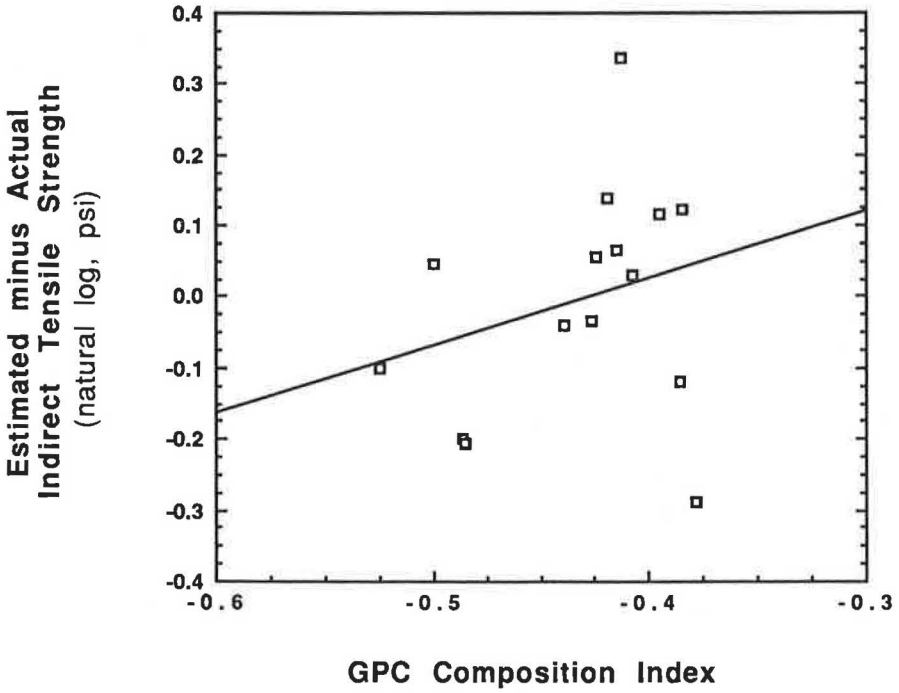

FIGURE 15 Effect of composition on IDTS: gravel mix, 8 percent voids, 5.5 percent AC.

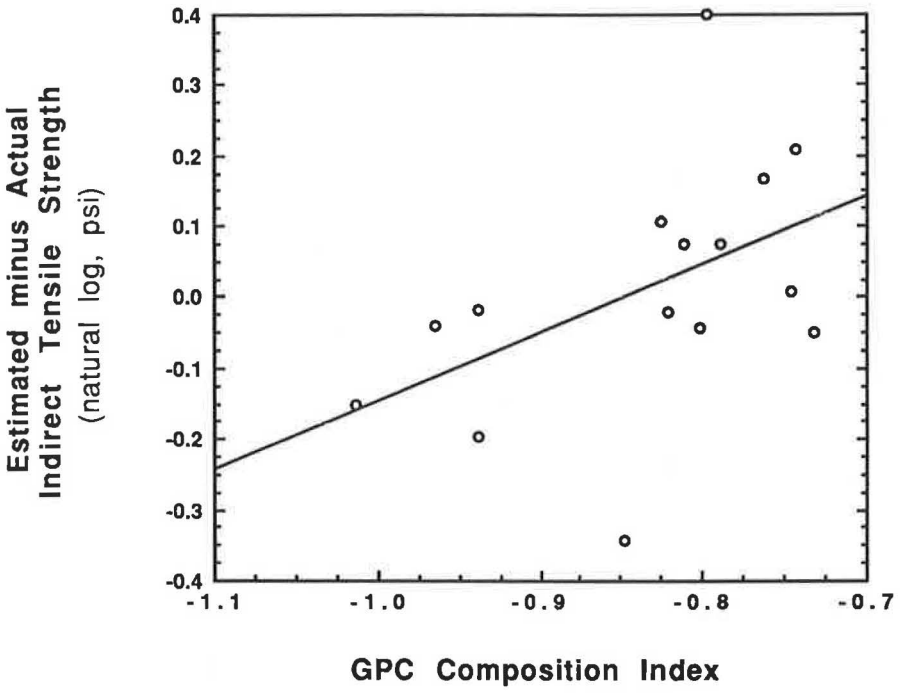

FIGURE 16 Effect of composition on IDTS: gravel mix, 6 percent voids, 4.8 percent AC.

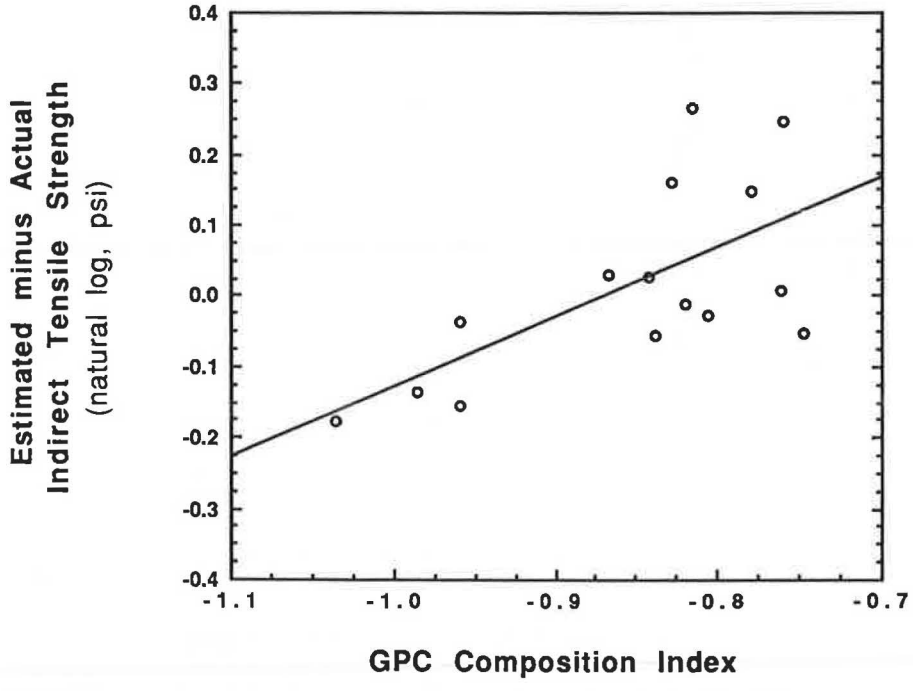

FIGURE 17 Effect of composition on IDTS: gravel mix, 6 percent voids, 5.5 percent AC.

SUMMARY

The effects of asphalt properties on the IDTS of a mix were examined. A strong correlation was observed between penetration of the TFOT residue and IDTS. The IDTS increases as penetration decreases.

The slope of the relationship between penetration and tensile strength varies significantly with aggregate type. The data suggest that the gravel mixes are more susceptible to temperature changes (in IDTS values) than the traprock mixes.

Aggregate type was also found to have a significant effect on the magnitude of the IDTS value of a given type of mix. In general, gravel mixes have higher tensile strength than equivalent traprock mixes with the same asphalt. However, the differences between two types of mixes with the same asphalt varied from asphalt to asphalt.

Asphalt composition was another factor that appeared to play a role in determining the IDTS of some mixes. For the traprock mixes, asphalt composition may account for differences of up to 55 percent in the IDTS. The effect of asphalt composition on gravel mixes was generally much less pronounced.

Overall, the IDTS of a given mix is clearly related to the consistency and composition of the asphalt. GPC is an effective method for characterizing the effects of asphalt composition on tensile strength.

ACKNOWLEDGMENTS

The authors would like to thank the Connecticut Department of Transportation (DOT) for sponsoring this project through the Joint Highway Research Advisory Council of the Connecticut DOT and the University of Connecticut. The authors would also like to thank the Institute of Material Science at the University of Connecticut for allowing them to use the GPC system in their laboratories.

REFERENCES

1. T. W. Kennedy, D. Little, H. L. Von Quintus, and J. Scherocman. Development of Asphalt-Aggregate Mixture Analysis System. *Proc., Association of Asphalt Paving Technologists*, Vol. 57, St. Paul, Minn., 1988, pp. 262–290.
2. J. W. Button, D. N. Little, B. M. Gallaway, and J. A. Epps. *NCHRP Report 268: Influence of Asphalt Temperature Susceptibility on Pavement Construction and Performance*. TRB, National Research Council, Washington, D.C., 1983.
3. P. E. Graf. Factors Affecting Moisture Susceptibility of Asphalt Concrete Mixes. *Proc., Association of Asphalt Paving Technologists*, Vol. 55, St. Paul, Minn., 1986, pp. 175–212.
4. E. L. Dukatz, Jr. and R. S. Phillips. The Effect of Air Voids on the Tensile Strength Ratio. *Proc., Association of Asphalt Paving Technologists*, Vol. 56, St. Paul, Minn., 1987, pp. 517–554.
5. H. W. Busching, S. N. Amirkhanian, J. L. Burati, J. M. Alewine, and M. O. Fletcher. Effects of Selected Asphalts and Antistripping Additives on Tensile Strength of Laboratory-Compacted Marshall Specimens—A Moisture Susceptibility Study. *Proc., Association of Asphalt Paving Technologists*, Vol. 55, St. Paul, Minn., 1986, pp. 120–148.
6. P. S. Kandhal. Evaluation of Six AC–20 Asphalt Cements by Use of the Indirect Tensile Test. In *Transportation Research Record 712*, TRB, National Research Council, Washington, D.C., 1979, pp. 1–8.
7. N. W. Garrick and L. E. Wood. Relationship between High-Pressure Gel Permeation Chromatography Data and the Rheological Properties of Asphalts. In *Transportation Research Record 1096*, TRB, National Research Council, Washington, D.C., 1986, pp. 35–41.

Publication of this paper sponsored by Committee on Characteristics of Bituminous Materials.

Use of HPGPC with UV Detection for Determination of Molecular Size Distribution of Asphalt Cement After Quantitative Corrections for Molar Absorptivity Variation and Saturated Oils

S. W. BISHARA AND R. L. MCREYNOLDS

A method is described for calculating molecular size distribution (MSD) of asphalt cement using ultraviolet (UV) detection. A 5-μm, 500Å phenogel column is used to fractionate a known amount of a whole asphalt sample. Tetrahydrofuran:pyridine (95:5) serves as mobile phase. After passing through the UV detector at 345 nm, the eluent is fractionated at arbitrarily selected intervals. The fractions are collected in weighed petri dishes and left to dry. A computer generates a slice report showing percent material eluting at successive retention times. The injection is repeated and eluting fractions collected in volumetric flasks. After removing the column, a known volume of a given fraction is injected and the maximum absorbance reading for each fraction is recorded. The second set of fractions is then poured into the petri dishes containing the fractions from the first injection. Then, the molar absorptivity a is calculated. Using ASTM Method D4124-86(B), the percent saturates is determined. The saturates are injected, a differential refractive index detector is used to get an MSD value, and a computer generates a slice report. The data generated for the whole asphalt sample are treated mathematically, first, to account for variation of a and, second, for undetectability of saturates by UV. For six samples, comparison of data readily available from the slice report with those obtained after treatment reveals differences of up to 65 percent for some fractions. Reproducibility of the system and of the proposed method proved satisfactory. Excluding the separation of saturates, the proposed method consumes 7 to 8 hr; in series less than 4 hr.

The revival of liquid chromatography in its modern version, high-performance liquid chromatography (HPLC), has paved the way for scientists to investigate highly complex organic and inorganic systems. Companies using polymers as raw material rely primarily on high-performance gel permeation chromatography (HPGPC) to fingerprint an incoming batch of polymer. For a batch to be accepted, the molecular size distribution (MSD) profile of the raw material has to match, by overlay, the profile already available for an ideal batch. HPGPC serves as well for quality control of the finished polymer product.

HPLC and HPGPC have been used to study the chemistry of asphalt cement (AC) (*1–9*). The two techniques, together with other investigations on the rheological behavior of materials (e.g., peeling, viscoelasticimetry, and viscosity of ultrathin films) show that ACs with the same specifications may in fact have substantially different chemical compositions and rheological behaviors (*5*). Brule (*3–5*), therefore, has emphasized the practical application of physicochemical methods such as HPGPC for the characterization of road asphalts.

Materials and Research Center, Kansas Department of Transportation, 2300 Van Buren St., Topeka, Kans. 66611.

In the HPGPC study of asphalt, two main types of detection are generally used—namely, the differential refractive index (RI), and ultraviolet (UV) absorption. The RI detector has the advantage of being able to analyze almost all types of organic structures, including the saturated oils (saturates). This advantage, however, is offset by drifting of the baseline, low sensitivity, and, more significant, the lack of reproducibility (*4*). The UV detector, on the other hand, is characterized by high sensitivity, stability, excellent reproducibility, and a wide range of applicability. For the analysis of road asphalts, however, two difficulties arise.

1. The saturates, which usually constitute 10 to 25 percent of the material, do not absorb UV radiation. Because the UV detector fails to respond to this class of compounds, the slice report, which lists how much material elutes at a given time, does not account for the saturates.
2. Unlike other polymers, any point on the MSD profile is governed by the amount of material eluting from the column as well as by the molar absorptivity (extinction coefficient) of the complex mixture eluting from the column at this particular point (*4,8,10*). The chemical composition of the asphalt material eluting from the GPC column varies with the retention volume (or time), thus causing the molar absorptivity to be a variable that has to be considered in determining the molecular size distribution of a chemically complex mixture such as asphalt. Unless the molar absorptivity is accounted for mathematically, the percent material reported at a given time will not only be a function of the amount passing through the detector, but also would depend on the molar absorptivity of such material.

These difficulties restrict the usefulness of the slice report and shift the burden of characterization of an asphalt sample to the MSD profile by itself. For many asphalt samples, however, the differences between the corresponding profiles are too subtle to provide decisive answers. Furthermore, two apparently identical MSD profiles can in fact belong to two different asphalts if the molar absorptivity of the constituents is distributed in a manner that tends to minimize the inherent differences.

A semipreparative GPC column fractionated a whole asphalt sample solution into a number of fractions at arbitrarily chosen time intervals. The slice report generated by the computer determined the percent of material eluting in each fraction. For each fraction, the molar absorptivity was determined in a manner similar to that described by Bishara and Wilkins (*11*). Another sample weight was then analyzed using ASTM Method D4124-86(B) to isolate the saturates; the solvent (hexane) evaporated and the percent of saturates was determined gravimetrically, as usual. After dissolution, an aliquot of the saturates was run across the same GPC column under conditions similar to those used for the whole asphalt sample, but using RI detection. The computer generated a slice report that determined the percent of saturates that eluted in each fraction. From this information, the percent of material in each fraction of the whole asphalt sample was then analyzed mathematically, to account for variation of molar absorptivity and for the undetectability of saturates by the UV detector.

EXPERIMENTAL

Apparatus

A Waters HPLC consisting of a Waters 600 multisolvent delivery system, a U6K injector, a UV-visible liquid chromatographic spectrophotometer (Lambda-Max, Model 481), and a Waters differential refractometer, Model R 401; and a Phenomenex, 5-μm, 500Å phenogel semipreparative column (300 × 22.5 mm) with tetrahydrofuran (THF) as the solvent were used. The data were received by a Waters 840 data and chromatography control station, consisting of a Digital Equipment Corporation (DEC) computer (Professional 380), a DEC LA Printer, and a Waters system interface module (SIM).

Materials

- THF, Optima HPLC-grade, freshly distilled and filtered through 0.2-μm membrane;
- Pyridine, distilled and filtered through 0.2-μm membrane;
- n-Hexane, distilled;
- Helium gas, 99.9 percent pure for sparging;
- Nylon 66 membranes, 47 mm in diameter, 0.2-μm, for solvent and sample purification;
- Whatman Glass microfiber filters, GF/F, 4.25 cm in diameter, for separating the asphaltenes as specified in ASTM D4124-86(B);
- Alumina, activated, chromatographic grade, 80–200 mesh, Type F–20, calcined at 775°F (413°C) for 16 hr, and stored in a desiccator; and
- Toluene, methanol, and trichloroethylene used to elute the asphalt sample solution through the alumina column.

Procedures

Step I—Separation of Saturates

The ASTM method D4124-86(B) was followed to separate the saturates. The rest of the sample, i.e., the naphthene aromatics and polar aromatics, were then eluted out of the column. The percent of saturates was determined gravimetrically, as usual.

Step II—Molecular Size Distribution of Saturates

The saturates were dissolved qualitatively in about 10 mL of THF and filtered through a 0.2-μm membrane. About 150 μL of the solution were injected into the HPLC and a mobile phase composed of 100 percent THF was used at a flow rate of 6.0 mL/min. The phenogel column was maintained at ambient temperature, and the RI detector was activated. A detailed slice report was programmed that showed the percent saturates eluting, e.g., every 0.1 min. From the slice report, the percent saturates eluting within the arbitrary time intervals T_1 (4.5 to 7.5 min), T_2 (7.5 to 8.5 min), T_3 (8.5 to 9.5 min), T_4 (9.5 to 10.5 min), and T_5 (10.5 to 14.0 min) following injection were obtained. Once selected, these intervals had to be maintained throughout the rest of the procedure.

Step III—Molecular Size Distribution of Whole Asphalt

An asphalt sample in the range 2.0 to 2.5 g was weighed accurately (to within 0.01 mg). About 25 mL of THF was added and the mixture was sonified for 15 min at room temperature. The solution was transferred quantitatively to a 50-mL volumetric flask, completed to volume V with THF, and filtered through a 0.2-μm membrane.

1. An exact aliquot (100 to 200 μL) chosen to contain 6 to 8 mg of the asphalt sample was injected. A mobile phase composed of 95 percent THF and 5 percent pyridine was used at a flow rate of 6.0 mL/min. The phenogel column was maintained at ambient temperature. The wavelength of absorption on the UV detector was set to 345 nm. The eluting material was collected in a series of five small, glass, accurately weighed (to within 0.01 mg) petri dishes at the same set of time intervals used in Step II. Petri Dishes 1 to 5 were set aside to allow for the solvent to evaporate. A detailed slice report that showed the percent of material eluting, say, every 0.2 min, was programmed. From this slice report, the percent of asphalt material eluting in each fraction, F_1 through F_5, was determined.
2. Under exactly the same conditions, the injection was repeated using an aliquot equal to that used in Step I. The eluting fractions were collected in a series of five volumetric flasks numbered 1 through 5. Because the fraction volumes were not uniform, each of the first and fifth fractions was collected in a 25-mL volumetric flask; each of the remaining fractions was collected in a 10-mL volumetric flask. The solution volume in each flask was filled to the mark with THF.

Step IV—Determination of Molar Absorptivity of Fractions of Whole Asphalt

To determine the molar absorptivity of each of the fractions collected in Step III, Part 2, the column was removed from the HPLC system and the two lines, originally joined to the column, were connected to each other.

1. Measurement of A. THF was used as the mobile phase at a flow rate of 0.2 mL/min. About 30 μL of the solution in Volumetric Flask 1 was injected. With the wavelength on the UV detector set at 345 nm, the absorbance reading increased, gradually reaching a maximum before declining back to the initial value (0.001). The maximum absorbance reading A_1 was recorded and used to substitute for the absorbance A in Beer's law

$$A = abc \tag{1}$$

where a = molar absorptivity, b = optical path length, and c = concentration. Because the same sample cell was used in all the work, and because relative rather than absolute value of molar absorptivity was sought, the optical path length could be eliminated, and the equation simplified to

$$A = ac \tag{2}$$

or

$$a = A/c \tag{3}$$

The value of the absorbance A was then obtained and recorded for each of the other fractions.

2. Calculation of c and a. The contents of each volumetric flask collected in Step III, Part 2, was poured into the corresponding petri dish from Step III, Part 1, and rinsed quantitatively. The petri dishes were set aside until dry, then heated in an oven at 160°C for 90 min. They were cooled in a desiccator until weight was constant. Setting S = weight in milligrams of saturates in the sample volume injected in Step III, Part 2,

$$S = \frac{W \times 1{,}000 \times \text{IV} \times \text{PS}}{V \times 1{,}000 \times 100} \tag{4}$$

where

W = sample weight (g),
IV = injection volume (μL),
PS = percent saturates (%), and
V = total volume (Step III) (mL).

For example, setting s_1 = weight in milligrams of saturates in Volumetric Flask 1,

$$s_1 = \frac{S \times \text{PS}_1}{100} \tag{5}$$

where PS_1 is the percent saturates eluting in time interval T_1 in Step II.

The weight in milligrams of UV-absorbing material in Volumetric Flask 1 is given by

$$X_1 = \frac{W_1}{2} - s_1 \tag{6}$$

where W_1 is the weight in milligrams of material in Petri Dish 1 from Step IV, Part 2.

Therefore,

$$c_1 = \frac{x_1 \times 1{,}000 \times 30}{v_1 \times 1{,}000} \tag{7}$$

where c_1 is the concentration of absorbing material in the (IV_1 = 30 μL) injection volume and v_1 is the volume in milliliters of Volumetric Flask 1. Equation 3 was used to calculate the corresponding value of a. Similarly, c and a were calculated for the rest of the fractions.

Calculation

Correction for Molar Absorptivity

For each fraction, the percent material as obtained from the slice report in Step III, Part 1, was divided by the molar absorptivity of the fraction concerned. The result was termed the "interim percent material." In this manner, the effect of molar absorptivity on the apparent value of eluting percent material was nullified (although the sum of the interim percent material for all the fractions was more than 100 percent).

Correction for Saturates

For the whole asphalt sample under consideration, the percent of UV-absorbing material was calculated by subtracting the percentage of saturates (Step I) from 100.0. For each fraction, the interim percent material was multiplied by the percent of UV-absorbing material and divided by the sum of interim percent materials to get the correct percent material in this fraction, i.e., to get the percent of absorbable components present in the given fraction. The sum of correct percent materials of the five fractions was the percent of UV-absorbing material in the given asphalt sample.

RESULTS AND DISCUSSION

Since the introduction of HPGPC as a polymer fractionation method, the technique has proved to be a reliable tool for characterization of polymers (*12*,*13*). Although not a polymer in the strict sense of the word, asphalt cement has also been analyzed by this technique. Not many detectors are suitable, and UV detection, though not perfect, is the most advantageous. From the MSD profile obtained, the computer sliced the area under the chromatogram and generated a report (slice report) that listed the percent material that eluted at a given retention time. Unlike polymers (and because of the chemical complexity of asphalt), for these values of percent eluting material to have any significance, the effect of variation of molar absorptivity with retention time had to be offset. Another variable was the undetectability of the saturated compounds by the UV detector.

One approach for addressing these problems was to use a relatively large GPC column that allowed injection of larger sample concentrations, collect the eluting material at different time intervals, generate an MSD profile of the whole asphalt sample, and then determine the molar absorptivity of each

fraction. The saturates were separated, weighed, dissolved, and eventually run through the HPGPC system to obtain an MSD profile.

Development and Limitation

Preliminary investigations to select the highest possible sample load on the column, without much loss of resolution, revealed that a 6- to 8-mg sample, run at a solvent flow rate of 6.0 mL/min, is optimum (Figure 1). As mentioned before, the method depended on fractionizing a whole asphalt sample into a number of fractions. Obviously, the higher the number of fractions collected, the closer would be the results to the actual values. However, the following limitations applied: (a) the maximum sample load allowed, which was a function of the column packing and dimensions, and (b) the capability of the balance used for weighing each fraction. As a tradeoff to these limitations, five fractions were selected as a reasonable number. However, to have fraction weights large enough to be accurately weighed by the balance available at the time of this study, the whole-asphalt sample injection had to be done twice. To facilitate computations, the two injection volumes were identical.

That the time elapsed between dissolution and injection might affect the MSD profile of an asphalt sample was already known. Figure 2 shows three runs for the same sample injected at 1, 2, and 4 hr from dissolution. Curve B demonstrates that after 2 hr the large molecular-weight region (t_R = 6 to 7 min) exhibited a slight decrease in detector response that later on (4 hr from dissolution, Curve C) led to a corresponding increase at the small-molecular-weight region (t_R = 11 to 12 min). The dissociation of larger molecules into smaller ones over time has been described by Brule (*4*). Therefore, the time interval between dissolution and injection was kept to a minimum, preferably 2 hr.

The time intervals set for collecting the eluent were arbitrarily set to provide a reasonable weight in each fraction. Although the cut times could be altered, once selected they had to be maintained throughout the procedure, or for a whole set of comparative analyses.

In an early stage of this study and to keep the error in weighing a fraction at a minimum, light polythene beakers were used for collection. On drying and heating, however, negative weights were frequently encountered, apparently as a result of the THF partially dissolving the container material to yield volatile by-products. The problem disappeared once glass petri dishes were substituted.

Sonification for 15 min at room temperature proved adequate for quantitatively dissolving any of the samples under investigation. To elute an asphalt sample of 6 to 8 mg out of the 300- × 22.5-mm semipreparative GPC column, a mobile phase of THF flowing at 6.0 mL/min was used at first. But the chromatogram was found to extend beyond the total column void volume, i.e., outside the useful range of separation by GPC. Some of the smaller molecules, particularly the strongly polar ones, are retained within the column by an adsorption mechanism. Use of a mobile phase composed of 95 percent THF plus 5 percent pyridine overcame the forces of adsorption, and enhanced elution.

The importance of asphaltenes in the asphalt macrostructure model of Yen (*14*) is known. Interactions between the π electrons of the pericondensed polynuclear aromatics provide cohesion for the sheets to form the asphaltene micelles. Under favorable conditions, these combine to form aggregates. Polynuclear aromatics are therefore important, and use of a long wavelength (345 nm) of UV absorption was warranted.

Analysis of Samples

Six asphalt cement samples from five different refineries and covering a wide range of viscosities were selected. Each sample was analyzed by the proposed method, and the results are given in Table 1.

As expected, the results show that the molar absorptivity depends on retention time. For some samples, e.g., Sample 85–1147, the range of variation was 0.1 to about 0.6. This value also varies from one sample to the other. These variations highlight the significance of including the value of molar absorptivity in MSD calculations. For the six samples analyzed, the percent saturates ranged between 10 and 23. Reliable information about the MSD of an asphalt sample using UV detection should account for the amount as well as the MSD of the saturates themselves within the sample in question.

Comparison between the treated and untreated data (those readily generated by the computer) in Table 1 reflects the influence that the molar absorptivity and saturates may exercise on the MSD data. Apart from Fraction 5, the difference was detectable for all fractions of the six samples analyzed, and was quite significant for some samples and for certain fractions reaching about −65 percent for F_1 of Sample 88–1043 and about +60 percent for F_3 of Sample 86–4292.

For laboratories where the analysis of asphalt into four fractions according to the ASTM method D4124-86(B) is a routine test, the time required for Steps II through IV of the proposed procedure is approximately 7 to 8 hr. In series, it takes less than 4 hr.

Reproducibility

To test reproducibility of the HPGPC system, a set of six polystyrene standards and toluene, run 11 days apart, were compared (Table 2). In either case, 100 μL of about 0.25

TABLE 2 COMPARISON OF RETENTION TIMES FOR A SET OF POLYSTYRENE STANDARDS AND TOLUENE, RUN 11 DAYS APART

Standard	Molecular Weight	Retention Time (min)	
		1st Day	12th Day
F–2	16,700	5.66	5.66
F–1	10,300	6.16	6.16
A–5000	6,200	6.78	6.78
A–2500	2,800	7.59	7.58
A–1000	950	8.70	8.70
A–300	402	9.75	9.75
Toluene	92	12.28	12.28
Correlation		0.9999176	0.9999195
Standard error of estimate		0.16848	0.16358

TABLE 1 MOLECULAR SIZE DISTRIBUTION OF ASPHALT CEMENT SAMPLES BEFORE AND AFTER CORRECTION FOR MOLAR ABSORPTIVITY VARIATION AND SATURATED OILS

Sample No.	Fraction	Percent Saturates *	Molar Absorptivity**	Percent Whole Asphalt Material		
				Untreated Data	Interim Data	Treated Data ***
	F_1	2.2	0.200	49.3	246.5	31.3
	F_2	6.9	0.098	17.2	175.5	22.3
85-2754	F_3	0.7	0.089	16.7	187.6	23.7
	F_4	0.1	0.184	14.3	77.7	10.0
	F_5	0.0	0.106	2.5	23.6	2.8
	Total	9.9		100.0	710.9	90.1
	F_1	3.2	0.308	44.1	143.2	21.6
	F_2	3.3	0.103	17.7	171.8	26.0
85-1147	F_3	4.1	0.098	17.8	181.6	27.5
	F_4	2.1	0.242	19.4	80.2	12.1
	F_5	0.0	0.572	1.0	1.7	0.3
	Total	12.7		100.0	578.5	87.5
	F_1	4.2	0.210	58.4	278.1	33.9
	F_2	8.5	0.089	17.8	200.0	24.3
85-2357	F_3	3.9	0.096	14.5	151.0	18.4
	F_4	0.0	0.166	9.0	54.2	6.6
	F_5	0.0	0.283	0.3	1.1	0.1
	Total	16.6		100.0	684.4	83.3
	F_1	1.5	0.297	43.7	147.1	21.5
	F_2	10.3	0.124	19.3	155.6	22.7
86-4292	F_3	2.6	0.093	19.3	207.5	30.3
	F_4	0.3	0.238	13.7	57.6	8.4
	F_5	0.0	0.246	4.0	16.3	2.4
	Total	14.7		100.0	584.1	85.3
	F_1	1.4	0.307	23.3	75.9	8.5
	F_2	14.1	0.301	23.0	76.4	8.6
88-1043	F_3	6.6	0.065	23.7	364.6	41.0
	F_4	0.7	0.150	23.0	153.3	17.2
	F_5	0.0	0.397	7.0	17.6	2.0
	Total	22.8		100.0	687.8	77.3
85-3890	See Table 3					

*Calculated as percentage of the whole asphalt sample.

** These are not absolute values.

*** Does not include saturates, i.e., only covers the UV-absorbing material.

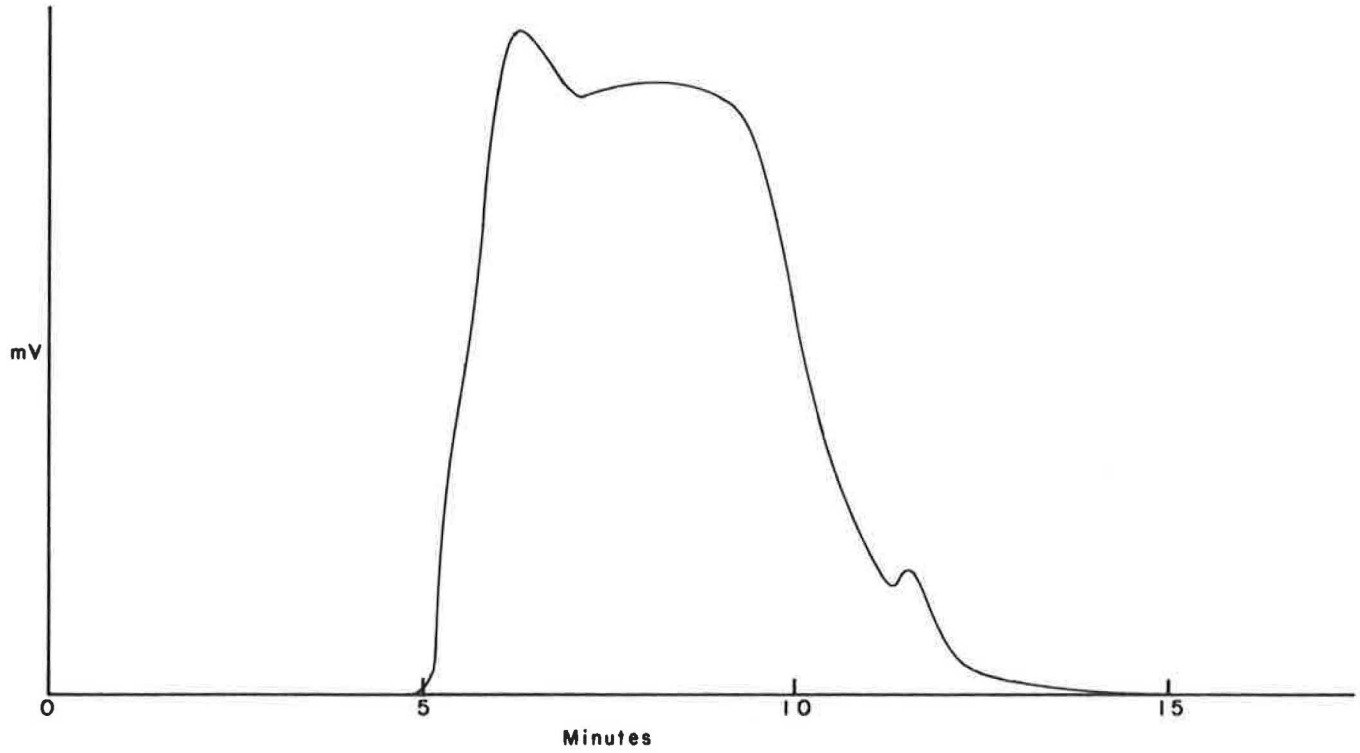

FIGURE 1 MSD profile for 7.99416 mg of Sample 86–4292 using 95 percent THF + 5 percent pyridine at 6.0 mL/min, ambient temperature, and one 500Å phenogel column (300 × 22.5 mm), UV at 345 nm.

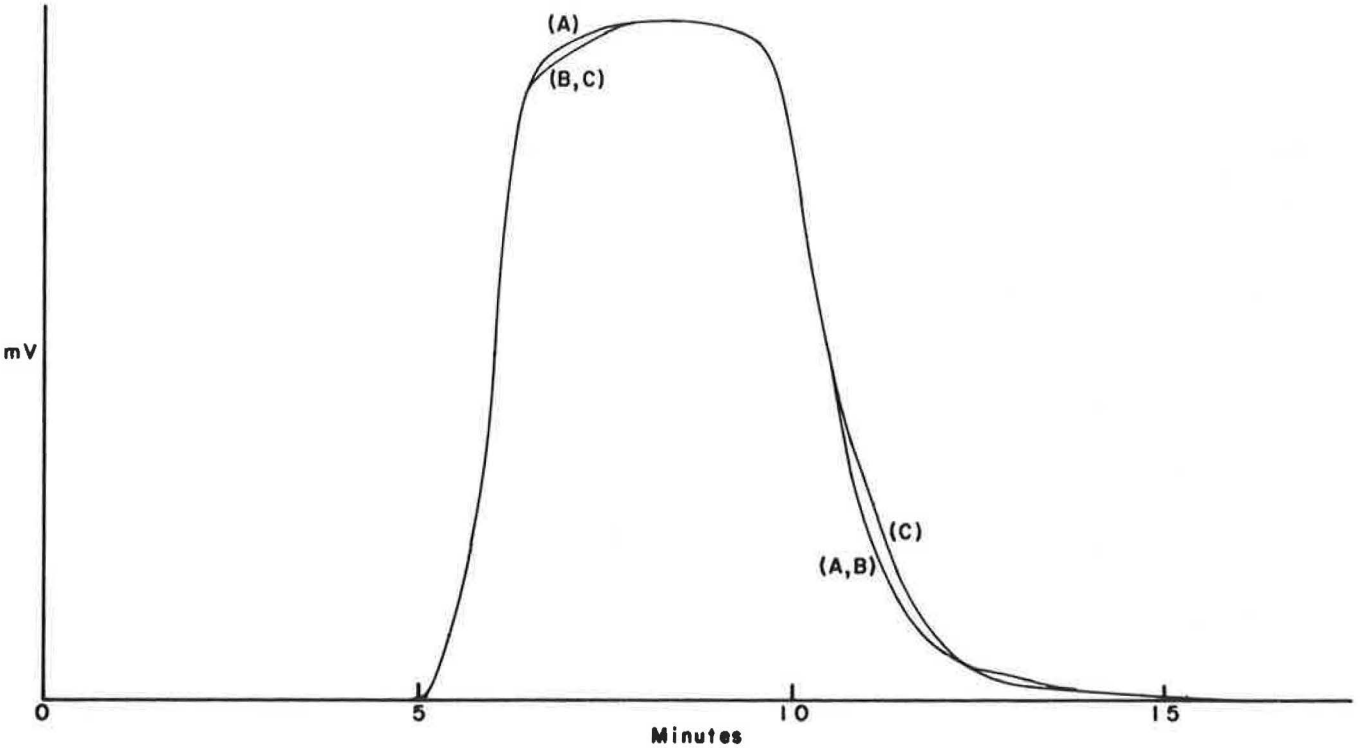

FIGURE 2 Comparison of three runs of Sample 85–3890 at different times from injection; 95 percent THF + 5 percent pyridine used as a mobile phase at 6.0 mL/min, UV at 345 nm, one 500Å phenogel column (300 × 22.5 mm); Curve *A*, 1 hr; Curve *B*, 2 hr; Curve *C*, 4 hr.

TABLE 3 RESULTS OF ANALYSIS OF SAMPLE 85-3890 TWICE, 10 DAYS APART

Fraction	Percent Saturates *	Molar Absorptivity ** (i)+	(ii)+	Percent Whole Asphalt Material (i)+ Untreated Data	(i)+ Treated Data ++	(ii)+ Untreated Data	(ii)+ Treated Data ++
F_1	1.2	0.237	0.231	36.7	20.2	37.0	19.1
F_2	2.2	0.124	0.099	21.7	22.9	21.2	25.5
F_3	4.4	0.088	0.079	21.3	31.7	21.1	31.8
F_4	2.5	0.169	0.176	16.9	13.1	17.5	11.9
F_5	0.0	0.256	0.259	3.4	1.7	3.2	1.5
Total	10.3			100.0	89.6	100.0	89.8

* Calculated as percentage of the whole asphalt sample.

** These are not absolute values.

\+ (i) Test run the first time; (ii) test run ten days later.

++ Does not include saturates, i.e., only covers UV-absorbing material.

percent polystyrene solution was injected, one 500Å phenogel column (300 × 22.5 mm) maintained at ambient temperature was used, and THF at 6.0 mL/min served as the mobile phase (the inclusion of 5 percent pyridine in the mobile phase did not seem to affect the retention time, and therefore was dispensed with). On the first day, the UV detector at 272 nm was used; on the 12th day, the RI detector was used.

To test reproducibility of the proposed method, Sample 85-3890 was tested twice under the same conditions but with 10 days separating the two runs. For each run, however, a fresh sample weight was used. Table 3 presents the two sets of measurements. All of the figures, with one exception, revealed a satisfactory level of reproducibility. Only Fraction 2 showed a deviation of 2.6 percent (absolute). This deviation occurred although the fraction weight was practically the same for the two tests (4.45 mg for the first run compared with 4.58 mg for the second run, with a relative error of 2.9 percent). The injected sample weights were also practically identical (16.55 and 16.54 mg, respectively, with a 0.06 percent difference). The difference in the values of A, however, was unexpectedly high, with 25 percent relative error (Table 3). Therefore, the deviation of the results of Fraction 2 was attributed to an odd reading of the absorbance.

CONCLUSION

In the study of the MSD of asphalt cement using HPGPC with UV absorption for detection, two difficulties have to be considered. First, the saturated compounds (usually 10 to 25 percent of sample) do no absorb electromagnetic radiation in the UV region. Second, because of the chemical complexity of asphalt, the molar absorptivity varies with the retention time. The data provided by the slice report depicting the percent material eluting at successive retention times (and correspondingly of decreasing molecular weights) has to be treated mathematically to account for these difficulties. To achieve this, a whole asphalt sample is fractionated, and the molar absorptivity determined for each fraction. The saturates are separated, and their MSD is determined.

ACKNOWLEDGMENTS

This work was accomplished in cooperation with FHWA under the "Implementation of Research and Development" line item in the Annual Work Program. There is no doubt that the FHWA Region 7 and the Kansas Department of Transportation's flexibility in administration of this line item has contributed significantly to the rapid and successful completion of this research.

Thanks are also due to Condie Erwin for entering the manuscript on the word processor.

REFERENCES

1. C. Such, B. Brule, and C. Baluja-Santos. Characterization of Road Asphalt by Chromatographic Techniques (GPC and HPLC). *Journal of Liquid Chromatography*, Vol. 2, 1979, pp. 437-453.
2. H. V. Drushel and W. W. Schultz. Effect of Solvents and Temperatures on the Separation of Asphaltenes by Gel Permeation

Chromatography. Presented at Symposium on Techniques for Characterization of Residual Fuels. American Chemical Society, San Francisco, Calif., 1980.
3. B. Brule. Characterization of Bituminous Compounds by Gel Permeation Chromatography (GPC). *Journal of Liquid Chromatography*, Vol. 2, 1979, pp. 165–192.
4. B. Brule. Contribution of Gel Permeation Chromatography (GPC) to the Characterization of Asphalts. In *Liquid Chromatography of Polymers and Related Materials II*, (J. Cazes and X. Delamare, eds.), Marcel Decker, New York, 1980, pp. 215–248.
5. B. Brule, G. Ramond, and C. Such. Relationships Between Composition, Structure, and Properties of Road Asphalts: State of Research at the French Public Works Central Laboratory. In *Transportation Research Record 1096*, TRB, National Research Council, Washington, D.C., 1986, pp. 22–34.
6. L. Caylor and T. Sharp. Asphalt Characterization and Performance Study. *Report No. 8301*, Georgia Department of Transportation, Atlanta, March 1987, pp. 1–64.
7. G. R. Donaldson, M. W. Hlavinka, J. A. Bullin, C. J. Glover, and R. R. Davison. The Use of Toluene as a Carrier Solvent for Gel Permeation Chromatography Analysis of Asphalt. *Journal of Liquid Chromatography*, Vol. 11, 1988, pp. 749–765.
8. J. A. S. Pribanic, M. Emmelin, and G. N. King. Use of Multiwavelength UV-VIS Detector with HP–GPC to Give a Three-Dimensional View of Bituminous Materials. In *Transportation Research Record 1228*, TRB, National Research Council, Washington, D.C., 1989, pp. 168–176.
9. A. S. Noureldin and L. E. Wood. Variations in Molecular Size Distribution of Virgin and Recycled Asphalt Binders Associated with Aging. In *Transportation Research Record 1228*, TRB, National Research Council, Washington, D.C., 1989, pp. 191–197.
10. L. R. Snyder. Determination of Asphalt Molecular Weight Distributions by Gel Permeation Chromatography. *Analytical Chemistry*, Vol. 41, 1969, pp. 1223–1227.
11. S. W. Bishara and E. Wilkins. Rapid Method for the Chemical Analysis of Asphalt Cement: Quantitative Determination of the Naphthene Aromatic and Polar Aromatic Fractions Using High-Performance Liquid Chromatography. In *Transportation Research Record 1228*, TRB, National Research Council, Washington, D.C., 1989, pp. 183–190.
12. J. J. Cazes. Chemical Instrumentation. Gel Permeation Chromatography. *Journal of Chemical Education*, Vol. 43, 1966, pp. A567–A568 and A625–A626.
13. J. J. Cazes. Current Trends in Gel Permeation Chromatography. Part Two: Methodology. *Journal of Chemical Education*, Vol. 47, 1970, pp. A505–A514.
14. T. F. Yen. Chemistry of Asphaltenes (J. W. Burger, ed.). *ACS Series*, Division of Petroleum Chemistry, American Chemical Society, Washington, D.C., 1981.

Publication of this paper sponsored by Committee on Characteristics of Bituminous Materials.

Adsorption of Asphalt and Asphalt Functionalities onto Aggregates Precoated with Antistripping Agents

CHRISTINE W. CURTIS, JEONGHYEON BAIK, AND YOUNG W. JEON

The adsorption behavior of asphalt and functionalities representative of those present in asphalt on aggregates precoated with antistripping agents was investigated. The amount of adsorption obtained was compared with that of uncoated aggregate. The aggregates used were a high-surface-area synthetic silica and low-surface-area actual siliceous aggregates; Warrior River sand from Alabama; and greywacke from California. The aggregates were precoated with commercial polyamine antistripping agents. The acidic functionalities benzoic acid and phenol demonstrated enhanced adsorption with the antistripping agent precoating, whereas the nonacidic functionalities phenylsulfoxide, benzylbenzoate, benzophenone, quinoline, and pyrene did not. The adsorption of AC–20 asphalt onto precoated silica and Warrior River sand showed decreased adsorption compared to that on the uncoated aggregate. The adsorption of AC–10 on precoated greywacke also showed decreased adsorption compared to uncoated greywacke. The ranking of the AC–20 adsorption on different uncoated aggregates when aggregate surface area was taken into account was Warrior River sand > silica > greywacke. Likewise, AC–20 adsorbed more on precoated Warrier River sand than on precoated silica. Desorption of AC–20 asphalt from precoated silica using distilled water appeared to be less than that from uncoated silica.

Asphalt serves as the binder for aggregates in road pavements. The adhesion of the binder to the aggregate is of utmost importance for achieving and maintaining long-lived, well-performing pavements. Adhesion of the asphalt to the aggregate can be examined in the laboratory using liquid-phase adsorption of asphalt onto different aggregate surfaces. Previous work performed by Plancher et al. (*1*) and Petersen et al. (*2*) has indicated the importance of the polar functionalities present in asphalt for providing a binding, strongly adsorbing layer at the interface between asphalt and aggregate. Plancher et al. (*1*) found that benzoic acid adsorbed most on all of the aggregates used whereas quinoline was preferentially adsorbed with acidic aggregates (quartzite and granite). Phenylsulfoxide, benzophenone, and phenol were favorably adsorbed onto either acidic or basic aggregate (limestone), whereas the other functionalities, benzylbenzoate, 1,2,3,4-dibenzanthracene, and naphthalene, showed little affinity for any of the aggregates. Curtis et al. (*3*) examined the competitive adsorption of heteroatomic model compounds onto dry and moist silica surfaces. The competitive affinity observed for dry silica was in the order of phenylsulfoxide > quinoline > phenol > benzoic acid, whereas for moist silica the order was phenylsulfoxide > phenol > benzoic acid > quinoline.

Chemical Engineering Department, Auburn University, Auburn, Ala. 36849.

Fritschy and Papirer (*4*) examined the adsorption of asphalt onto different surface area Aerosils that are nonporous pyrogenic silicas. Multilayer adsorption of the asphalt was observed with the most strongly adsorbing fraction appearing to be asphaltenes. Curtis et al. (*5*) examined the adsorption of asphalt with different degrees of oxidation onto model and actual aggregates. AC–20 achieved a higher level of adsorption on all of the aggregates than did the more highly oxidized asphalts. Moisture on the aggregate surface had different effects on the amount of adsorption, depending on the type of aggregate used.

The stripping or removal of asphalt from the aggregate because of water penetrating between the layer of asphalt and the aggregate surface causes many pavements to fail. Many different antistripping agents have been developed over the years to reduce the stripping propensity of different aggregates; however, many of them are composed of polyamines [for example, Mathews (*6*), Dybalski (*7*), Kartashevskii et al. (*8*), Brown and Swidler (*9*)]. Mathews (*10*) reported that using cationic surfactants as antistripping agents promoted adhesion between asphalt and aggregate and effectively reduced water damage. The action of these cationic surfactants is to migrate to the aggregate surface and render the surface lipophilic for facile adsorption of asphalt. Dybalski (*11*) proposed a method of directly applying antistripping agents to the surface. This method would obviate the possibility that the polyamine antistripping agents would react with acidic components in the asphalt and be rendered inactive. However, the best method for introducing antistripping agents is still in question.

This study investigated the effect of adsorbed antistripping (AS) agents on the chemistry and adsorption behavior of asphalt and asphalt functionalities at the asphalt-aggregate interface. The primary objective was to ascertain the adsorption behavior of asphalt and asphalt functionalities onto synthetic and actual aggregates precoated with AS agents and to compare their adsorptive behavior without AS agents. The asphalts used in this study were an AC–10 and an AC–20. The aggregates used were Warrior River sand; a greywacke; and a high-surface-area, porous silica. The model functionalities representing chemical functionalities present in asphalt selected for this study were carboxylic acids represented by benzoic acid, phenolics by phenol, sulfoxides by phenylsulfoxide, nitrogen bases by quinoline, ketones by benzophenone, esters by benzylbenzoate, and polynuclear aromatics by pyrene. Commercial polyamine antistripping agents were used to precoat the aggregates. Asphalt adsorption was performed from toluene solution using a continuous system,

whereas the asphalt functionalities were adsorbed from cyclohexane solutions using batch adsorption.

EXPERIMENTAL

Materials Used

Two commercially available polyamine AS agents (AS1 and AS2) were used as received. The AC–10, labeled in the figures as AAD–1, was produced from California Coastal crude; the AC–20, obtained from Hunt Oil, was produced from 18 percent Maya crude, 65 percent Mississippi-Alabama pipeline crude, and 17 percent Boscan crude. The seven model compounds representing chemical functionalities present in asphalt used were benzoic acid (purity >99 percent), quinoline (>99 percent), phenylsulfoxide (97 percent), phenol (>99 percent), benzophenone (>99 percent), benzylbenzoate (>99 percent), and pyrene (>99 percent), all supplied by Aldrich. The organic solvents used were dichloromethane (>99 percent, spectrophotometric grade, Aldrich) for adsorption of the AS agents, cyclohexane (>99 percent, spectrophotometric grade, Aldrich) for adsorption of the model compounds, and toluene (spectranalyzed grade, Fisher) for adsorption of the asphalts. Distilled water was also used as a desorption solvent for asphalt. The liquid model compounds and the organic solvents were dried before use by adding activated Type 4A molecular sieves, whereas the solid compounds were dried in a vacuum desiccator.

The adsorbents used were Warrior River sand, an aggregate from Alabama; a greywacke, a siliceous aggregate obtained from Kaiser Sand and Gravel, Pleasenton, California; and a silica gel purchased from Alltech Associates, Inc., and manufactured by Davison Chemical Division, W. R. Grace and Company. The aggregate surface areas, obtained using multipoint nitrogen adsorption, are as follows:

Aggregate	*Surface Area (m^2/g)*
Warrior River sand	0.6
Greywacke	2.5
Silica	294

The aggregates were dried before use at 150°C for 24 hr to remove physisorbed water and volatile organics.

Equipment

The asphalt adsorption experiments were performed using a continuous system described previously [Curtis et al. (*3*)], consisting of a thermojacketed column containing the aggregate and toluene circulating through the system. The column temperature was maintained at 25°C and the change in concentration was monitored by visible spectroscopy. The AS agents and model functionalities were adsorbed from dichloromethane and cyclohexane, respectively, using batch adsorption. Their change in concentration was monitored by ultraviolet (UV) spectroscopy. The adsorption vessels were agitated using a Model 3528CC microprocessor-controlled orbit shaker manufactured by Lab-line Instruments. Adsorption temperature, speed, and agitation time were controlled at 25°C ± 0.65°C, 250 ± 10 rpm, and 60 min, respectively.

Preparation of Precoated Aggregate

Each AS agent was dissolved into dichloromethane to make solutions with initial concentrations ranging from 0.5 to 10 g/L. The insoluble fraction consisting of about 5 percent of the AS agent was removed by vacuum filtering the solution through a Whatman 934 AH glass microfilter. The solution concentration was corrected by subtracting the insoluble fraction from the initial amount of the AS agent introduced. The flasks containing AS agent solution were placed in the orbit shaker for 1 hr to allow equilibration of the solution to 25°C. Then, 2 g of dried aggregate was introduced into 95 mL of AS agent solution, and the solution mixture was stirred for 1 hr, which was sufficient for attaining equilibrium for adsorption. Samples of 5-mL aliquots were taken before and after adsorption by filtering them through 0.22-μm MSI Teflon membrane filters. The weakly adsorbed AS1 fraction on silica was removed by washing the silica three times with 100 mL of pure dichloromethane.

When precoated silica was prepared for the asphalt adsorption studies, only 1 g of silica was introduced to the AS1 solution resulting in a somewhat higher AS1 monolayer amount than with 2 g. When Warrior River sand and greywacke were precoated, 5 g of each material was added to each adsorption flask for precoating with AS1. Neither Warrior River sand nor greywacke was washed with dichloromethane. After precoating, the aggregates were dried for 24 hr at room temperature in a vacuum desiccator.

Adsorption of Model Compounds onto Precoated Silica

Model compounds were each dissolved into cyclohexane to make solutions with various initial concentrations up to 15 g/L. The sample solutions were placed in the orbit shaker for 1 hr to equilibrate at 25°C. Then, 0.5 g of precoated silica was added into 95 mL of model compound solution, and the solution mixture was agitated for 1 hr to attain equilibrium. Samples of 5-mL aliquots were taken before and after adsorption.

Analysis

Samples taken in the adsorption experiments were analyzed by UV-visible spectroscopy using a Model 250 Gilford UV-visible spectrometer. The characteristic wavelengths used for each compound are as follows:

Test Compound	*Solvent*	*Wavelength (nm)*
AS1	Dichloromethane	270
AS2	Dichloromethane	270
Quinoline	Cyclohexane	274
Phenylsulfoxide	Cyclohexane	252
Phenol	Cyclohexane	271.5
Benzoic acid	Cyclohexane	274
Benzophenone	Cyclohexane	250
Benzylbenzoate	Cyclohexane	247
Pyrene	Cyclohexane	295
AC–10	Toluene	410
AC–20	Toluene	375

Quantitation was based on Beer's law, $A = abc$, where A, a, b, and c denote UV or visible absorbance, absorptivity (L/g-cm), cell pathlength (1 cm), and solution concentration (g/L), respectively. The calibration curves for the asphalts, AS agents, and model compounds were developed using standard solutions of known concentrations. From the absorbance readings, the solution concentration as well as the amount adsorbed was calculated by using the equations given in the following paragraphs.

AS Agent Loading on Silica from Dichloromethane Solution

$$C/C_0 = \text{Abs}/\text{Abs}_0 \quad (1)$$

$$AW = V(C_0 - C) \quad (2)$$

$$DW = VC_D = V(\text{Abs}_D/ab) \quad (3)$$

$$\sigma = A - D \quad (4)$$

where

C_0 = initial solution concentration (g/L),
C = equilibrated solution concentration (g/L),
Abs_0 = UV absorbance of initial solution,
Abs = UV absorbance of equilibrated solution,
A = amount adsorbed per gram of silica (g/g silica),
W = quantity of silica used (g),
V = solution volume (L),
D = amount desorbed per gram of silica (g/g silica),
C_D = solution concentration resulting from washing (g/L),
Abs_D = UV absorbance of wash solution,
a = absorptivity of AS agent (L/g-cm),
σ = amount of AS loading on silica obtained after removing the weakly adsorbed fraction (g/g silica), and
b = cell pathlength (cm).

Model Compound Adsorption from Cyclohexane Solution

Equations 1 and 2 suffice to describe the adsorption from cyclohexane solution.

Adsorption of Asphalt onto Aggregate

Asphalt solutions were prepared using dry spectroanalyzed toluene. The concentration ranges used were from ~0.4 to 53.5 g/L for silica, 0.02 to ~1.4 g/L for Warrior River sand, and 0.02 to 0.54 g/L for greywacke. The asphalt in toluene solution was introduced to the column and allowed to equilibrate for approximately 5 min. The flow rate of 0.58 mL/sec was then set without aggregate in the column. Aggregate, both precoated and uncoated, consisting of 1 g of silica or 5 g of either Warrior River sand or greywacke, was then added to the column and the experiment begun. The visible absorbance reading was obtained at the wavelengths presented in Table 2 (the last two entries) after each solution had reached equilibrium. The equilibrium time was 8 hr for silica and Warrior River sand and 12 hr for greywacke.

Desorption of AC–20 from Precoated Silica and Uncoated Silica

The desorption experiment was performed by first adsorbing nearly equivalent amounts of AC–20 onto AS1 precoated and uncoated silica. The silica with preadsorbed AC–20 was dried for 48 hr at room temperature in a vacuum desiccator, then placed in 25 or 50 mL of distilled water, and finally agitated for 2 hr at 25°C. The asphalt was extracted from the water phase by toluene. Aliquots (5 mL) of the organic phase were taken for quantitative analysis by visible spectroscopy.

Asphalt Adsorption and Desorption on Aggregate

Adsorption

$$C/C_0 = \text{Abs}/\text{Abs}_0 \quad (5)$$

$$AW_A = V(C_0 - C) \quad (6)$$

$$A = VC_0(\text{Abs}_0 - \text{Abs})/W_A\text{Abs}_0 \quad (7)$$

Desorption

$$D_wW_A = V_wC_w = V_w(\text{Abs}_w/a_wb)$$

$$D_w = V_w(\text{Abs}_w/a_w)/W_A \quad (8)$$

where

W_A = quantity of aggregate used (g),
V_w = solution volume used for extraction (L),
D_w = amount of asphalt desorbed per gram of aggregate (g/g),
C_w = solution concentration after extraction (g/L),
Abs_w = absorbance of extracted solution, and
a_w = absorptivity of asphalt in toluene solution (L/g-cm).

RESULTS AND DISCUSSION

Adsorption Isotherms of AS Agents on Silica

Both AS1 and AS2 were precoated onto silica from a dichloromethane solution. AS1 exhibited a Langmuir-type monolayer adsorption that was characterized by the formation of a plateau at high concentrations, whereas AS2 did not. AS2 had a continuously increasing adsorption with increased concentration. AS2 adsorbed more than AS1 at concentrations below 1 g/L, whereas the reverse was observed between 1 and 8 g/L. At high concentrations (>8 g/L), AS2 again adsorbed more onto the silica than did AS1.

The Langmuir equation having the form

$$C/q = C/q_m + 1/b'q_m$$

where

C = equilibrium concentration,
q = amount adsorbed per gram of silica,
q_m = saturated monolayer amount, and
b' = a constant, respectively,

was applied to the adsorption isotherms (*12*). The monolayer amounts obtained for AS1 and AS2 on silica, when 2 g of silica was introduced, were 138 and 139 mg per gram of silica, respectively.

The adsorptions of AS1 on dry and moist silica were also compared as shown in Figure 1. In this case, only 1 g of silica was introduced to the AS1 batch adsorption flask compared to the 2 g in the above experiments. The moisture content of silica was ~4.6 weight-percent moisture, a value that was obtained by placing dry silica in a humidifying chamber containing distilled water. The adsorption behaviors of AS1 on the moist and dry silica were similar although the amount of AS1 adsorbed onto moist silica appeared to be higher than that onto dry silica. The data, when fitted to the Langmuir adsorption model, yielded monolayer values of 265.5 and 217.8 mg per gram of silica with correlation coefficients of 0.991 and 0.981 for moist and dry silica, respectively.

Adsorption of Model Compounds on Precoated Silica

Seven model functionalities were adsorbed onto AS1- and AS2-precoated silica using cyclohexane as the adsorption medium at 25°C. The adsorption of the acidic functionalities benzoic acid and phenol was enhanced when compared to the adsorption on dry silica by the precoating of the AS agents on silica. The adsorption of the compounds representing nonacidic functionalities, such as phenylsulfoxide, quinoline, pyrene, benzylbenzoate, and benzophenone, underwent a large reduction.

Table 1 presents the effect of precoated silica on the adsorption of model functionalities on the basis of the amount adsorbed as determined at an equilibrium concentration of 5 g/L and 25°C. The acidic compounds benzoic acid and phenol had enhanced adsorption for the precoated silica ranging from 8 to 57 percent. The largest increase in benzoic acid adsorption of 57 percent was obtained with the 6 to 7 weight-percent AS2-coated silica, whereas the largest increase in phenol adsorption of 25 percent was obtained with the 6 to 7 weight-percent AS1-coated silica. The two acidic functionalities showed different adsorption behaviors; the benzoic acid adsorption was enhanced on the precoated silica over the entire equilibrium concentration range when compared to dry silica whereas phenol was only enhanced at high concentrations.

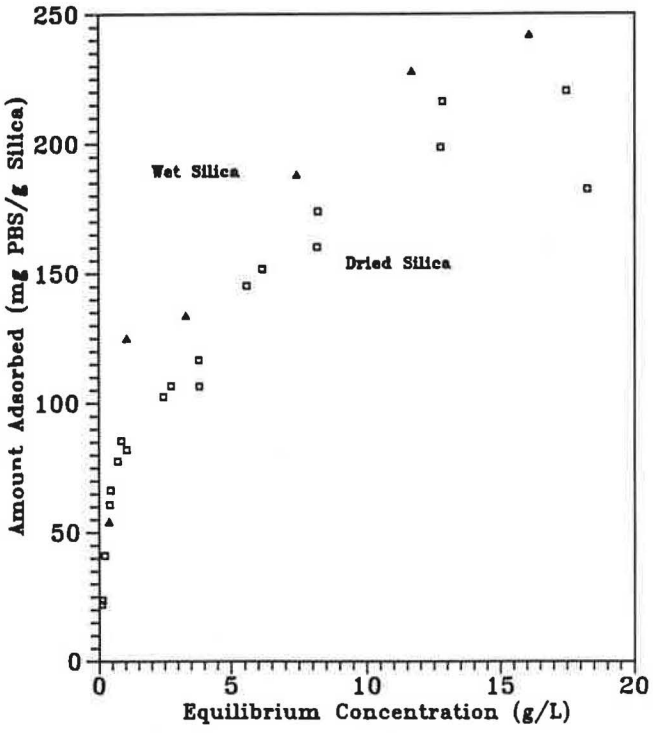

FIGURE 1 Adsorption of antistripping agent onto dried silica and wet silica.

A proposed mechanism for the interaction of the acidic compounds with the polyamine AS agents is the transfer of a proton from the acidic functionality to the amine group of the AS agent. The acidic molecule is thus negatively charged whereas the amine group has a positive charge by forming a quaternary ammonium ion. As a result, a charge attraction exists between the acidic molecule and the ammonium ion. This acid-base interaction may explain the enhancement by AS agents in the adsorption of acidic compounds benzoic acid and phenol onto the precoated silica. Through hydrogen bonding, benzoic acid and phenol in cyclohexane can also be adsorbed onto the silanols of the silica surface unoccupied by the precoated AS agents.

The other model functionalities underwent more than 80 percent reduction in their adsorption onto the precoated silica when compared to uncoated silica adsorption. Because these AS agents are primarily composed of polyamines as their primary constituents, they do not readily interact with nonacidic functionalities. Amine groups can act as Lewis bases, i.e., as proton acceptors or electron pair providers (*13*). However, none of the five functionalities has a free proton to release to the Lewis base; therefore, they remain unreactive with the basic AS agents. As a result, the adsorption of these nonacidic functionalities onto the silica surface was inhibited by the preadsorbed AS agents, compared to the uncoated silica.

A second probable mechanism that can be proposed for reduced adsorption of the nonacidic functionalities on the AS1- and AS2-precoated silica is competitive adsorption. The AS agents, which are Lewis bases, may be competing for the same aggregate sites as the nonacidic functionalities that are themselves Lewis bases. The AS agents may occupy the same sites on the uncoated silica surface as would have been occupied by the nonacidic functionalities and, hence, restrict the adsorption of the nonacidic functionalities.

Adsorption of Asphalt onto Precoated and Uncoated Silica

The adsorption behaviors of AC–20 asphalt onto dry, uncoated silica and onto silica precoated with 8 to 9 percent AS1 agent were compared. The adsorption isotherms developed for these two silicas are shown in Figure 2. The isotherm for the uncoated silica followed the Freundlich model better than the Langmuir model, whereas that for the precoated followed the Langmuir model. However, because the correlation coefficients for the Langmuir model were high for both—0.984 for uncoated and 0.993 for precoated—the Langmuir model was used to obtain the amount of asphalt monolayer coverage for both materials.

TABLE 1 THE EFFECT OF PRECOATED ANTISTRIPPING AGENTS ON SILICA ON THE ADSORPTION OF ASPHALT MODEL FUNCTIONALITIES

Asphalt Functionality	Amount Adsorbed (g/g silica)[1]		
	Uncoated Silica	6 -7 wt% AS1 Coated Silica	6 -7 wt% AS2 Coated Silica
Benzoic Acid (Carboxylic Acid)	0.105	0.140 (33%)[2]	0.165 (57%)
Phenol (Phenolic)	0.120	0.150 (25%)	0.130 (8%)
Quinoline (N-Base)	0.145	0.012 (-92%)	0.020 (-86%)
Phenylsulfoxide (Sulfoxide)	0.185	0.034 (-82%)	0.040 (-78%)
Benzophenone (Ketone)	0.095	0.010 (-89%)	NP
Benzylbenzoate (Ester)	0.103	NP[3]	0.007 (-93%)
Pyrene (Polynuclear Aromatic)	0.030	0.003 (-90%)	NP

[1] Determined at an equilibrium concentration of 5 g/L and 25°C
[2] % Change in Adsorption = [(B-A)/A] x 100
where A = Uncoated silica adsorption
B = AS agent coated silica adsorption
[3] NP = not performed

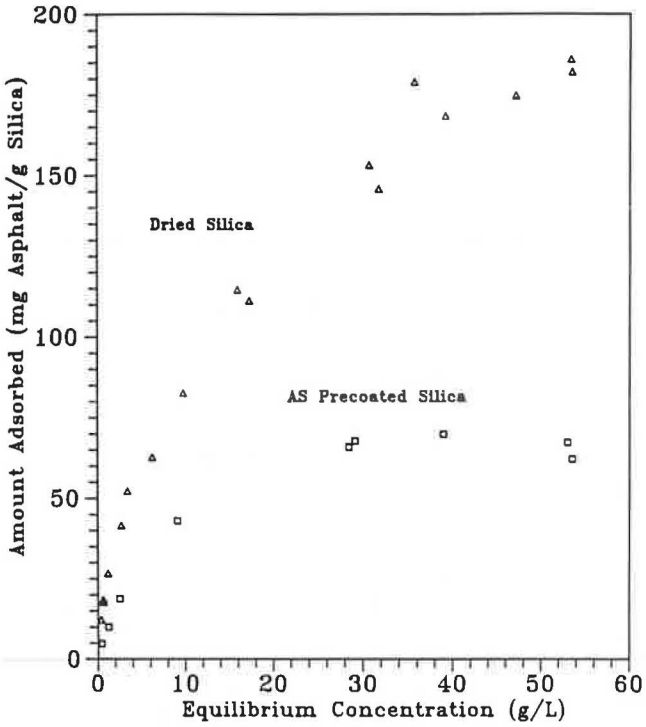

FIGURE 2 Adsorption of asphalt onto dried silica and silica precoated with antistripping agent.

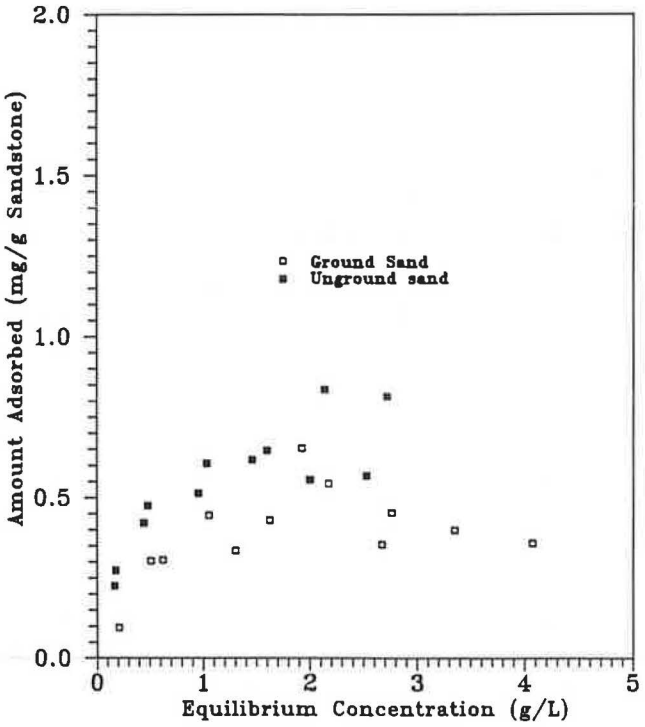

FIGURE 3 Adsorption of antistripping agent onto ground WRS and unground WRS.

The Langmuir equation was applied in the same form as was stated earlier. The monolayer amount obtained for AC–20 asphalt adsorbed by uncoated silica was 214 mg/g, whereas that for the AS1-precoated silica was 75.7 mg/g. A decrease of nearly 65 percent in the monolayer amount of AC–20 adsorbed was observed with the AS1 precoating of the aggregate.

Adsorption of AS1 on Warrior River Sand and Greywacke

The preparation of the AS1 agent precoating on Warrior River sand and greywacke followed the same procedure as that for silica; however, the actual aggregates were not washed with dichloromethane before being used in the asphalt adsorption experiments. As shown in Figure 3, adsorption of AS agent onto Warrior River sand followed the Langmuir model. A coating of 0.012 weight-percent AS1 was obtained.

The Warrior River sand used in this experiment, as well as that for asphalt adsorption, was sieved material of the quarry mixture consisting of particles between −40 and +80 mesh. Some material ground from larger sizes from −40 to +80 mesh was also used for the adsorption of AS1, as is also shown in Figure 3. The adsorption behavior for these two sands was different even though they were both obtained from the same material and had the same particle size range. The monolayer amounts obtained for AS1 adsorption on the unground and ground sand were 0.789 and 0.423 mg/g, respectively, indicating that the unground sand adsorption was about 86 percent greater than the ground sand. Hence, the grinding of the sand sufficiently affected the aggregate surface chemistry and properties to reduce the adsorption of the AS1 agent.

In contrast to the adsorption behavior of Warrior River sand, the adsorption of AS1 on greywacke followed a Freundlich isotherm behavior rather than the Langmuir model. The Freundlich model is represented by the equation

$$\ln q = \ln K + (1/n) \ln C$$

where q and C denote the amount adsorbed per unit weight of adsorbent and the equilibrium adsorbate concentration, respectively, K and n being constants. The Freundlich model generally represents a heterogeneous surface and physisorption, whereas the Langmuir model generally represents a homogeneous surface and chemisorption. The fact that different models were followed indicates a difference in the interaction between the AS1 agent and the surface of the two aggregates. The greywacke was precoated with approximately 0.04 weight-percent AS1 agent, more than three times the amount adsorbed on Warrior River sand. The larger adsorption of AS1 agent by greywacke followed the same trend as the surface areas because greywacke had four times as much surface area as Warrior River sand.

Adsorption of AC–20 on Warrior River Sand

AC–20 asphalt was adsorbed on both dry and AS1 precoated Warrior River sand. An adsorption versus time study indicated that within 8 hr adsorption on both the precoated and uncoated Warrior River sand reached equilibrium. The adsorption isotherms of both uncoated and precoated Warrior River sand shown in Figure 4 had Langmuir behavior characterized by formation of a plateau at high concentrations. The monolayer amounts obtained were 0.251 and 0.982 mg of asphalt per gram of uncoated sand. The amount of asphalt adsorbed on the AS1-precoated sand was about four times less than that adsorbed onto uncoated sand. Hence, the types and number of functionalities adsorbing on the precoated Warrior River sand were much less than those on the uncoated sand.

Adsorption of AC–10 and AC–20 onto Greywacke

An adsorption-versus-time experiment for the adsorption of AC–10 on greywacke indicated that 8 hr was required to achieve a saturated equilibrium amount for the precoated greywacke and 12 hr for the uncoated greywacke. The adsorption isotherms performed using both precoated and uncoated greywacke exhibited Langmuir adsorption behavior yielding monolayer amounts of 0.4 and 1.0 mg/g, respectively (Figure 5). The decrease in adsorption caused by aggregate precoating was 60 percent. AC–20 asphalt was also adsorbed onto the uncoated greywacke and followed a similar behavior to that of AC–10. The AC–20 asphalt adsorbed a slightly higher monolayer amount of 1.17 mg/g.

Comparisons of Different Asphalt-Aggregate Systems

A comparison of the monolayer amounts obtained from the different asphalt-aggregate combinations is presented in Table 2. Each aggregate, whether synthetic or actual, yielded asphalt monolayer amounts for the AS1-precoated aggregates that

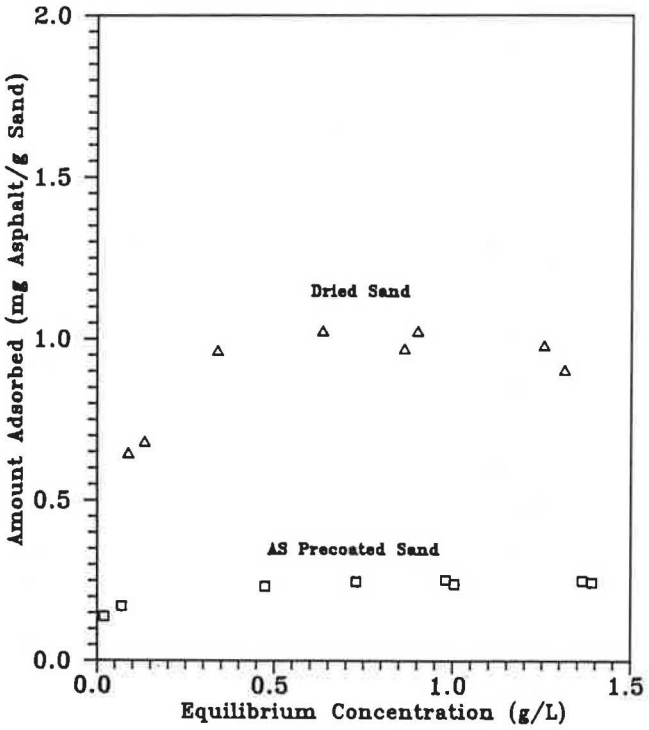

FIGURE 4 Adsorption of asphalt onto dried WRS and AS1-precoated WRS.

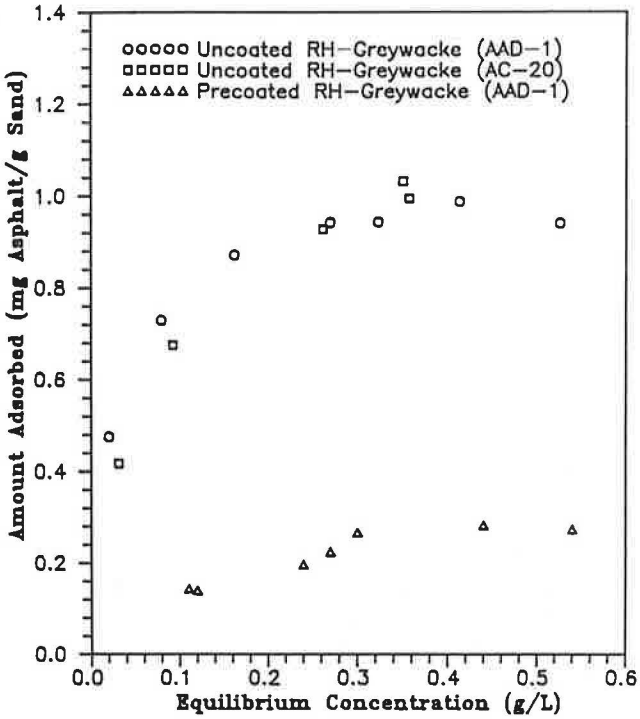

FIGURE 5 Adsorption of AAD-1 and AC-20 asphalts onto uncoated RH-greywacke and precoated RH-greywacke.

were one-fourth to one-third of those for uncoated aggregate. Thus, the uncoated aggregate adsorbed a greater quantity of asphalt than the precoated aggregate regardless of the type of siliceous aggregate used. The model functionality study indicated that only acidic functionalities were promoted by the precoating of siliceous aggregates with polyamines. All of the other functionalities tested were inhibited. Hence, the adsorbing species from the AC-10 and AC-20 asphalts used appeared to be composed of substantial quantities of compounds that were not acidic and, hence, did not adsorb on the precoated aggregates.

Because these siliceous aggregates possessed substantially different surface areas, comparison on the basis of surface area allows direct comparison of the amount adsorbed among the different aggregates. The adsorption of AC-10 and AC-20 asphalts on the basis of surface area is shown in Figure 6. The adsorption behavior of the two asphalts was nearly equivalent on greywacke. By contrast, on the basis of surface area the AC-20 adsorbed much more on Warrior River sand.

The same types of comparisons can be made from the data presented in Table 2. The adsorption behavior of the three uncoated aggregates on the basis of surface area for AC-20 ranked as Warrior River sand > silica > greywacke. The precoated Warrior River sand also adsorbed more AC-20 than did precoated silica on the basis of surface area. These results suggest that the aggregate had a substantial effect on the adsorption of the AC-20 asphalt. For uncoated greywacke, AC-10 adsorption was slightly less than AC-20, suggesting that asphalt type and composition had a small effect on adsorption behavior. The more influential factors on asphalt adsorption were aggregate type and surface properties as changed by precoating with AS1 agents.

Desorption Behavior of AC-20 Asphalt

AC-20 asphalt was adsorbed at an equivalent amount on both AS1-precoated and uncoated silicas. Desorption with distilled water resulted in removing 0.7 to 1.9 percent of the preadsorbed asphalt from uncoated silica and 0.4 to 0.9 percent from precoated silica. These results were obtained when 25 mL of distilled water was used for desorption; however, when 50 mL of distilled water was used, the amount of asphalt desorbed from uncoated silica for two samples ranged from 8.4 to 9.0 percent, whereas that from AS1-precoated silica ranged from 0.39 to 0.46 percent. These results indicated that the precoating of silica with AS1 agents rendered the asphalt surface less susceptible to desorption by water. Although the adsorption of asphalt was reduced by the precoating of aggregate with AS agents, asphalt retention in the presence of water was increased.

TABLE 2 COMPARISON OF MONOLAYER AMOUNTS OBTAINED FROM DIFFERENT ASPHALT AND AGGREGATE COMBINATIONS

Aggregate	Asphalt	Pretreatment	Monolayer (mg/g)	Monolayer (mg/m^2)	% Difference from Uncoated Aggregate[1]
Silica	Hunt AC-20	Uncoated	213.9 ± 9.24	0.73 ± 0.03	NA[2]
Warrior River Sand	Hunt AC-20	Uncoated	0.98 ± 0.04	1.63 ± 0.07	NA
Greywacke	Hunt AC-20	Uncoated	1.17 ± 0.04	0.47 ± 0.02	NA
Greywacke	AC-10 (AAD-1)	Uncoated	1.01 ± 0.02	0.40 ± 0.01	NA
Silica	Hunt AC-20	Precoated	75.7 ± 3.48	0.26 ± 0.01	-64.6
Warrior River Sand	Hunt AC-20	Precoated	0.25 ± 0.01	0.42 ± 0.01	-74.5
Greywacke	AC-10 (AAD-1)	Precoated	0.39 ± 0.20	0.16 ± 0.08	-61.4

[1] % Difference = [(B-A)/A] x 100
where A = Monolayer of Uncoated Aggregate
B = Monolayer of Precoated Aggregate

[2] NA = Not Applicable

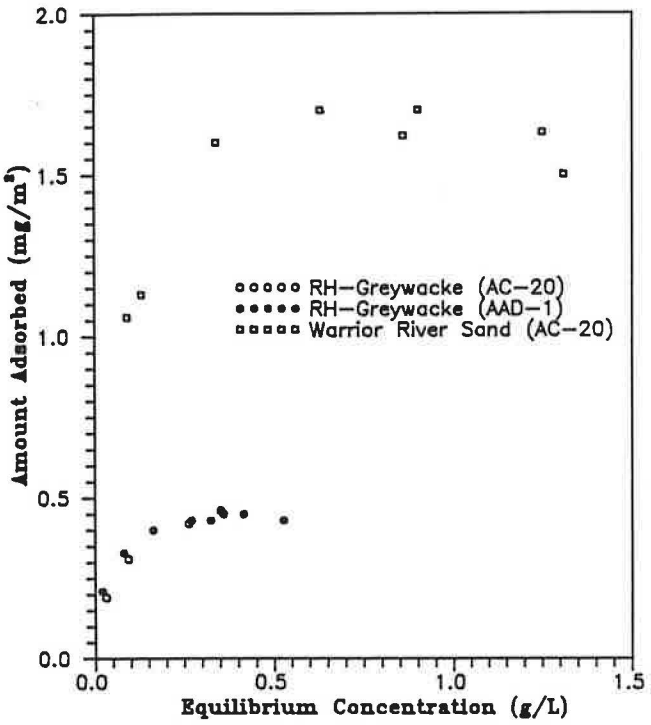

FIGURE 6 Adsorption of AC–20 and AAD–1 asphalts onto Warrior River sand and RH–greywacke on the basis of surface area.

SUMMARY AND CONCLUSIONS

The adsorption behavior of asphalt and asphalt functionalities was substantially affected by precoating the aggregate surface with AS agents. Acidic functionalities increased in adsorption on the precoated silica compared to the uncoated silica whereas the nonacidic functionalities decreased. This behavior may be explained by acid-base interactions between the acidic functionalities and the Lewis base AS agents and by repulsion between the AS agents and the nonacidic functionalities that are also Lewis bases. Another possible explanation for the decreased adsorption of the nonacidic functionalities is that the preadsorbed AS agents were occupying sites on the aggregate that would have been otherwise occupied by the nonacidic functionalities. The nonacidic functionalities were unable to replace the preadsorbed AS agents and, hence, showed minimal adsorption. These results indicate that if aggregate was precoated with AS agents or if the surface of the aggregate became coated with the AS agent because of migration of the AS agent to the aggregate surface, then the aggregate surface chemistry changed substantially. This change directly affected the adsorption behavior of different asphalt functionalities and the character of the asphalt-aggregate bond.

Substantial reductions in the asphalt adsorption onto aggregates precoated with AS agents were also observed. Because the amount of asphalt adsorbed decreased for the precoated aggregate compared to the uncoated, the functionalities involved at the uncoated interface most likely were composed of nonacidic as well as acidic functionalities. The presence of some asphalt adsorption indicated that some of the bonding functionalities were acidic or at least were able to replace the AS agents on adsorption sites on the aggregate surface.

Insights were gained into the chemistry occurring at the asphalt-aggregate interface when AS agents are present. The AS agent changed the chemistry at the interface. Less asphalt was adsorbed with precoated aggregate but less asphalt was desorbed also. Recommendations for actual practice must await further research investigating the asphalt-aggregate bond and its link to performance.

ACKNOWLEDGMENTS

The National Center for Asphalt Technology and the Strategic Highway Research Program are gratefully acknowledged for support of this work. The companies that supplied asphalt (Hunt Oil), antistripping agents (Morton-Thiokol and Scanroad), and aggregates (SHRP) are also gratefully acknowledged.

REFERENCES

1. H. Plancher, S. M. Dorrence, and J. C. Petersen. Identification of Chemical Types in Asphalts Strongly Adsorbed at the Asphalt-Aggregate Interface and Their Relative Displacement by Water. *Proc., Association of Asphalt Paving Technologists*, Vol. 46, St. Paul, Minn., pp. 151–175.
2. J. C. Petersen, H. Plancher, E. K. Ensley, R. L. Venable, and G. Miyake. Chemistry of Asphalt-Aggregate Interaction: Relationship With Pavement Moisture-Damage Prediction Test. In *Transportation Research Record 843*, TRB, National Research Council, Washington, D.C., 1982, pp. 95–104.
3. C. W. Curtis, Y. W. Jeon, and D. J. Clapp. Adsorption of Asphalt Functionalities and Oxidized Asphalts on Aggregate Surfaces. *Fuel Science and Technology International*, Vol. 7, No. 9, 1989, pp. 1225–1268.
4. G. Fritschy and E. Papirer. Interactions Between a Bitumen, Its Components and Model Fillers. *Fuel*, Vol. 57, 1978, pp. 701–704.
5. C. W. Curtis, Y. W. Jeon, D. J. Clapp, and B. M. Kiggundu. Adsorption of Model Asphalt Functionalities, AC–20, and Oxidized Asphalts in Aggregate Surfaces. In *Transportation Research Record 1228*, TRB, National Research Council, Washington, D.C., 1989.
6. D. H. Mathews. Effect of Cationic Surface-Active Agents in the Adhesion of Bituminous Binders to Road Stones. Chemistry and Physics of Applied Surface Active Substances, *Proc., 4th Inst. Congress, Meeting Data, 1964*, Vol. 3, C. Paquot, ed., Gordon Breach, London, 1967, pp. 777–786.
7. J. N. Dybalski. *Bitumen Dispersion with Improved Adhesion*. German Patent No. DE 2005618, Armour Industrial Chemical Co., Sept. 3, 1970. (In German.)
8. A. I. Kartashevskii, E. S. Tetel'baum, and T. A. Meizler. Production of Adhesion Additives for Highway Bitumens. *Neftepererab, Neftekhim*, Moscow, Vol. 9, 1971, pp. 6–7. (In Russian.)
9. L. H. Brown and R. Swidler. Corrosion Inhibitor Composition. U.S. Patent No. 3899535, Tallow Co., USA, Aug. 12, 1975.
10. D. H. Mathews. Surface-Active Agents in Bituminous Road Materials. *Journal of Applied Chemistry*, Vol. 12, 1962, pp. 56–64.
11. J. N. Dybalski. Cationic Surfactants in Asphalt Adhesion. *Proc., Association of Asphalt Paving Technologists*, Vol. 51, St. Paul, Minn., 1982, pp. 293–307.
12. C. S. Brooks. Competitive Adsorption of Aliphatic Compounds and Water on Silica Surfaces. *Journal of Colloid Science*, Vol. 13, 1958, pp. 522–536.
13. R. S. Drago and N. A. Matwiyoff. *Acids and Bases*. D. C. Heath, Lexington, Mass., 1968.

Publication of this paper sponsored by Committee on Characteristics of Nonbituminous Components of Bituminous Paving Mixtures.

Comparison of Dolomitic and Normally Hydrated Lime as Antistripping Additives

MARY STROUP-GARDINER AND DAVID NEWCOMB

Five paving mixtures typical to Utah and Nevada were prepared with and without 1.0 and 1.5 percent (by weight of aggregate) of dolomitic Type S or normally hydrated high-calcium (Type N) lime. The temperature and moisture susceptibility of each of the mixtures was determined. A slight increase in mixture stiffness resulted from the addition of either type of lime. Moisture sensitivity substantially decreased for all mixtures when lime, regardless of type, was used. The magnitude of the improvement appears to be unique for each asphalt-aggregate combination.

The stripping of asphalt from aggregate surfaces is a complex physical-chemical process that can result in early pavement distress. A popular method of combating the stripping problem is to introduce chemicals into the mixture that increase the attraction between polar sites in the asphalt and aggregate surfaces. Such chemicals are known as antistripping agents, the most popular of which is lime.

Lime is produced from high-calcium or dolomitic limestone. High-calcium limestone is almost pure calcium carbonate, whereas dolomitic limestone is a combination of calcium and magnesium carbonates (*1*). These differences in chemical composition require that each type of limestone be processed specially to obtain the final product of lime.

High-calcium limestone is calcined (i.e., burned) to produce calcium oxide (quicklime, CaO). The quicklime is then hydrated to produce hydrated lime. Lime produced in this manner is marketed as Type N lime.

Dolomitic limestone, once calcined, requires prolonged contact with water to completely hydrate the magnesium oxide and convert it into hydroxide. Because this prolonged contact is not economical, a continuous, high-pressure system is used to complete the hydration. The designation Type S indicates this type of manufacturing process.

Historically, only Type N lime has been used as an antistripping additive in asphalt concrete mixtures. However, in certain instances, Type N lime can be economically prohibitive. In these cases, substituting Type S lime for the traditional Type N would be economically preferable. This substitution can be widely accepted because of the benefits obtainable from Type S lime.

RESEARCH PROGRAM

This research program was designed to show the effectiveness of pressure-hydrated dolomitic lime in relationship to normally hydrated high-calcium lime in preventing moisture damage to asphalt concrete. Five aggregates commonly used by the Utah and Nevada Departments of Transportation were obtained. Asphalt cements commonly used for highway construction in these states were also obtained. Various combinations of these materials were used to produce typical paving mixtures, both with and without dolomitic or normally hydrated lime. Mixtures were evaluated for

1. Changes in temperature susceptibility, and
2. Resistance to moisture damage.

MATERIALS

Aggregates

Aggregates were obtained from five pits in Utah and Nevada that have evidenced a history of stripping problems:

1. Helm's Construction Company, Sparks, Nevada;
2. Interstate Highway 70 (IH-70), Utah;
3. Redmond pit, Utah;
4. Staker pit, Utah; and
5. Weaver Canyon, Utah.

The physical properties of these aggregates are presented in Table 1. Aggregate bulk specific gravities range from 2.427 to 2.803. Aggregate absorption capacities range from less than 1 percent to more than 4 percent.

All aggregate stockpiles were separated into 10 individual fractions: ½-in., ⅜-in., No. 4, No. 8, No. 16, No. 30, No. 50, No. 100, No. 200, and passing No. 200. Aggregates for each sample were then recombined into the gradations presented in Table 2, which are representative of typical highway construction projects for both states.

Asphalt Cement

Three asphalt cements were used during the course of this project:

1. Witco AR–4000,
2. Sahauro AC–10, and
3. Conoco AC–20R.

One type of asphalt cement was selected for each aggregate source.

M. Stroup-Gardiner, University of Nevada, Building SEM, Room 105, Reno, Nev. 89557. D. Newcomb, Department of Civil and Mineral Engineering, University of Minnesota, Minneapolis, Minn. 55455.

TABLE 1 PHYSICAL PROPERTIES OF AGGREGATES ON THE BASIS OF RECOMBINED GRADATION

Aggregate Source	Bulk Specific Gravity	Bulk Specific Gravity (SSD)	Apparent Specific Gravity	Absorption Capacity (%)
Helm's				
Fines	2.478	2.602	2.795	4.36
Coarse	2.542	2.596	2.705	2.31
Weaver				
Fines	2.572	2.597	2.637	0.95
Coarse	2.534	2.577	2.648	1.71
Staker				
Fines	2.785	2.811	2.859	0.93
Coarse	2.803	2.818	2.845	0.53
IH-70				
Fines	2.644	2.690	2.771	1.72
Coarse	2.543	2.594	2.680	2.00
Redmond				
Fines	2.427	2.520	2.627	2.58
Coarse	2.432	2.504	2.621	2.97

The AR–4000 was obtained from Witco's Golden Bear refinery in Oildale, California. Both the AC–10 (Sahauro Petroleum) and AC–20R (Conoco) were supplied by the Utah Department of Transportation. The physical properties of these asphalts are presented in Table 3.

Lime

The dolomitic lime was pressure-hydrated under 60 psi and was manufactured and supplied by Chemstar Lime Co., Inc., of Henderson, Nevada. The normally hydrated, high-calcium lime was also manufactured and supplied by the same source.

The chemical compositions of the limes were not available.

SAMPLE PREPARATION AND TESTING PROGRAM

The research was performed in two phases:

1. Determining optimum asphalt content, and
2. Evaluating temperature and moisture sensitivity of various mixtures.

These phases are described in detail in the following paragraphs.

The various combinations of asphalt cements and aggregates selected were

- AC–20R and IH-70 aggregate (Utah),
- AC–10 and Redmond pit aggregate (Utah),
- AC–10 and Staker pit aggregate (Utah),
- AC–10 and Weaver aggregate (Utah), and
- Witco AR–4000 and Helm's aggregate (Nev.).

TABLE 2 AGGREGATE GRADATIONS USED FOR PREPARING LABORATORY SAMPLES

Sieve Size	Cumulative Percent Passing
3/4-inch	100
1/2-inch	92
3/8-inch	80
No. 4	57
No. 8	40
No. 16	28
No. 30	20
No. 50	12
No. 100	8
No. 200	4

Optimum Asphalt Content

Previous research has indicated that the presence of lime does not significantly affect the optimum asphalt content (*2*). Therefore, only one mix design for each aggregate source was performed. The mix design test results for each aggregate source are presented in Table 4.

The optimum asphalt content was determined by the Marshall mix design procedure (*3*). Briefly, aggregates and asphalt were heated to at least 300°F before mixing; temperature was dependent on the type of binder used. Samples were immediately compacted with 50 blows per side. Optimum asphalt content was based on Marshall stability and flow, air voids, and unit weight. All mixtures had voids in mineral aggregate (VMA) greater than the minimum of 14 percent.

Sample Preparation for Temperature and Moisture Susceptibility Specimens

A Hveem kneading compactor was used to compress all the samples prepared for this testing with sufficient energy to

TABLE 3 PHYSICAL PROPERTIES OF ASPHALT CEMENT

Test	Witco AR4000	AC 10	AC 20R
Viscosity:			
140F, Poise	2184		1071
275F, cSt	268		---
Penetrations:		Not Available	
77F, 100g/5sec.	54		---
Ductility, cm			
Toughness and	---		85.7
Tenacity	---		75.2
(20-in./min in. lb.)			
After Aging:			
Viscosity:			
140F, Poise	3880		
275F, cSt	345		3427

Penetrations:		Not Available	
77F, 100g/5sec.	34		---
Ductility, cm	100+		31

TABLE 4 RESULTS OF MARSHALL MIX DESIGNS

Aggregate/ Asphalt	Marshall Stability (lbs.)	Marshall Flow (0.01 in.)	Air Voids (%)	Unit Weight (pcf)	Asphalt Content+ (%)	
Helm's Agg.						
AR 4000	1350	8	7.4	137.2	5.5	
	1410	8	6.2	138.0	6.0	
	1678	11	4.7	139.2	6.5	
	2354	11	3.4	140.3	7.0	*
	1569	11	0.32	138.9	7.5	
IH-70 Agg.						
AC 20R**	2325	14	11.2	138.8	4.5	
	2464	15	8.2	144.8	5.0	
	2471	17	7.8	141.5	5.5	*
	2007	14	6.7	141.1	6.0	
	1912	13	5.9	135.4	6.5	
Redmond Agg.						
AC 10	1275	14	5.5	139.0	4.5	
	1498	16	4.4	139.7	5.0	*
	1378	14	2.6	141.6	5.5	
	1360	13	1.6	142.0	6.0	
	1299	16	0.5	142.8	6.5	
Staker Agg.						
AC 10	1757	12	4.4	150.7	4.5	*
	1654	11	3.1	151.5	5.0	
	1514	14	2.4	151.6	5.5	
	1338	20	1.3	152.1	6.0	
	1242	18	0.6	152.3	6.5	
Weaver Agg.						
AC 10	1335	10	7.7	138.9	4.5	
	1586	12	5.3	141.5	5.0	
	1385	10	4.4	141.9	5.5	*
	1335	10	3.7	142.0	6.0	
	1242	11	3.1	142.1	6.5	

* Asphalt cement content chosen as optimum

** Difficulties were encountered in achieving air voids; opt. asphalt content was based on maximum stability.

\+ By dry weight of aggregate.

produce samples with air voids between 6 and 8 percent (30 blows, 250 psi, and leveling load of 11,600 lb). A change from Marshall to Hveem compaction achieved an aggregate-asphalt matrix that would better simulate field conditions (*4*). A set of six samples was prepared for each mixture.

Samples were stored at 140°F for 15 hr, and then moved to a 230°F oven 2 hr before compaction (*5*). They were then tested according to the flow chart shown in Figure 1. Resilient moduli values were determined at a load duration and interval of 0.1 and 2.9 sec, respectively. Values were determined for 0°F, 34°F, 77°F, and 104°F according to ASTM D4123.

Indirect tensile strengths were determined using a constant 2-in./min deformation rate at 77°F (ASTM D4123).

ANALYSIS OF TEST RESULTS

Temperature Susceptibility

Table 5 indicates that some stiffening of the mixture generally existed, in agreement with previous research (*6,7*).

Figures 2 and 3 show examples of typical resilient modulus versus temperature for two of the mixtures. The changes in temperature susceptibility vary between mixtures. Figure 2 shows that the mixtures with Helm's aggregate and AR–4000 varied at temperatures less than 77°F, and exhibited little change at 104°F. Figure 3 shows trends exhibited by the remaining materials—addition of lime slightly stiffens the mixtures, regardless of type or percentage of lime.

Moisture Susceptibility

The addition of lime has various effects both on the absolute values of the resilient modulus and on tensile strengths, with either initial or Lottman conditioning (see Table 6). In two cases (see Figures 4 and 5) there is a slight softening (i.e., decrease in resilient modulus) of approximately 50 ksi from the initial material stiffness. However, this decrease may not be significant. Figures 6–8 show a slight-to-moderate increase of 75 to 250 ksi in initial material stiffness when either lime is added. The absolute value for resilient modulus after conditioning shows improvement in all cases (see Figures 4–8).

Both the initial and conditioned tensile strengths generally exhibit trends similar to those for resilient modulus. A slight initial decrease in resilient modulus with the addition of lime results in a corresponding trend for the tensile strength (see Figure 4). The addition of lime increases the after-conditioned tensile strengths (see Figures 4–8) for all mixtures, regardless of type of binder or aggregate source. These increases varied from as little as 15 psi to as much as 50 psi over the original values.

Overall moisture sensitivity, as determined by the ratios, decreased for all mixtures regardless of binder type or aggregate source. Figure 4 shows an improvement of 30 to 40 per-

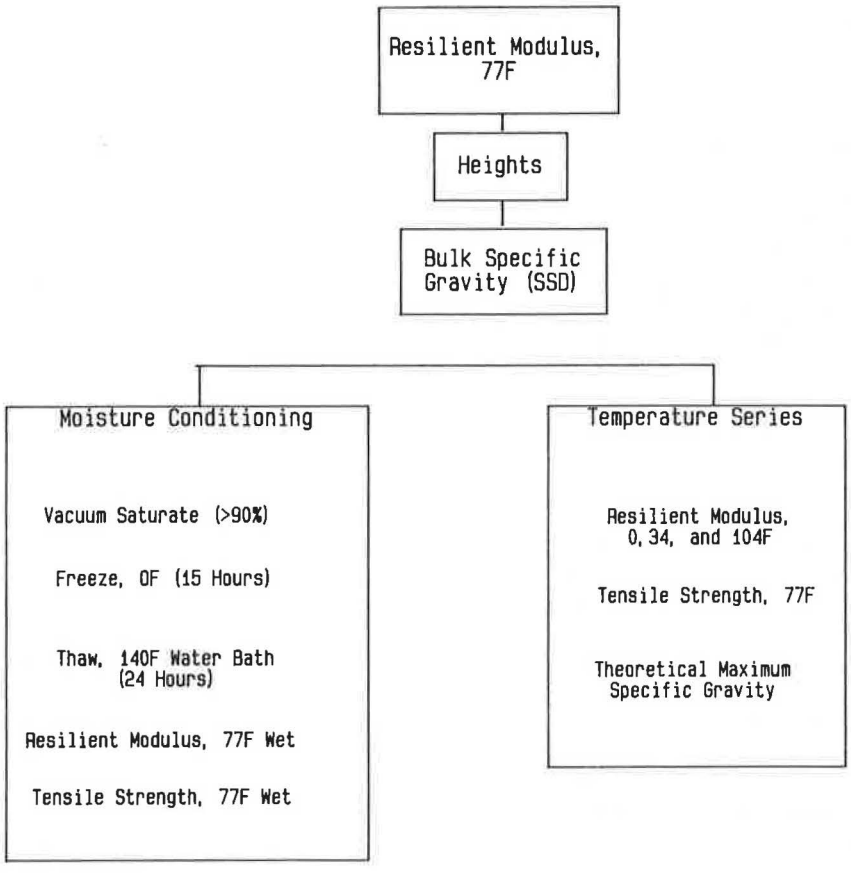

FIGURE 1 Flow chart of testing sequence.

TABLE 5 TEST RESULTS FOR LOTTMAN-ACCELERATED CONDITIONING

Aggregate Source	Resilient Modulus, 1000 psi			Tensile Strength, psi		
	77°F Dry	77°F Wet	Ratio	77°F Dry	77°F Wet	Ratio
Helm's-AR 4000						
No Lime	474	262	54	168	89	53
Dolomitic						
1.0 Percent	NA	NA	NA	159	123	78
1.5 Percent	400	341	85	155	131	84
Normally Hydrated						
1.0 Percent	NA	NA	NA	134	104	78
1.5 Percent	430	414	96	157	140	89
IH-70-AC 20R						
No Lime	167	52	31	59	32	54
Dolomitic						
1.0 Percent	148	91	62	56	46	82
1.5 Percent	122	104	88	67	65	97
Normally Hydrated						
1.0 Percent	178	116	66	63	63	101
1.5 Percent	235	153	65	64	72	112
Redmond-AC 10						
No Lime	228	121	53	78	46	59
Dolomitic						
1.0 Percent	346	232	67	78	85	101
1.5 Percent	309	244	79	72	62	89
Normally Hydrated						
1.0 Percent	273	220	80	65	59	92
1.5 Percent	304	279	92	64	68	105
Staker-AC 10						
No Lime	214	64	30	80	23	30
Dolomitic						
1.0 Percent	288	158	65	87	59	68
1.5 Percent	317	182	58	83	59	71
Normally Hydrated						
1.0 Percent	273	132	49	78	53	69
1.5 Percent	434	159	37	189	67	36
Weaver-AC 10						
No Lime	110	24	23	66	34	52
Dolomitic						
1.0 Percent	137	94	69	82	72	88
1.5 Percent	179	131	74	78	76	98
Normally Hydrated						
1.0 Percent	162	126	78	91	92	101
1.5 Percent	168	143	85	102	87	85

cent for either resilient modulus or tensile strength ratios for mixtures with the Nevada aggregate and AR–4000 binder. Figure 5 shows an improvement of over 50 percent for either ratio for mixtures with a Utah aggregate (IH-70) and a latex-modified AC–20R binder. Figures 6–8 show improvements of 20 to 60 percent for either ratio for mixtures with various Utah aggregates and an AC–10 binder.

In summary, all mixtures show a substantial decrease in moisture susceptibility with either dolomitic or normally hydrated lime. The magnitude of improvement appears to depend on both the quantity of a particular lime and the specific aggregate-asphalt mixture.

CONCLUSIONS

The following conclusions can be drawn from this research:

1. The addition of either dolomitic or normally hydrated lime, in the quantities covered by this research program, appears to cause a slight increase in mixture stiffness.
2. All mixtures studied had a significant decrease in moisture sensitivity when either dolomitic or normally hydrated lime was added, regardless of the various aggregates sources (Nevada and Utah) and binder types (AR–4000, AC–20R, AC–10) used in this study.

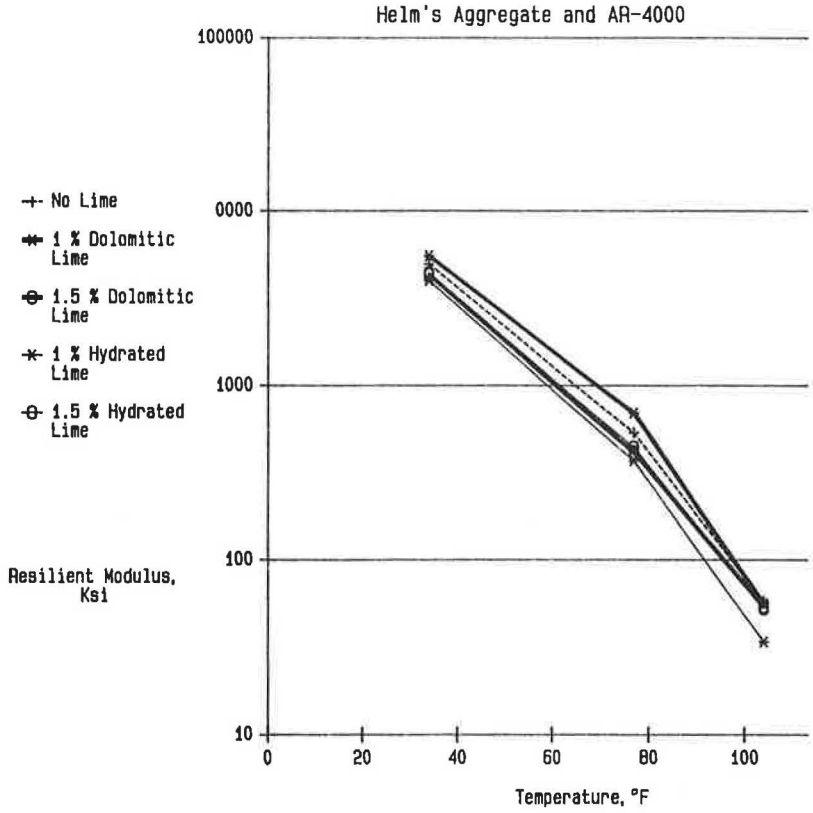

FIGURE 2 Resilient modulus at various test temperatures for mixtures prepared with Helm's aggregate and various types of lime.

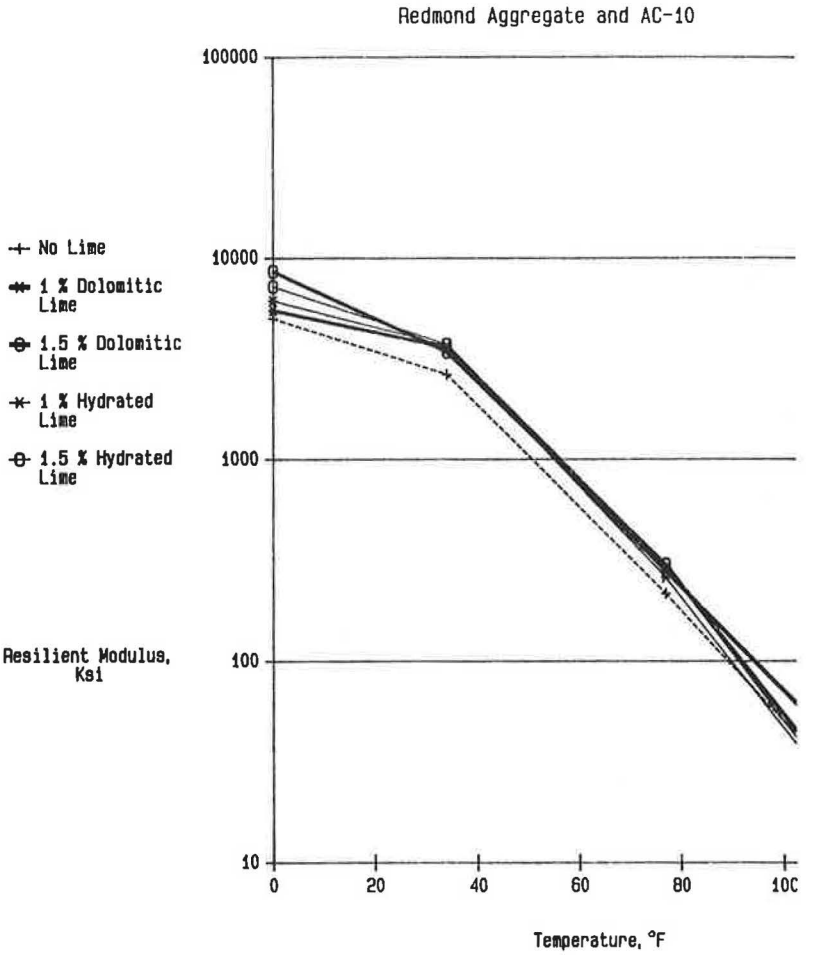

FIGURE 3 Resilient modulus at various test temperatures for mixtures prepared with Redmond aggregate and various types of lime.

TABLE 6 RESILIENT MODULUS VALUES AT VARIOUS TEST TEMPERATURES—HELM'S AGGREGATE WITH AR-4000

Aggregate Asphalt	Resilient Modulus, 1000 psi			
	0°F	34°F	77°F	104°F
Helm's-AR 4000				
No Lime	10956	5854	567	38
Dolomitic				
1.0 Percent	100018	5551	695	56
1.5 Percent	5996	5976	502	55
Normally Hydrated				
1.0 Percent	7612	3996	369	34
1.5 Percent	12014	6883	528	45
IH-70-AC 20R				
No Lime	4169	1128	152	19
Dolomitic				
1.0 Percent	2985	1880	159	23
1.5 Percent	4928	2223	239	30
Normally Hydrated				
1.0 Percent	4521	1806	211	27
1.5 Percent	5399	1553	201	27
Redmond-AC 10				
No Lime	4995	2644	216	39
Dolomitic				
1.0 Percent	5502	3583	279	56
1.5 Percent	5245	2674	305	47
Normally Hydrated				
1.0 Percent	5416	2428	251	41
1.5 Percent	5220	3165	306	50
Staker-AC 10				
No Lime	12042	2800	201	34
Dolomitic				
1.0 Percent	*	3504	383	56
1.5 Percent	*	3533	402	62
Normally Hydrated				
1.0 Percent	*	2867	261	44
1.5 Percent	7089	3955	427	74
Weaver-AC 10				
No Lime	5285	2115	101	15
Dolomitic				
1.0 Percent	6675	3157	166	23
1.5 Percent	7048	1859	179	23
Normally Hydrated				
1.0 Percent	*	4812	143	21
1.5 Percent	*	5775	190	27

* Values in excess of equipment range

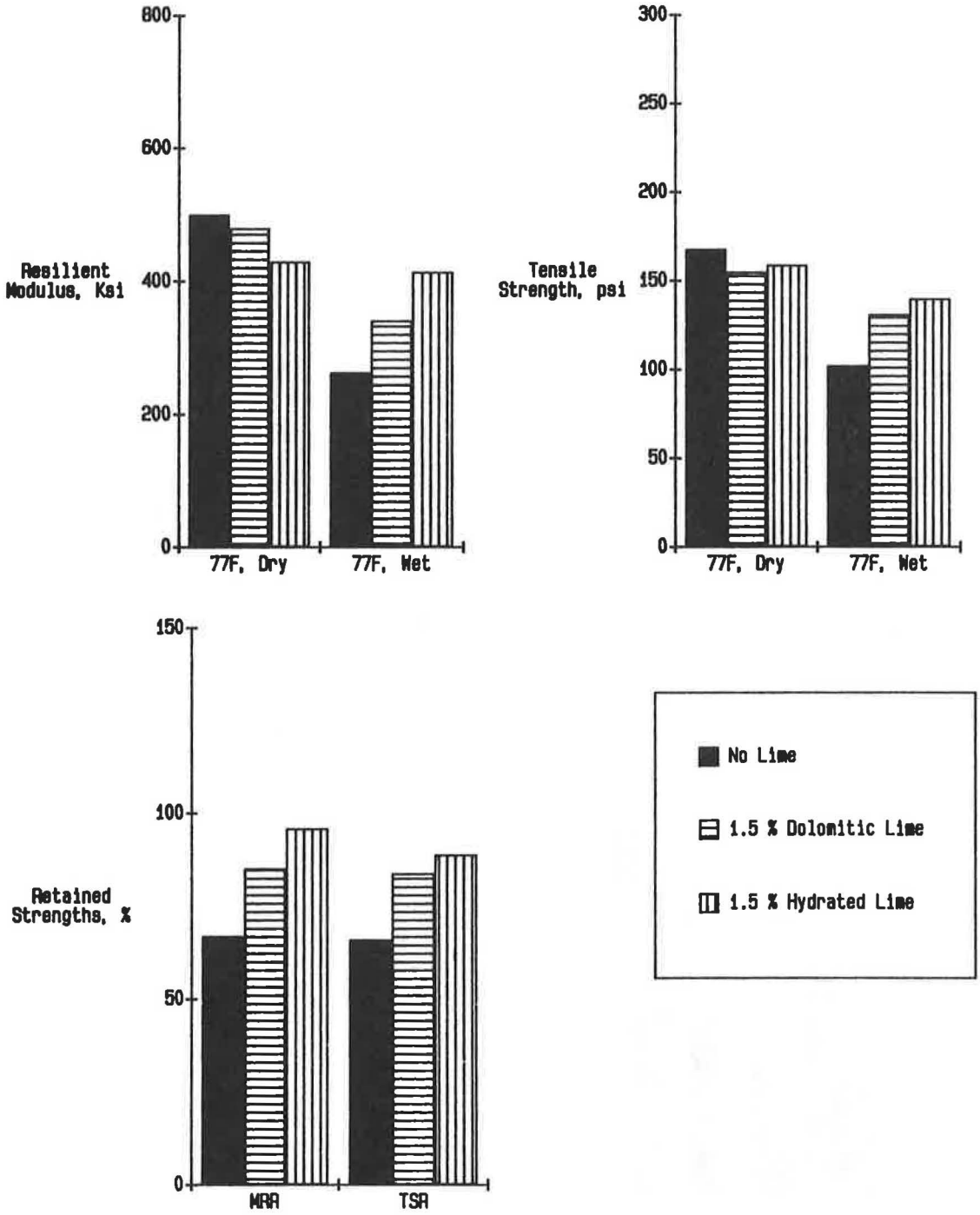

FIGURE 4 Test results after Lottman conditioning for Helm's aggregate.

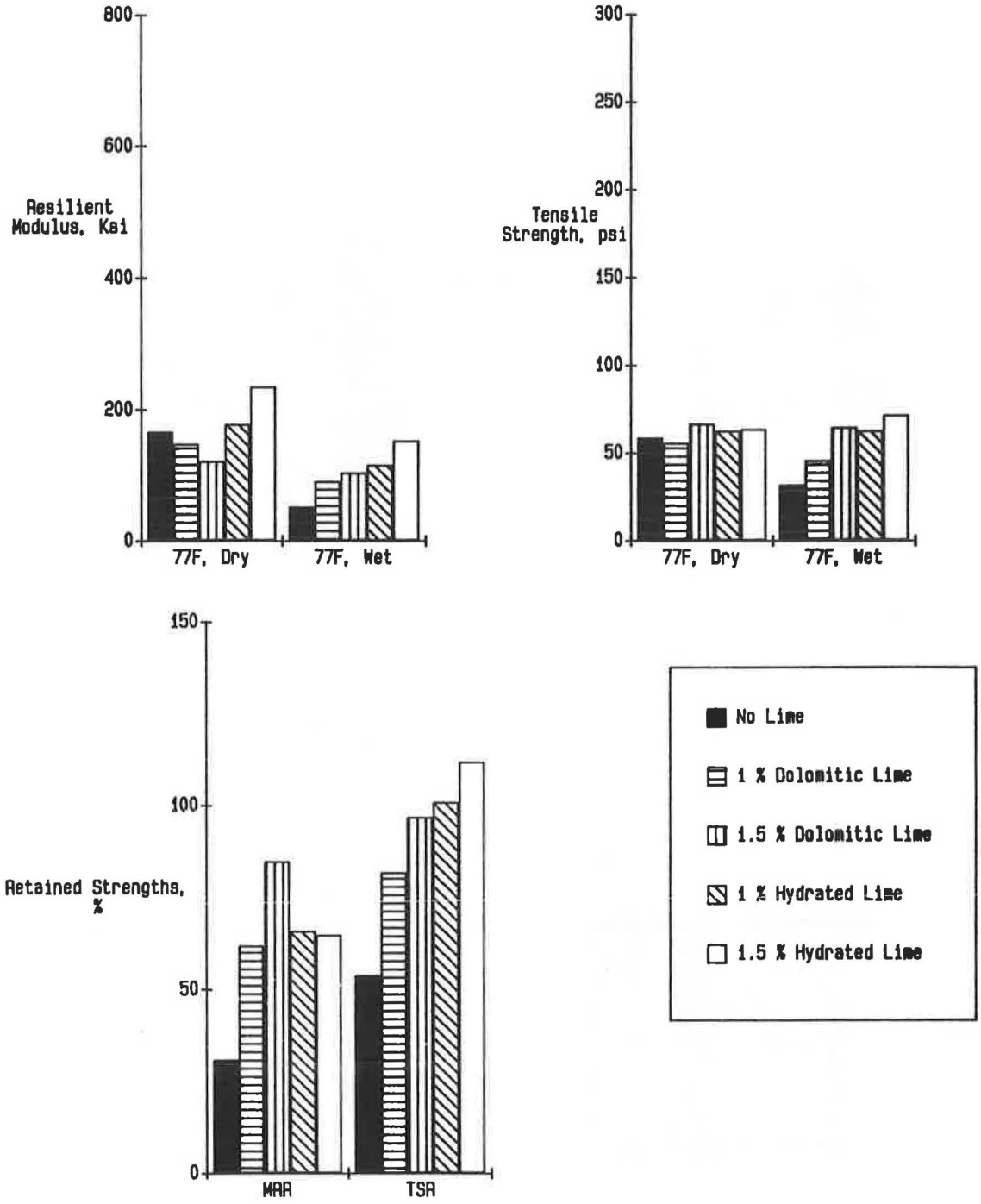

FIGURE 5 Test results after Lottman conditioning for IH-70 aggregate.

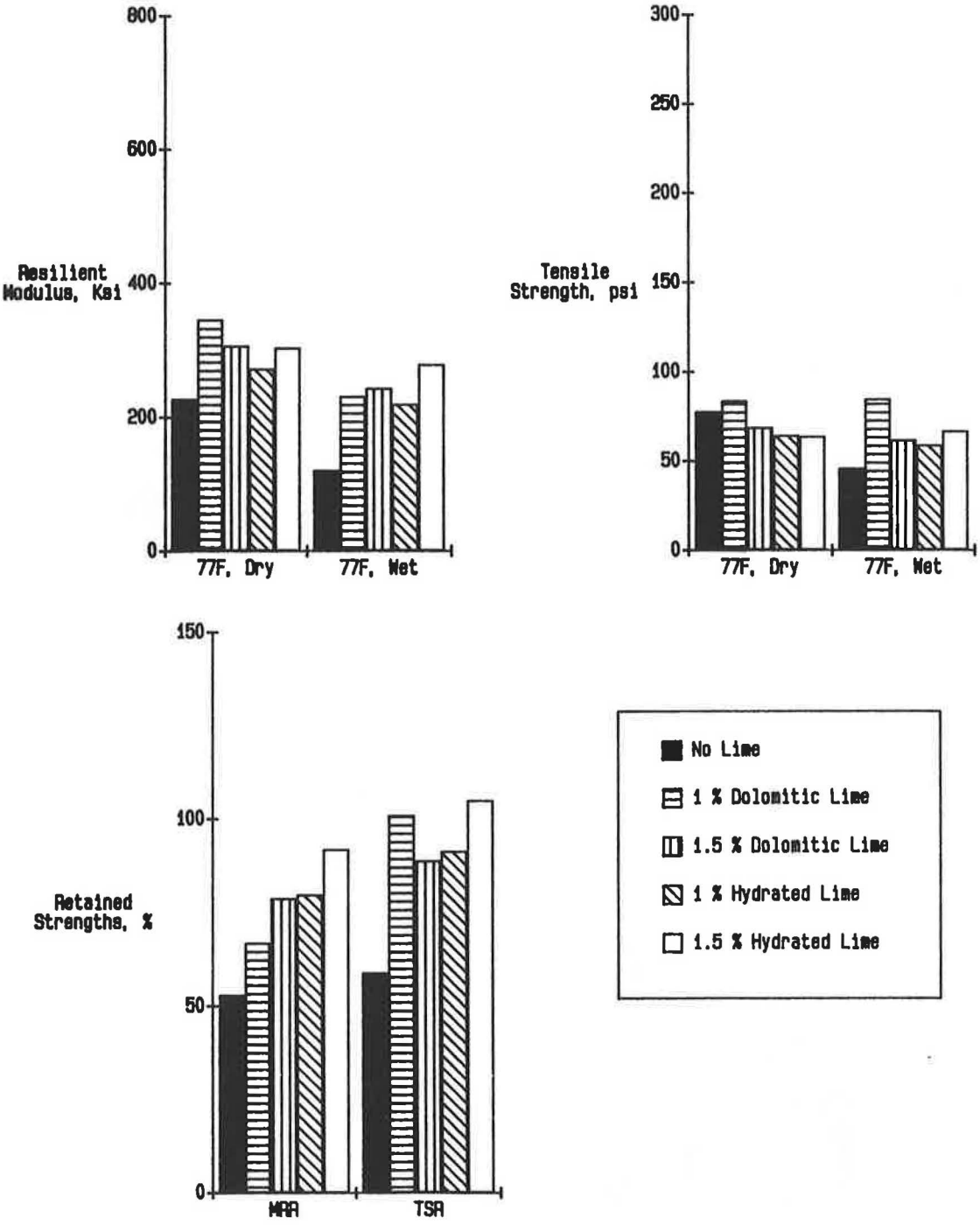

FIGURE 6 Test results after Lottman conditioning for Redmond aggregate.

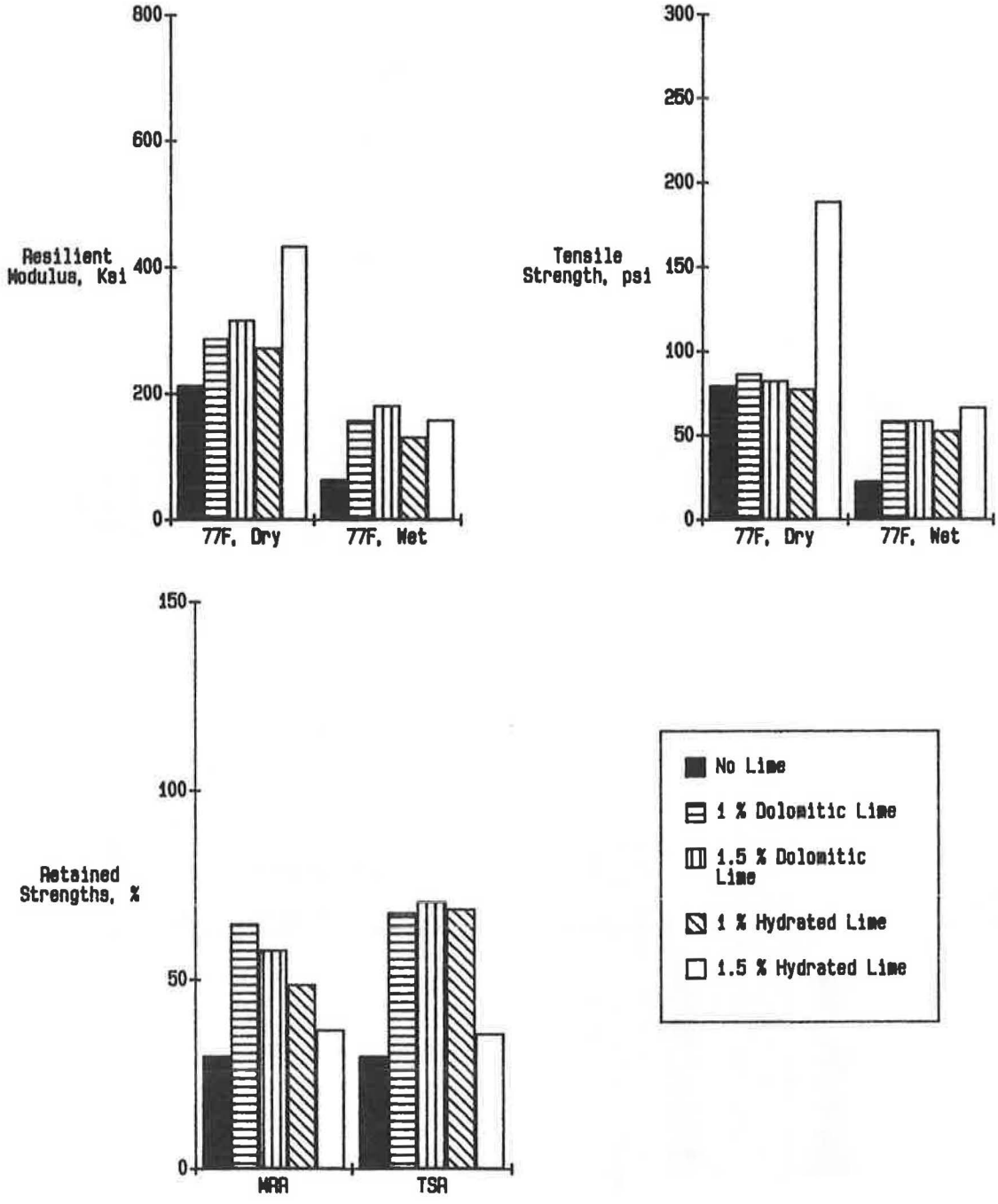

FIGURE 7 Test results after Lottman conditioning for Staker aggregate.

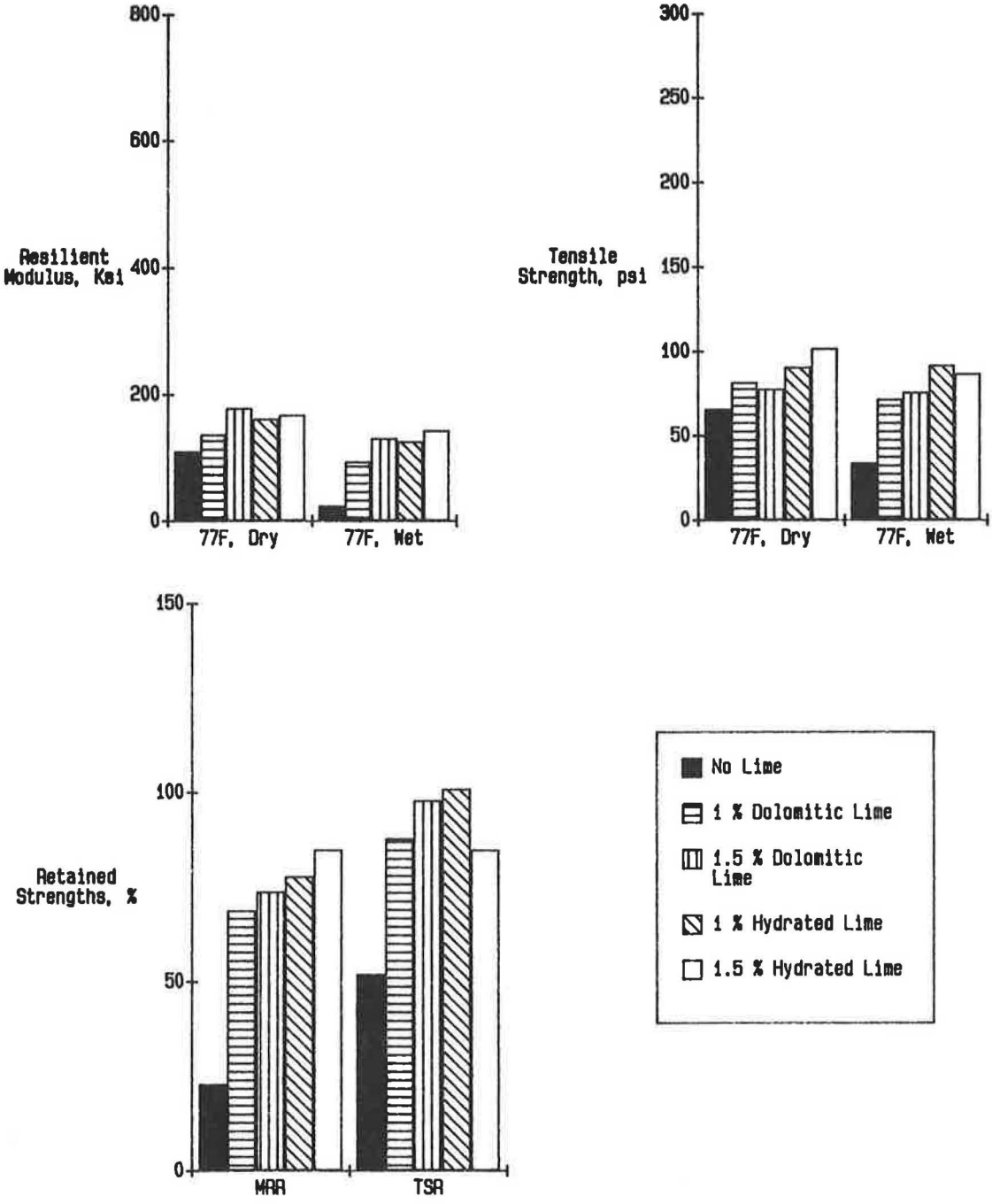

FIGURE 8 Test results after Lottman conditioning for Weaver aggregate.

3. The magnitude of the improvement appears to be unique to each aggregate-asphalt-lime system.

ACKNOWLEDGMENT

The authors would like to thank Chemstar Lime Co., Inc., for continuing support of research related to identifying methods of decreasing the moisture sensitivity, and thereby increasing the life, of asphalt concrete pavements.

REFERENCES

1. *Lime Plants and Products*. Chemstar (formerly Genstar) Cement and Lime Co., Henderson, Nev., undated.
2. M. Stroup-Gardiner, D. E. Newcomb, H. Anderson, and J. E. Epps. *Influence of Lime on the Fines Content of Asphalt Concrete*. ASCE, Nashville, Tenn., Feb. 1988.
3. *Mix Design Methods for Asphalt Concrete*. Manual Series No. 2, The Asphalt Institute, Lexington, Ky., 1984.
4. H. L. Von Quintus, J. A. Scherocman, C. S. Hughes, and T. W. Kennedy. *AAMAS-Procedures Manual for Asphalt-Aggregate Mixture Analysis, Phase II*, Vol. III, Brent Rauhut Engineering, Austin, Tex., Sept. 1988.
5. *Manual of Testing*, Vol. 2, No. 304, Transportation Laboratory, California Department of Transportation, 1978.
6. M. Stroup-Gardiner, J. A. Epps, and H. Waite. Four Variables That Affect the Performance of Lime in Asphalt-Aggregate Mixtures. In *Transportation Research Record 1115*, TRB, National Research Council, Washington, D.C., 1987.
7. D. Dunn, M. Stroup-Gardiner, and D. Newcomb. *The Effectiveness of Lime as an Anti-Strip Additive with Various Aggregate Sources*. Department of Civil Engineering, University of Nevada, Reno, Dec. 1987.

Publication of this paper sponsored by Committee on Characteristics of Nonbituminous Components of Bituminous Paving Mixtures.

Comparative Study of Manganese-Treated and Conventional Asphalt Concrete Mixtures and Pavements

J. LUDWIG FIGUEROA AND KAMRAN MAJIDZADEH

A typical rehabilitation alternative of roadways that have reached their serviceability level is the construction of asphalt concrete (AC) overlays on either rigid or flexible pavements. However, overlays constructed with conventional AC tend to reflect the cracking and jointing patterns of existing pavements a short time after their placement. Other typical distresses observed in conventional AC mixtures are fatigue cracking, stripping, and moisture damage. A manganese-based AC additive (CTI–101, Chemkrete) has been claimed to minimize some of these problems. The Ohio Chemkrete test section was built at a location subjected to average climatic and traffic conditions. Whether the additive led to any beneficial performance gains or, at least, to equal performance for the same cost of conventional AC overlays was studied. The study compared condition surveys (consisting of pavement condition rating and crack surveys), Dynaflect deflection measurements, and laboratory testing of field-procured specimens that obtained values of resilient modulus, Marshall stability, indirect tensile strength, fracture toughness, creep compliance, and fatigue. Results of laboratory tests performed on field-procured cores indicated better performance by conventional AC specimens than by the Chemkrete-treated specimens. On the basis of results of core testing, VESYS III computer model rut depth calculations predicted that rut depths would be approximately twice the magnitude along the Chemkrete-treated section than along the control section. Dynaflect deflection measurements indicated a slightly better performance on the control section than on the Chemkrete-treated section. No significant gains in the engineering properties of AC mixtures are obtained with the addition of Chemkrete.

Prolonging the service life of pavements has been a subject of major concern for highway and materials engineers. As the expansion of the highway network reached its apparent limit in the United States, and with the increased amount of traffic on most of these roads, attention has been directed towards maintenance and rehabilitation.

A typical rehabilitation alternative is the construction of asphalt concrete (AC) overlays on either rigid or flexible pavements that have reached their minimum acceptable serviceability level. However, a short time after their placement overlays constructed with conventional AC tend to reflect the cracking and jointing patterns of the existing pavements. Other typical distresses observed in conventional AC mixtures are fatigue cracking, stripping, and moisture damage. Some of these problems may be minimized with the use of additives in the AC. These additives are claimed to affect the properties of the AC by producing mixtures in which softer asphalts can be used without impairing the high-temperature stability of the mixture, while not becoming as brittle at low temperatures (*1*).

A manganese-based AC additive (CTI–101) developed by Chemkrete Technologies, Inc., has been claimed to produce these beneficial effects (*1,2*). The apparent success in improving desirable properties in the laboratory, reported by several authors, has encouraged state highway officials to set up experimental pavement sections containing this additive to determine whether or not pavement performance improvements result under actual working conditions (*1,3–6*).

Several test sections containing CTI–101 (Chemkrete) as an additive, as well as adjacent control sections containing conventional AC, have been built in several states, with mixed performance results. The Ohio Chemkrete test section was built at a location subjected to average climatic and traffic conditions. The objective of the study was to determine whether the additive led to any beneficial performance gains or, at least, equal performance for the same cost of AC overlays.

PREVIOUS LABORATORY EXPERIENCE

Extensive laboratory testing of Chemkrete-modified and conventional AC specimens was undertaken by several researchers to determine if the addition of Chemkrete produced any significant improvement in the physical and engineering properties of asphalt concrete mixtures (*1,4,6*).

Chemkrete-modified AC mixtures had a more desirable behavior than conventional AC mixtures when tested in the laboratory. However, a significant amount of curing time was required before these beneficial properties materialized. This result may have some implications on placement conditions as well as on the length of time before allowing traffic on a new construction project. The most important gains, in some cases, were a reduction in the temperature susceptibility, as indicated by a flatter temperature-viscosity relationship and the possibility of using marginal-quality aggregates in the preparation of AC mixtures.

PREVIOUS FIELD EXPERIENCE

Experimental pavement sections using Chemkrete have been built in several states with various degrees of success (*7–10*). Moulthrop and Higgins (*3*) also reported a total of 44 projects

J. L. Figueroa, Department of Civil Engineering, Case Western Reserve University, Cleveland, Ohio 44106. K. Majidzadeh, Resource International, Inc., Westerville, Ohio 43081.

containing Chemkrete-modified asphalts built in a variety of climates in the United States between January 1980 and August 1984.

In previous studies, it was expected that the addition of Chemkrete to AC mixtures would result in a reduction of their temperature susceptibility leading to less rutting or shoving at high temperatures and less thermal distress at low temperatures. Other benefits would include (a) a longer pavement life because of greater load-carrying capacity as a result of resilient modulus and indirect tensile strength increases at high temperature, (b) lower cost because of reduced section thickness for equal performance, and (c) the possibility of using less costly aggregates. These studies indicated that Chemkrete-modified AC yielded more desirable properties than conventional AC when subjected to adequate curing in the laboratory. Conventional AC pavement sections, however, performed substantially better than Chemkrete-modified AC pavement sections when subjected to identical curing, climatic, and traffic conditions.

PROJECT DESCRIPTION

The Ohio Chemkrete test section is located on US-23 near the Delaware-Marion county line. At that location, US-23 is a 4-lane, divided highway carrying an average daily traffic of 18,425 vehicles, with a direction distribution factor of 50 percent, and 23 percent of the traffic consisting of trucks.

Two Chemkrete test sections were placed in July 1984; a 2-mi-long section in the travel lane of the northbound direction, and a 1-mi-long section, also in the travel lane, of the southbound direction. The original plans called for the passing lanes in both directions to be used as control sections; however, because of the difference in the number and composition of traffic this procedure was changed to select the control sections on the travel lanes (northbound and southbound), following the Chemkrete-modified sections.

The existing pavement consisted of 9 in. of badly cracked portland cement concrete pavement on 6 in. of granular subbase, placed on a gently rolling terminal moraine deposit. The project called for the placement of a 3-in.-thick overlay consisting of a 1¼-in.-thick wearing course (Ohio Department of Transportation Type 404) on a 1¾-in.-thick leveling course (Type 402). Approximately 25 percent of the joints were full-depth repaired before overlay.

Mixture and Placement Characteristics

Limestone aggregate was mixed with AC–5 asphalt cement treated with 4 percent of Chemkrete (CTI–101) for the Chemkrete test section, whereas AC–20 asphalt cement was mixed with the same aggregate for the control section. A laboratory analysis of the AC–5 asphalt cement treated with 4 percent of Chemkrete yielded a dynamic viscosity equal to 250 poises. The test was conducted at 140°F following AASHTO T202 specifications.

The grain size distribution for the aggregate used in the AC for the wearing course met Ohio 848, Type I, specifications. The grain size distribution for the aggregate used in the AC for the leveling course met Ohio 848, Type II, specifications. The maximum-sized aggregate was limited to 1 in. for the leveling course and to ½ in. for the wearing course.

Mixture design, by the Marshall method, indicated required AC contents of 5.9 percent by weight for the wearing course and 5.1 percent by weight for the leveling course. A recommended 4 percent Chemkrete dosage by weight of binder yielded an average 0.089 percent manganese content by weight of binder (after testing representative samples), as compared to a target of a 0.08 percent content. Tested samples ranged from 0.082 to 0.104 percent in manganese content by weight of binder.

Construction Procedure

The construction procedure for Chemkrete-modified AC pavements is similar to that of conventional AC pavements. The only variation is the addition of Chemkrete to the AC before blending it with the aggregate. The Chemkrete AC blending may be done in a heated storage tank that requires prolonged mixing or at the nozzle before spraying the AC on the heated aggregate.

The AC used in the construction of the test section was prepared with the specified proportions at a mixing plant and transported to the site where it was compacted with a pneumatic breakdown roller, followed by a vibratory intermediate, and a heavy, tandem finish roller.

Temperature during placement ranged between 255°F and 275°F. Minor cracking was noticed in the northbound Chemkrete section after rolling; however, overnight traffic knitted the pavement together. The southbound section showed heavy segregation and low AC content, leading to raveling when traffic was permitted onto this section. The section was immediately removed and repaved (*2*).

Initial Performance Observations

Initial performance observations obtained 5 months after overlay placement are presented in Table 1 (*2*). Before the first winter, the conventional AC pavement section was performing better than the Chemkrete-treated AC pavement section. No apparent drainage-associated distress was observed at either the Chemkrete or the control sections. Although some of the most distressed joints were full-depth repaired along both the Chemkrete and the control sections, reflection cracking still occurred at these joints, showing not one but two reflected cracks.

TESTING PROGRAM AND ANALYSIS

The investigation of Chemkrete-modified AC pavements included the comparison of their performance with that of conventional AC pavements. The comparison included PCR and crack condition surveys, Dynaflect deflection measurements, and the laboratory testing of field-procured specimens to obtain pertinent physical and engineering properties.

The following discussions will be limited to the presentation of test results and the identification of any noticeable and consistent behavioral trends of field-obtained, Chemkrete-

TABLE 1 INITIAL PERFORMANCE OBSERVATIONS

	Control Section	Chemkrete Section
Texture	Good	Good
Edge Cracking	None	None
Reflective Cracking	Many Joints	Almost every Joint
Average Crack Spacing	98.3	58.9*
Spacing (ft)		

*Approximate Joint Spacing

modified and conventional AC specimens, as well as of the actual field test sections.

Condition Survey

The field condition survey included periodic PCR determinations and crack surveys to ascertain the pavement overlay performance with time and an increased number of vehicles, for both Chemkrete-treated and untreated pavement sections.

Reflection cracking surveys were conducted in December 1984, in May and October 1985, and in April 1986, leading to the results presented in Table 2. Pavement condition surveys were also performed on May 17, 1985, and April 7, 1986 (see Table 3).

Comparisons can be made between the PCR obtained on the Chemkrete and the control sections. Results of the earlier PCR determination indicated that the Chemkrete-treated section was performing slightly better than the control section. The second and more detailed (on a joint by joint basis) PCR determination, obtained approximately 1 year later, indicated slightly better performance on the control section than on the Chemkrete section.

Dynaflect Deflection Measurements

Dynaflect deflection measurements, provided by ODOT, were used as an added method to measure the relative performance of Chemkrete-treated AC pavements with respect to the performance of conventional AC pavements. Existing data, however, do not distinguish between deflection measurements obtained at the joint on the approach or leave slab or at midslab, making it difficult to draw any conclusions regarding pavement performance with respect to time or seasonal variations.

Dynaflect deflection measurements were obtained on two different occasions: September 27, 1984, and December 4, 1985. Figures 1 and 2 show the deflection measured with the first sensor (W1), and the spreadability (SPR%) defined by the equation

$$\text{SPR}\% = \frac{W1 + W2 + W3 + W4 + W5}{5\,W1} \times 100 \qquad (1)$$

where $W1$, $W2$, $W3$, $W4$, and $W5$ are the deflections measured with the first, second, third, fourth, and fifth sensors, respectively.

Measurements at the two different times have been presented to determine whether there are any significant changes

TABLE 3 AVERAGE PAVEMENT CONDITION RATINGS

	MAY 1985	APRIL 1986
CHEMKRETE (Northbound)		
20.0 - 20.5 (DEL)	93.0	84.0
20.5 - 21.0 (DEL)	90.0	89.0
21.0 - 21.5 (DEL)	91.0	82.0
00.0 - 0.5 (MAR)	90.0	89.0
CONTROL (Pass-Northbound)		
0.5 - 1.0 (MAR)	89.0	87.0
1.0 - 1.5 (MAR)	89.0	89.0

DEL = Refers to Delaware County Log Mile on US-23

MAR = Refers to Marion County Log Mile on US-23

TABLE 2 REFLECTION CRACKING SURVEY

DATE	CHEMKRETE	CONTROL
December, 1984	Low	Very Low
May, 1985	Low-Medium and Extensive	Medium and Extensive
October, 1985	Medium and Extensive	Medium and Extensive
April, 1986	Medium and Extensive	Medium and Extensive

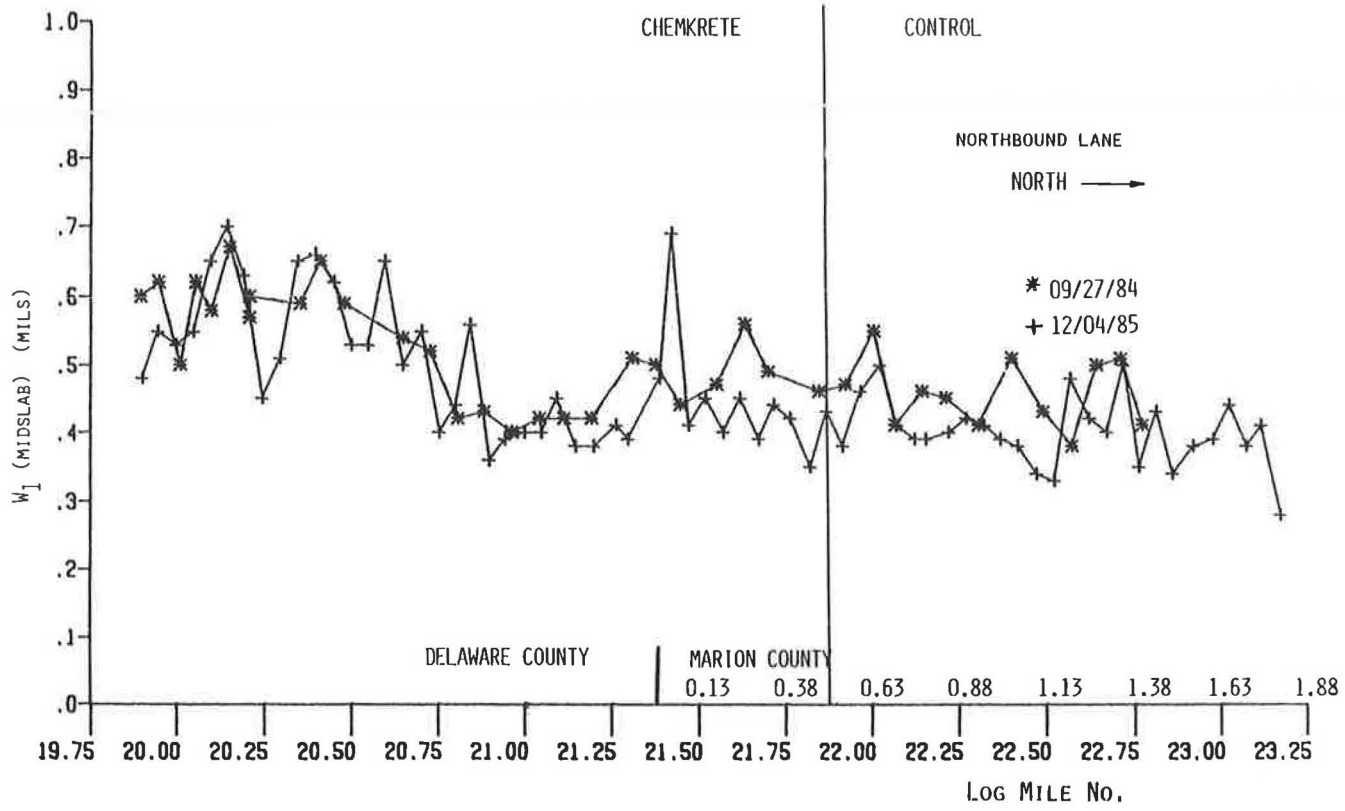

FIGURE 1 First sensor Dynaflect deflections along the Chemkrete and control sections.

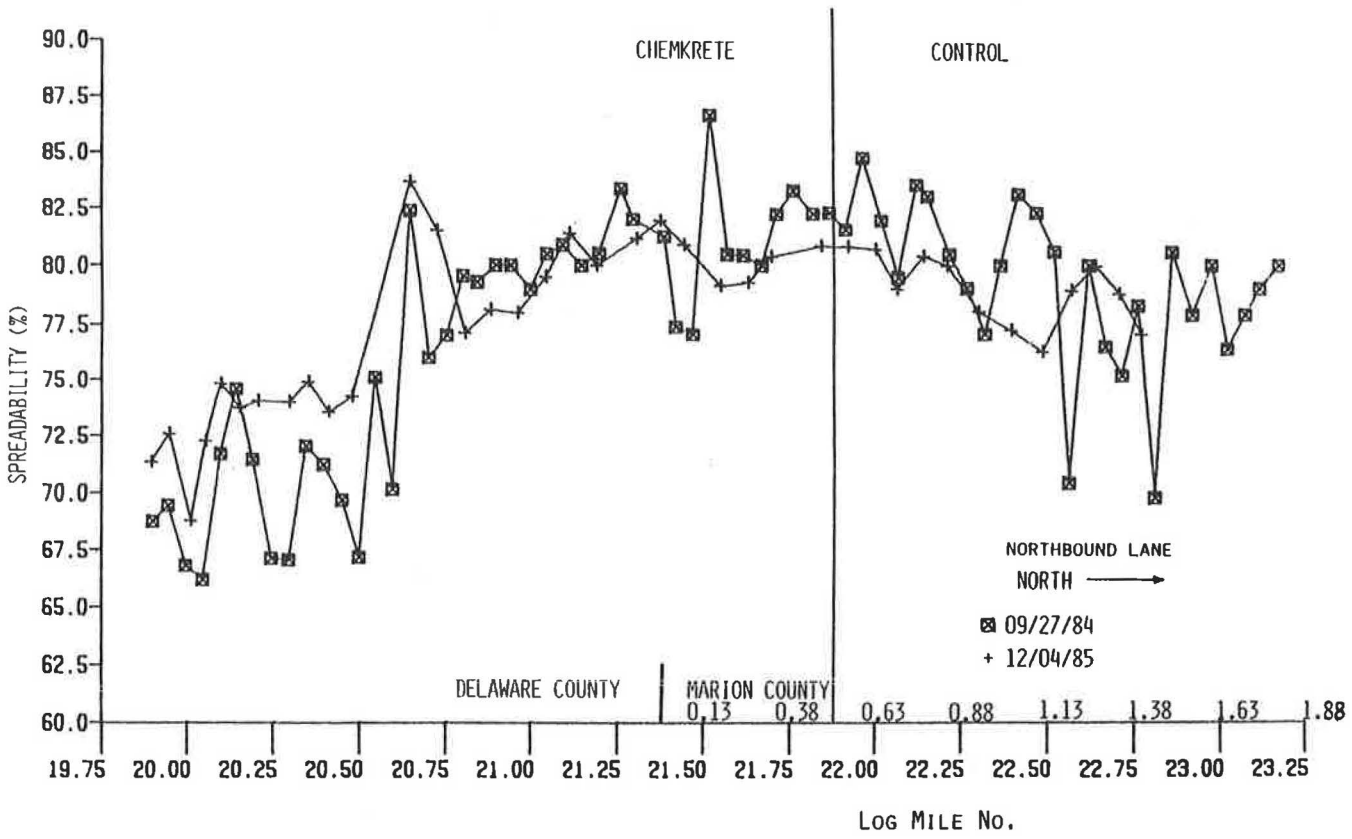

FIGURE 2 Spreadability (from Dynaflect measurements) along the Chemkrete and control sections.

in the relative performance of the Chemkrete and control sections with time and additional traffic.

The observation of the deflection measurements obtained with the first sensor, *W*1 (see Figure 1), generally indicated that higher deflections (less favorable) were obtained on the Chemkrete-treated section than on the control section. Near the boundary between the Chemkrete and control sections, the variations in *W*1 and spreadability were less than at stations farther apart. This result may indicate the influence of subgrade variability on the Dynaflect deflection measurements. Spreadability values were, in general, lower on the Chemkrete section (also less favorable) than on the control section as shown in Figure 2. Dynaflect testing results indicate slightly more favorable values on the conventional AC than on the Chemkrete-treated section.

Laboratory Testing of Field Cores

Field-extracted cores from both the Chemkrete-modified and control sections were subjected to resilient modulus, Marshall stability, indirect tensile strength, fracture toughness, creep compliance, and fatigue tests. All extracted cores were 4 in. in diameter and extended through both the wearing and leveling courses. In some cases, it was difficult to drill through the leveling course because some of the cores crumbled during extraction, probably from lack of adequate compaction during construction or lack of adequate curing. Wearing course specimens, in some cases, were also thinner than 1 in., which presented difficulties in the testing of the disc-shaped specimens.

The diametrical modulus of resilience is commonly applied to asphaltic mixtures. A dynamic load of known duration and magnitude (below the indirect tensile strength of the sample) is applied across the vertical diameter of a Marshall-sized specimen, and the elastic deformation across the horizontal diameter is measured with displacement transducers. The resilient modulus M_r is calculated using the equation

$$M_r = \frac{P\,(\mu + 0.2734)}{\Delta t} \tag{2}$$

where

P = magnitude of dynamic load,
μ = Poisson's ratio,
t = specimen thickness, and
Δ = total deformation.

The ultimate strength of asphaltic mixtures under an indirect tensile stress field is obtained after diametrically applying a vertical load, at a rate of advance of the load piston of 0.065 in./min, until the maximum load (yield strength) that the specimen is able to withstand is reached. The indirect tensile strength σ_y is calculated using the equation

$$\sigma_y = \frac{2P}{\pi D t} \tag{3}$$

where

P = maximum load (lb),
D = specimen diameter (in.), and
t = specimen thickness (in.).

Both resilient modulus and indirect tensile strength tests were conducted at 40°F, 70°F, and 100°F to account for temperature influences expected during the life of the pavement.

Some of the specimens tested for resilient modulus and indirect tensile strength were subjected to Lottman's accelerated moisture damage system to determine their durability under freezing and thawing. The procedure consists of the vacuum saturation of Marshall-sized specimens after which they are subjected to freezing at 0°F for 15 hr while the specimens are wrapped, followed by their submersion in a 140°F distilled water bath for 24 hr.

The Ohio State University procedure was used to determine the fracture toughness K_{1c} of Marshall-sized specimens. The method consists of cutting a right-angled wedge into a Marshall-sized specimen and initiating a crack (usually 0.25 in. long) at the apex of the notch. The specimen is set on a base with the notch pointing upwards, and a vertical load is applied to it through a three-piece set-up consisting of two plates (placed against the sides of the wedge) and a semicircular rod placed between the two plates to transmit the load by wedging to the sides of the notch. The results of tests conducted at room temperature allowed the calculation of K_{1c} from the equation

$$K_{1c} = \frac{P}{t}\,(0.92 + 0.284c + 0.552c^2) \tag{4}$$

where

P = maximum applied load (lb),
t = specimen thickness (in.), and
c = initial crack length (in.).

The fracture toughness test provides pavement engineers with an additional parameter for evaluating cracking potential (one of the controlling asphalt pavement design criteria). K_{1c} is a material constant independent of crack geometry, loading conditions, or other physical variables (*11*).

The creep compliance and permanent deformation tests have been developed to determine the long-term effects of static and dynamic loads on the behavior of asphaltic mixtures. The contribution of asphaltic layers to rutting is measured in the laboratory by testing cylinders in dynamic compression or static creep, as specified in the VESYS II User's Manual (*12*). The procedure includes an incremental static-dynamic test in which specimens measuring 4 in. in diameter by 8 in. in height are used to determine the primary response, expressed as the creep compliance function, and the permanent deformation properties of asphaltic mixtures.

The permanent deformation properties are derived from incremental static-dynamic compression tests to define the fraction of the predicted total strain that is permanent, as a function of load cycles. The permanent strain, measured during the test, is plotted versus the number of load repetitions on a log-log scale, and a straight line is drawn to approximate the permanent strain within the expected range of loading. The permanent deformation properties are characterized by the parameters μ and α, defined as

$$\alpha = 1 - s \tag{5}$$

$$\mu = \frac{Is}{\varepsilon_{200}} \tag{6}$$

where

s = slope of the drawn line,
I = intercept at one load repetition, and
ε_{200} = resilient strain at the 200th load repetition.

The standard-sized specimen designated by the VESYS II procedure (cylindrical specimens, 4 in. in diameter by 8 in. in height) has been modified to accommodate field cores using specimens 4 in. in diameter by 1¼ to 1¾ in. in height. Values obtained from creep compliance and permanent deformation tests are used in conjunction with the VESYS III computer model to predict the amount of rutting in the treated and untreated pavements after a defined period of time.

Fatigue tests are useful in developing damage functions for the design of AC pavements when pavement failure by fatigue is identified as the design control factor. Results of fatigue testing were statistically analyzed to develop regression equations for damage functions of the form

$$N_f = K(1/\sigma)^n \quad (7)$$

where

N_f = number of load applications to failure,
σ = applied stress, and
K, n = regression constants.

Three sets of cores each were obtained at the Chemkrete and control sections to determine changes in engineering properties with time and traffic. The cores were obtained in September 1984, October 1985, and October 1986. It was particularly difficult to obtain enough intact cores in September 1984, because they crumbled during extraction. As previously indicated, this behavior probably results from insufficient curing of the mixture. Tables 4 and 5 present the results of laboratory testing of cores obtained in October 1985. These tables represent typical behavior observed at different sampling periods. A complete summary of all testing conducted at each sampling period has been provided by ODOT (*13*).

Test results indicate that specimens obtained from the control section yield, in general, slightly more desirable results than specimens obtained from the Chemkrete-treated section.

TABLE 4 PHYSICAL AND ENGINEERING PROPERTIES OF FIELD CORES AND WEARING COURSE CORES OBTAINED OCTOBER 1985

PARAMETER	UNTREATED	CHEMKRETE TREATED
	Average Value	Average Value
Thickness (in)	1.36 NB	1.36 NB
	1.08 SB	1.35 SB
Unit Weight (pcf)	142.1 NB	142.3 NB
	141.4 SB	143.9 SB
MR @ 40°F (x10^{6}psi)	2.19	1.32
MR @ 70°F (x10^{6}psi)	1.39	0.76
MR @ 70°F (x10^{6}psi) (a)	1.31	0.75
MR @ 70°F (x10^{6}psi) (b)	0.69	0.38
MR @ 100°F (x10^{6}psi)	0.26	0.14
σ_y @ 70°F (psi)	193	96
σ_y @ 70°F (psi) (a)	208	109
σy @ 70°F (psi) (b)	117	60
K_{1c} (psi $\sqrt{in}$)	917	419

(a) Vacuum Saturation Only

(b) Freeze and Thaw (Lottman's Procedure)

NB = Northbound Lane Specimens

SB = Southbound Lane Specimens

TABLE 5 PHYSICAL AND ENGINEERING PROPERTIES OF FIELD CORES AND LEVELING COURSE CORES OBTAINED OCTOBER 1985

PARAMETER	UNTREATED	CHEMKRETE TREATED
	Average Value	Average Value
Thickness (in)	1.81 NB 2.37 SB	1.82 NB
Unit Weight (pcf)	143.1 NB	145.7 NB
MR @ 40°F (x10^{6}psi)	1.84	1.87
MR @ 70°F (x10^{6}psi)	1.10	0.90
MR @ 70°F (x10^{6}psi) (a)	0.91	1.01
MR @ 70°F (x10^{6}psi) (b)	0.76	0.60
MR @ 100°F (x10^{6}psi)	0.28	0.15
σ_y @ 70°F (psi)	171	121
σ_y @ 70°F (psi) (a)	190	171
σy @ 70°F (psi) (b)	114	70
K_{1c} (psi $\sqrt{in}$)	600	418

(a) Vacuum Saturation Only

(b) Freeze and Thaw (Lottman's Procedure)

NB = Northbound Lane Specimens

SB = Southbound Lane Specimens

This conclusion is based on the comparison of test results of resilient modulus, indirect tensile strength, fracture toughness, and Marshall stability.

In addition to testing, field-obtained cores were subjected to fatigue testing to compare the relative performance of the Chemkrete-treated and conventional AC pavement sections. Fatigue testing was performed on leveling and wearing course cores and the results are shown in Figures 3 and 4 for cores obtained in October 1986. Similar trends were observed on the fatigue testing of cores obtained in October 1985, and the corresponding results have also been provided by ODOT (*13*). No fatigue testing was performed on cores obtained in September 1984 because of the difficulty in obtaining sufficient intact specimens. Regression equations following the form of Equation 7, their coefficient of determination R^2, and their standard error of estimate Sx are shown next to the corresponding curves, when appropriate. These curves indicate that cores from the control sections performed substantially better than cores from the Chemkrete-treated sections. These cores already had some accumulated fatigue damage from the applied traffic between the time of construction and the time of testing.

Pavement deformation characteristics of field-compacted, Chemkrete-treated, and conventional (control) AC were investigated through creep compliance and permanent deformation tests, as previously described. The average results of three specimens tested for each type of mixture are presented in Table 6. These results were used in conjunction with the VESYS III computer model to obtain expected rut depths versus time along the Chemkrete-treated and control sections. Layer properties used in the VESYS III analyses are presented in Table 7. The control section generally exhibited more desirable permanent deformation characteristics than the Chemkrete-treated section. The calculated rut depths (through VESYS III analyses and shown in Figure 5) along the Chemkrete-treated section are approximately double the magnitude of those of the control section.

SUMMARY AND CONCLUSION

Results of laboratory tests performed on field-procured cores indicated better performance of the control specimens than that of the Chemkrete-treated specimens. Properties such as

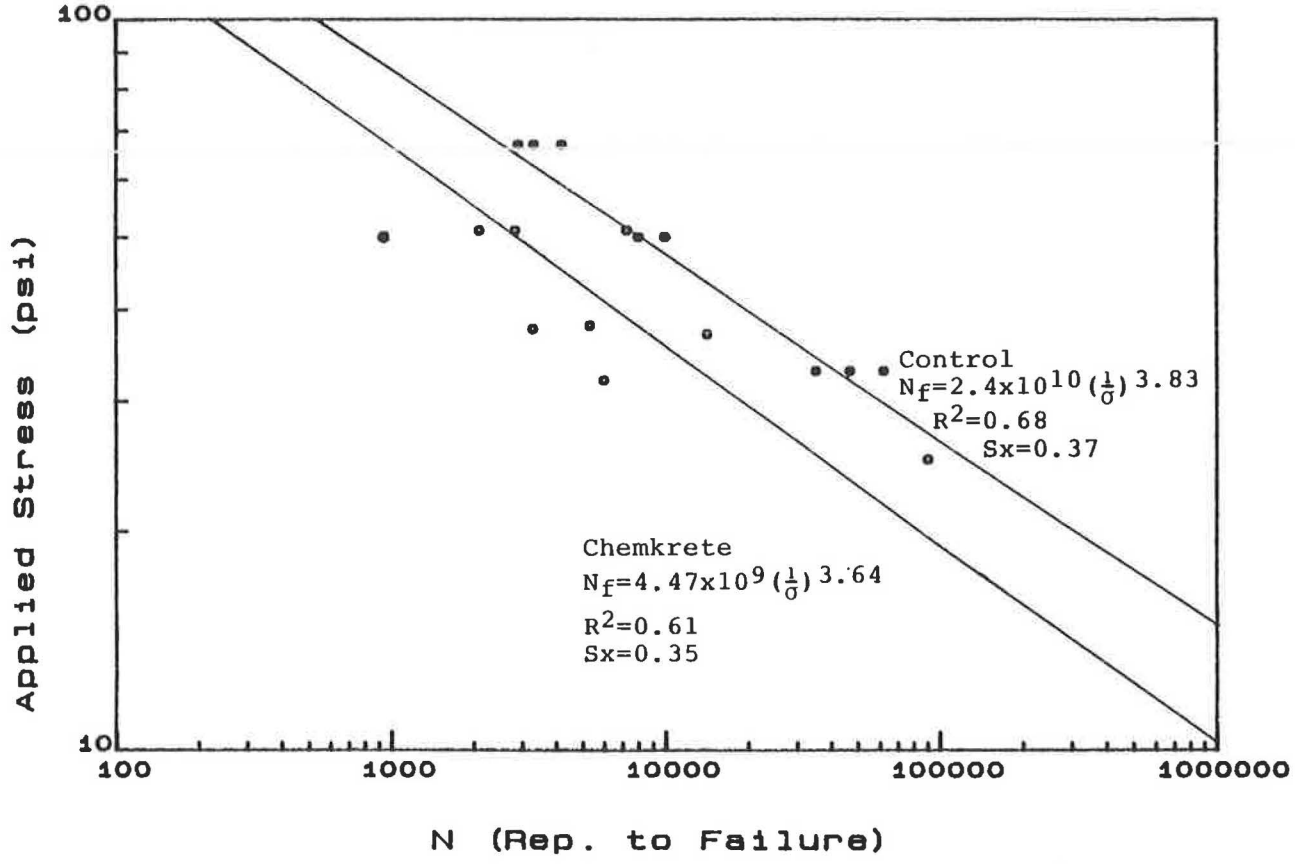

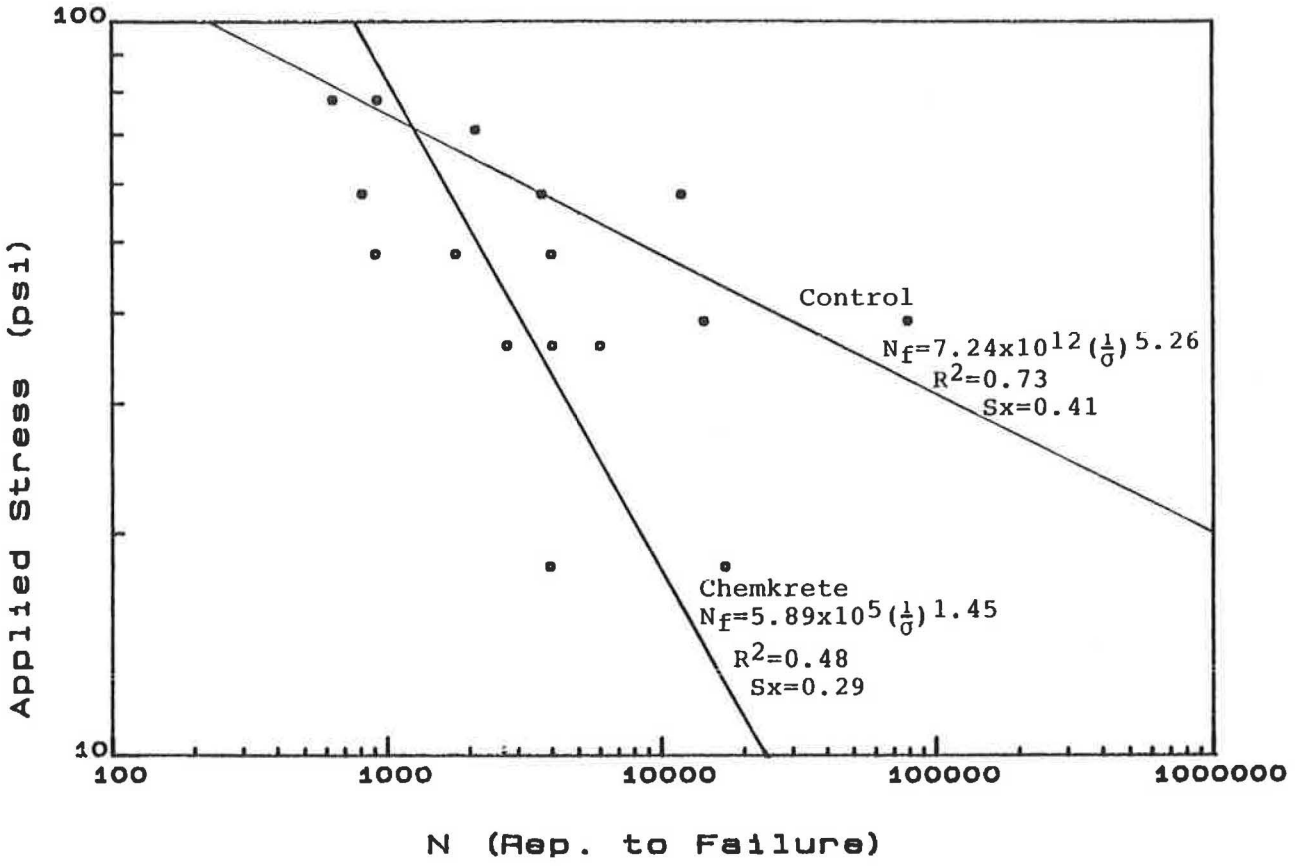

FIGURE 4 Fatigue curves (leveling course cores obtained October 1986).

TABLE 6 CREEP COMPLIANCE TEST RESULTS

Course	Section	I $*10^{-6}$	s	ϵ_{200} $*10^{-6}$	μ	α
Wearing	Chemkrete	3.47	0.49	3.95	0.43	0.51
	Control	0.91	0.56	2.32	0.22	0.44
Levelling	Chemkrete	4.17	0.47	4.32	0.45	0.53
	Control	1.23	0.31	2.30	0.17	0.69

* Refer to Equations 5 and 6 for Symbol Equivalencies.

TABLE 7 MATERIAL PROPERTIES FOR VESYS III ANALYSES

Layer		Thickness (in)	Mr $*10^6$ (psi)	μ	α
ODOT 404	Chemkrete	1.25	1.06	0.43	0.51
	Control	1.25	1.27	0.22	0.44
ODOT 402	Chemkrete	1.75	0.63	0.45	0.53
	Control	1.75	0.99	0.17	0.69
PCC		9.00	3.60	0.10	0.95
Gravel Base		6.00	0.07	0.05	0.60
Subgrade		Semi-Infinite	0.02	0.0075	0.85

* Refer to Equations 5 and 6 for Symbol Equivalencies

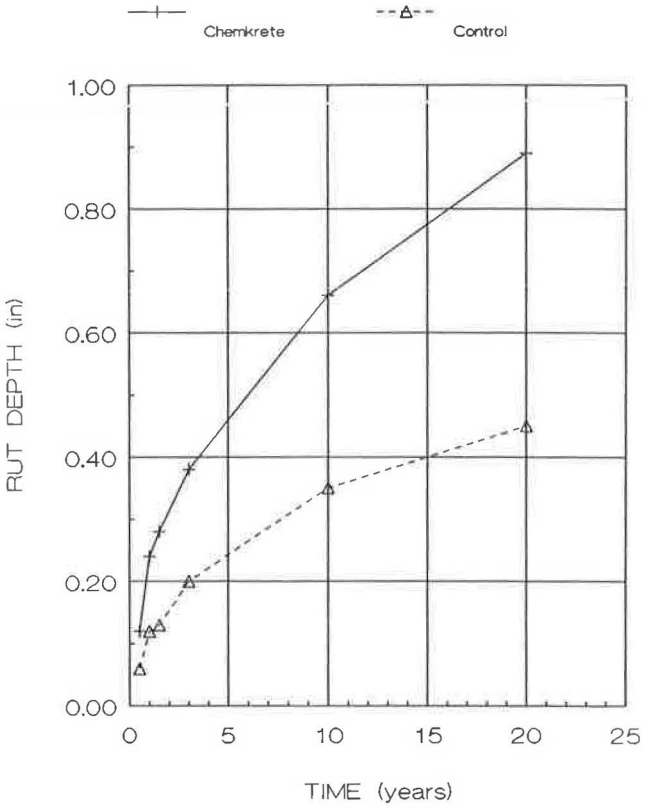

FIGURE 5 Predicted rut depth (VESYS III analyses).

modulus of resilience, indirect tensile strength, and fracture toughness were consistently higher on the control specimens than on the Chemkrete-treated specimens. Control section cores also exhibited longer fatigue life and more desirable creep and permanent deformation characteristics than Chemkrete-treated section cores. VESYS III computer model rut depth calculations also indicated predicted rut depths of approximately twice the magnitude along the Chemkrete-treated section than along the control section.

Dynaflect deflection measurements also indicated a slightly better performance on the control section than on the Chemkrete-treated section. The difference, however, was almost imperceptible in measurements obtained near the boundary of the two sections. Subjective field observations (PCR) also indicated a slightly better performance of the control section than that of the Chemkrete-treated section. Because both Chemkrete-treated and control sections had the same overlay thickness, no apparent beneficial gains are obtained in the performance of AC mixtures with the addition of Chemkrete to the AC.

No significant gains in the engineering properties of AC mixtures are obtained with the addition of Chemkrete, consistent with experience in other states, as previously discussed. Laboratory testing of field-obtained cores subjected to similar climatic and traffic conditions indicates that Chemkrete appears to adversely affect the engineering properties of AC. This behavior may be attributed to the lack of proper curing within a reasonable period of time before the road is opened to traffic.

ACKNOWLEDGMENT

This work was conducted by Resource International, Inc., under a contract with the Ohio Department of Transportation. The authors gratefully acknowledge the assistance of engineers from the Research and Development Division at ODOT.

REFERENCES

1. T. W. Kennedy, J. C. Peterson, D. Anderson, R. Haas, and J. Epps. Chemistry, Rhelosy and Engineering Properties of Manganese-Treated Asphalt Mixtures. In *Transportation Research Record 1096*, TRB, National Research Council, Washington, D.C., 1986.
2. Chemkrete Technologies, Inc. *Interim Project Evaluation Report—US Highway 23, Delaware, Ohio*. Ohio Department of Transportation, Columbus, Aug. 1985.
3. J. S. Moultrop and W. A. Higgins. Manganese Modified Asphalt Pavements: A Status Report. In *Transportation Research Record 1034*, TRB, National Research Council, Washington, D.C., 1985.
4. J. D. Perkins. *Laboratory Evaluation of Chem-Crete Processed Asphalt for Use with Marginal Construction Material*. U.S. Army Engineer Waterways Experiment Station, Vicksburg, Miss., Jan. 1981.
5. E. J. Barenberg. *Performance Analysis of Pavements with Chem-Crete Modified Asphalts*. Chem-Crete Corporation, Menlo Park, Calif., June 1981.
6. D. E. Carey and H. R. Paul. *Laboratory Evaluation of Modified Asphalt—Final Report*. Louisiana Department of Transportation and Development, Baton Rouge, Jan. 1981.
7. D. B. Mellot. *Field Evaluation of Chemkrete Modified Asphalt*. Research Project No. 81–15, Pennsylvania Department of Transportation, Harrisburg, July 1985.
8. W. B. Brewer. *Chemkrete and Rubber Mixtures at Seiling, Oklahoma*. Oklahoma Department of Transportation, Oklahoma City, Jan. 1984.
9. G. W. Maupin, Jr. *Evaluation of Chem-Crete—Final Report*. Virginia Highway and Transportation Council, Charlottesville, Va., Dec. 1982.
10. K. T. Diringer and J. Smith. *Asphalt Additives Study Construction Report*. New Jersey Department of Transportation, Trenton, Feb. 1985.
11. K. Majidzadeh et al. *Evaluation of Asphalt Pavement Recycling in Ohio: A Laboratory and Field Investigation—Final Report on EES599*. Department of Civil Engineering, Ohio State University, Columbus, Oct. 1985.
12. *Predictive Design Procedure—VESYS User's Manual. An Interim Design Method for Flexible Pavements Using the VESYS Structural System*. Report FHWA-RD-TI-154, FHWA, U.S. Department of Transportation, 1978.
13. Resource International, Inc. *A Preliminary Study of Chemkrete Additives*. Project OD-4068, Ohio Department of Transportation, Columbus, Oct. 1987.

Publication of this paper sponsored by Committee on Characteristics of Bituminous Paving Mixtures To Meet Structural Requirements.

Some Effects of Rubber Additives on Asphalt Mixes

R. J. SALTER AND J. MAT

The effects of three types of rubber on the behavior of asphaltic concrete (AC) mixes have been investigated by first determining the changes that rubber additives have on the properties of the bitumen binder. Changes in penetration, softening point, and penetration temperature susceptibility with rubber-bitumen blends are reported. Force ductility tests were also carried out to investigate the changes in the properties of rubber-modified binders at low temperatures. The Marshall method was used to determine changes in optimum binder content consequent to incorporation of rubber into the mix. Flexural testing of beam specimens was carried out using cyclic loading to investigate the changes in the fatigue properties of AC mixes caused by the addition of rubber. Within the limitations of the experimental work, the incorporation of the rubber into binders generally improved the properties of binders and mixes as determined by laboratory testing.

Increasing traffic flows and associated increases in axle loading experienced on highway systems in the developed and developing world together with demands that maximum life and minimum maintenance costs be achieved have led highway engineers to investigate how the properties of asphaltic highway pavement materials might be improved by the use of additives.

The effects of rubber were investigated as an additive to asphaltic mixes, a topic of particular interest to highway engineers in Malaysia. The following three types of natural rubber were used in the experimental work:

1. Pulvatex, manufactured in Great Britain by Rubber Latex, is an unvulcanized rubber powder manufactured from concentrated natural latex, of composition 60 percent natural rubber powder and 40 percent separator.
2. Crusoe Standard, manufactured in Great Britain by Harrison and Crossfield, is an unvulcanized spray-dried rubber powder containing approximately 6 percent silica filler and 1 percent calcium stearate as a partitioning agent.
3. LCS Revertex, manufactured in Great Britain by Revertex, is an unvulcanized latex concentrated by evaporation to 68 percent solids and stabilized with potassium hydroxide and soap.

The experimental work investigated the following effects of addition of natural rubber powders:

1. Effects on physical properties of the bitumen,
2. Effects on design of asphaltic concrete (AC) mixes (investigated using the Marshall method), and
3. Effects on fatigue life of AC beam specimens when tested under constant strain.

R. J. Salter, University of Bradford, Emm Lane, Bradford, England. J. Mat, University of Technology, Jalan, Gurney, Kuala Lumpur, Malaysia 54100.

BINDER PROPERTIES AND RUBBER BITUMEN BLENDS

Materials used in the experimental investigation were selected so as to be similar to those used in Malaysian practice and to comply with current Public Works Department specifications. The bitumen, supplied in Great Britain by Croda Hydrocarbons, had a penetration of 98 at 25°C and a ring- and ball-softening point of 47°C. Blends of natural rubber-bitumen were prepared using concentrations of 3, 5, and 7 percent by mass of rubber to bitumen. The blends were prepared in the laboratory with the blend at a temperature of approximately 135°C; stirring of the rubber into the bitumen took place for 30 min.

All prepared blends were given separate designations for identification in subsequent testing. Details of the mixes used are presented in Table 1.

Penetration tests were carried out on the rubber-bitumen blends and on the control of unmodified bitumen. The results are presented in Table 2 and indicate decreasing penetration with increasing rubber content, the greatest reduction in penetration being obtained from Revertex. Table 2 also presents the softening points of the blends, which increased with increasing rubber content for all blends, the greatest increase in softening point occurring with the use of Revertex as an additive.

For the blends tested, the maximum reduction in penetration, which occurred with 7 percent blends, was 29.5 percent for blends containing Pulvatex, 22 percent for blends containing Crusoe Standard, and 35 percent for blends containing Revertex. Comparison of softening point values indicated an increase of 28 percent in softening point obtained with the liquid latex Revertex with 7 percent additive.

Penetration indices for the blends were also calculated because this index was considered a good indicator of the temperature susceptibility of the blend. The index proposed by Pfeiffer has been commonly used in rubber-bitumen investigations. The calculation was carried out in two stages, the first stage determining the penetration temperature susceptibility (PTS) from the relationship

$$\text{PTS} = \frac{\log 800 - \log p}{t - 77}$$

where p is the penetration (25°C, 100 g, 5 sec) and t is the softening point (°F).

TABLE 1 RUBBER-BITUMEN BLEND DESIGNATIONS

Binder Designation	Additive	Additive Content (percent)
P100	none	0
PVT3	Pulvatex	3
CST3	Crusoe	3
LCR3	Revertex	3
PVT5	Pulvatex	5
CST5	Crusoe	5
LCR5	Revertex	5
PVT7	Pulvatex	7
CST7	Crusoe	7
LCR7	Revertex	7

TABLE 2 PENETRATION AND SOFTENING POINT VALUES FOR RUBBER-BITUMEN BLENDS

Binder Designation	Penetration	Softening Point (°C)
P100	98.0	47.0
PVT3	81.5	51.4
CST3	84.0	50.2
LCR3	78.2	51.8
PVT5	73.1	53.6
CST5	79.1	52.4
LCR5	67.4	54.6
PVT7	69.1	57.1
CST7	76.0	55.0
LCR7	63.6	60.0

TABLE 3 PENETRATION TEMPERATURE SUSCEPTIBILITY AND PENETRATION INDEXES FOR RUBBER-BITUMEN BLENDS

Binder Designation	PTS	PI
P100	0.0230	−0.236
PVT3	0.0209	0.409
CST3	0.0216	0.183
LCR3	0.0210	0.389
PVT5	0.0202	0.650
CST5	0.0204	0.587
LCR5	0.0202	0.658
PVT7	0.0184	1.281
CST7	0.0190	1.084
LCR7	0.0175	1.669

The second stage of the calculation determined the penetration index PI from the relationship

$$PI = \frac{30}{1 + 90PTS} - 10$$

Calculated values are presented in Table 3.

The indices presented in Table 3 show a reduction in temperature susceptibility over all the blends used when compared with the control binder. Because the penetration susceptibility index is the slope of the log penetration versus temperature curve for the respective penetration p and temperature t, its values indicate that the slope becomes less steep as the amount of rubber increases. This effect is similar to that described by Bokma (*1*) for the influence of rubber on penetration at varying temperature. In these experiments, the slope of the penetration-temperature curve decreased as the amount of rubber in the mix increased. These relationships demonstrated that rubber-bitumen blends are harder at higher temperatures and softer at lower temperatures than unmodified binders. The decreased temperature susceptibility, decreased penetration, and increased softening point are the major benefits of the use of rubber-bitumen blends. Al-Abdullah and Mesdary (*2*) found that the addition of natural rubber to 60/70 Kuwaiti bitumen results in a binder equivalent to heavy-duty bitumen, as recommended by the Transport and Road Research Laboratory for carrying heavy commercial vehicles in Great Britain. Heavy-duty bitumen has a penetration of 40 ± 10 and a softening point of 58°C to 68°C.

FORCE DUCTILITY TESTS

In addition to penetration and softening point tests, force ductility testing was carried out on the rubber-binder blends. The test measured tensile load-deformation characteristics of binders. The test apparatus consisted of apparatus for the ductility test (ASTM D113) using briquet specimens of the binder that were pulled apart by a tensile force while immersed in water at 4°C. The apparatus was modified by adding a load cell mounted in series between the drive mechanism and the sample. The force generated in the sample was measured using a data logger and microcomputer.

Force ductility results were reported as load required to cause elongation of the briquet sample. During the first 30 mm of elongation, the load was measured at every 1 mm of elongation and thereafter at every 10 mm of elongation until the specimen ruptured. A typical plot of the results obtained is shown in Figure 1, where the behavior of the specimen under load can be clearly seen. As the sample is pulled apart, the force increases until it reaches a peak; then the force decreases as the elongation of the specimen increases and finally becomes zero when the specimen ruptures. Figure 1 shows the force versus elongation relationship obtained for blends containing 7 percent additive.

Results of the force ductility tests, including the maximum tensile force, elongation of the specimen at maximum force, and elongation at rupture, are presented in Table 4.

The results indicate that rubber-modified binders exhibit higher maximum tensile load than the control binder except for blends containing 5 and 7 percent Crusoe Standard additive. The blend containing 7 percent liquid rubber (Revertex) demonstrated a 63.5 percent increase in strength.

MARSHALL TESTING PROCEDURE

An investigation into the effect of rubber blends on AC mix design was carried out using the Marshall mix design procedure as used by the Malaysian Public Works Department. This method is the only mechanical mix design test in current Malaysian practice.

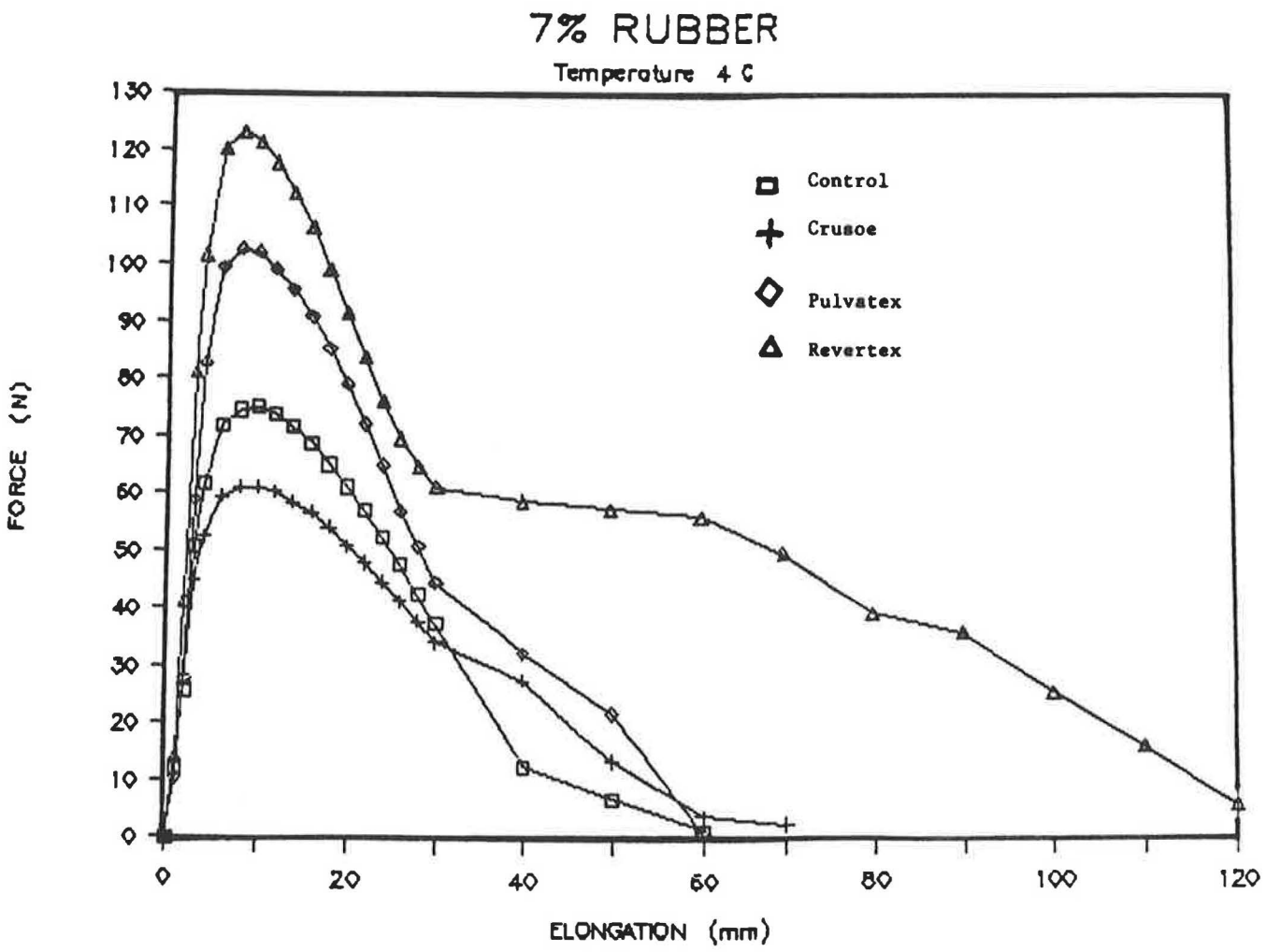

FIGURE 1 Force ductility test graphical output.

TABLE 4 RESULTS OF THE FORCE DUCTILITY TESTS

Binder Designation	Maximum Tensile Force (N)	Elongation at Maximum Force (mm)	Elongation at Rupture (mm)
P100	76.735	9	60
PVT3	79.330	10	70
CST3	83.795	9	60
LCR3	82.944	9	100
PVT5	96.475	8	70
CST5	75.993	8	70
LCR5	93.231	8	120
PVT7	102.776	8	60
CST7	61.536	9	70
LCR7	125.482	9	120

Materials for the AC mixes were typical of those used in Malaysia; limestone was used for both fine and coarse aggregate, and rubber-bitumen blends and control binder were used as previously described. Nominal size of the aggregate was 25 mm; the grading was in accordance with the Malaysian Public Works Department grading for binder courses.

Testing of the rubber-bitumen and control bitumen mixes was carried out in accordance with the Marshall procedure. The following parameters were related to binder content: unit weight, stability, air voids, voids in the mineral aggregate, and flow. Best-fit curves were obtained. A typical example for mixtures containing a 7 percent blend of Pulvatex and bitumen is shown in Figure 2.

For AC, mix design requirements of the Roads Division of the Malaysian Public Works Department specify values of stability, flow, voids in the total mix, voids filled with bitumen, and residual stability. Table 5 presents specified values for a binder course.

The binder contents corresponding to maximum stability, maximum unit weight, and midpoint (5 percent) of allowable air voids were determined. Optimum binder content was the average of these binder contents read from the smoothed curves of which Figure 2 is an example. Tables 6 and 7 present a summary of the mix design results for the rubber-bitumen blends and the control binder.

The Malaysian method of determining optimum binder content, previously described, differs from the method used in Great Britain (*4*) for hot-rolled asphalt wearing course. In the

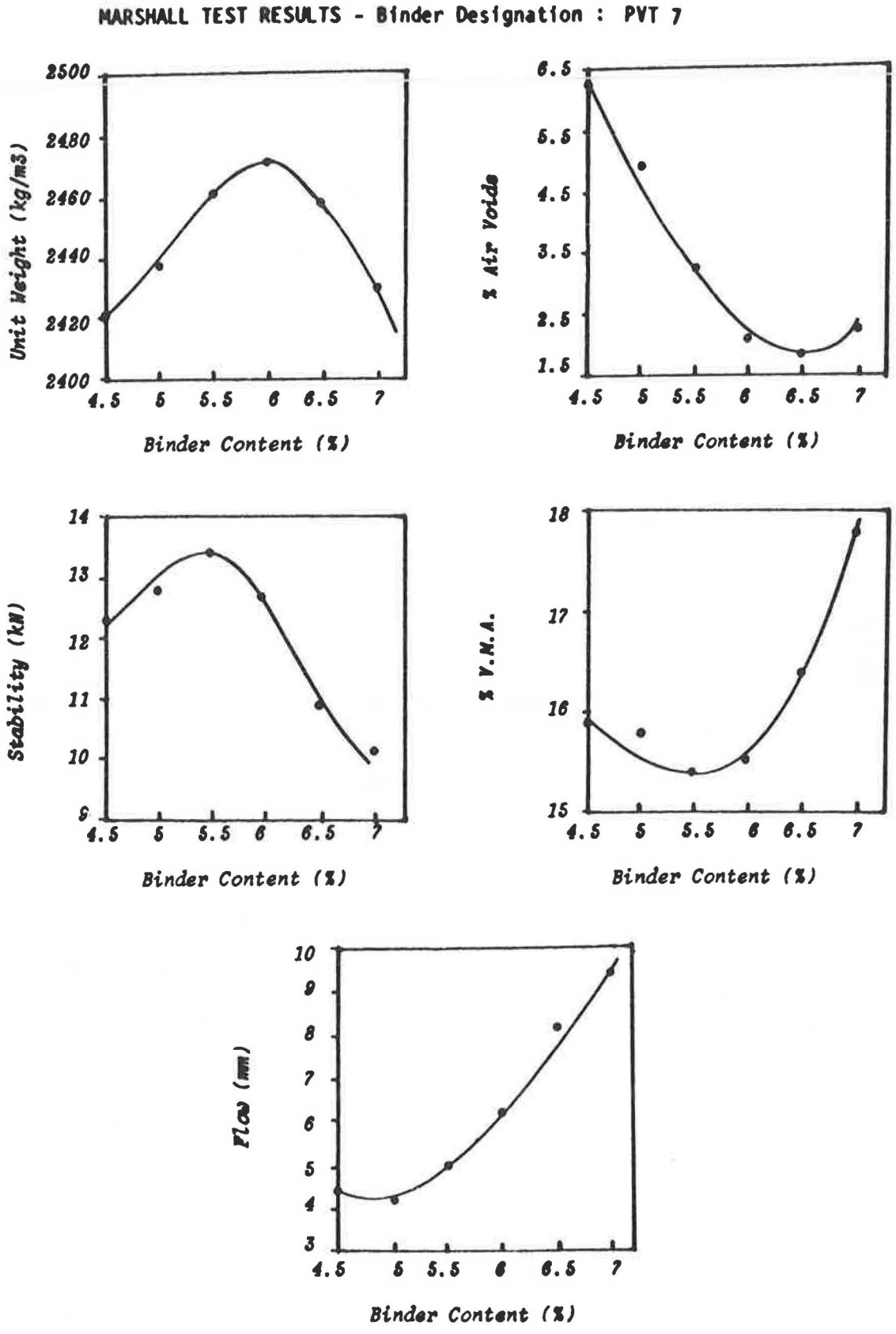

FIGURE 2 Determination of optimum binder content.

TABLE 5 REQUIREMENTS OF THE MALAYSIAN PUBLIC WORKS DEPARTMENT FOR AC BINDER COURSES

Stability (kg)	Not less than 500
Flow (1/100 cm)	20–40
Voids in total mix (percent)	3–7
Voids filled with bitumen (percent)	65–75
Residual stability (immersed percent)	Not less than 75

TABLE 6 DETERMINATION OF OPTIMUM BINDER CONTENT BY THE MALAYSIAN METHOD

Binder Designation	Binder Content at Maximum Unit Weight	Binder Content at Maximum Stability	Binder Content at 5 Percent Air Voids	Optimum Binder Content (percent)
P100	5.5	5.6	5.4	5.5
PVT3	5.7	5.8	5.2	5.6
PVT5	5.9	6.0	5.1	5.7
PVT7	6.0	5.5	5.0	5.5
CST3	5.7	6.0	5.5	5.7
CST5	6.0	5.8	6.0	5.9
CST7	6.2	6.0	6.1	6.1
LCR3	5.8	6.0	5.3	5.7
LCR5	6.0	6.2	5.1	5.8
LCR7	6.1	6.5	5.0	5.9

British method, evaluation of the design binder content is based on the average of the binder contents at maximum stability, mix density, compacted aggregate density, and flow, together with the addition of a factor depending on the coarse aggregate content of the mix. The difference between the two methods for determining optimum binder contents is obtained by comparing Tables 6 and 8. Except for the control mix and those containing Crusoe Standard, the British method yields higher optimum binder contents.

The basic difference between the methods is that the Malaysian approach is suited to the design of an AC mix in which voids are of considerable importance. Too high a binder content and a low voids content will lead to excess binder's reaching the surface of the pavement under traffic action in Malaysian climatic conditions. On the other hand, excessive air voids will lead to low durability. Sufficient binder should be used to produce air voids between 3 and 5 percent. The behavior of AC is sensitive to this figure; different target values should be used for different climatic and traffic conditions.

Within the limitations of the tests performed, the addition of rubber to the binder did affect the optimum binder content. For Pulvatex, the increase was inconsistent and relatively small. For 7 percent rubber-bitumen blends, no increase was observed, while at 3 and 5 percent a small increase was noted using the Malaysian method. Using the British method, a small increase was noted at all rubber concentrations. For Crusoe Standard and LCS Revertex, the optimum binder was increased for all rubber concentrations as determined by both the Malaysian and British methods.

Addition of rubber significantly affected the unit weight of the compacted mixes. For mixes containing Pulvatex and LCS Revertex, increasing the rubber content generally caused an increase in unit weight. For the samples containing Crusoe Standard, the unit weight decreased with increasing rubber content, an effect considered to be caused by the coarser grading of the rubber particles, which affected the compatibility of the specimens.

TABLE 7 MARSHALL QUOTIENT VALUES ON THE BASIS OF THE MALAYSIAN METHOD

Binder Designation	Stability at Optimum Binder (kN)	Flow at Optimum Binder (mm)	Marshall Quotient (kN/mm)
P100	11.0	3.6	3.06
PVT3	11.6	3.8	3.05
PVT5	12.5	4.7	2.66
PVT7	13.4	5.0	2.68
CST3	11.1	4.3	2.58
CST5	11.3	4.6	2.46
CST7	9.8	5.0	1.96
LCR3	11.8	4.3	2.74
LCR5	12.7	5.2	2.44
LCR7	12.8	6.1	2.10

TABLE 8 DETERMINATION OF OPTIMUM BINDER CONTENT BY USING THE BS 598 METHOD

Binder Designation	Binder Content at Maximum Unit Weight	Binder Content at Maximum Stability	Binder Content at Maximum Compacted Aggregate Density	Optimum Binder Content (percent)
P100	5.5	5.6	4.9	5.3
PVT3	5.7	5.8	5.3	5.6
PVT5	5.9	6.0	5.6	5.8
PVT7	6.0	5.5	5.7	5.7
CST3	5.7	6.0	5.4	5.7
CST5	6.0	5.8	5.7	5.8
CST7	6.2	6.0	5.9	6.0
LCR3	5.8	6.0	5.5	5.8
LCR5	6.0	6.2	5.9	6.0
LCR7	6.1	6.5	6.0	6.2

Rubber content also affected the Marshall stability. For Pulvatex and LCS Revertex, stability increased as rubber concentration increased. For Crusoe Standard, increase in stability was not observed; the specimens containing a 7 percent blend had decreased stability, an effect associated with the decreased unit weight of these specimens.

Addition of Pulvatex and LCS Revertex caused air voids to decrease as the rubber content increased, while for specimens containing Crusoe Standard blends air void contents increased with increasing rubber contents.

Voids in the mineral aggregate (VMA) has been the most important mix design parameter affecting the durability of an AC mix (*5*). Except for Crusoe Standard, the addition of rubber reduced the VMA values compared to the control mix. In Malaysian practice, to satisfy the requirement for voids filled with bitumen indicated in Table 5 the minimum VMA value is about 14 percent. All the mixes investigated had a value that exceeded this minimum.

Increasing rubber content increased flow values. All the specimens containing rubber, except PVT3, had flow values that exceeded the maximum specified for Malaysian conditions. As the unmodified control specimens had flow values

approaching the maximum, a revised grading may have reduced the extent of the excess flow values.

Values of the Marshall quotient indicate the effect of addition of rubber to the mix. The increased values of flow cause a decrease in Marshall quotient despite increased values of stability.

FLEXURAL TESTING

Following the Marshall test procedure, a series of beam flexure tests were carried out on AC laboratory-prepared specimens to determine the effects of natural rubber powders and latex on fatigue life and dynamic modulus.

TABLE 9 EFFECT OF RUBBER-BITUMEN BLENDS ON FATIGUE LIFE OF AC BEAM SPECIMENS

	Mean Number of Cycles to		Percentage Increase in	
Sample	Fatigue Life	Severe Cracking	Fatigue Life	Severe Cracking
P100	23,568	27,500		
PVT3	28,825	35,625	22.3	29.6
PVT5	40,321	49,997	71.1	81.8
PVT7	44,359	50,010	88.2	81.9
CST3	29,725	36,876	26.1	34.1
CST5	36,251	43,672	53.8	58.8
CST7	35,285	44,997	49.7	63.6
LCR3	33,277	41,250	41.2	50.0
LCR5	37,753	50,718	60.2	84.4
LCR7	41,516	50,013	76.2	81.9

Constant-strain testing was adopted because it simulated strain conditions for pavements with relatively thin bituminous layers over granular bases. Sinusoidal loading was used with a frequency of 2 Hz; test temperature was 20°C ± 1°C. Binder and aggregate type and grading were as for the previously described Marshall testing program. Binder content was the optimum determined by the Malaysian method.

Specimens were prepared in the laboratory with a procedure similar to that used by the California kneading compactor. This method of specimen compaction simulated actual rolling conditions on the highway. Originally compacted to a size of 100 × 100 × 375 mm, specimens were cut to produce finished beam specimens measuring 37.5 × 37.5 × 375 mm.

Because the main objective of the testing program was to study the effect of natural rubber powders and latex on the fatigue life of the AC specimens under repetitive constant strain conditions, the criterion of failure was defined as the number of strain repetitions corresponding to a reduction in the load applied to the beam to half its value after the first 200 repetitions of load.

Four beams of each mix type were tested. The application of sinusoidal load was continued until cracking was observed in the beam specimens. Results of the test are presented in Table 9, in which considerable increases both in fatigue life and in cycles to cracking can be seen.

During testing, the variation in applied load with increasing cycles of applied load was noted. Relationships between load and repetitions are shown graphically in Figures 3–5, in which the behavior of specimens containing the three types of rubber additive and the control mix is compared.

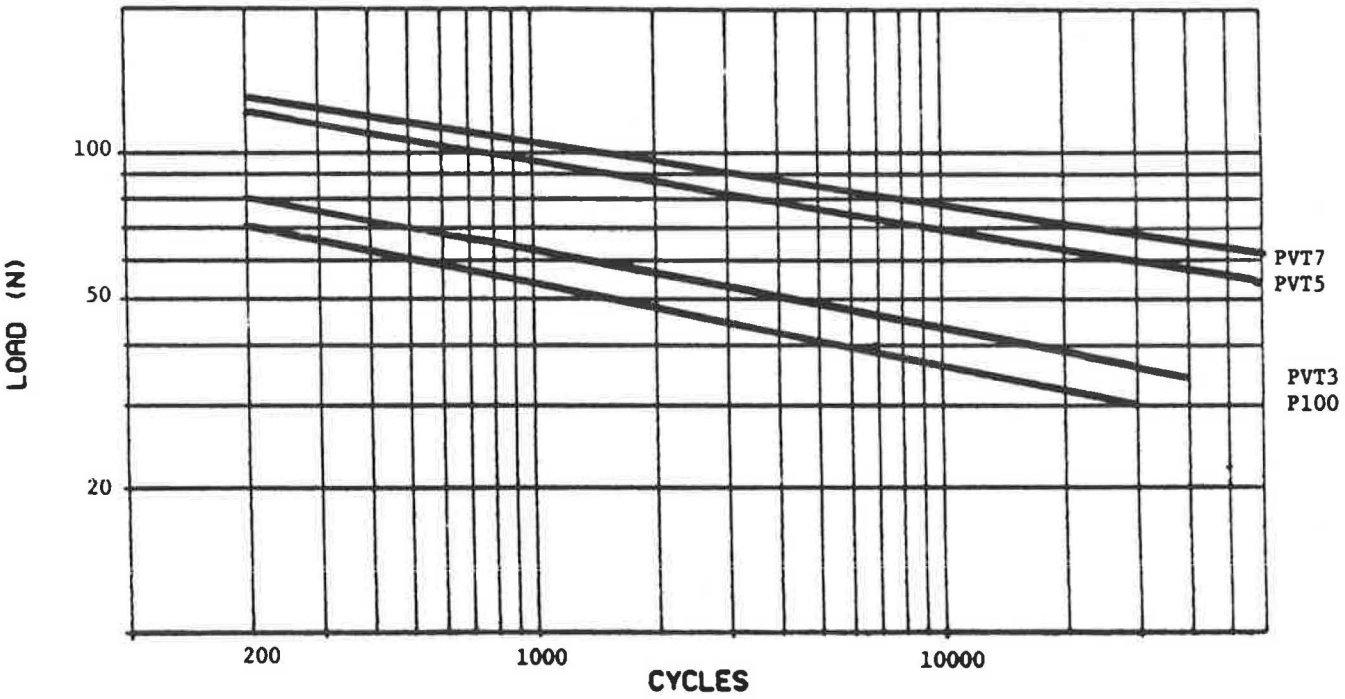

FIGURE 3 Relationships between applied load and cyclic loading for PVT mixes.

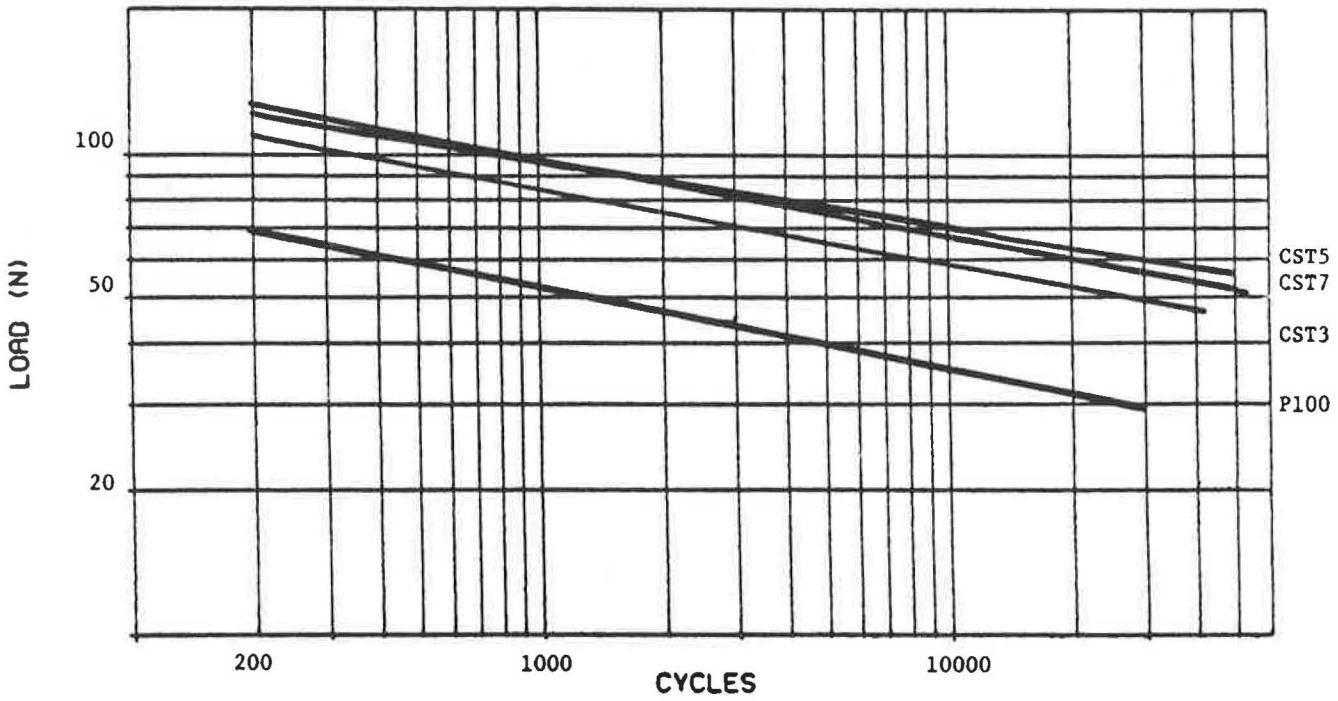

FIGURE 4 Relationships between applied load and cyclic loading for CST mixes.

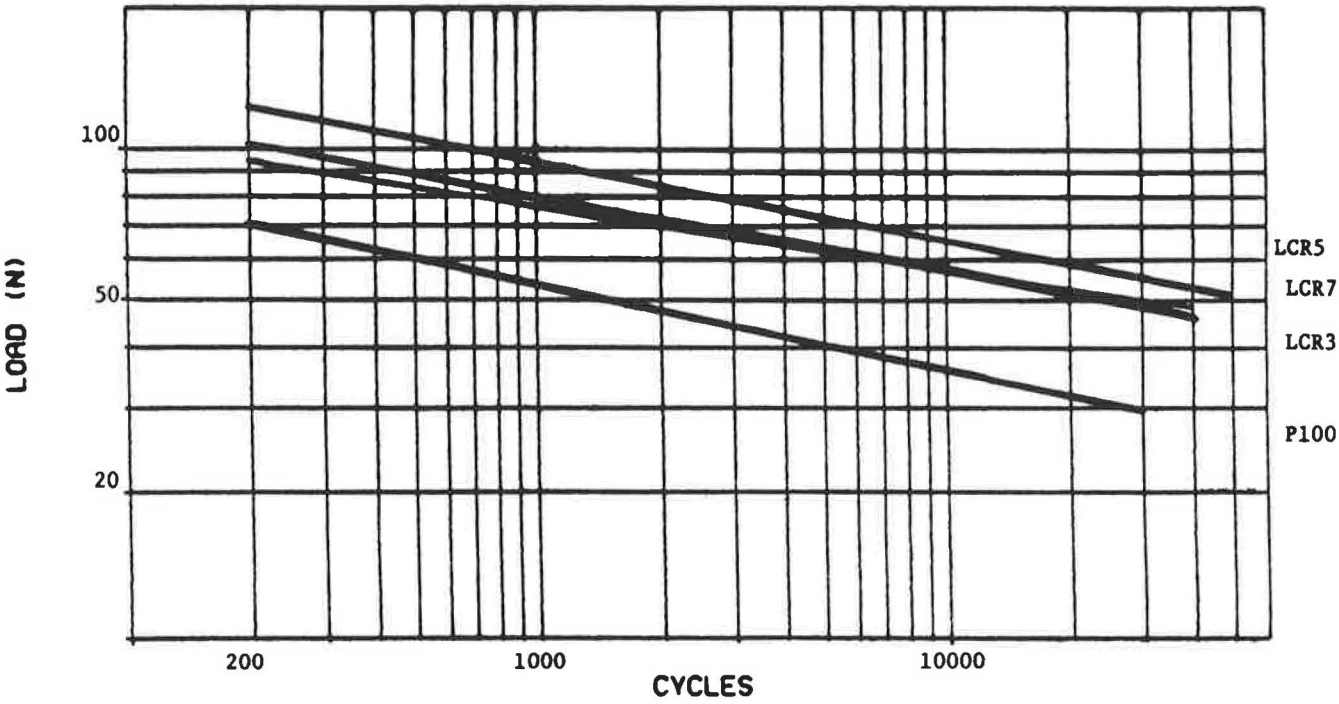

FIGURE 5 Relationships between applied load and cyclic loading for LCR mixes.

CONCLUSIONS

During the testing, the addition of all three types of rubber additive caused a decrease in penetration and an increase in softening point compared to the unmodified binder. Little variation in these properties was observed between the three types of rubber additive. An investigation into the temperature susceptibility of rubber-bitumen blends demonstrated decreased susceptibility compared to the unmodified binder.

Force ductility tests on modified and unmodified specimens at 4°C indicated that rubber-modified binders, with the exception of blends containing Crusoe Standard additive, exhibited higher maximum tensile loads during testing.

The Marshall testing program revealed a small increase in optimum binder content for most of the rubber-bitumen blends tested. The addition of rubber increased Marshall stability values for Pulvatex and LCS Revertex blends, but not for blends containing Crusoe Standard additive. Flow values were increased by the addition of rubber, a factor that should be considered in the overall design of mixes.

In a series of fatigue tests using beam bending to constant strain, the increase in fatigue resistance for rubber-bitumen blends was clearly indicated. When beam failure was defined as the reduction in applied load to half its initial value, improvements of up to 88 percent were noted in fatigue life. Similar improvements were found when the point of failure of specimens was defined as the onset of crack formation in the specimens.

REFERENCES

1. F. T. Bokma. The Use of Rubber in Bituminous Road Construction. *Communication 96, Rubber-Stichting*, Delft, Holland, 1949.
2. A. Al-Abdullah and M. S. Mesdary. The Impact of Research on Road Development in Kuwait. *Proc., 3rd IRF Middle East Regional Meeting*, Vol. 4, Riyadh, Saudi Arabia, 1988, pp. 263–280.
3. *Design and Construction of Asphalt Pavements*. Roads Division, Public Works Department, Malaysia, 1984.
4. *Sampling and Examinations of Bituminous Mixtures for Roads and Other Paved Areas*. British Standard 598: Part 3. British Standards Institution, London, 1985.
5. P. S. Kandhal and W. S. Koehler. The Marshall Mix Design Method, Current Practices. *Proc., Association of Asphalt Paving Technologists*, Vol. 54, St. Paul, Minn., 1985, pp. 284–303.

Publication of this paper sponsored by Committee on Characteristics of Nonbituminous Components of Bituminous Paving Mixtures.

Moisture Damage Cutoff Ratio Specifications for Asphalt Concrete

ROBERT P. LOTTMAN AND STEPHEN BREJC

Moisture susceptibility of asphalt concrete (AC) mixtures is identified by performing laboratory tests on dry- and wet-accelerated conditioned specimens. Excessive moisture susceptibility is associated with low ratios of wet-to-dry mechanical properties. Highway agencies use values of cutoff wet-to-dry ratios for resilient modulus and for indirect tensile strength as specifications. Mixtures having wet-to-dry ratios lower than the cutoff ratios have excessive moisture susceptibility and require treatment before paving. Currently, most highway agencies apply either a resilient modulus cutoff ratio of 0.70 or an indirect tensile strength cutoff ratio of 0.75. The University of Idaho AC moisture damage analysis system (ACMODAS) programs on field performance are applied to predict cutoff ratios, compare predicted cutoff ratios to currently used ratios, classify AC mixture moisture susceptibility, and recommend cutoff ratios to be used in practice. Two cutoff ratios are necessary to control moisture susceptibility both for fatigue cracking and for wheelpath rutting field distresses. These cutoff ratios are 0.80 for resilient modulus and 0.85 for indirect tensile strength, and both should be applied simultaneously. [Simultaneous application of the (lower) currently used cutoff ratios may only control fatigue cracking.] Applying individual cutoff ratio values to each material, about 25 percent of mixtures, which cannot be treated by conventional additives or other means to obtain desired fatigue cracking performance because of water-induced brittleness, have cutoff ratios >1. However, the other mixtures can be treated, if need be, to obtain desired performance; their cutoff ratios are <1. Identification of these mixtures is discussed.

Moisture damage in asphalt concrete (AC) mixtures as pavements occurs in many locations and results in loss of performance life. Application of related control specifications is a strong factor in AC mixture design for highway agency laboratories. Cutoff ratios will continue to be used in the near future as moisture damage specifications.

Controlling fatigue cracking distress in the design of AC mixes is based on a resilient modulus cutoff ratio as well as a tensile strength cutoff ratio. In addition, a resilient modulus cutoff ratio is necessary to control wheelpath rutting distress. Each mixture and pavement situation provides specific values and a unique relationship between these cutoff ratios.

Most highway agencies currently use only one cutoff ratio to control moisture damage. A two-ratio control method is necessary to minimize field damage from the occurrence both of fatigue cracking and of rutting when pavements become wet. Routine ability is needed to perform both the indirect tensile strength and resilient modulus tests in highway agencies. Fortunately, these test activities are increasing steadily because of awareness of other uses for these test data for the evaluation of AC mixtures.

Department of Civil Engineering, University of Idaho, Moscow, Idaho 83843.

The objective is to predict cutoff ratios and to combine them in a practical form that will provide rational specifications to control the field distresses of fatigue cracking and wheelpath rutting.

Cutoff ratios obtained through the ACMODAS prediction models are related to ratios currently in use that have been based on experience. The simpler approach to specifications is the application of universal cutoff ratio values rather than of specific cutoff values associated with each type of AC mixture.

Use of cutoff ratios implies that decisions of satisfactory field performance are based on comparative or relative behavior. A cutoff ratio defined for AC moisture sensitivity is the value of the mechanical property of the wet specimen divided by the value of the mechanical property of the dry specimen. Ratios much lower than 1.0 indicate high moisture sensitivity and a potential for severe loss of field life when the AC becomes wet.

Magnitudes of cutoff ratios should be independent of the laboratory wet-accelerated conditioning test used. These ratios are specifications that set a standard for limiting moisture-induced damage in the field to a predetermined level. Separately, the laboratory test procedure is developed on the merits of producing adequate moisture damage potential for AC mixtures. The test-obtained mechanical property ratios are compared to the cutoff ratios.

Application of cutoff ratios as specifications is several decades old. Early tests screened AC mixtures in the laboratory before paving by using unconfined compressive strength. Specimens were wet-accelerated conditioned by soaking for 24 hr at 140°F. On the average, the specific AC mixture was satisfactory if its wet-to-dry ratio or cutoff ratio was equal to or greater than 0.85. Currently, indirect tension tests are being used from which wet-to-dry resilient modulus ratios (MrR) and tensile splitting strength ratios (TSR) are applied for control before paving. These biaxial stress tests bring out adhesion effects more readily than the unconfined compressive strength tests. Also, the wet-accelerated conditioning is a forced saturation by vacuum on which is superimposed a freeze-thaw cycle or a 24-hr, 140°F water soak, or both, producing somewhat more severe conditioning than in the unconfined compressive strength test. These factors have led highway agencies to establish cutoff ratios of 0.70 for MrR and 0.75 for TSR, lower than the 0.85 value for the unconfined compressive strength test. These cutoff ratios vary by ± 0.05 around the country, depending on the experience of the highway agency.

Highway agencies use only one cutoff ratio, either an MrR or TSR value. The approach of this study is based on the simultaneous application of both ratios.

Further discussion of cutoff ratios, including quantitative relationships, has been provided by Lottman et al. (*1*).

PERCENTAGE ALLOWABLE REDUCTION

The universal acceptance of using cutoff ratios lower than 1 by highway agencies implies a philosophy that there is an acceptable loss of pavement performance life (i.e., AC mixture durability) caused by moisture damage. The acceptable loss of life can be translated into percentage allowable reduction (of all-dry performance life) (PAR). At present, PAR is determined subjectively, but results of life cycle cost and performance determination procedures will improve the selectivity of PAR. The average highway agency PAR is 10 percent, with range from 0 to 20 percent. For example, suppose PAR is 10 percent and an all-dry performance life is assumed to be 12 years, then the maximum allowable wet performance life of the AC must be no less than 10.8 years.

The cutoff ratio is a function both of PAR and of the association of the field performance life relationship with AC mechanical properties.

Evaluation of PAR with cutoff ratios indicates that

1. Efficient programming for pavement life cycle costing will require that PAR be small;
2. Practicalities, including imperfect treatments of moisture-sensitive AC mixtures, will keep PAR greater than zero; and
3. Severity of the laboratory specimen wet-accelerated conditioning is independent of establishing values for the cutoff ratios when considering the application of PAR.

In this study, PAR = 10 percent is used to develop the cutoff ratios.

ANALYSIS PROGRAM

The ACMODAS programs were developed several years ago by the University of Idaho for predicting relative wet-pavement performance life of moisture-sensitive AC. The programs are mechanistically based. The program inputs are wet and dry mechanical properties of resilient modulus and tensile splitting strength for a specific AC mixture, PAR, and pavement climate factor. The mechanistic models in the programs translate the laboratory-determined mechanical properties to performance life, in years. They are also used to predict the MrR and TSR cutoff ratios. Technical background and application of the programs were described by Lottman and Frith (*1*,*2*).

ACMODAS C consists of two programs, one each for the two prominent field distresses related to moisture sensitivity:

1. ACMODAS 2, for effect of moisture on wheel load (or fatigue) cracking; and
2. ACMODAS 3, for effect of moisture on wheelpath permanent deformation or rutting.

The Idaho Research Foundation, Moscow, Idaho, provides the ACMODAS C diskette and operator manual in response to inquiries.

Using ACMODAS C, cutoff ratios are obtained for MrR and TSR for fatigue cracking, and for MrR for wheelpath rutting. Values of the three ratios are usually not the same, even for a specific AC mixture.

For fatigue cracking, both cutoff ratios of MrR and TSR are required to control or limit the moisture sensitivity because the ACMODAS 2 model incorporates relative fatigue strength and toughness as a measure of moisture resistance, which, in turn, is related to both stiffness and strength. For wheelpath rutting, an MrR cutoff is used without a TSR cutoff because the ACMODAS 3 model incorporates relative shear strain permanent deformation, which, in turn, is related to stiffness. Because these field distresses are different physically, the MrR cutoff ratios from ACMODAS 2 and 3 have different values.

The ACMODAS 2 and 3 programs of ACMODAS C were applied to develop cutoff ratios for specific AC mixtures containing different asphalt binders and aggregates. These mechanistic-based, predicted cutoff ratios are independently determined.

AC MIXTURE VARIABLES

AC mixtures from the following two categories were investigated:

1. Highly strippable aggregate from a constant source with variable asphalt binders [three asphalt sources, approximately 25 asphalt treatments (antistripping additives, i.e., liquid chemicals and lime), polymeric modifiers, and combinations of additives and modifiers]. The total amounted to 58 different AC mixtures. Further description of the variables and properties was provided by Lottman and Mesch (*3*). The wet-accelerated conditioning in NCHRP Report 246 (*4*) (90 percent saturation by vacuum plus freeze and 24 hr, 140°F water soak) was used.
2. Variable strippable aggregate from a nonconstant source with specific asphalt for each aggregate. Mixtures were made with and without additives. Further description of the variables and properties was provided by Brent Rauhut Engineering (*5*). Both NCHRP Report 246 (*4*) wet-accelerated conditioning and AASHTO T-283 wet-accelerated conditioning (67 percent saturation by vacuum plus freeze and 24 hr, 140°F water soak) were used.

Specimens representing each of these AC mixtures, having different input wet and dry mechanical properties, provided a varied-population data base from which to predict and evaluate cutoff ratios using ACMODAS C. The variation of proportionality between modulus and strength properties in both wet and dry conditions affected the magnitude of cutoff ratio predicted for a specific mixture. The type of wet-accelerated conditioning test used did not seem to be a factor in changing the proportionality; the test mainly is responsible for the magnitude of these input mechanical properties.

GROUPING OF RESULTS AND EXAMPLES

Moisture Effect Categories

As previously mentioned the cutoff ratios determined by the ACMODAS C program are related to specific field distresses

of fatigue cracking and wheelpath rutting. The results, therefore, are separated as follows:

Distress	*Cutoff Ratios*
Fatigue cracking	MrR, TSR
Wheelpath rutting	MrR

Also, the cutoff ratios obtained by the ACMODAS C program can be separated into three mixture-moisture effect categories, each with a specific relationship to specifications and control. These categories are as follows:

1. Cutoff Ratios >1.0. No conventional routine mixture improvement, e.g., additive application, will make MrR and TSR >1.0. Thus, mixtures requiring cutoff ratios >1.0 will not perform in the field to the level of the designated PAR.
2. Cutoff Ratios <1.0 with MrR Cracking Cutoff Larger Than MrR Rutting Cutoff. When quality additive application is necessary, ratios equal to or larger than the cutoff ratios can be produced so that these mixtures will perform at PAR in the field for both distresses. Control set by the MrR and TSR cracking cutoffs becomes the specification; the MrR rutting cutoff is automatically achieved.
3. Cutoff Ratios <1.0 with MrR Rutting Cutoff Larger Than MrR Cracking Cutoff. Quality additive application should also produce input ratios equal to or larger than cutoff ratios to perform at PAR for both distresses. A cutoff-setting procedure is required. The TSR cracking cutoff is increased to retain relative wet-mixture toughness because the larger MrR cutoff, the one for rutting, controls. The MrR cracking cutoff is increased to equal the MrR rutting cutoff, thus the TSR cracking cutoff is also increased.

Figure 1 is a specification chart giving example cutoff ratios for a specific AC with given mechanical properties and a PAR

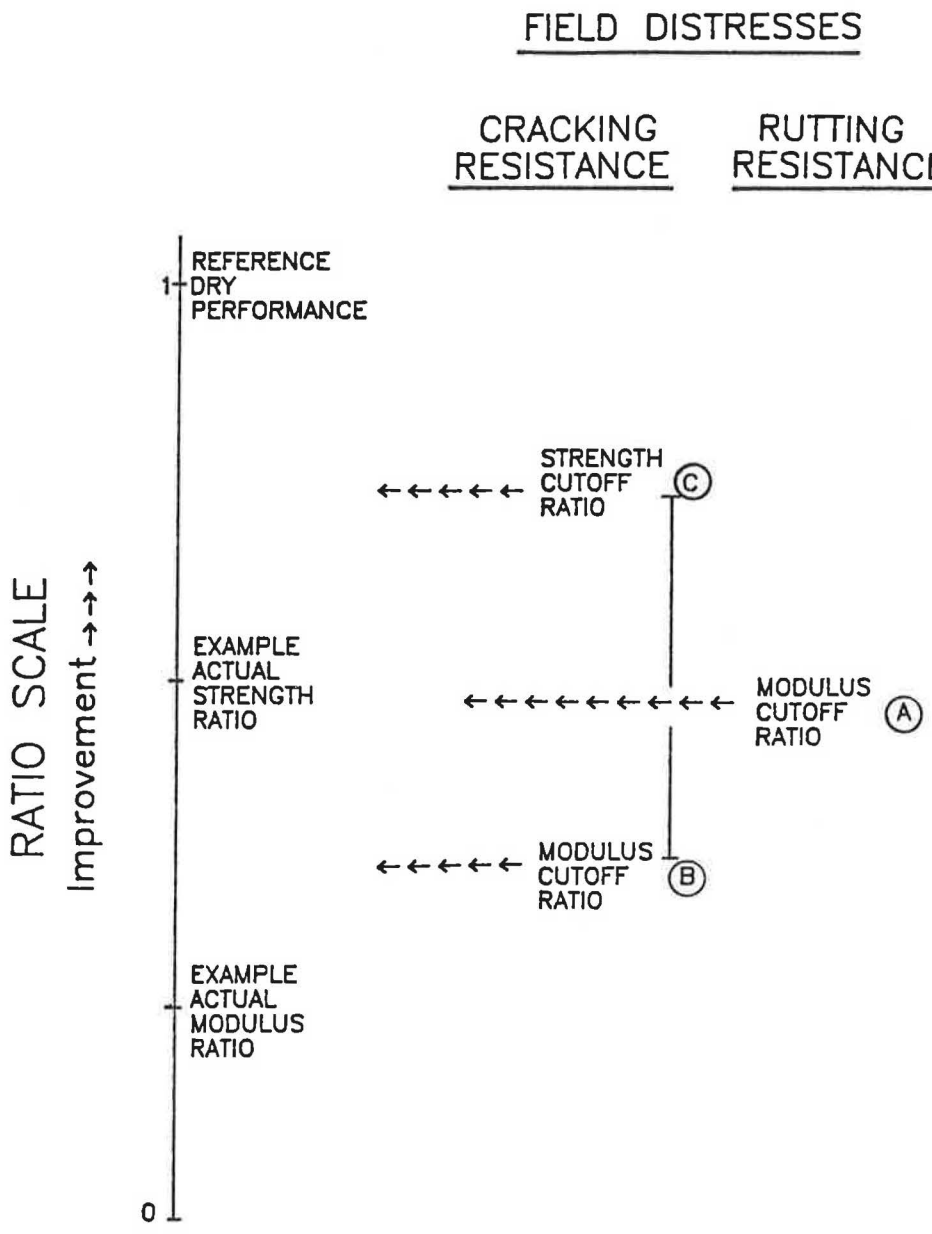

FIGURE 1 Interactive cutoff ratio specifications.

specified by a highway agency. Here, MrR and TSR obtained from the specimen tests reflect excessive moisture damage because the ratios are smaller than the corresponding cutoff ratios required for each distress. The change to be effected in this asphalt concrete before paving requires a specimen MrR increase to satisfy the MrR rutting cutoff A. The MrR cracking cutoff becomes equal to the MrR rutting cutoff (B increases to A), because the same mixture (i.e., specimen) cannot possess different values of the modulus ratio at the same time. The TSR cracking cutoff now must increase to a value $>C$ to satisfy the required proportionality between cutoff ratios B and C. This $B-C$ proportionality maintains satisfactory resistance against onset of cracking fatigue and crack propagation, which will be quantified in a following section. In order to meet the cutoff ratio specifications for both field distresses, the AC in this example will require a new mixture design, or inclusion of additives, to achieve the required MrR cutoff A and the new TSR cutoff value that is larger than C.

Examples of Categories

Table 1 contains examples of ACMODAS C predicted cutoff ratios for five different AC mixtures using a PAR value = 10 percent.

The interactive requirements when using the cutoff ratios as specifications are illustrated by the following brief evaluation, in detail, for each pavement mixture specified in Table 1:

- Pavement C. To meet the MrR cutoff for rutting of 0.88, the standards for cracking must increase, so that MrR cutoff for cracking increases from 0.45 to 0.88; the associated TSR cutoff of 0.65 must increase in proportion. The net result on the pavement will be that the AC will perform better than PAR for cracking and equal to PAR for rutting.
- Pavement M. To meet the MrR cutoff for cracking of 1.09, the standard for rutting must increase so that MrR rutting cutoff increases from 0.69 to 1.09. In the pavement, this increase will result in the AC having a better performance than PAR for rutting and equal to PAR for cracking. (This situation is theoretical, because an MrR cutoff of 1.09 cannot practically be met because it is larger than 1.)
- Pavement T. Because both MrR cutoff values are about the same, PAR for both rutting and cracking will be met by achieving an MrR cutoff of 0.77 and a TSR cutoff of 0.83.
- Pavement V. Similar evaluation to Pavement C.
- Pavement W. Similar evaluation to Pavement M.

The AC for pavements M and W will have a wet life smaller than the allowable 10 percent life reduction because of moisture damage (or PAR). This result follows from the problematic wet-to-dry strength-modulus relationships that exist in these ACs that cannot be easily remedied without chemical modification.

TABLE 1 EXAMPLE OF ACMODAS PREDICTED CUTOFF RATIOS

Pavement	Fatigue Cracking		Wheelpath Rutting
	TSR Cutoff	MRR Cutoff	MRR Cutoff
C	0.65	0.45	0.88
M	0.95	1.09	0.69
T	0.83	0.76	0.77
V	0.80	0.72	0.85
W	0.97	1.03	0.72

VALUES OF CUTOFF RATIOS AND PRACTICAL IMPLICATIONS

Average values of cutoff ratios determined by the ACMODAS C program are listed by cutoff ratio category in this section, along with related findings.

Cutoff Ratios >1

Approximately 25 percent of the mixtures required cutoff ratios >1 for the control of fatigue cracking.

It is not practical to treat or improve these mixtures to get an MrR or TSR value >1 to achieve PAR = 10 percent. Unfortunately, one has to settle for PAR value >10 percent, perhaps 20 or 25 percent, for the reduction of dry life (determined by fatigue cracking) caused by moisture damage.

These mixtures should be screened out, especially if they are problematic regarding other performance criteria. They can be identified because their MrR values are larger than their TSR values. This effect seems to be caused by water-induced brittleness.

However, the value of the MrR cutoff for wheelpath rutting is almost always <1, which is always practically achievable, so that a PAR = 10 percent can be reached for controlling wheelpath rutting.

Cutoff Ratios <1, with MrR Cracking Cutoff Larger Than MrR Rutting Cutoff

Approximately 30 percent of the mixtures are in this category. Moisture sensitivity control is achieved through the fatigue cracking cutoff ratios of MrR and TSR. Because the MrR cracking cutoff is larger than the MrR rutting cutoff, wheelpath rutting is automatically controlled by using the larger MrR cutoff value, which is for fatigue cracking.

An example for a specific mixture is MrR cracking cutoff = 0.78, TSR cracking cutoff = 0.84, and MrR rutting cutoff = 0.74. In application, MrR cutoff = 0.78 and TSR cutoff = 0.84 would be used for the moisture sensitivity control of this mixture.

In this category, for all the mixtures tested the average cutoff ratios were found to be MrR cracking cutoff = 0.85, TSR cracking cutoff = 0.80, and MrR rutting cutoff = 0.75. The MrR cracking cutoff of 0.85 and the TSR cracking cutoff of 0.80 would be simultaneously applied for overall control in this category.

Cutoff Ratio <1, with MrR Rutting Cutoff Larger Than MrR Cracking Cutoff

Approximately 45 percent of the mixtures are in this category. They will require the B–C TSR cutoff shift as shown in Figure

1. In this case, the MrR cutoff is based on rutting. Because it is required that the value of the MrR cracking cutoff be equal to that of the MrR rutting cutoff, the TSR cracking cutoff is shifted to a larger value. The value of the larger TSR cutoff can be calculated from the following equation:

$$TSR_2 = TSR_1 (MrR_2/MrR_1)^{0.50} + 0.02 \quad (1)$$

where

TSR_2 = new, larger required TSR cracking cutoff,
TSR_1 = original TSR cracking cutoff,
MrR_1 = original MrR cracking cutoff, and
MrR_2 = required MrR cutoff (= MrR rutting cutoff).

Equation 1 has $r^2 = 0.95$. In the equation, MrR Subscripts 1 and 2 correspond to *A* and *B*, respectively, in Figure 1, and TSR Subscript 1 corresponds to *C* in Figure 1.

Average values of the cutoff ratios obtained for all mixtures in this study are (a) fatigue cracking cutoffs of $MrR_1 = 0.65$ and $TSR_1 = 0.75$ (corresponding to MrR_1 and TSR_1 in Equation 1), and (b) wheelpath rutting cutoff of $MrR_2 = 0.80$ (corresponding to MrR_2 in Equation 1).

If only the fatigue cracking cutoff ratios of MrR_1 and TSR_1 (0.65 and 0.75, respectively) are used for control, rutting will not be controlled to the desired level (10 percent) of PAR. The loss of rutting life will be greater than required. On the other hand, if the MrR_2 cutoff ratio is used with TSR_1 (0.80 and 0.75, respectively), cracking will not be controlled to the desired level of PAR because TSR_1 is now too low. Thus, a higher-strength cutoff ratio is required, i.e., TSR_2. Substitution of MrR_1, MrR_2, and TSR_1 into Equation 1 yields $TSR_2 = 0.85$. Therefore, the control of both cracking and rutting in this category to achieve PAR = 10 percent requires an MrR cutoff of 0.80 and a TSR cutoff of 0.85 to be simultaneously applied for overall control.

RECOMMENDATION

The preceding results of the evaluation of individual cutoff ratio categories obtained from the ACMODAS C program are now overviewed for current practice. This examination requires that MrR and TSR values obtained by laboratory test for a specific AC mixture be compared to overall predetermined cutoff ratios. The recommended approach is as follows:

1. Determine if the AC mixture is in the minority category, cutoff ratios >1. These mixtures can be identified by MrR > TSR after wet-accelerated conditioning. Treatment may reduce the water sensitivity of these mixtures, but they still would remain more water sensitive to fatigue cracking than the limit set by PAR = 10 percent.

2. Remaining mixtures will have cutoff ratios <1. They can be conventionally treated and improved. The recommended approach is to make sure that the MrR and TSR values are equal to or greater than overall predetermined cutoff ratios to achieve control both of cracking and of rutting at PAR = 10 percent (10 percent loss of dry performance life). The values of these cutoff ratios are (a) MrR cutoff = 0.80, and (b) TSR cutoff = 0.85.

Both cutoff ratios should be simultaneously applied, i.e., at the same time for the same mixture. If MrR and TSR input values are smaller than the cutoff ratios, then treatment or different mixture constituents to reduce the water sensitivity will be required. Because of the need to control wheelpath rutting as well as fatigue cracking, the values of the recommended cutoff ratios are 0.10 higher than the values currently used by most highway agencies.

ACKNOWLEDGMENTS

This research study was one of three in the first series of research projects funded at University of Idaho under the TRANSNOW Northwest Transportation Center program in cooperation with the U.S. Department of Transportation. The authors appreciate the support of these agencies and also of the Idaho Transportation Department, which provided a portion of the local matching funds.

REFERENCES

1. R. P. Lottman, L. J. White, and D. J. Frith. Methods to Predict and Control Moisture Damage in Asphalt Concrete. In *Transportation Research Record 1171*, TRB, National Research Council, Washington, D.C., 1988, pp. 1–11.
2. R. P. Lottman, and D. J. Frith. Predicting the Effects of Moisture on Wheelpath Rutting in Asphalt Concrete. In *Transportation Research Record 1228*, TRB, National Research Council, Washington, D.C., 1989.
3. R. P. Lottman and K. A. Mesch. Effect of Microadditives on Asphalt Concrete. Final Project Report ECE-8411271, National Science Foundation, Washington, D.C., April 30, 1988.
4. R. P. Lottman. *NCHRP Report 246: Predicting Moisture-Induced Damage to Asphalt Concrete*, TRB, National Research Council, Washington, D.C., 1982.
5. Brent Rauhut Engineering. Development of Asphalt-Aggregate Mixture Analysis System: AAMAS. *Phase II Vol. II Preliminary Draft Final Report*. NCHRP Project 9-6(1). TRB, National Research Council, Washington, D.C., Sept. 1988.

Publication of this paper sponsored by Committee on Characteristics of Nonbituminous Components of Bituminous Paving Mixtures.

Laboratory Evaluation of Recycled Asphalt Pavement Using Nondestructive Tests

A. SAMY NOURELDIN AND LEONARD E. WOOD

Many tests have been devised for measuring the characteristics of bituminous materials. These tests can be divided into four categories: (a) destructive tests that are associated with fundamental elastic and viscoplastic behavior such as the indirect tensile tests; (b) destructive tests that are arbitrary (in the sense that their usefulness lies in the correlation of their results with field performance), such as the Marshall and Hveem stability tests; (c) nondestructive tests that are associated with fundamental elastic and viscoplastic behavior such as the resilient modulus test; and (d) nondestructive tests that are arbitrary, such as the sonic pulse velocity test. The nondestructive resilient modulus and sonic pulse velocity tests were used for characterization of hot-mix recycled asphalt paving mixtures. Asphalt specimens were tested for pulse velocity, resilient modulus, and Marshall stability. Analysis and evaluation of the test data indicated sensitivity of the resilient modulus to mix design parameters. The test was identified as an additional criterion for design and evaluation of hot-mix recycled asphalt pavement. Pulse velocity data were not sensitive to the mix design used. However, the modulus of elasticity estimated from the test indicated low statistical variations, suggesting the use of test values as input for pavement thickness design related to layered theory solutions. Stiffness and strength characteristics of the recycled mixtures were comparable to those of a companion virgin bituminous mix, with no recycled materials.

Hot-mix bituminous pavement recycling is a process in which reclaimed bituminous pavement materials, reclaimed aggregate materials, or both, are combined with new bitumen, rejuvenating agents, or virgin aggregate, as necessary, to produce hot-mix paving mixtures that meet standard materials specifications and construction requirements for the type of mixture being produced.

The increase in recycling operations has resulted in an increased awareness that the recycled materials must be properly characterized to ensure a high-quality pavement. The cost and energy savings obtained during construction may be lost through excessive maintenance if the recycled pavements undergo severe deterioration. Initial indications are that a high-quality recycled pavement is being constructed using conventional design methods. However, there are several fundamental questions still unanswered in the area of hot-mix recycling that require research. These include its homogeneity, compatibility, and rate of hardening of a recycled mix when compared to a virgin mix. In addition, assurance is needed that weathering actions, long-term behavior, mechanical properties of compacted recycled mixtures, and the effect of repeated loads on recycled pavements are not problems.

A. S. Noureldin, Public Works Department, Cairo University, Cairo, Egypt. Current affiliation: Ministry of Communications, King Abdel Aziz Road, Riyadh 11178, Saudi Arabia. L. E. Wood, Department of Civil Engineering, Purdue University, West Lafeyette, Ind. 47907.

A laboratory investigation was performed to characterize the performance of the hot-mix recycled asphalt pavement in comparison with a virgin mix. A virgin mixture and three recycled mixtures were evaluated. Marshall size specimens were prepared and evaluated using the pulse velocity, resilient modulus, and Marshall stability tests. Subjective conclusions were established for the performance of recycled mixtures under various conditions.

Study results will provide the highway engineer with a better understanding of the effect of different factors on the resilient characteristics of hot-mix recycled bituminous paving mixtures.

SAMPLING PLAN AND MATERIALS

Recycled Asphalt Pavement

A stockpile of representative salvaged asphalt pavement was obtained for laboratory evaluation. The material used was milled from US-52, a highway south of Indianapolis, Indiana, that was randomly selected and was under the supervision of the Indiana Department of Highways personnel for the purpose of this study. Sampling of the laboratory-created stockpile was also randomly selected to obtain statistically representative asphalt materials for the study.

Samples of the Recycled Asphalt Pavement (RAP) were randomly chosen, reduced in size, and characterized. Asphalt extraction and recovery was conducted using ASTM D2172 method A and the Abson method, ASTM D1856. The salvaged binder was characterized by means of penetration, softening point, and viscosity tests. Amount of asphalt present was determined, and the salvaged aggregate obtained from extraction was characterized by sieve analysis.

Tables 1 and 2 present the characteristics of the extracted hard asphalt and the gradation of salvaged aggregate, respectively. The Indiana State Highway *Standard Specifications* (*1*) for No. 12 surface were also included in Table 2 for comparison purposes and for future determination of the feasibility of the salvaged aggregate for use as a high-quality hot surface mix. The recovered aggregate consisted mainly of crushed limestone as coarse aggregate (material retained on No. 4 sieve) and crushed sand as fine aggregate (material passing No. 4 sieve). The sieve analysis of the salvaged aggregate indicated a gradation that is within the specification for No. 12 surface.

Recycling Agents (Rejuvenators)

Three types of recycling agents were selected for use in combination with the age-hardened salvaged asphalt binder. The

TABLE 1 CHARACTERISTICS OF EXTRACTED HARD ASPHALT

Test	Value
Penetration, 77°F, 100 gm, 5 sec.	28
Viscosity, 140°F, Poises	20,888
Kinematic visc., 275°F, c. st.	726
Softening Point, °F	137
Asphalt Content (Total Wt.)	6%

selections were based on their previous usage in other recycling techniques, wide variation between their natures, and knowledge of their physical and chemical properties. The following recycling agents were used:

- AC-2.5, ASTM designation, produced by Amoco Oil Company.
- AE-150, Indiana-designated high-float, medium-setting-type asphalt emulsion, supplied by McConnaughy, Inc.
- Mobilsol-30, ASTM-designated Type 101 oil, produced by McConnaughy, Inc.

Tables 3–5 present the characteristics of AC-2.5, AE-150, and Mobilsol-30.

Virgin AC-20

The three recycling agents were to be used to restore the old binder present in the RAP to the AC-20, ASTM designation, classification range. A virgin AC-20 was obtained from Amoco Oil Company to use in comparing virgin and recycled hot mixes. Virgin AC-20 was not used in any combination with recycled mixtures. Table 6 gives the characteristics of AC-20. The choice of AC-20 was based on its usage in Indiana to produce hot-mix asphalt pavements.

Virgin Aggregate

Crushed limestone and crushed sand were selected to represent the coarse and fine aggregate material for the virgin aggregate, the same as for recovered salvaged aggregate.

TABLE 3 CHARACTERISTICS OF AC-2.5

Test	Value
Penetration, 100 gm, 77°F, 5 sec., 0.1 mm	200
Absolute viscosity, 140°F, Poise	292
Specific Gravity, 77°F	1.024
Ductility, 77°F, 5 cm/min., cm.	150+

TABLE 4 CHARACTERISTICS OF AE-150

Test	Value
Residue by Distillation	68%
Penetration of Residue	
100 gm, 5 sec, 787°F, 0.1 mm	200
Specific Gravity of Residue, 77°F	1.01
Float, 1140°F, sec.	1200+
Absolute Viscosity of Residue,	
140°F, Poise	270

DETERMINATION OF THE AMOUNT OF REJUVENATOR

The Asphalt Institute curves (*2*) were used to determine an initial value for the percentage of rejuvenator (AC-2.5 and AE-150) to be added to the old binder to restore the properties to AC-20 range of classification. The AC-20 classification range was a target for its wide usage in producing high-quality hot-mix paving mixtures in Indiana. The curves suggest the rejuvenator percentage on the basis of its viscosity at 140°F, the old binder viscosity at 140°F, and the required viscosity for the new rejuvenated binder at 140°F. The initial value for the percentage of Mobilsol-30 was chosen on the basis of previous recycling projects (*3,4*).

A series of extraction and recovery tests were conducted to justify these initial values. Table 7 shows the characteristics

TABLE 2 GRADATION OF SALVAGED AGGREGATE

Sieve Size	3/8	#4	#8	#16	#30	#50	#100	#200
% Passing	98	74	62	44	28	15	7.5	5
IND. spec for #12 Surface	96-100	70-80	36-66	19-50	10-38	5-26	2-17	0-8

TABLE 5 CHARACTERISTICS OF MOBILSOL-30

Percent Asphaltenes*	0
Percent Polar Compounds*	8
Percent Aromatics*	79
Percent Saturates*	13
Percent Residue in Emulsified Form	66.7
Flash Point*, °F	505
Kinematic Viscosity* at 140°F, c.st.	164
Specific Gravity*	0.974

*Properties of Residue

Note: Constituents were obtained using Clay-Gel Analysis (ASTM D2007-75)

TABLE 6 CHARACTERISTICS OF AC-20

Test	Value
Penetration, 100 gm, 5 sec., 77°F, 0.1 mm	65
Absolute Viscosity, 140°F, Poise	1890
Softening Point, °F	122
Ductility, 77°F, 5 cm/min., Cm	150+

of salvaged asphalt, the rejuvenators, and the three rejuvenated binders, together with the amount of rejuvenator being used.

TESTING PROGRAM TO EVALUATE COMPACTED HOT-MIX RECYCLED ASPHALT PAVEMENT

Virgin mixtures containing virgin AC-20 and No. 12 surface virgin aggregate were compared with three other recycled mixtures. Salvaged binders present in recycled mixtures were restored to AC-20 range of classification by using (60 percent AC-2.5 + 40 percent old asphalt), (55 percent AE-150 + 45 percent old asphalt), and (85 percent Mobilsol-30 + 15 percent old asphalt). Salvaged and virgin aggregate combinations in recycled mixtures were adjusted to have the gradation of No. 12 surface. This adjustment was not complicated because the gradation of the salvaged aggregate was within No. 12 surface specification limits, and the virgin aggregate gradation was selected to be the specification midpoint of No. 12 surface.

The four mixes prepared were designated as $(AC)_0$, $(AC\text{-}20)_1$, $(AC\text{-}20)_2$, and $(AC\text{-}20)_3$. All mixtures had the same aggregate gradation (No. 12 surface) and binders satisfying AC-20 specifications. The only difference was that the first was a completely virgin mix and the other three were recycled mixtures with AC-2.5, AE-150, and Mobilsol-30, respectively, as rejuvenating agents.

Three asphalt contents were used in mix preparations: 5.5 percent, 6 percent (original asphalt content present in RAP), and 6.5 percent by total weight of mixture. The mixtures were compacted using the kneading compactor and evaluated using the pulse velocity, resilient modulus, and Marshall stability tests.

TABLE 7 CHARACTERISTICS OF SALVAGED ASPHALT REJUVENATORS AND REJUVENATED BINDERS

Binder	Penetration	Vis. 140°F, Poises
Old Asphalt	28	20,888
AC-2.5	200	292
AE-150 Residue	200	270
40% Old Asphalt + 60% AC-2.5	62	2112
45% Old Asphalt + 55% AE-150 Residue	68	1994
85% Old Asphalt + 15% Mobilsol-30 Residue	69	1974
AC-20 spec.	60+	1600-2400

Note: Mobilsol-30 characteristics are given in Table 5.

Preparation of Specimens

Samples of the recycled asphalt pavement (RAP), virgin aggregate, and virgin AC-20 were heated in an oven at 240°F for 1 hr. The rejuvenators AC-2.5, AE-150, and Mobilsol-30 were heated in an oven at 180°F. The RAP, virgin aggregate, and one rejuvenator were mechanically hot-mixed for 2 min. Absolute virgin mixtures containing AC-20 and virgin aggregate were hot-mixed similarly.

The loose samples containing 5.5, 6, and 6.5 percent asphalt binder for $(AC\text{-}20)_0$ and $(AC\text{-}20)_1$, $(AC\text{-}20)_2$, and $(AC\text{-}20)_3$ specimens were stored in an oven at 140°F for 15 hr. The mixtures were then reheated to 240°F and compacted using the standard California kneading compactor, ASTM D1561, to form specimens of 4-in. diameter and approximately 2.5-in. height.

Tests on Compacted Specimens

The merit in using conventional design indices such as the Marshall or the Hveem stabilities exists in the need for similarity of design procedures for the recycled mix and conventional mixtures.

Pieces of equipment used were the pulse velocity, resilient modulus, and Marshall testing equipment.

Pulse Velocity Test

Pulse velocity tests have been used since the 1940s for evaluating the elastic properties of solid composite materials such as rocks and concrete blocks (*5*). Sonic testing has been used for studying the elastic constants of bituminous mixtures over a wide range of temperature (*6*). The pulse velocity procedure has not been widely used for evaluating conventional bituminous mixtures and investigators have not reported its use for characterizing recycled mixtures. Some studies, however, show that this procedure may be suitable for studying changes taking place in asphalt mixtures with time (*7*).

The pulse velocity determination consists of measuring the rate of propagation of sound waves in a test specimen. The sound wave velocity for elastic materials is a function of elastic modulus, Poisson ratio, and density (*5*,*7*) and can be determined from the following equation:

$$E = v^2 d/c \tag{1}$$

where

E = material elastic modulus,
d = material density,
v = pulse velocity,
$c = 1/(3 - 6\mu) + 2/(3 + 3\mu)$, and
μ = Poisson ratio.

The material modulus can be estimated using this relationship, the pulse velocity measurements, and a proper measurement or assumption of the Poisson ratio. Correlations have been found between the concrete modulus estimated by the pulse velocity measures and from the flexural strength test (*5*).

Bituminous materials are viscoelastic and experience variations in their modulus and Poisson ratio with time and temperature. However, the change in Poisson ratio is not so great, relatively, as is the change in the modulus. A single value can be assumed for the ratio so that the modulus estimation can be used to obtain comparative values between different bituminous mixtures although no exact value can be determined. In addition, pulse velocity may be used directly as the criterion for evaluating asphalt mixtures and thus need not be converted to a modulus value (*7*).

The pulse velocity test is independent of the size and shape of the specimen being tested (*5*). Thus, the procedure is potentially adequate for both laboratory and field testing applications. The test is simple, inexpensive, and more important, nondestructive. Additional testing can be conducted on the same sample in the laboratory.

The pulse velocity test equipment used in this study is the same as that required in the standard test on rocks, ASTM D2845. The equipment briefly consists of a sample holder (a Marshall-type specimen can be used), two transducers, and a pulse generator with a timing unit. The sample height divided by the time measured is the pulse velocity.

The transducers are to be connected to the transmitter and receiver nodes of the pulse generator. The pulse generator is allowed to send mechanical pulses through the transducer connected to the transmitter node. These pulses pass through the compacted specimen and are received by the transducer connected to the receiver. The time taken by this pulse is displayed on the timing unit screen, read, and recorded.

The test was conducted at room temperature, 72°F. A sample holder was used to maintain contact between the transducers and the specimen. In addition, a thin coating of starch gel enhanced the contact between the sample and transducers. For pulse velocity computations, sample height was measured to the nearest 0.1 mm. Specimen weight and height were used to estimate the unit weight of the compacted mixtures.

The following parameters (response variables) were used to characterize the compacted mixtures:

$$V = 32.81\ H/t \tag{2}$$

where

V = pulse velocity (ft/sec/1,000),
H = specimen height (cm),
t = time displayed on screen (μsec), and
32.81 = constant for units adjustment.

$$E = V^2 d/C \tag{3}$$

where

E = instantaneous elastic modulus,
V = pulse velocity,
d = density,
$C = 1/(3-6\mu) + 2/(3+3\mu)$, and
μ = Poisson ratio.

To estimate the instantaneous elastic modulus a value for μ was assumed. The theoretical value ranges between 0 and 0.5 and depends on the materials property. Asphalt mixtures are believed to have values in the range 0.25 to 0.45. Schmidt (*8*) used a value of 0.35 at ambient temperature in the computations of the diametral resilient modulus. Mamlouk (*9*) indicated difficulties in laboratory determination of the Poisson

ratio value; instead, he assumed values for μ of 0.3, 0.35, and 0.4 at 50°F, 75°F, and 100°F, respectively.

The estimation of E from pulse velocity test results of this study was based on assuming a Poisson ratio of 0.35 for a test temperature of 72°F. Using this assumption and adjusting the units, Equation 3 can be expressed as

$$E = V^2d/7{,}442 \quad \text{at } 72°F \tag{4}$$

Resilient Modulus Test

The resilient modulus, the modulus of elasticity when the theory of elasticity is applied to bituminous mixtures to analyze the stress-strain relationship, is the ratio of the applied stress to the recoverable strain when a dynamic load is applied.

The resilient modulus for an asphalt mix can be determined in the laboratory using the diametral compression mode in which Marshall-sized specimens can be used. The test method is based on the fact that when a viscoelastic material is loaded for a short duration of time, its response is mainly elastic.

Schmidt (*8*) developed a procedure in which a pulsating load is applied across the vertical diameter of a Marshall specimen every 3 sec with 0.1-sec duration and the corresponding horizontal deformation is recorded. The fact that the test is not only sensitive, but also rapid and nondestructive makes it an excellent tool for design and characterization of hot-mix recycled asphalt pavement.

The resilient modulus test equipment used in this study consists mainly of a load cell, specimen restraint, diaphragm air cylinder, source of compressed air, solenoid valve system, two transducers, and a control panel. The compressed air source is connected to the diaphragm air cylinder through the solenoid valve system. The solenoid valve is electrically activated and turned on for a duration of 0.1 sec every 3 sec, causing a pulse of compressed air to pass through the air cylinder and to create a pulse load along the vertical diameter of the test specimen.

The magnitude of the pulse load is controlled through adjustment of the compressed air. The horizontal deformation of the specimen is measured by the two transducers that are adjusted to lie on opposite sides of the horizontal diameter of the specimen. The magnitude of the load and resultant deformation are displayed on a detector on the electronic control panel. They can be read easily and recorded.

The horizontal transducers were moved until they just contacted the properly aligned specimen. The load was applied across the vertical diameter of the specimen using two curved loading strips of 0.5-in. width and 2-in. radius (same as the specimen). The magnitude of the applied load was controlled by adjusting the pressure regulator for the compressed air to 35 and 50 lb. Horizontal deformations corresponding to each of the applied loads were displayed on the recorder screen and recorded.

Resilient modulus MR values corresponding to each load magnitude and resulting deformation were computed using the following equation:

$$\text{MR} = \frac{P(\mu + 0.2734)}{hD} \tag{5}$$

where

P = compressed air pressure (lb),
MR = resilient modulus (psi),
h = specimen height (in.),
D = deformation (in.), and
μ = Poisson ratio, assumed to be 0.35 at a test temperature of 72°F.

Marshall Stability Test

The autographic Marshall testing apparatus was used to conduct the Marshall stability tests on the recycled mixtures. The recorder provides a continuous load-deformation plot as a specimen is being loaded to failure. Load at failure is the specimen stability, while total deformation at failure is its flow in units of 0.01 in.

The Marshall stability test was conducted on $(AC\text{-}20)_0$, $(AC\text{-}20)_1$, $(AC\text{-}20)_2$, and $(AC\text{-}20)_3$ specimens previously tested by the nondestructive pulse velocity and resilient modulus tests.

CHARACTERISTICS OF COMPACTED SPECIMENS

Pulse Velocity Test

Pulse Velocity

Table 8 presents pulse velocity values for different compacted mixtures at different asphalt contents. The analysis of variance (ANOVA) results suggested that there were no significant differences between the pulse velocity values caused by change of asphalt content. However, the mean value at 6.5 percent was slightly lower than those values at 5.5 and 6.0 percent. Pulse velocity values of compacted recycled mixtures $(AC\text{-}20)_2$ with AE-150 as a recycling agent were slightly lower than those values for absolute virgin mix $(AC\text{-}20)_0$. Other recycled mixtures, $(AC\text{-}20)_1$ and $(AC\text{-}20)_3$, did not demonstrate significant differences in the pulse velocity values compared to the $(AC\text{-}20)_0$ mix.

Density

Table 9 presents density values for the different compacted specimens at asphalt contents of 5.5, 6.0, and 6.5 percent. Analysis of variance indicated no significant difference between density values at the three asphalt contents. The density was determined by measuring the specimen weight and average specimen height. The limited accuracy of this method in determining density could be a factor in the lack of variation in density with change in asphalt content. In addition, the three asphalt contents (5.5, 6.0, and 6.5 percent) may be at or around the optimum content for maximum density, explaining the resulting insignificant differences. The statistical analysis also indicated a slight difference between density values of the virgin and two recycled mixtures. This difference might indicate better compactibility of recycled mixtures prepared using AE-150 and Mobilsol-30 as recycling agents.

TABLE 8 PULSE VELOCITY ($\times$ 1,000 ft/sec) AT 72°F FOR COMPACTED MIXTURES AT DIFFERENT ASPHALT CONTENTS

	Mixture Types				
%A.C.	$(AC\text{-}20)_0$	$(AC\text{-}20)_1$	$(AC\text{-}20)_2$	$(AC\text{-}20)_3$	Mean
	11.14	10.66	11.25	10.69	
5.5%	11.55	11.24	10.49	10.65	10.99
	11.16	10.99	11.10	11.00	
	11.09	10.86	10.71	11.19	
6.0%	11.27	11.23	10.63	11.28	11.04
	10.74	11.36	10.87	11.28	
	10.84	10.53	10.52	10.90	
6.5%	11.21	10.79	10.98	10.51	10.80
	11.19	11.11	10.37	10.62	
Mean	11.13	10.97	10.77	10.90	

TABLE 9 DENSITY (g/cm^3) FOR COMPACTED MIXTURES OF DIFFERENT ASPHALT CONTENTS

	Mixture Types				
%A.C.	$(AC\text{-}20)_0$	$(AC\text{-}20)_1$	$(AC\text{-}20)_2$	$(AC\text{-}20)_3$	Mean
	2.33	2.35	2.39	2.40	
5.5%	2.39	2.37	2.39	2.41	2.38
	2.35	2.35	2.39	2.41	
	2.37	2.34	2.36	2.40	
6.0%	2.36	2.37	2.39	2.40	2.37
	2.35	2.34	2.37	2.39	
	2.36	2.32	2.36	2.40	
6.5%	2.37	2.38	2.38	2.40	2.37
	2.35	2.37	2.37	2.38	
Mean	2.36	2.36	2.38	2.40	

Note: (1) Density values were rounded to two decimal places.

(2) Statistical Analyses were based on non-rounded data.

Modulus of Elasticity

Table 10 presents the estimated modulus of elasticity values for the absolute virgin mixture $(AC\text{-}20)_0$ and the recycled mixtures $(AC\text{-}20)_1$, $(AC\text{-}20)_2$, and $(AC\text{-}20)_3$ at 5.5, 6.0, and 6.5 percent binder contents. The ANOVA suggests that the modulus of elasticity estimation by pulse velocity is neither sensitive to the binder type nor to the change in asphalt content. No significant differences were detected at $\alpha = 0.05$. However, recycled mixtures, especially those modified by AE-150, provided slightly lower modulus values than those of virgin mixtures. In addition, mixtures containing 6.5 percent binder content also provided slightly lower modulus values than those containing 5.5 and 6.0 percent.

Resilient Modulus Test

The diametral resilient modulus test was conducted on the same specimens tested by the nondestructive pulse velocity test. Table 11 presents the modulus values corresponding to 5.5, 6.0, and 6.5 percent binder contents and the various mixture types. The test was sensitive both to binder content and to binder type present in the virgin and recycled mixtures (unlike the pulse velocity test), and significant differences were detected. Asphalt content of 5.5 percent appears to be the optimum content for maximum modulus values. The increase in asphalt content from 5.5 to 6.0 percent resulted in a significant decrease in the modulus value. Resilient modulus values at 6.5 percent asphalt content were also slightly lower than those values at 6.0 percent, but significantly lower than the modulus values at 5.5 percent.

Virgin mixture $(AC\text{-}20)_0$ showed higher modulus values over recycled mixtures, as indicated in Table 11. Virgin mixture $(AC\text{-}20)_0$ provided the highest modulus values, followed by recycled mixture with Mobilsol-30 as rejuvenator; $(AC\text{-}20)_3$; and the recycled mixtures containing AC-2.5 and AE-150, with $(AC\text{-}20)_1$ and $(AC\text{-}20)_2$, respectively, as modifiers. $(AC\text{-}20)_2$ mixtures provided the lowest modulus values. The trend is identical to that obtained for pulse velocity and modulus of elasticity estimated from pulse velocity tests. However, the statistical significance was detected herein, whereas it was not detected from pulse velocity test results.

Marshall Stability Test

Specimens tested by the nondestructive pulse velocity and resilient modulus tests were loaded to failure by the Marshall loading mechanism, after placing them in an oven at 140°F for 2 hr.

Table 12 presents the Marshall stability values for virgin and recycled mixtures. Marshall stability values were sensitive to binder type in the various mixtures as well as the asphalt content, and significant differences were detected by ANOVA results. Virgin mixtures $(AC\text{-}20)_0$ provided the highest Marshall stability values, followed by RAP modified by Mobilsol-30, RAP modified by AC-2.5, and RAP modified by AE-150. Flow values, which were almost identical for all mixtures, ranged between 11.0 and 14.0 (in 0.01 in.).

DISCUSSION OF RESULTS

Some empirical values are presented that can give a general idea about the characteristics of asphalt paving mixtures. The usual judgment of a highway engineer is that for two asphaltic mixtures having Marshall stabilities of 700 and 2,000 lb to be

TABLE 10 MODULUS OF ELASTICITY ($\times 10^6$ psi) AT 72°F FOR COMPACTED MIXTURES AT DIFFERENT ASPHALT CONTENTS

	Mixture Types				
%A.C.	$(AC\text{-}20)_0$	$(AC\text{-}20)_1$	$(AC\text{-}20)_2$	$(AC\text{-}20)_3$	Mean
	2.421	2.234	2.531	2.302	
5.5%	2.672	2.505	2.205	2.290	2.408
	2.452	2.375	2.469	2.439	
	2.447	2.316	2.274	2.515	
6.0%	2.513	2.502	2.262	2.555	2.423
	2.268	2.532	2.346	2.546	
	2.326	2.159	2.191	2.387	
6.5%	2.499	2.318	2.404	2.224	2.317
	2.462	2.454	2.133	2.250	
Mean	2.451	2.377	2.313	2.390	

TABLE 11 DIAMETRAL RESILIENT MODULUS ($\times 10^6$) AT 72°F FOR COMPACTED MIXTURES AT DIFFERENT ASPHALT CONTENTS

	Mixture Types				
%A.C.	$(AC\text{-}20)_0$	$(AC\text{-}20)_1$	$(AC\text{-}20)_2$	$(AC\text{-}20)_3$	Mean
	0.755	0.653	0.675	0.671	
5.5%	0.936	0.648	0.706	0.697	0.717
	0.717	0.659	0.736	0.752	
	0.690	0.440	0.466	0.610	
6.0%	0.689	0.510	0.404	0.645	0.590
	0.738	0.596	0.556	0.739	
	0.726	0.434	0.353	0.635	
6.5%	0.615	0.594	0.462	0.466	0.543
	0.642	0.593	0.336	0.658	
Mean	0.723	0.570	0.522	0.653	

NOTES: Least significant difference between means, mixture type = 0.07 * 10^6 psi.
Least significant difference between means, %AC = 0.06 * 10^6 psi.
$\alpha = 0.05$.

TABLE 12 MARSHALL STABILITY AT 140°F FOR DIFFERENT COMPACTED MIXTURES

	Mixture Types				
%A.C.	$(AC\text{-}20)_0$	$(AC\text{-}20)_1$	$(AC\text{-}20)_2$	$(AC\text{-}20)_3$	Mean
	2450	2050	1850	2150	
5.5%	2500	2150	1900	2350	2138
	2550	1950	1750	2000	
	2250	1850	1700	1900	
6.0%	2200	1750	1600	1800	1929
	2300	1950	1750	2100	
	2000	1650	1500	1900	
6.5%	1950	1750	1550	1700	1721
	2050	1600	1400	1600	
Mean	2250	1856	1667	1944	

Notes:

*L.S.D., Mix Type = 91 pounds
*L.S.D., % AC = 79 pounds

used in pavement construction, the first is generally a poor mixture and the second is generally a good mixture. However, familiarity with other mechanical property values is not the same as for the better-known Marshall stability values. The following empirical values, the overall means of the various response variables obtained in this study, can give a rough idea about other mechanical property values. Asphalt mixtures with a Marshall stability value in the range of 1,400 to 2,550 lb and 1,930 lb average value, have roughly the following empirical values at ambient temperature (72°F):

- Pulse velocity through compacted specimens is in the range 10,500 to 11,500 ft/sec with an average value of 11,000 ft/sec. This value for structural concrete is roughly 15,000 ft/sec. Sonic pulse velocities are approximately 1,100 and 17,000 ft/sec in air and steel, respectively.
- Modulus of elasticity in the range 2.1 to 2.7 $\times$ 10^6 psi with an average of 2.4 $\times$ 10^6 psi.
- Resilient modulus in the range of 340 to 940 ksi with an average of 620 ksi.

The total variation from the mean was approximately ± 4.5 percent for pulse measurements, ± 12.5 percent for modulus of elasticity computations, ± 30 percent for Marshall stability measurements, and ± 47 percent for resilient modulus measurements. That the compacted specimens were identical in gradation and binder consistency characteristics implied that the resilient modulus test was the most sensitive to binder type (virgin or recycled). However, the sensitivity of the Marshall stability test was also good enough to identify mixtures with higher strength (stability).

Lower variation in sonic pulse velocity and modulus of elasticity values—estimated from pulse velocity measurement—suggest them as better candidates for pavement thickness design. Both measurements are closer to the elastic range of bituminous materials than is the resilient modulus and therefore they may be more appropriate for the application of elastic layered theory solutions for pavement thickness.

SUMMARY OF RESULTS

Three hot-recycled bituminous mixtures in the compacted state were characterized using the pulse velocity, resilient modulus, and Marshall stability tests. The recycled mixtures contained binders with the same consistency as AC-20 and the aggregate gradation of No. 12 surface. The three recycling agents used in the mixtures were AC-2.5, AE-150, and Mobilsol-30. Every recycled mixture contained old asphalt, salvage aggregate, virgin aggregate, and only one of these recycling agents. A virgin mixture containing virgin aggregate and virgin AC-20 was characterized by the same tests for comparative purposes. Binder contents in the mixtures were 5.5, 6.0, and 6.5 percent by total weight of the mix. The main findings are summarized as follows:

- Virgin mixture stiffness (resilient modulus) and strength values (Marshall stability) were in general higher than those of recycled mixtures.
- The stiffness and strength values of the recycled mixture with AE-150 as a rejuvenator were remarkably low. AE-150 may be a poor choice of rejuvenator for hot-mix recycling.
- Pulse velocity test parameters were neither sensitive to binder content nor to the binder type present in the mixtures. This result could be attributed to the similarity between all mixtures in the elastic range caused by the high rate of application of pulses.
- Resilient modulus test results were sensitive to both binder content and type. The test can be used for the design of asphalt mixture (virgin or recycled) and the evaluation of recycling agent used.
- The conventional Marshall stability test was appropriate enough to identify binders (virgin or recycled) with potential to produce mixtures with higher strength (stability).
- Low statistical variations obtained from pulse velocity and modulus of elasticity measurements may suggest their use for pavement thickness design on the basis of layered elastic theory solutions.

ACKNOWLEDGMENTS

This research was carried out at Purdue University. The authors are grateful for the support of the Indiana Department of Highways and the U.S. Department of Transportation, FHWA.

REFERENCES

1. *Standard Specifications*. Indiana Department of Highways, West Lafayette, 1988.
2. *Asphalt Hot-Mix Recycling*. MS–20, The Asphalt Institute, Lexington, Ky., 1981.
3. A. Iida. *The Effects of Added Softening Agents Upon The Behavior of Cold Recycled Asphalt Mixtures*. Report FHWA/IN/JHRP-80/13. Purdue University, West Lafayette, Ind., 1980.
4. N. Khosla. *Effect of Emulsified Modifiers on the Characteristics of Recycled Mixtures*. Preprint, Association of Asphalt Paving Technologists, St. Paul, Minn., Feb. 1982.
5. B. G. Long, H. J. Kartz, and T. A. Sandenau. An Instrument and a Technique for Field Determination of the Modulus of Elasticity and Flexural Strength of Concrete (Pavements). *Proc., American Concrete Institute*, Vol. 41, Chicago, Ill., 1945, p. 217.
6. W. H. Goetz. Sonic Testing of Bituminous Mixtures. *Proc., Association of Asphalt Paving Technologists*, Vol. 34, St. Paul, Minn., 1955, p. 332.
7. P. G. Manke and B. M. Gallaway. Pulse Velocities in Flexible Pavement Construction Materials. In *Highway Research Record 131*, HRB, National Research Council, Washington, D.C., 1966, p. 128.
8. R. J. Schmidt. A Practical Method for Measuring the Resilient Modulus of Asphalt-Treated Mixes. In *Highway Research Record 404*, HRB, National Research Council, Washington, D.C., 1972, pp. 22–32.
9. M. S. Mamlouk. *Characterization of Cold Mixed Asphalt Emulsion Treated Bases*. Report JHRP-79-19, Purdue University, West Lafayette, Ind., 1979.
10. A. S. Noureldin. *Material Characterization of Hot Mix Bituminous Pavement Recycling*. Ph.D. dissertation. Purdue University, Civil Engineering Department, West Lafayette, Ind., 1987.

Publication of this paper sponsored by Committee on Characteristics of Bituminous Paving Mixtures To Meet Structural Requirements.

Development of the Pressure Method for Determining Maximum Theoretical Specific Gravity of Bituminous Paving Mixtures

COLIN A. FRANCO AND K. WAYNE LEE

The viability of using an air meter (Type B) for determining the maximum theoretical specific gravity (MTSG) of asphalt mixtures was evaluated. The air meter normally has been used for determining the percentage of air in fresh portland cement concrete. A series of experiments were performed using this new method (herein called the "pressure method") and the current standard (Rice) method. The primary experiment involved determining MTSG by two methods on 10 asphalt mixtures with varying asphalt contents. There was good correlation and no significant difference in the performance or precision between the two methods. There was little difference in obtaining the optimum asphalt content by the two methods. The results of the additional experiments with aggregates from three different sources indicated no difference in precision between methods or operators. Suggestions were made for modifying and improving the air meter for pressure method testing, to add versatility in the options for determining the MTSG of asphalt mixtures (and other materials of a porous or water-absorbent nature).

The maximum theoretical specific gravity (MTSG) of asphalt concrete (AC) is the specific gravity at which zero air voids are present in the mixture (*1,2*). MTSG is one of the most important properties of an asphalt mixture; not only does it provide an upper limit for the possible compaction in the field, but its determination is also critical in later computing the voids in the compacted asphalt pavement (*3,4*). MTSG is also used in the computation of voids filled with asphalt (VFA), which is a measure of asphalt cement coating on the mineral aggregate. These two parameters play important roles in determining engineering properties of asphalt mixtures and in evaluating potential for pavement distress modes such as raveling, shoving, rutting, flushing, and cracking.

In addition, the Marshall method of asphalt mix design requires that the optimum asphalt content (OAC) be found using the voids criteria, among others, which require the determination of the MTSG.

Proper and precise determination of the MTSG is important in the asphalt mix design procedure and in evaluating performance of asphalt pavements, which make up approximately 70 percent of the nation's highway system.

The current experimental method is the Rice method (AASHTO T-209 and ASTM D2041–78), which uses a volumetric flask, vacuum apparatus, and water (see Figure 1). The Rice method is primarily a displacement method in which a known mass of prepared asphalt mixture is introduced into an empty flask of known volume, which is then filled with water. Air entrapped within the asphalt and water mixture in the flask is expelled by a vacuum. The MTSG is then calculated by computing the displaced volume of water. All of the air is not expelled during the application of the vacuum, possibly because of the affinity of air for the asphaltic compounds in the mixture. The new method does not have this problem, because the entrapped air is accounted for in the computation.

The new method, herein called the "pressure method," makes use of the Type B air meter (AASHTO T-152-82 and ASTM C231-80), which works on the principle of Boyle's law, i.e., the operational principle of this meter consists of equalizing a known volume of air at a known pressure in a sealed air chamber with an unknown volume of air in the sample of asphalt mixture and water. The dial on the pressure gauge is calibrated in terms of percent of air for the observed pressure at which equalization takes place (see Figure 2).

In the pressure method, a weighed sample of prepared asphalt mixture is introduced into the bowl of the air meter, and the meter is filled to capacity with water. No attempt is made to remove any entrapped air. The filled air meter is weighed, and the weight of water obtained. The air content of the meter is then determined in accordance with the method in AASHTO T-152. Back calculations are performed and the volume of the sample of asphalt mixture is found. The MTSG is then the weight in grams of the sample divided by its volume in cubic centimeters.

The objectives of this study were

1. Evaluation of the viability of the pressure method to determine MTSG (Experiment 1),
2. Confirmation of the viability of the method using various types of aggregates from three different sources (Experiment 2), and
3. Verification of the precision and repeatability of the pressure method (Experiments 3A and 3B).

EXPERIMENTAL PROGRAMS

Experimental programs included the sampling and processing of the aggregates (both coarse and fine), producing the asphalt

C. A. Franco, Materials Section, Division of Public Works, Rhode Island Department of Transportation, Providence, R.I. 02903. K. W. Lee, Department of Civil Engineering, University of Rhode Island, Kingston, R.I. 02881.

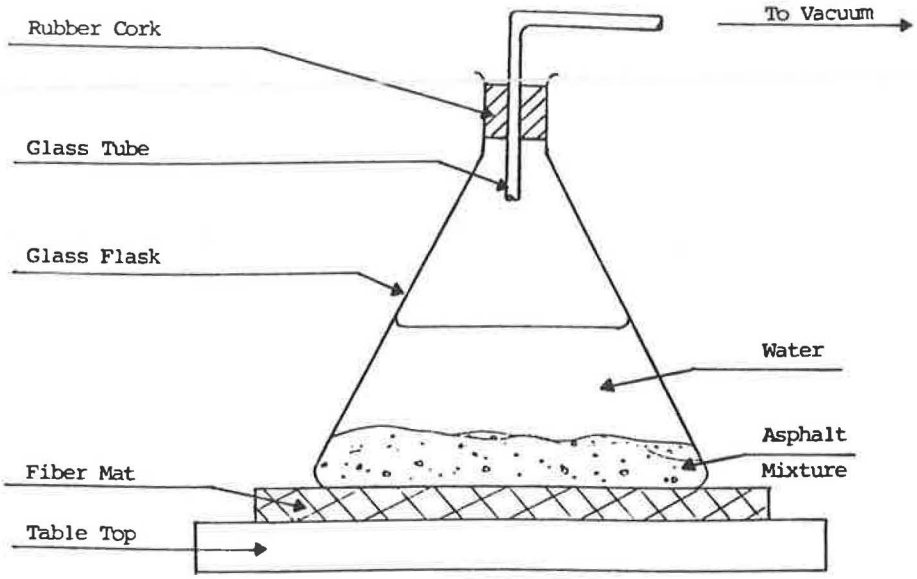

FIGURE 1 Schematic diagram of the experimental setup for the Rice method.

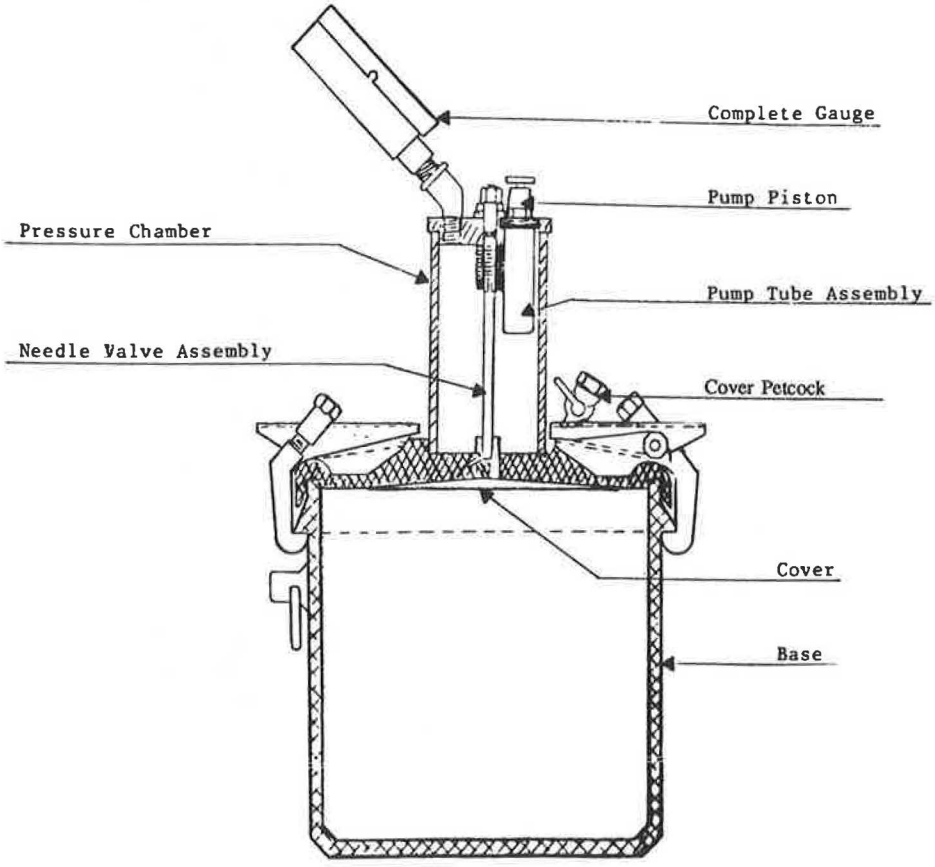

FIGURE 2 A cross section of an air meter indicating main components.

mixtures, fabrication of Marshall core specimens when required, testing of specimens, comparative analysis of the methods used, and drawing conclusions.

Materials

Mineral Aggregates

Coarse aggregates from three local suppliers were used. Two of the aggregate sources were of fine-grained, trap rock with low absorption characteristics. The other source was a crushed gravel, which also had low absorption characteristics (see Table 1). The aggregates were sieved into their individual sizes. The fine aggregates consisted of crushed-stone and natural sand; their characteristics are presented in Table 2. The aggregates were sieved into individual-sized fractions as presented in Column C of Table 3. Both crushed and fine aggregates were blended to have the gradation of Rhode Island Class I–1 standard-surface course mix with a maximum size of ¾ in.

For Experiment 1, aggregates were obtained from one supplier and sieved into individual sizes in sufficient quantity to produce enough material for 10 sets of cores. For Experiment 2, aggregates were obtained from three different suppliers and sieved into individual sizes in sufficient quantity to produce enough material for 4 sets of cores.

Asphalt Cement

AC–20 from a single source was used; it was obtained in a number of quart-sized containers.

Plant Asphalt Hot-Mix

In conducting Experiment 3, a production mix from one of the three suppliers, consisting of the same class of asphalt mixture, i.e., Class I–1 surface course, was used.

TABLE 1 PHYSICAL PROPERTIES OF COARSE AGGREGATE

Aggregate Supplier	Apparent Specific Gravity	Absorption (percent)	Unit weight (lbs./ cu. ft.)	Bulk Specific Gravity
Gammino Inc.	2.757	1.10	102.90	2.674
Forte Bros.	2.789	0.97	100.73	2.715
Cardi Corp.	2.668	1.16	94.80	2.588

TABLE 2 PHYSICAL PROPERTIES OF FINE AGGREGATE

Aggregate Supplier	Apparent Specific Gravity	Absorption (percent)	Unit Wt. (lbs./ cu. ft.)	Bulk Specific
Gammino Inc.	2.738	1.10	117.14	2.659
Forte Bros.	2.777	0.45	119.10	2.750
Cardi Corp.	2.668	0.71	121.9	2.618

TABLE 3 GRADATION OF RHODE ISLAND CLASS I-1 MIX FOR SURFACE COURSE

(A) Sieve Opening	(B) Percent Passing	(C) Aggregate Size	(D) Percent of Individual Size
3/4"	100.0	3/4" - 1/2"	10.0
1/2"	90.0	1/2" - 3/8"	10.0
3/8"	80.0	3/8" - #4	20.0
#4	60.0	#4 - #8	17.5
#8	42.5	#8 - #30	19.0
#30	23.5	#30 - #50	5.5
#50	18.0	#50 - #100	6.0
#100	12.0	#100 - #200	6.5
#200	5.5	passing #200	5.5

Testing Programs

Experiment 1

Asphalt cores were made by combining the coarse and fine aggregate together with the AC. In 10 different sets of four cores each, the asphalt content values were, 4.0, 4.3, 4.6, 4.9, 5.2, 5.5, 5.8, 6.1, 6.4, and 6.7 percent. The bulk specific gravity was determined for each set of cores according to Method B of AASHTO T-166. The cores were then tested for stability and flow according to Sections 4 and 5 of AASHTO T-245.

Preparation of Samples. The four cores of the set were heated in an oven at 105°C to remove traces of moisture and to separate the particles of the sample as described in the Rice method procedures. The separated sample was then split into two portions, with the portion for the Rice method weighing approximately 1,500 to 1,600 g.

Rice Method. The MTSG was determined according to the Rice method procedure (AASHTO T-209, Section 6.7, Flask Determination). This sample portion was then retained, air-dried, and rerun to obtain a second result. The average of two results was taken for analysis and comparison.

Pressure Method. The MTSG was determined for the second portion of samples according to the following procedures:

1. The air meter to be used was cleaned, calibrated, and weighed. The initial air line was determined before commencement of the experiment.
2. The volume of the air meter was ascertained by filling the bowl with distilled water and introducing additional water into the petcocks until overflow occurred. The temperature of the water was noted, as well as the weight of the air meter filled with water. From the differences in weight, the amount of water required to fill the meter was determined. Then, using the temperature correction factor for the water, the volume of the air meter was calculated to the nearest 0.1 mL. The water was then discarded, and the meter was dried completely.
3. The sample was weighed accurately in the dry bowl of the meter to the nearest 0.1 g.
4. Distilled water was introduced to the bowl with the sample, and the bowl was agitated by tapping on the sides to expel large air bubbles.
5. The top of the meter was then placed securely to the bowl, and additional water was inserted through the petcocks until overflow occurred.
6. The pump was primed until the needle rested on the initial pressure line.
7. The petcocks were closed, and the meter was wiped dry so as not to leave any overflow water on the outside.
8. The air meter, water, and sample were then weighed to the nearest 0.1 g.
9. The air valve was opened to equalize the pressure between the chambers, and the percentage of air was read on the dial (AASHTO T-152, Section 7.3).
10. This procedure was repeated twice to obtain two more air percentage readings.
11. The pressure was then released, and the temperature of the water in the meter was recorded.
12. The sample was saved, air-dried, and retained to obtain the second set of air percentage readings.
13. The MTSG was calculated with temperature correction. The reported MTSG was then the average of the three results. A form for determination of specific gravity by the pressure method is shown in Figure 3.

Air Meter #:_____ Date:_____
Balance #: _____ Name of Tester:_____
Sample # & I.D.:_____ Sampled By:_____

Test Procedure

1) Wt. of Air Meter (dry)			_____	gms.
2) Wt. of Air Meter & Asphalt Sample			_____	gms.
2b) (zero or tare the balance)				
2c) (fill meter with water)	Run 1	Run 2	Run 3	
3) Wt. of Water in Meter				gm
4) Temp. of Water				°C
4b) (correction factor F)				
5) Air Reading (percent)				
6) Wt. of Air Meter & Water (full)			_____	gms.

Calculations

	Run 1	Run 2	Run 3	
7) Vol. of Air Meter [(6)-(1)]/(4b)				ml
8) Vol. of Water in Air Meter (3)/(4b)				ml
9) Vol. of Air (5)X(7)/100%				ml
10) Wt. of Asphalt Mix (2)-(1)				gm
11) Vol. of Asphalt (7)-(8)-(9)				ml
12) Specific Gravity [(10)/(11)]/(4b)				

Maximum Specific Gravity of Mix (Avg. of Runs) = _____

FIGURE 3 A form for the determination of specific gravity by the pressure method.

Experiment 2

Aggregate materials from three different suppliers were obtained and processed. Asphalt mix designs for the standard RI Class I–1 mix were made for each of the materials, using the Marshall method. Four sets of four cores were made for each mix design at asphalt contents of 5.0, 5.5, 6.0, and 6.5 percent. The average bulk specific gravity for each set was determined. The cores were then tested (AASHTO T-245) and each set of cores was dried and prepared (AASHTO T-209). The tests were performed by both the Rice and pressure methods and repeated after the samples were thoroughly air-dried.

The mix design results were plotted for each of the three different mixes, and a voids analysis was carried out using the MTSG obtained by the Rice and pressure methods. Comparative analysis of results determined the following:

- Confirmation of viability of the pressure method and results obtained in Experiment 1, and
- Any significant impact on the mix design (i.e., whether the OAC values were more or less the same).

Experiment 3

Experiment 3A. A standard RI Class I–1 production mix sample was obtained weighing approximately 100 kg and prepared as previously (*1*). This production sample was then subdivided into 17 lots using a sample splitter. Each lot was further divided to provide two test samples, of approximately 1,500 to 1,600 g for the Rice method and of approximately 3,400 to 3,500 g for the pressure method.

The samples for this series of 17 dual tests were run only once with the following stipulations:

- The tests were run on two different sets of apparatuses for both methods,
- Two operators were interchanged midway during the test programs, and

• The two methods were run simultaneously on the same day and within 1 hr of each other.

Experiment 3B. Two out of 17 subsamples were tested repeatedly (eight times) following the same test procedures as described previously, except that the operators were not interchanged; each test method had a unique operator.

RESULTS

Experiment 1

The results of Experiment 1 are presented in Table 4, and further analysis was carried out, as follows:

• Statistical Comparison. A statistical comparison of the results obtained by the two methods indicated that there was no significant difference in performance between the Rice and pressure methods. Figure 4 shows a comparison of MTSG results from these methods.

• Precision. The analysis did not detect a difference in precision between the two methods.

• Sensitivity. The Rice method was more sensitive to the change in asphalt content because as the asphalt content increased, the MTSG of the mix decreased at a relatively uniform rate. For the pressure method, the MTSG did not always decrease at a uniform rate with increase of asphalt content (see Figure 5).

• Marshall Mix Design. The difference in the OAC values determined by the air voids obtained by the Rice and pressure methods was about 0.1 percent.

Experiment 2

Table 5 presents three suppliers of aggregates, asphalt content of each of the mixes, calculated MTSG, two Rice method results, two pressure method results, and the average of results. Further analysis was performed as follows:

• Average Values. The average values of the MTSG obtained by the Rice and pressure methods were within 0.08 percent of each other. The calculated average value for the MTSG was 0.8 percent lower than for the other methods. Table 6 presents the voids analysis for the mix design by calculation, Rice, and pressure methods.

• Standard Deviations. The standard deviation for the calculated MTSG was lower than that for the Rice and pressure methods. The standard deviations for the Rice and pressure methods were of the same magnitude.

• Performance. No difference in performance was detected from individual Rice method runs, individual pressure method runs, or runs between two methods (see Table 7).

• Correlation. There was good correlation between the three methods (see Table 7).

• Mix Design. Figure 6 shows a typical Marshall properties plot for one of the three different mixes used to determine OAC values. The OAC value determined by the three methods did not vary by more than 0.1 percent.

Experiment 3A

Tables 8 and 9 present the subsamples, operators, apparatus, and MTSG obtained by the Rice and pressure methods,

TABLE 4 MTSG OF BITUMINOUS MATERIALS—RESULTS OF RICE AND PRESSURE METHODS FOR EXPERIMENT 1

a) Results of Rice Method

Day	AC (%)	Rice Method			
		Run1	Run2	Avg.	d_{1-2}
1	4.0	2.553	2.552	2.553	0.001
2	4.3	2.574	2.570	2.572	0.004
3	4.6	2.561	2.559	2.560	0.002
4	4.9	2.545	2.542	2.544	0.003
5	5.2	2.542	2.539	2.541	0.003
6	5.5	2.521	2.522	2.522	-0.001
7	5.8	2.519	2.519	2.519	0.000
8	6.1	2.504	2.505	2.505	-0.001
9	6.4	2.494	2.495	2.495	-0.001
10	6.7	2.493	2.491	2.492	0.002

Note: d_{1-2} = Result of Run 1 - Result of Run 2

(*continued on next page*)

TABLE 4 (*continued*)

b) Results of the Pressure Method

Day	AC (%)	Pressure Method			
		Run1	Run2	Avg.	d_{1-2}
1	4.0	2.565	2.563	2.564	0.002
2	4.3	2.566	2.567	2.567	-0.001
3	4.6	2.549	2.548	2.549	0.001
4	4.9	2.555	2.552	2.554	0.003
5	5.2	2.525	2.524	2.525	0.001
6	5.5	2.520	2.530	2.525	-0.010
7	5.8	2.528	2.528	2.528	0.000
8	6.1	2.517	2.510	2.514	0.007
9	6.4	2.502	2.503	2.503	-0.001
10	6.7	2.494	2.493	2.494	0.001

Note: d_{1-2} = Result of Run 1 - Result of Run 2

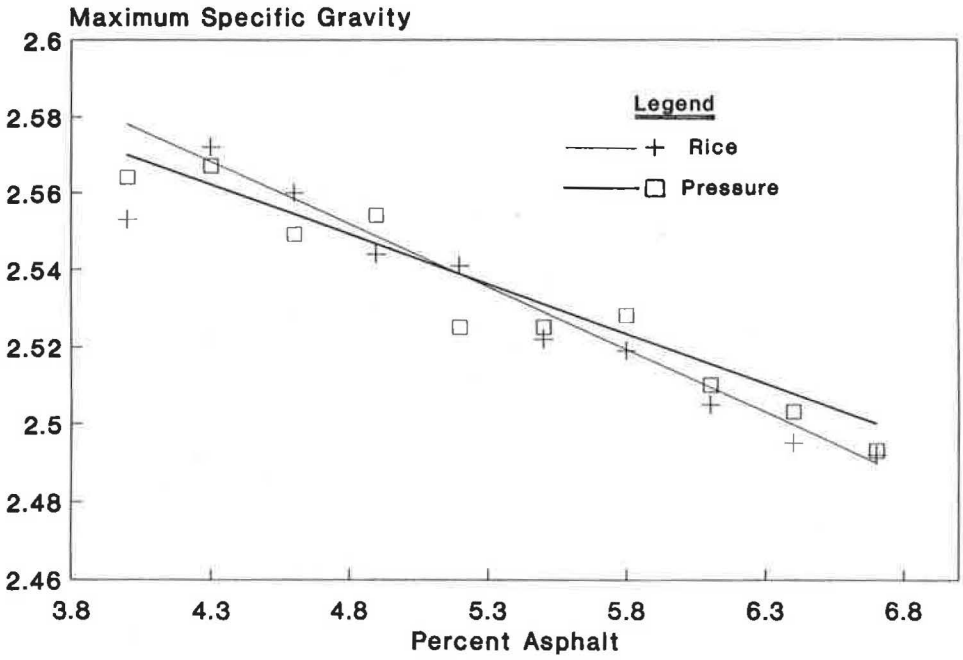

FIGURE 4 Maximum specific gravity versus asphalt content for Experiment 1.

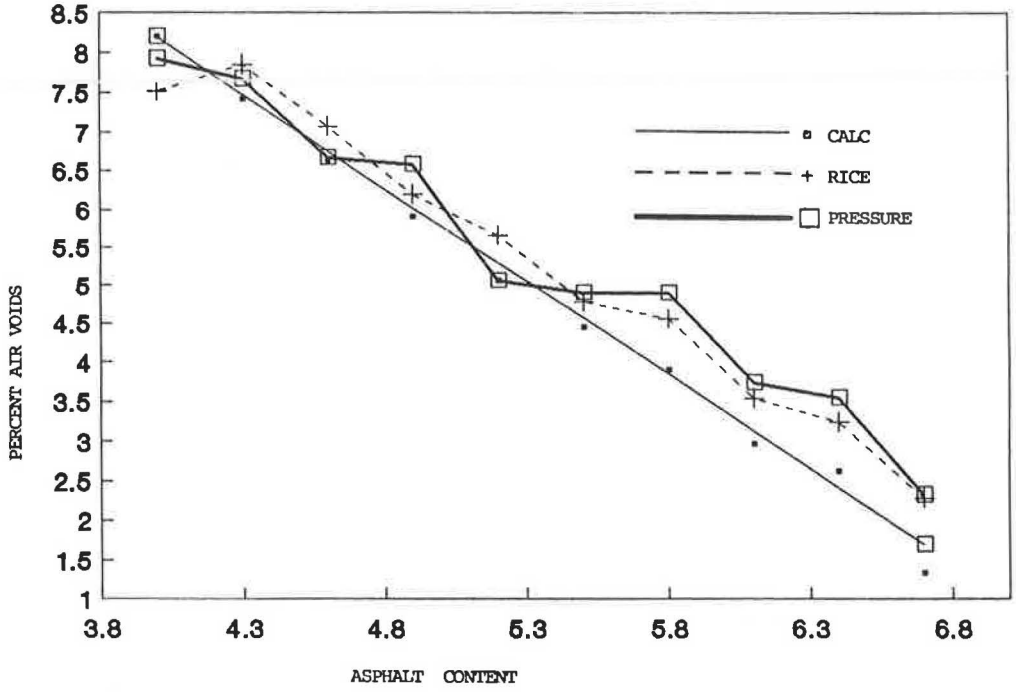

FIGURE 5 Total air voids versus asphalt content using the three different methods for Experiment 1.

TABLE 5 TESTING RESULTS OF RICE AND PRESSURE METHODS FOR EXPERIMENT 2

a) Results of Rice Method

Supplier	AC (%)	Calc.	Rice			
			FL	R1	R2	Avg. R
Cardi	5.0	2.470	II	2.445	2.439	2.442
	5.5	2.452	I	2.450	2.434	2.442
	6.0	2.434	II	2.421	2.421	2.421
	6.5	2.417	I	2.419	2.419	2.419
Forte	5.0	2.567	II	2.572	2.562	2.567
	5.5	2.547	I	2.547	2.542	2.545
	6.0	2.527	II	2.525	2.551	2.538
	6.5	2.508	I	2.527	2.531	2.529
Gammino	5.0	2.532	II	2.591	2.592	2.592
	5.5	2.513	I	2.583	2.575	2.579
	6.0	2.494	II	2.562	2.570	2.566
	6.5	2.475	I	2.553	2.544	2.549
n		12		12	12	12
$\bar{x}$		2.495		2.516	2.515	2.516
s		0.0462		0.0645	0.0662	0.0651

Notes: FL = Flask number. R1 = Results of Run 1.
R2 = Results of Run 2.

(continued on next page)

TABLE 5 *(continued)*

b) Results of Pressure Method

Supplier	AC (%)	Calc.	Pressure FL	P1	P2	Avg. P
Cardi	5.0	2.470	II	2.452	2.452	2.460
	5.5	2.452	I	2.441	2.421	2.431
	6.0	2.434	II	2.423	2.409	2.416
	6.5	2.417	I	2.415	2.404	2.410
Forte	5.0	2.567	II	2.578	2.566	2.572
	5.5	2.547	I	2.591	2.569	2.580
	6.0	2.527	II	2.544	2.522	2.533
	6.5	2.508	I	2.528	2.511	2.520
Gammino	5.0	2.532	II	2.525	2.601	2.563
	5.5	2.513	I	2.576	2.570	2.573
	6.0	2.494	II	2.603	2.548	2.576
	6.5	2.475	I	2.536	2.530	2.533
n		12		12	12	12
$\bar{x}$		2.495		2.518	2.510	2.514
s		0.0462		0.0678	0.0686	0.0664

Notes: FL = Flask number. P1 = Results of Run 1.
P2 = Results of Run 2.

TABLE 6 MIX DESIGN VOIDS ANALYSIS FOR EXPERIMENT 2

Spec. Set No.*	Asphalt Content (%)	Bulk S.G.	Theoretical Spec. Gravity Calc. Method	Rice Method	Pressure Method
A1	5.0	2.371	2.471	2.442	2.460
A2	5.5	2.382	2.453	2.442	2.431
A3	6.0	2.382	2.436	2.421	2.417
A4	6.5	2.382	2.418	2.419	2.410
B1	5.0	2.483	2.570	2.567	2.572
B2	5.5	2.476	2.550	2.545	2.572
B3	6.0	2.486	2.531	2.538	2.533
B4	6.5	2.487	2.511	2.529	2.520
C1	5.0	2.460	2.534	2.592	2.563
C2	5.5	2.486	2.515	2.579	2.573
C3	6.0	2.493	2.496	2.566	2.576
C4	6.5	2.500	2.472	2.549	2.533

Spec. Set No.*	Asphalt Content (%)	Bulk S. G.	Total Voids in Mix Calc. Method	Rice Method	Pressure Method
A1	5.0	2.371	4.05	2.91	3.62
A2	5.5	2.382	2.89	2.46	2.02
A3	6.0	2.382	2.22	1.61	1.45
A4	6.5	2.382	1.49	1.53	1.16
B1	5.0	2.483	3.38	3.27	3.46
B2	5.5	2.476	2.90	2.71	4.03
B3	6.0	2.486	1.78	2.05	1.86
B4	6.5	2.487	0.96	1.67	1.31
C1	5.0	2.460	2.92	5.09	4.02
C2	5.5	2.486	1.15	3.61	3.38
C3	6.0	2.493	0.12	2.84	3.22
C4	6.5	2.500	-0.93	1.92	1.30

* A - Cardi, B - Forte, C - Gammino

Note: Cardi, Forte, and Tilcon Gammino were the three aggregate suppliers used in this study.

TABLE 7 COMPUTATIONS FOR PERFORMANCE ANALYSIS FOR EXPERIMENT 2

Supplier	AC	R1-R2	P1-P2	R-P	R-C	P-C
Cardi	5.0	0.0060	-0.0150	-0.0175	-0.0280	-0.0105
	5.5	0.0160	0.0200	0.0110	-0.0100	-0.0210
	6.0	0.0000	0.0140	0.0050	-0.0130	-0.0180
	6.5	0.0000	0.0110	0.0095	0.0020	-0.0075
Forte	5.0	0.0100	0.0120	-0.0050	0.0000	0.0050
	5.5	0.0050	0.0220	-0.0355	-0.0025	0.0330
	6.0	-0.0260	0.0220	0.0050	0.0110	0.0060
	6.5	-0.0040	0.0170	0.0095	0.0210	0.0115
Gammino	5.0	-0.0010	-0.0760	-0.0285	0.0595	0.0310
	5.5	0.0080	0.0060	0.0060	0.0660	0.0600
	6.0	-0.0080	0.0550	-0.0095	0.0720	0.0815
	6.5	0.0090	0.0060	0.0155	0.0735	0.0580
n		12	12	12	12	12
$\bar{x}_d$		0.0013	0.0078	0.0019	0.0210	0.0191
s_d		0.0109	0.0309	0.0167	0.0367	0.0336
u		0.0069	0.0196	0.0106	0.0233	0.0213
Difference in Performance		No	No	No	No	No

Note: R indicates results of Rice Method
P indicates results of Pressure Method
C indicates results of Calculation Method

If $|\bar{x}_d| < u$, a difference in performance is not indicated.

respectively. The statistical analysis of the results is presented in Tables 10 and 11.

- Average Value. The difference in the average MTSG values between the two methods was 0.14 percent.
- Standard Deviation. The standard deviation of the MTSG for the pressure method was greater than that for the Rice method.
- Performance. No significant difference in performance between the two methods (see Table 10) was discernable.
- Precision. The analysis detected a difference in precision between the two methods. Though the Rice method was more precise, the difference was not significant (see Table 11).

Experiment 3B

Tables 12 and 13 present results of the single-operator precision study for better methods. Further analysis was carried out as follows:

- Average Values. The differences in average MTSG values for samples 2R and 13R were 0.21 and 0.25 percent, respectively.
- Standard Deviation. The standard deviation for the pressure method was greater than for the Rice method.
- Precision. The statistical analysis did not detect any difference in the precision between the two methods or between the four sets of tests, i.e., 2R, 13R, 2A, and 13A (see Table 14 and the Appendix).

DISCUSSION OF RESULTS

Comparison for the Time and Performance

The Rice method is simple, but needs a laboratory setup primarily because of the necessity of a vacuum. Relatively easy to perform, the Rice method requires a moderate amount of technique to obtain good consistency. It has a 15-min actual run time for the expulsion of air from the flask and requires an additional 5 to 10 min to prepare the weighing of the sample and water in the flask. Should the method need to be repeated, 20 to 25 min would be added. Generally, one run of the test after sample preparation takes between 25 and 30 min.

The pressure method requires the use of a calibrated air meter and balance accurate to 0.1 g. This method does not require a laboratory setup and could be easily used in the field, making it a versatile method for computing the MTSG of an asphalt mix. It is relatively easy to perform and does not require much skill, except that care should be taken to ensure that the weights and temperatures are recorded accurately.

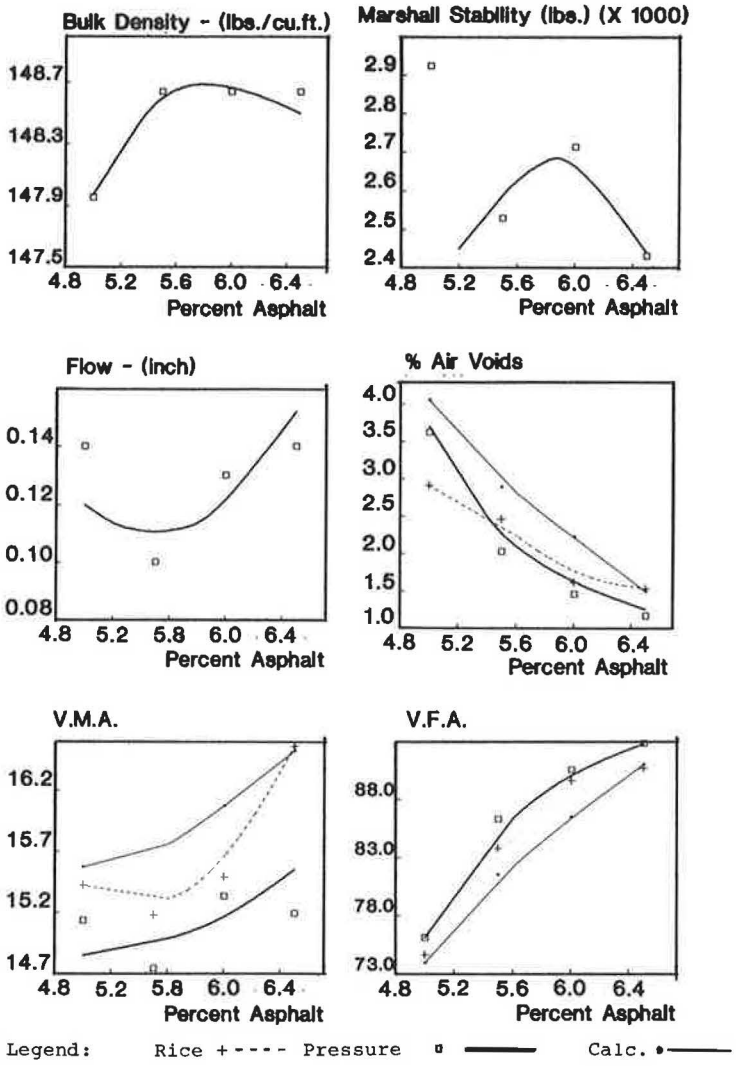

FIGURE 6 A typical Marshall mix design plot for the Cardi mix for Experiment 2.

TABLE 8 OVERALL PRECISION ANALYSIS FOR THE RICE METHOD FOR EXPERIMENT 3A

Sample	Operator	Date	Flask	Specific Gravity
1	1	10-31-88	II	2.492
2		10-31-88	I	2.481
3		10-31-88	II	2.485
4		10-31-88	I	2.493
5		11-01-88	II	2.506
6		11-01-88	I	2.482
7		11-01-88	II	2.472
8		11-02-88	I	2.492
9		11-04-88	II	2.488
10		11-04-88	I	2.496
11	2	11-07-88	II	2.482
12		11-07-88	I	2.479
13		11-09-88	I	2.389*
14		11-09-88	II	2.499
15		11-09-88	I	2.489
16		11-10-88	II	2.491
17		11-10-88	I	2.505

Note: Samples with 6% asphalt content from Forte (supplier) were divided into 17 subsamples.

Note: Sample No. 13 is an outlier. Therefore sample No. 13 was not included in computation.

TABLE 9 OVERALL PRECISION ANALYSIS FOR THE PRESSURE METHOD FOR EXPERIMENT 3A

Sample	Operator	Date	Meter	Readings 1	2	3	Average
1	2	10-31-88	F947	2.491	2.486	2.486	2.488
2		10-31-88	F947	2.449	2.446	2.450	2.448
3		10-31-88	F947	2.476	2.475	2.477	2.476
4		11-01-88	F947	2.493	2.492	2.485	2.490
5		11-01-88	F947	2.509	2.481	2.508	2.499
6		11-01-88	F947	2.484	2.482	2.486	2.484
7		11-02-88	F947	2.481	2.478	2.475	2.478
8		11-02-88	F947	2.462	2.464	2.463	2.463
9		11-04-88	D676	2.487	2.489	2.488	2.488
10	1	11-04-88	D676	2.520	2.504	2.505	2.510
11		11-09-88	D676	2.490	2.486	2.485	2.487
12		11-09-88	D676	2.510	2.500	2.511	2.507
13		11-09-88	D676	2.494	2.488	2.487	2.490*
14		11-10-88	D676	2.504	2.505	2.502	2.504
15		11-10-88	D676	2.481	2.476	2.480	2.479
16		11-10-88	D676	2.487	2.483	2.483	2.484
17		11-14-88	D676	2.491	2.488	2.488	2.489

Notes: Samples were 6 percent asphalt content from Forte supplies and were divided into 17 subsamples.
Sample No. 13 is an outlier. Therefore sample No. 13 was not included in computation.

TABLE 10 COMPUTATIONS FOR PERFORMANCE ANALYSIS FOR EXPERIMENT 3A

Sample	Rice	Pressure	$x_d=x_A-x_R$
1	2.492	2.488	-0.004
2	2.481	2.448	-0.033
3	2.485	2.476	-0.009
4	2.493	2.490	-0.003
5	2.506	2.499	-0.007
6	2.482	2.484	0.002
7	2.472	2.478	0.006
8	2.492	2.463	-0.029
9	2.488	2.488	0.000
10	2.496	2.510	0.014
11	2.482	2.487	0.005
12	2.479	2.507	0.028
13	2.389*	2.490*	
14	2.499	2.504	0.005
15	2.489	2.479	-0.010
16	2.491	2.484	-0.007
17	2.505	2.489	-0.016
n	16	16	16
$\bar{x}$	2.490	2.486	-0.003625
s	0.00930	0.0158	0.01494
u			0.007959

$|x_d|<u$. Therefore, the pressure method does not differ from the Rice Method in performance.

Note 1: Forte sample with 6% binder was divided into 17 subsamples.

Note 2: Sample no. 13 is an outlier. Therefore, sample no. 13 was not included in computation.

The size and weight of the air meter with sample plus water (approximately 17 to 18 kg) could be a problem to an operator of slight build. The actual run time is approximately 5 to 7 min, including securing the top of the meter to the bowl, filling up the petcock with water, wiping the meter dry, pumping up the chamber and setting the needle to the initial pressure line, taking a reading, weighing the meter with the sample and water, and noting the temperature of the water. The repeated runs take approximately 4 to 5 min each, and the whole experiment can be accomplished in 15 to 20 min. Although this method is faster, it also reduces the potential for procedural error, because no agitation of the meter is required. (With the Rice method, the flask has to be agitated for 2 min every 15 ± 2 min).

The air meter should be accurately calibrated before beginning the experiment; otherwise, the results will be erroneous. For this project, the calibration was performed before the start of each series of experiments. The pressure method apparatus also is capable of rough handling because there are no delicate components. Hence, it is suitable for field use.

TABLE 11 STATISTICAL ANALYSIS RESULTS FOR OVERALL PRECISION FOR EXPERIMENT 3A

	Rice	Pressure
$\bar{x}$	2.490	2.486
s	0.00930	0.0158
s^2	8.64EE-5	2.49EE-4

F-Test for comparison of variances, $\alpha = 0.05$

$$F = \frac{s_{P_2}^2}{s_R^2} = \frac{2.49EE\text{-}4}{8.64EE\text{-}5} = 2.884$$

$F_{\alpha/2,15,15} = 2.86$

$F > F_{0.025,15,15}$. Therefore, the F-Test has detected a difference in precision. Pressure Method is less precise than the Rice Method.

Interpretation of Results

- Performance. The average values of the MTSG obtained by the two methods were in close agreement, inferring that implementation of the pressure method would be a viable alternative. Confirmed by the statistical analysis, there is no significant difference in performance between the two methods.
- Precision. The results and analysis also show that there was no significant difference in precision between the Rice method and the pressure method.
- Sensitivity. Experiment 1 indicated that the Rice method was more sensitive to change in asphalt content than the pressure method; the Rice method results were also more consistent than those of the pressure method.

TABLE 12 SINGLE OPERATOR PRECISION ANALYSIS FOR THE RICE METHOD FOR EXPERIMENT 3B

Operator	Sample	Date	Flask	Specific Gravity	
2	2R	11-10-88	I	2.483	$\bar{x}$ = 2.480
	2R	11-15-88	I	2.483	s = 0.00542
	2R	11-15-88	I	2.486	s^2 = 2.93EE-5
	2R	11-16-88	I	2.484	
	2R	11-17-88	II	2.477	
	2R	11-17-88	II	2.476	
	2R	11-18-88	II	2.471	
	13R	11-09-88	I	2.389*	Omitting the outlier value 2.389:
	13R	11-10-88	II	2.496	
	13R	11-15-88	II	2.494	
	13R	11-15-88	II	2.498	$\bar{x}$ = 2.501
	13R	11-16-88	I	2.508	s = 0.00505
	13R	11-17-88	IV	2.505	s^2 = 2.55EE-5
	13R	11-18-88	IV	2.502	
	13R	11-18-88	IV	2.503	Including the Value 2.389:
					$\bar{x}$ = 2.487
					s = 0.0398
					s^2 = 0.00159

Note: Forte samples 2R and 13R are from a larger sample of RI Class I-1 mixture with 6% binder content.

TABLE 13 SINGLE OPERATOR PRECISION ANALYSIS FOR THE PRESSURE METHOD FOR EXPERIMENT 3B

Operator	Sample	Date	Meter	Reading 1	Reading 2	Reading 3	Average Reading
1	2A	11-14-88	D676	2.478	2.477	2.475	2.477
	2A	11-17-88	F947	2.468	2.471	2.469	2.469
	2A	11-18-88	F947	2.485	2.480	2.488	2.484
	2A	11-21-88	F947	2.477	2.476	2.478	2.477
	2A	11-22-88	F947	2.488	2.486	2.484	2.486
	2A	11-22-88	F947	2.469	2.470	2.463	2.467
	2	11-23-88	f947	2.462	2.462	2.464	2.463
	13A	11-09-88	D676	2.494	2.488	2.487	2.490
	13A	11-17-88	F947	2.506	2.504	2.500	2.503
	13A	11-18-88	F947	2.493	2.492	2.491	2.492
	13A	11-21-88	F947	2.510	2.508	2.506	2.508
	13A	11-21-88	F947	2.494	2.498	2.493	2.495
	13A	11-22-88	F947	2.473	2.482	2.480	2.478
	13A	11-23-88	F947	2.496	2.497	2.494	2.496

Note: Forte sample 2R, 13R are from a larger sample of RI Class I-1 mixture with 6% binder content.

Note:

Sample	x	s	s^2
2A	2.475	0.00864	7.56ee-5
13A	2.495	0.00962	9.26ee-5
2A + 13A	2.485	0.136	1.84ee-4

TABLE 14 ANALYSIS FOR SINGLE OPERATOR PRECISION FOR EXPERIMENT 3B

Rice Method					
Operator	Sample	Repeat Runs	$\bar{x}$	s^2	#
1	2R	7	2.480	2.93EE-5	1
Flasks:	13R	7	2.501	2.55EE-5	2
I,II,IV	2R+13R	14	2.490	1.42EE-4	3

Pressure Method					
Operator	Sample	Repeat Runs	$\bar{x}$	s^2	#
2	2A	7	2.4751	7.56EE-5	4
Meters:	13A	7	2.4951	9.26EE-5	5
D676,F947	2A+13A	14	2.4851	1.84EE-4	6

Suggested Improvements for the Apparatus of the Pressure Method

Some improvements for the apparatus of the pressure method are as follows:

1. The air meter is a cumbersome piece of equipment weighing approximately 8.3 kg empty and approximately 17.5 kg filled. Reducing its size and weight would allow smaller samples to be taken and decrease the physical strain on the operator, making the testing effort much easier.

2. The air meter dial has a logarithmic scale running from 0 to 100 percent. In this experiment, the air percentage readings were in the range of 0 to 2 percent. It would be an improvement if the range of the air meter could be reduced to 0 to 5 percent, and spread out over the present scale. The intermediate graduations could also be given to the nearest 0.01 percent, which would increase the accuracy of the reading. Interpolation was used to determine the air percentage to the nearest 0.01 percent. This process is difficult because it is more natural to interpolate arithmetically than logarithmically.

3. The pressure-sensing mechanism consists of a curved, hollow tube connected to the air chamber at the open end, which deflects under change of pressure in the chamber. At the closed end, a ratchet system is connected to the spring dial, which then reads the air percentage in the chamber on a logarithmic scale. In order to obtain more consistent and precise readings, mechanical improvements to this system should be further investigated.

CONCLUSIONS AND RECOMMENDATIONS

The pressure method is a viable tool for the determination of the MTSG of asphalt mixture. With the current apparatus, the pressure method would be appropriate for use in the Marshall mix design procedures, acceptance testing, and as a rapid test method in the field. For research and where sophisticated evaluation of the MTSG of an asphalt mixture is desired, the Rice method could be used concurrently. The pressure

method could also be used to determine the MTSG of materials that have an affinity for air when immersed in water, or have a porous structure from which all the free air would have to be expelled to determine the specific gravity, e.g., aggregates, porous concrete products, and bottom ash. This topic could undergo future research.

Efforts should also be made to improve the consistency and sensitivity of the air meter to attain greater precision in results. These efforts, which would require some research into mechanical aspects of the air meter, would be challenging for the mechanically inclined. In any case, the scope of the project will be broadened by soliciting other laboratories in the area to run MTSG tests by the pressure method so that interlaboratory results can be obtained and analyzed. The final goal is to have the pressure method accepted as an alternative to the Rice method for determining MTSG of asphalt mixtures.

ACKNOWLEDGMENTS

The authors would like to thank members of the Materials Section of the Rhode Island Department of Transportation who assisted throughout this project, especially D. Clarke and P. Carrier, who performed a major part of the sample preparation and testing, J. Fera for invaluable assistance in providing the statistical analysis and suggestions as the testing progressed, and M. Sock and I. Frament, for mastery in computing and word processing. Special appreciation is extended to M. Gill and W. Carcieri, Jr., who have been sources of encouragement and inspiration, notably in their sponsorship of the authors to various research meetings and seminars. The authors would also like to express their gratitude to W. Kovacs and S. Bose at the University of Rhode Island for their suggestions and guidance.

APPENDIX—THE *F*-TEST

To test the significance of variance differences; i.e., to test the null hypothesis $S_A^2 = S_B^2$:

$$F = S_A^2/S_B^2 \qquad \text{(A-1)}$$

where

S_A^2 = the larger variance estimate, $n - 1$ degrees of freedom,
S_B^2 = the smaller variance estimate, $n - 1$ degrees of freedom, and
α = 0.05, 95 percent confidence level.

$$S_1^2,\ S_2^2\text{: } F = \frac{2.93\text{EE} - 5}{2.55\text{EE} - 5} = 1.151$$

$$< F_{0.025,6,6} = 5.82 \qquad \text{(A-2)}$$

Therefore, no difference in precision.

$$S_5^2,\ S_4^2\text{: } F = \frac{9.26\text{EE} - 5}{7.56\text{EE} - 5} = 1.226$$

$$< F_{0.025,6,6} = 5.82 \qquad \text{(A-3)}$$

Therefore, no difference in precision.

$$S_4^2,\ S_1^2\text{: } F = \frac{7.56\text{EE} - 5}{2.93\text{EE} - 5} = 2.576$$

$$< F_{0.025,6,6} = 5.82 \qquad \text{(A-4)}$$

Therefore, no difference in precision.

$$S_5^2,\ S_2^2\text{: } F = \frac{9.26\text{EE} - 5}{2.55\text{EE} - 5} = 3.635$$

$$< F_{0.025,6,6} = 5.82 \qquad \text{(A-5)}$$

Therefore, no difference in precision.

$$S_6^2,\ S_3^2\text{: } F = \frac{1.84\text{EE} - 5}{1.42\text{EE} - 5} = 1.292$$

$$< F_{0.025,13,13} = 3.12 \qquad \text{(A-6)}$$

Therefore, no difference in precision.

REFERENCES

1. *Standard Specifications for Transportation Materials and Methods of Sampling and Testing. Part II. Methods of Sampling and Testing*, 14th ed. AASHTO, Washington, D.C., 1986.
2. *Annual Book of ASTM Standards*. ASTM, Philadelphia, Pa., 1989.
3. R. R. Johnson and U. L. Kelley. *Maximum Theoretical Specific Gravity of Bituminous Paving Mixtures*. Technical Report GL-87-8, U.S. Department of the Army, Waterway Experiment Station, Vicksburg, Miss., 1987.
4. *Mix Design Methods for Asphalt Concrete*. MS-2, The Asphalt Institute, Lexington, Ky., 1984.

Publication of this paper sponsored by Committee on Characteristics of Bituminous Paving Mixtures To Meet Structural Requirements.

Use of a Loaded-Wheel Testing Machine To Evaluate Rutting of Asphalt Mixes

JAMES S. LAI AND THAY-MING LEE

A loaded-wheel testing machine is used to evaluate the rutting characteristics of asphalt mixes. The 3- × 3- × 15-in. asphalt beam samples used for the test can be prepared by kneading compaction or by static compression. The rutting tests are normally conducted at an elevated temperature between 95°F and 105°F. The repeated loading on the beam sample is generated by a pressurized rubber hose placed lengthwise on top of the beam sample and a loaded wheel riding back and forth at 44 cycles/min along the rubber hose. The pressure in the hose is maintained at 100 psi, and the magnitude of the wheel load is 100 lb. The rut depth developed on the beam sample along the wheel path under the rubber hose is measured at different numbers of repetitions and is used for evaluating the rutting potential of the asphalt mixes. This repeated-load mechanism has several advantages over the conventional wheel-tracking mechanism. Asphalt mixes of the Georgia Department of Transportation standard Type B mix, Coarse B mix, base mix, and two other modified mixes using three different aggregate sources were tested by the proposed method to evaluate the effect of mix gradations and aggregate sources on rutting resistance. The results showed significantly different rutting resistance among the asphalt mixes tested.

Rutting on asphaltic pavement has become more serious as the wheel loads and tire pressure of truck traffic on highways have increased. Rutting reduces road serviceability and creates the problem of hydroplaning caused by the accumulation of water on the rutted wheel paths. Methods to eradicate rutting on asphaltic pavement usually involve asphalt concrete (AC) overlay. This rehabilitation process is costly and provides no assurance that the overlayed pavements will not rut again.

An asphaltic pavement can develop rutting because of inadequate structural capacity as a result of improper design, improper construction practices, or instability of the asphalt mix used in the pavement. Currently available mechanistic flexible pavement design and analysis procedures can be used to design a flexible pavement structure with adequate structural capacity to minimize rutting. But rutting still occurs because of lack of stability. Poor resistance to deformation of the asphalt mix itself must be mitigated by having a better asphalt mix design procedure through which asphalt mixes with better rutting resistance can be obtained.

Two commonly used methods for the design of asphalt mixes are the Marshall and the Hveem mix design methods. Although these two methods can probably screen out extremely unstable mixes, there is no assurance that an asphalt mix with properties satisfying the design criteria of either of these methods will not develop rutting under normal traffic conditions.

J. S. Lai, School of Civil Engineering, Georgia Institute of Technology, Atlanta, Ga. 30332. T.-M. Lee, National Expressway Engineering Bureau, Taipei, Taiwan, Republic of China.

Recent studies by Lai (*1–3*) demonstrated the inability of the Marshall method to assess the rutting potential of asphalt mixes. Many testing methods have been proposed to improve prediction of the rutting potential of asphalt mixes. These include the triaxial repeated-load test and the creep test. Some of the test methods have achieved varying degrees of success in predicting the rutting potential of asphalt mixes.

In a recent study conducted by Lai (*1*) for the Georgia Department of Transportation (GaDOT), the loaded-wheel testing (LWT) machine was demonstrated to be capable of evaluating the rutting characteristics of AC. Results of the LWT method were more compatible with the rutting characteristics normally experienced in asphaltic pavements under vehicular loading than results achieved by the permanent deformation of the same asphalt mixes tested under the triaxial repeated-load test and the creep test. In the second study (*2*), the LWT machine was used to assess the rutting potential of GaDOT Type B asphalt mixes and six different modified mixes using aggregates from three different sources. The mixes used fillers with different gradations and particle shape and size distributions. One of the mixes also contained polymer modifier. Although all 21 of the asphalt mixes met the Marshall mix criteria, they exhibited significantly different rutting characteristics under the LWT machine. From these test results, certain modified mixes that have the potential to give better resistance to rutting were identified.

In the third study (*3*), the same test method was used to evaluate the rutting potential of six asphalt mixes for potential use in base course. The gradation of the mixes varied in the maximum aggregate size and the fine aggregate portion. Again, the results from the LWT showed significant difference in rutting resistance among the mixes, even though all the mixes satisfied Marshall mix criteria. The LWT machine and the testing procedure are described in the following section, and some rutting characteristics of asphalt mixes determined by this testing procedure are presented.

DESCRIPTION OF LOADED-WHEEL TESTING MACHINE

The original version of the LWT machine was developed by Benedict Slurry Seal, Inc., for evaluating certain properties of asphalt slurry seals. A similar machine has been used elsewhere to evaluate the rutting potential of AC (*4,5*). The original machine was modified (*1,2*) to make it more applicable for evaluating the rutting behavior of asphalt mixes under a laboratory environment.

Figure 1 shows the main features of the modified LWT machine. The 3- × 3- × 15-in. beam sample (*A*) is placed in the sample-holding mold (*B*). The beam sample and the sample-holding mold are shown more clearly in Figure 2. The base of the sample-holding mold includes a removable 3- × 15- × ½-in. steel plate to simulate a rigid base-course condition. This steel plate can be replaced by an equally thick resilient rubber pad to simulate a flexible base. The sides and ends of the sample are partially confined by steel brackets. A pressurized rubber hose (*C*), also shown in Figure 2, is placed on top of the sample and is partially restrained at the ends. In addition to the loading wheel (*D*) shown in Figure 1, the components of the loading system consist of a ⅓-hp motor (*G*), 12-in. reciprocating-stroke arms (*E* and *F*), and the weight-holding box (*H*). The machine is equipped with dual counters, a resettable mechanical counter (*I*), and an electric counter activated by a photographic relay for recording the number of repetitions. The electric counter was installed on top of the environmental chamber lid, so that the number of cycles during the test can be read when the environmental chamber lid is closed. The entire testing machine is enclosed in this environmental chamber, which can maintain a constant temperature of up to 120°F throughout the test period. Details of the environmental chamber and the preheating box (for preheating the test samples) and other features of the LWT machine were described by Lai (*6*).

DESCRIPTION OF WHEEL-LOAD GENERATING SYSTEM

The original 1-in.-wide aluminum loading wheel had a 3-in. diameter and was fitted with a hard rubber tire. The tire would exert nonuniform contact pressure on the surface of an AC sample, particularly for the coarser mixes. It was decided that the hard rubber tire should be replaced with an inflatable tire, so the contact pressure could be more controllable.

At first, an approximately 1-in.-wide, off-the-shelf tire with tire pressure up to 120 psi was sought. No suitable tire could be found, so a loading wheel with the specified characteristics was developed in the laboratory.

The first version was an 8-in.-diameter aluminum wheel with a 1-in.-diameter high-pressure rubber hose wrapped around the rim. The hose could be pressurized and maintained at a controlled pressure up to 100 psi through an air-pressure system and a pressure regulator. This wheel assembly was fitted on the LWT machine, along with other necessary modifications to make the system compatible. Several preliminary

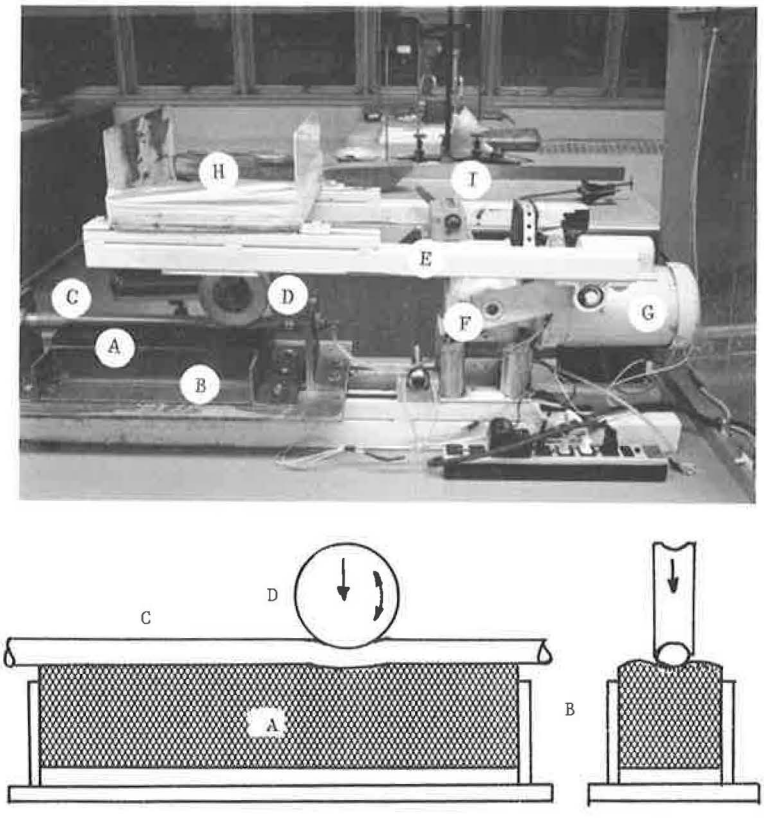

A: Beam Sample
B: Sample Holding Mold
C: Pressurized Rubber Hose
D: Loading Wheel
E & F: Reciprocating Arms
G: 1/3 hp Motor
H: Weight Holding Box
I: Restable Counter

FIGURE 1 Modified loaded-wheel testing machine.

rutting tests were performed on 3- × 3- × 15-in. asphalt beam samples. The wheel assemblage itself performed satisfactorily, with pressure in the hose kept relatively constant, but several problems were observed during the tests. The reciprocating action of the loaded wheel, which occurred at the end of each stroke, caused the rubber hose to generate excessive skidding against the rough surface of the sample near the ends of the stroke. The skidding caused excessive wear of the rubber hose and, more importantly, excessive rutting on the asphalt samples near the ends of the beam. Furthermore, because of the excessive ruts developed there, the wheel had the tendency to push near these regions, instead of just rolling along the wheel path. Shoving became evident along these regions and slowly progressed toward the center. For these reasons, this version of the wheel system was abandoned.

To overcome these problems, a rather novel concept of generating moving-wheel load was conceived. This loading system consisted of a flexible linear tube made of a high-pressure rubber hose, and a 3-in.-diameter aluminum wheel (see Figures 1 and 2). The rubber hose was pressurized to the prescribed pressure and placed on top of the AC specimen. The hose was stationary, loosely held in position on both ends by end clamps to maintain the longitudinal alignment along the center of the beam. The concave shape of the rim would keep the aluminum wheel on top of the rubber hose. The wheel was attached to the reciprocating arm of the machine. During the rutting test, the loaded aluminum wheel rode along

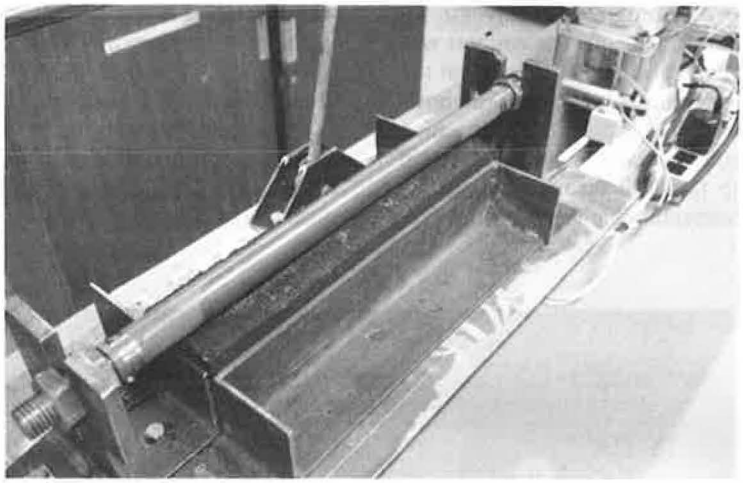

FIGURE 2 Linear-tube loading system.

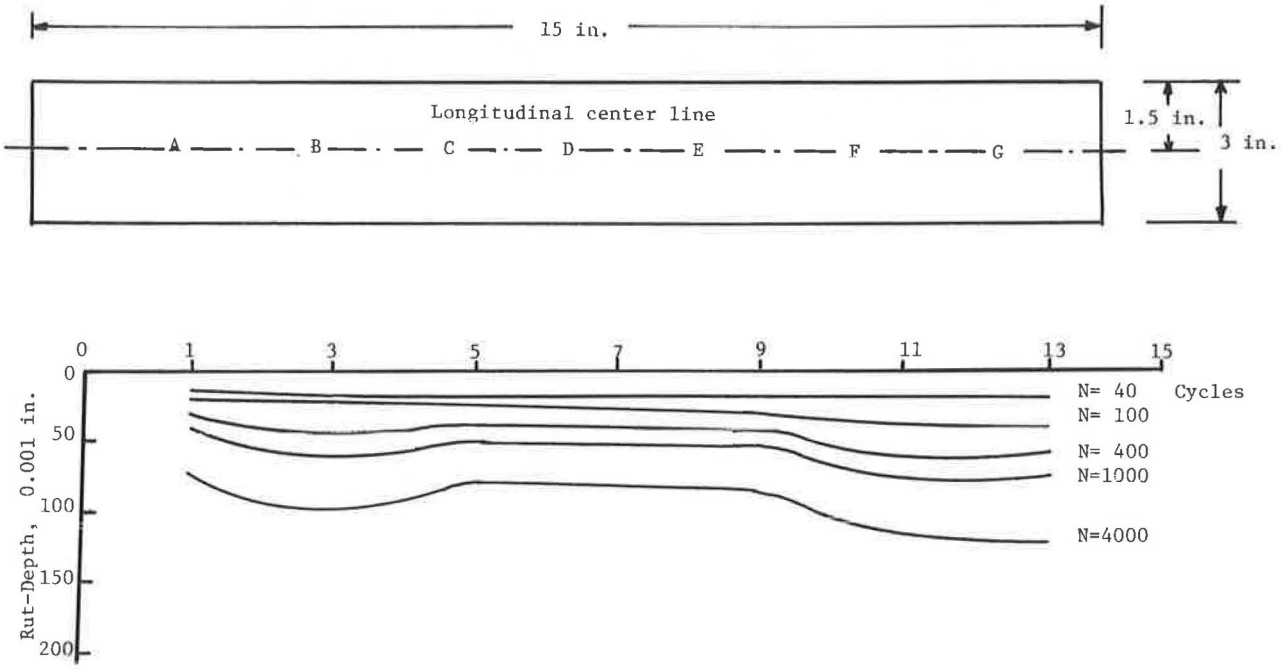

FIGURE 3 Rutting profile along the longitudinal centerline.

the pressurized rubber hose; at the point of contact, it generated pressure on the surface of the beam sample.

The linear-tube concept was tested, and the performance was satisfactory. The excessive rutting at both ends of the asphalt beam sample was substantially reduced. The magnitude of rutting at the end regions was still greater than that at the middle region (see Figure 3), probably because the total duration of loading was longer at the end regions than at the middle region because of the wheel's reverse movement at the end of the reciprocating action.

Because of the novelty of the linear-tube loading concept, some questions still needed to be answered. One concerned the nature of the contact pressure exerted on the test specimen. The other involved the effect of the stiffness of the rubber hose on the rutting of beam samples.

In order to evaluate the effect of the stiffness of the rubber hose, the imprints of the contact area between the rubber hose and the asphalt beam sample were measured for the two types of rubber hose, one relatively stiff and one relatively flexible, under 100-psi inflated pressure and at 100-lb weights. The imprints are shown in Figure 4. The stiffer rubber hose generated a more elongated and narrower contact area, whereas the more flexible hose generated a shorter and wider contact area. This information alone implied that the use of the stiffer hose may generate a greater rutting on the beam sample than the less-stiff hose would. A series of rutting tests was performed on the same asphalt mix using these two rubber hoses. The results (presented in Table 1) indicated that the flexible hose generated a slightly greater rutting on beam samples than the stiffer hose did. No direct measurement of the contact pressure between the rubber hose and the asphalt beam surface was taken.

ASPHALT BEAM SAMPLE PREPARATION PROCEDURE

In the previous studies (*1–3*), the 3- × 3- × 15-in. asphalt beam samples used for the rutting test were fabricated using a kneading compaction machine. The typical procedure was as follows. A Marshall mix design for an asphalt mix was followed; 50-blow compaction per side was used for preparing the samples. The optimum asphalt content for the mix was determined on the basis of air voids in the mix at approximately 4.5 percent. On the basis of the bulk density of the mix at the optimum asphalt content from the Marshall mix design and the known volume of the 3- × 3- × 15-in. beam mold, the weight of the aggregate samples for one-third beam

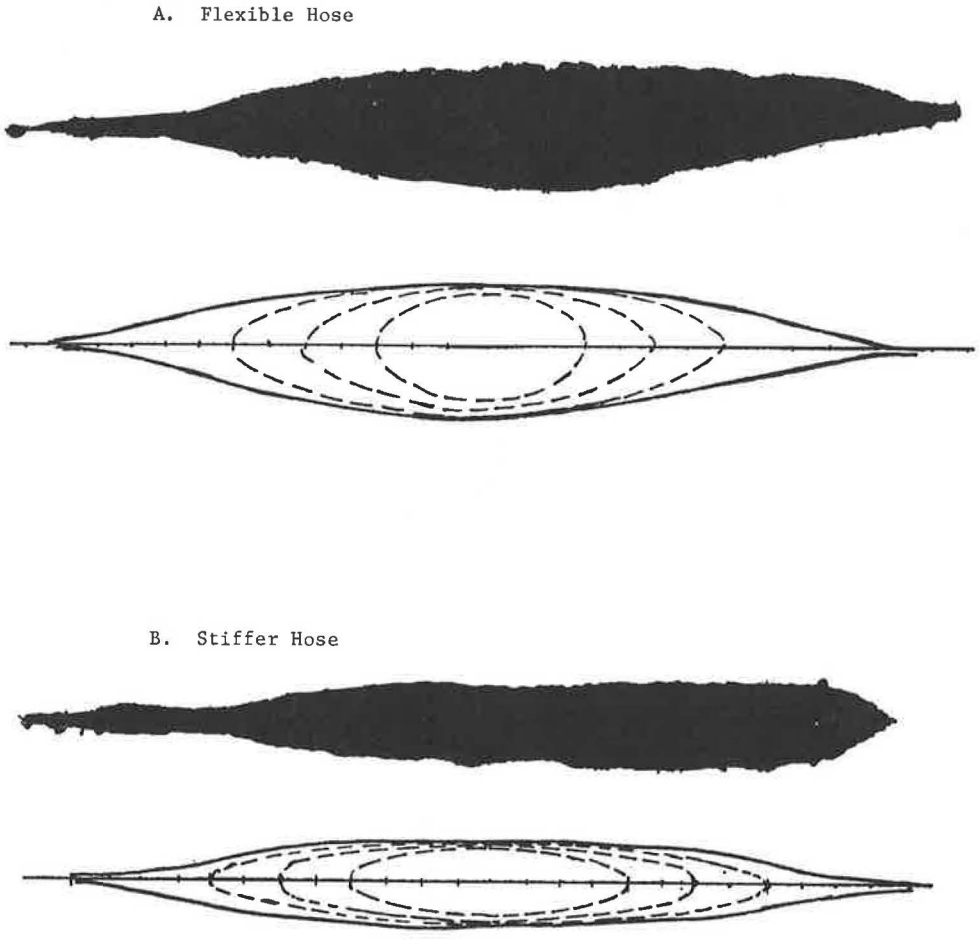

FIGURE 4 Contact imprints of the rubber hoses with asphalt beam sample at 100-lb load and 100-psi pressure.

TABLE 1 RUT DEPTHS USING FLEXIBLE AND STIFFER HOSES

	Flexible Hose		Stiffer Hose	
Number of Cycles	Test 1 (in.)	Test 2 (in.)	Test 3 (in.)	Test 4 (in.)
500	0.106	0.087	0.080	0.086
1,000	0.126	0.106	0.103	0.101
8,000	0.189	0.210	0.177	0.193

sample volume was calculated and batched. The heated aggregate sample was mixed with the predetermined amount of asphaltic cement, and the mix was placed in the heated beam mold. The 3- × 1-in. loading foot of the kneading compactor was activated to compress the asphalt mix placed in the mold. The asphalt mix was compacted in three lifts. After the third batch of the mix was in the mold and was compacted to approximately the required height, a heated 3- × 15-in.-thick plate was placed on top of the beam and high pressure was applied to compress the mix in the mold to the final required height, flush with the 3-in.-high mold. After the beam sample was allowed to cool, it was removed from the mold. The bulk density was determined

A simplified procedure to fabricate the beam samples by static compression using a universal testing machine was successfully developed (*6*). The potential advantages of using a static compression procedure are a simpler and shorter procedure and more readily available equipment. Because only about 50,000 lb of static compressive load are needed for fabricating 3- × 3- × 15-in. beam samples and most testing laboratories are equipped with a universal testing machine with a larger capacity (usually 100,000 to 200,000 lb), larger AC beam samples can be made. The static compression procedure is presently being used by GaDOT for fabricating asphalt beam samples for the rutting tests.

In the course of this investigation, some mixes (e.g., the base mix described in the next section) used a maximum aggregate size of 1½ in. This size appeared to be too large in relation to the beam size. For aggregate of this size, a large-beam cross section would be preferred.

RUTTING TEST PROCEDURE AND RESULTS

The rutting tests were conducted at temperatures ranging from 95°F to 105°F. In the previous studies (*1–3*), the testing machine was placed in an environmental room with the temperature controlled to the prescribed testing temperature. To make the testing machine more portable, an environmental chamber attached to the testing machine and a sample-preheating box were designed and constructed (*6*). The beam samples could be preconditioned in the preheating box for about 6 hr and then transferred to the testing machine for testing.

The following procedures were used for the rutting test. The preheated beam sample was placed in the sample-holding device. The initial sample surface elevation was measured using the rutting-profile measuring device (see Figure 5). Then the rubber hose was placed on top of the beam sample and the ends of the hose were loosely clamped down. The hose was pressurized to the preset pressure level of up to 100 psi. The loading assembly, including the aluminum wheel, was lowered so that the wheel rested on the rubber hose; appropriate weights were placed in the weight-holding box. The environmental chamber lid was then closed, and the testing machine was turned on. The reciprocating action of the machine caused the loaded aluminum wheel to move back and forth along the rubber hose, generating repeated loading on the beam sample. When the repeated loading reached the pre-

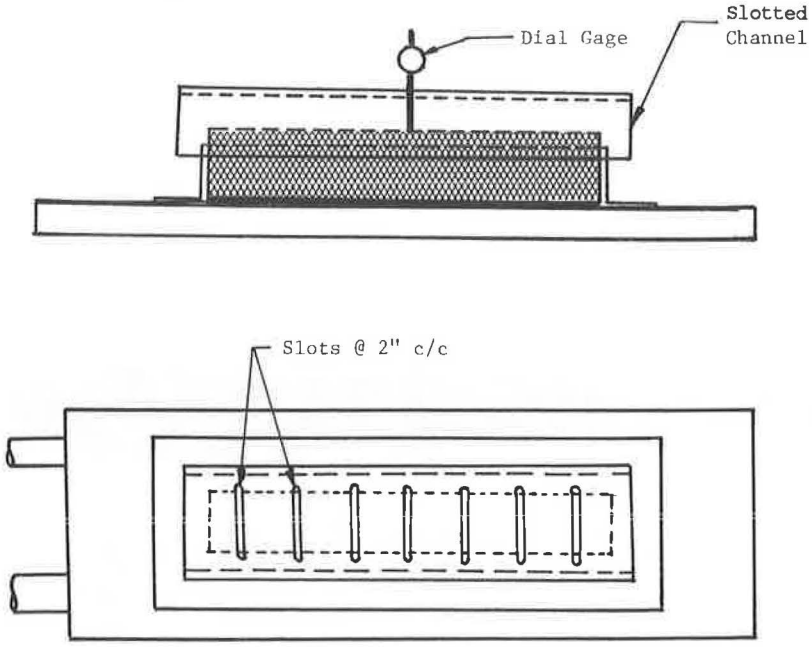

FIGURE 5 Rutting-profile measuring device.

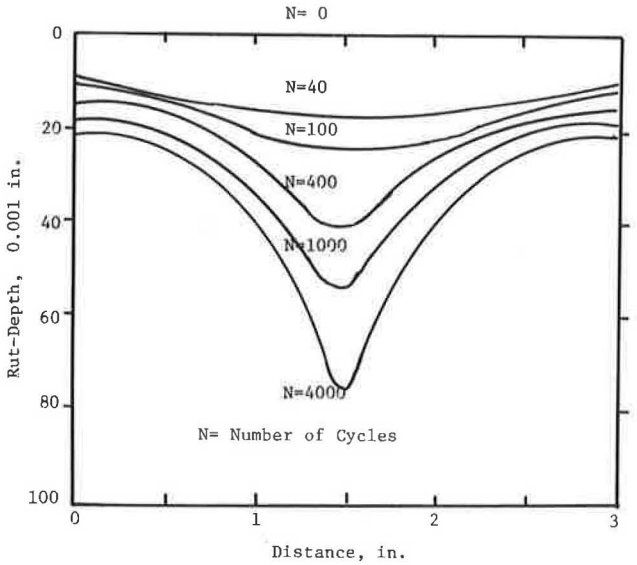

FIGURE 6 Typical transverse rutting profiles.

scribed number of repetitions, the machine was stopped, the environmental chamber lid was lifted, the weights were removed, the loading wheel was propped up, and the rubber hose was removed. The rut depths on the beam sample at three reference locations along the wheel path (directly underneath the rubber hose) were measured. If it was necessary to continue the test, the rubber hose was put back on top of the beam sample, the wheel was lowered, and the weights were put back in the weight-holding box. The chamber cover was lowered, and the machine was restarted.

In the initial investigation (*1*), transverse rutting profiles were taken at seven reference positions (*A* to *G*) along the centerline of the beam samples. Figure 6 shows the typical transverse rutting profiles at different cycle numbers, and Figure 3 shows the typical longitudinal centerline rutting profile. The longitudinal profiles show uneven rutting, with the heaviest rut developed at the rear end of the beam (closest to the pivot of the reciprocal arm). Excessive rutting at the end regions does not represent the normal rutting characteristics of the asphalt mix under repeated moving wheel loads. Rutting at the middle region (Reference Positions *C*, *D*, and *E* in Figure 6) was usually quite uniform. On the basis of these findings, the results of subsequent rutting tests were represented by the averaged value of the rut depths measured at these three positions, provided that the three readings were consistent.

In the initial investigation (*1*), four types of asphalt mixes were selected. These mixes had been used by GaDOT in four separate paving projects, and the pavements had shown varying degrees of rutting. In order to determine the best combinations of pressure and wheel-load magnitude, which would yield the most usable test results, two levels of pressure (75 and 100 psi) and three levels of loading (50, 75, and 100 lb) were used. The combination of 100-lb load and 100-psi pressure produced significant differences in rutting among the four mixes (see Figure 7); at 50-lb wheel load and 75-psi pressure, however, the effects of mix types on rutting became almost indistinguishable.

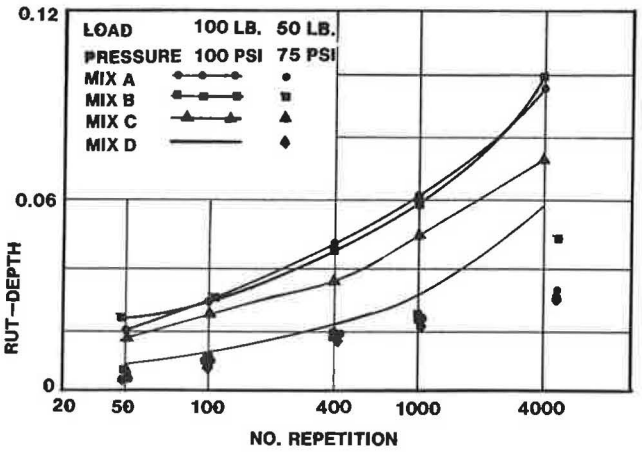

FIGURE 7 Loaded-wheel test results, rut depth versus load application.

EFFECT OF AGGREGATE GRADATION ON RUTTING OF ASPHALT MIXES

Segregation of AC paving mixtures has been an annoying problem in asphalt paving construction. These problems have become more noticeable since the advent of drum-mix plants with large-capacity storage silos. Other factors, such as placement procedures and coarse-mixture gradations, also affect the degree of segregation. One method of minimizing segregation is to reduce the largest size of aggregate particles normally used in a particular mixture. Although this approach may minimize the segregation problem, changing the size of coarse aggregate used could affect the properties of the asphalt mixes produced. Among the asphalt mix properties that could be affected by the change and have significant effect on the performance of asphalt pavements is the rutting resistance.

GaDOT initiated a research project to evaluate the effects that varying the maximum nominal-aggregate size and the fine-aggregate portion of asphalt mix gradations have on the rutting resistance of the asphalt mixes. Three aggregate sources commonly used for asphalt mixes in the Atlanta area were selected. Five different gradations, including the standard gradation for the Type B binder course, base course, Coarse B mix, and two modified gradations for each aggregate source, were prepared. The gradations were identified as follows:

Type	*Designation*	*Maximum Aggregate Size (in.)*	*Percent Passing No. 8 Sieve*
Standard Type B	B	1	38
Base mix	BA	1½	35
Coarse B mix	CB	1	33
Modified X mix	X	¾	30
Modified XX mix	XX	¾	38

All the mixes had 1 percent lime as a part of the filler. The coarse aggregate used in this study was 100 percent crushed. The fine aggregate used in all mixes was also 100 percent crushed, and no natural sand was used.

Marshall mix design (using 50 blows per side) was followed for the 15 mixes. Results of the Marshall mix design are presented in Table 2. The asphalt contents used for preparing the beam samples for each mix were based on the Marshall

mix design results at about 4.5 percent air voids. The actual air voids content in the corresponding Marshall mixes for the 15 mixes varied between 4.5 and 4.7 percent.

On the basis of unit weights and the asphalt content at 4.5 percent air voids (determined from the Marshall mix design), three 3- × 3- × 15-in. beam samples were prepared for each mix. Following the procedure described in the previous section, rutting tests using the LWT machine were performed. The following test conditions were used:

Temperature	105°F
Load	100 lb
Hose pressure	100 psi
Frequency	44 cycles/min

During the test, rutting profiles of the beam samples along the wheel path were measured initially, at 200, 500, and 1,000 cycles, and at every 1,000-cycle increment up to 8,000 cycles. Figure 8 shows the results of rut-depth growth versus number of load repetitions for the five gradations. The rut depths developed at 2,000- and 8,000-load repetitions for all the mixes are presented in Table 2. Additional test results and analyses of the results were described by Lai (*3*). Some of the more significant results from this study are presented in the following section.

COMPARISON OF MODIFIED X AND MODIFIED XX MIXES

Both the modified X and modified XX mixes have ¾-in. maximum aggregate size, which is smaller than the top aggregate size of the three other mixes (B, BA, and CB) commonly used for a binder course. The difference between the X mixes and the XX mixes is the percentage of fines. The X mixes have 30 percent passing No. 8 sieve; the XX mixes have 38 percent passing No. 8 sieve. These two percentages represent the extremes of the fines among the five mixes. The amount of fines between X and XX mixes has a significant effect on the rutting resistance of the mix. Table 3 presents the results of the rut depths measured at N = 8,000 cycles for these two mixes among the three aggregate sources.

These results clearly indicate that the X mixes, which contain 30 percent fines, can resist rutting much better than the XX mixes, which contain 38 percent fines. The results are consistent with what would normally be expected for asphalt mixes containing aggregates with a top size of ¾ in.

When the Marshall stability and flow values of the mixes are analyzed, as presented in Table 3, a different picture emerges. The stability values of the XX mixes are consistently higher than those of the X mixes. The flow values of these mixes are not significantly different. A comparison of the rut depth and the Marshall stability value of the five mixes from the same aggregate source (Figure 9) shows the advantage of using the LWT method to assess the rutting potential of asphalt mixes.

COMPARISON OF DIFFERENT AGGREGATE SOURCES

The purpose of this analysis was to determine whether aggregates from different sources affect the rutting characteristics

TABLE 2 MARSHALL MIX DESIGN AND RUTTING TEST RESULTS FOR DIFFERENT ASPHALT MIXES

Agg. Source & Mix Type	Marshall Mix Design Results					Rutting Test Results Rut-Depth, in.	
	Stab. lbs.	Flow 0.01"	Air Voids %	Unit Wt. pcf	Opt. AC %	N=2000	N=8000
D-BA	2140	11.6	4.6	156.5	4.5	0.118	0.182
D-B	2130	10.0	4.5	153.0	4.7	0.133	0.229
D-CB	1880	10.7	4.5	155.2	4.8	0.152	0.222
D-X	1810	12.2	4.5	153.5	5.2	0.138	0.218
D-XX	2120	11.0	4.3	155.4	5.1	0.147	0.294
K-BA	3000	10.2	4.7	153.4	4.8	0.100	0.184
K-B	3170	12.7	4.6	153.3	5.0	0.127	0.208
K-CB	2810	11.0	4.6	153.0	4.9	0.136	0.193
K-X	2880	11.6	4.6	152.5	5.3	0.097	0.163
K-XX	3010	11.8	4.6	152.3	5.3	0.128	0.217
L-BA	2970	10.8	4.6	145.9	4.8	0.124	0.218
L-B	2930	10.4	4.6	144.6	5.3	0.113	0.184
L-CB	2740	12.0	4.6	145.2	5.1	0.139	0.211
L-X	2580	10.0	4.5	144.5	5.5	0.109	0.162
L-XX	2710	9.6	4.6	144.2	5.3	0.137	0.220

Aggregate Sources: D=Dalton, GA
K=Kennesaw, GA
L=Lithia Springs, GA

TABLE 3 COMPARISON OF X MIX AND XX MIX PROPERTIES BY AGGREGATE SOURCE

	Mix X	Mix XX	Difference
Top aggregate size (in.)	¾	¾	–
Percent passing No. 8 sieve (%)	30	38	–
Rut depth at N = 8,000 (0.001 in.)			
D	218	290	76
K	163	217	54
L	162	220	58
AC content (%)			
D	5.2	5.1	–
K	5.3	5.3	–
L	5.5	5.3	–
Stability (lb)			
D	1,810	2,120	–
K	2,280	3,010	–
L	2,580	2,710	–
Flow (0.01 in.)			
D	12.2	11	–
K	11	11.8	–
L	10	9.6	–

NOTE: D (Dalton Springs), K (Kennesaw), and L (Lithia Springs) are aggregate sources.

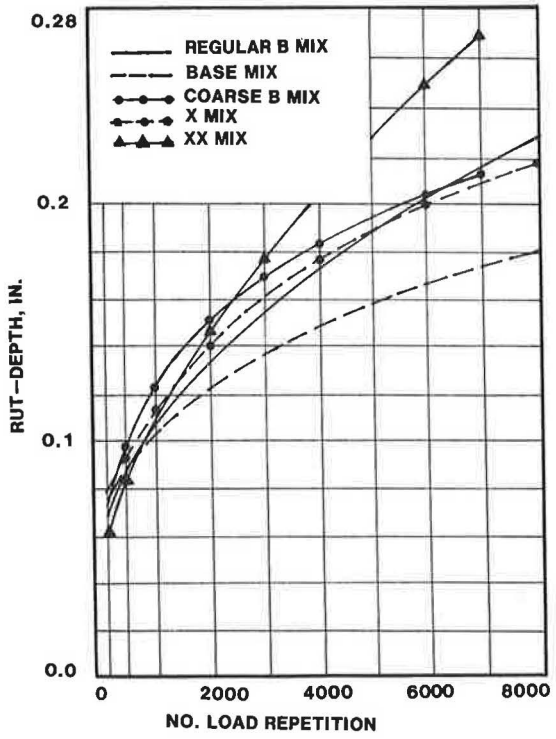

FIGURE 8 Rut depth versus number of load repetitions.

of asphalt mixes. Using the results presented in Table 2, the averaged rut depth values of the five mixes from the same aggregate source at N = 8,000 were calculated, as follows:

	Rut Depth at N = 8,000 (0.001 in.)	*Asphalt Content (%)*	*Marshall Stability (lb)*	*Marshall Flow (0.01 in.)*
Dalton	229	4.86	2,016	11.1
Kennesaw	193	5.06	2,974	11.3
Lithia Springs	199	5.2	2,786	10.6

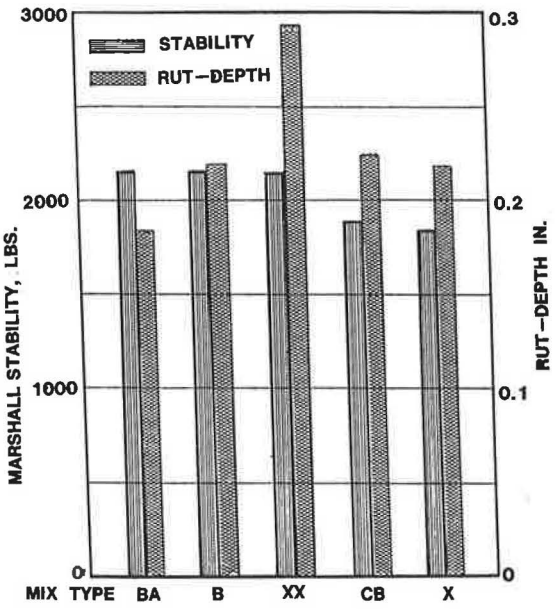

FIGURE 9 Comparison between Marshall stability value and rut depth of asphalt mixes.

The mixes using aggregates from Dalton showed significantly greater rutting than the mixes using the other two aggregates. The average rutting between mixes using aggregates from Kennesaw and mixes using aggregates from Lithia Springs was not significantly different. The averaged Marshall stability of the mixes using Dalton aggregate was lower than that of the mixes using the other two types of aggregates. These effects can be explained by the particle shape and the surface texture of the aggregates. The aggregate from Dalton is limestone type, and the particles of the coarse aggregates are more elongated and flaky, whereas the aggregates from Kennesaw and Lithia Springs are granite, the particles are more cubical, and the surface textures are rougher than the limestone from Dalton.

CONCLUSION

The modified LWT machine described in this paper has been used in several studies to evaluate the rutting resistance of asphalt mixes. The studies have shown that the LWT machine is relatively simple to operate in a laboratory environment and that the test can be used to assess the rutting characteristics of asphalt mixes.

ACKNOWLEDGMENT

This work was performed for GaDOT in cooperation with the U.S. Department of Transportation, FHWA, Office of Materials and Research.

REFERENCES

1. J. S. Lai. *Development of a Simplified Test Method to Predict Rutting Characteristics of Asphalt Mixes*. Research Project 8502,

Final Report, Georgia Department of Transportation, Atlanta, 1986.
2. J. S. Lai. *Evaluation of Rutting Characteristics of Asphalt Mixes Using Loaded-Wheel Tester*. Research Project 8609, Final Report, Georgia Department of Transportation, Atlanta, 1986.
3. J. S. Lai. *Evaluation of the Effect of Gradation of Aggregate on Rutting Characteristics of Asphalt Mixes*. Research Project 8706, Final Report, Georgia Department of Transportation, Atlanta, 1988.
4. M. Livneh and J. Greenstein. Influence of Aggregate Shape on Engineering Properties of Asphaltic Paving Mixtures. *Highway Research Record 404*, HRB, National Research Council, Washington, D.C., 1972, pp. 42–56.
5. J. Uzan. An Evaluation Scheme for Conventional Requirements of Design and Construction Quality for Asphalt Concrete. *Proc., Association of Asphalt Paving Technologists*, Vol. 51, 1982, pp. 129–148.
6. J. S. Lai. *Development of a Laboratory Rutting Resistance Testing Method for Asphalt Mixes*. Research Project 8717, Final Report, Georgia Department of Transportation, Atlanta, 1989.

Publication of this paper sponsored by Committee on Characteristics of Bituminous Paving Mixtures To Meet Structural Requirements.

Overview of a Rational Asphalt Concrete Mixture Design for Texas

KAMYAR MAHBOUB AND DALLAS N. LITTLE

A rational asphalt concrete (AC) mix design and analysis methodology was developed. The term "rational" meant that the material properties evaluated in the mixture design and analysis could be used with a layered-elastic pavement model and mechanistic-empirical formulations that relate to pavement performance. The procedures proposed in this study were intended to be used in conjunction with the current Texas State Department of Highway and Public Transportation method of mix design in a complementary fashion. Three major modes of pavement distress—(a) rutting, (b) flexural fatigue, and (c) low-temperature cracking—were addressed. In addition to mixture properties, structural arrangement of pavement layers and environmental factors have significant effects on the performance of AC mixtures. Therefore, a comprehensive mix design should not be performed independent of pavement structural design. Asphalt mix design and pavement structural design parameters were brought together in an integrated fashion.

Hot-mix asphalt (HMA) mix design has long been a trial-and-error process. Two major empirical methods of mix design have emerged as those most commonly used by the asphalt community. The Hveem (ASTM D1560) and Marshall (ASTM D1559) methods have evolved over the past four decades. They are both regarded as empirical methods. There are many variations of these basic methods (see Figure 1) in use among state highway agencies (*1*). Texas State Department of Highways and Public Transportation (SDHPT) has its own unique method of mix design, which is basically a modified Hveem procedure (*2*).

According to the Asphalt Institute (*3*), all mix design procedures must provide the following:

1. Sufficient asphalt to ensure a durable pavement;
2. Sufficient mixture stability to satisfy the demands of traffic without distortion or displacement;
3. Sufficient voids in the final compacted mix to allow for a slight amount of additional compaction due to traffic loading; sufficient voids for expansion of asphaltic cement without flushing, bleeding, and loss of stability; and low enough voids to keep out harmful air and moisture; and
4. Sufficient workability to permit efficient placement of the mix without segregation or shoving.

Historically, the Hveem and Marshall methods have served well; however, they are often used beyond their originally intended realm of empiricism. That is precisely why these methods have proven to be inadequate in addressing today's in-service performance problems. Such problems are associated with variations in the crude source and refining processes, use of additives and modifiers (*4*), type of mix (e.g., large-stone or open-graded) (*5*), and current trends toward heavier traffic loads and higher tire pressures (*6*).

Serious shortcomings of current methods of mix design have led researchers to search for mix design methods on the basis of mechanistic parameters. Recently, a study was funded by Texas SDHPT with the objective of developing a rational mix design and analysis procedure to address different modes of pavement distress in terms of HMA mechanistic parameters.

TEXAS MIX DESIGN METHODOLOGY

In Texas' present method of mix design (*2*), the basic philosophy is to produce a mix with adequate Hveem stability and a target air voids of 3 percent. The latter, which represents the void content in the pavement after its second summer in service, also requires that the aggregate have adequate polish resistance and a minimum of crushed surfaces.

The Texas gyratory-shear method of compaction is used in specimen fabrication. This method closely simulates the kneading action of roller compactors and further densification caused by traffic. As part of a study called "Asphalt Aggregate Mixture Analysis System (AAMAS)," sponsored by NCHRP, researchers (*7*) noted that the Texas gyratory-shear compactor was better at producing the densification and material properties similar to those developed through field compaction than the processes of the Marshall method.

RESEARCH APPROACH

The philosophy behind this improved mix design procedure is to design an HMA that will provide an adequate level of stiffness to protect the vulnerable subgrade by proper distribution of vertical compressive stresses. There is a tradeoff between the stiffness of HMA and its flexibility. An adequate level of flexibility must be demonstrated by the HMA for it to resist a load-induced, flexural fatigue mode of distress. Once the stiffness and flexibility properties are determined to be acceptable, the permanent deformation potential of HMA can be assessed by means of a constant-stress creep analysis.

Finally, the low-temperature fracture potential is evaluated on the basis of the HMA's stiffness and tensile strength. The temperature susceptibility of the HMA stiffness is characterized by variation of the diametral resilient modulus induced by changes in temperature. The HMA tensile strength is also

K. Mahboub, Kentucky Transportation Center, University of Kentucky, Lexington, Ky. 40506. D. N. Little, Texas Transportation Institute, Texas A&M University, College Station, Tex. 77843.

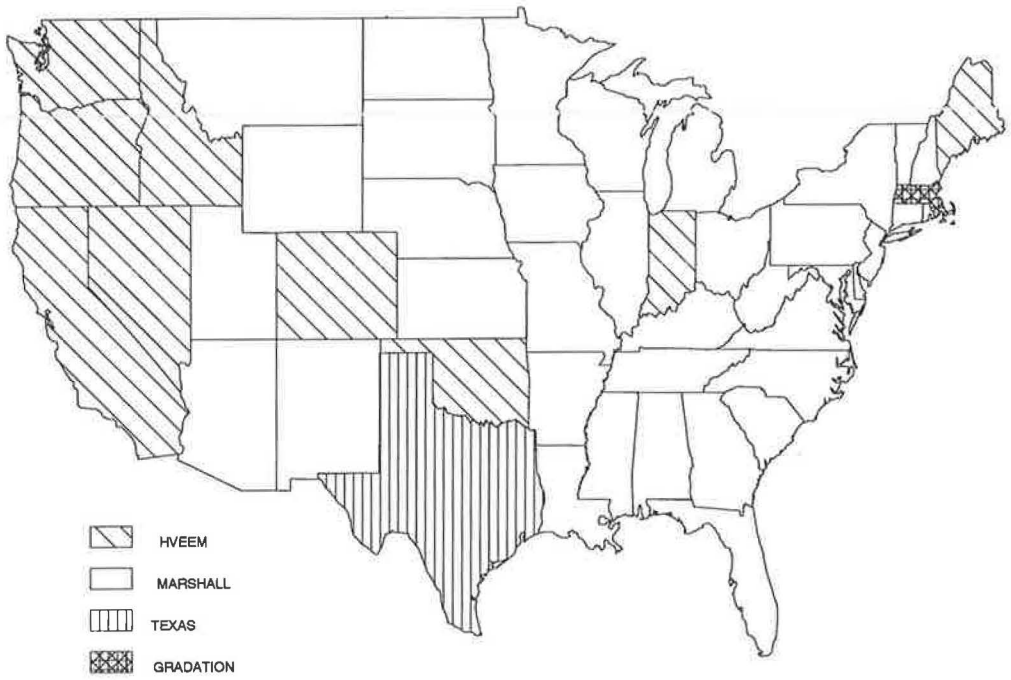

FIGURE 1 Distribution of mixture design methods common in the United States (*1*).

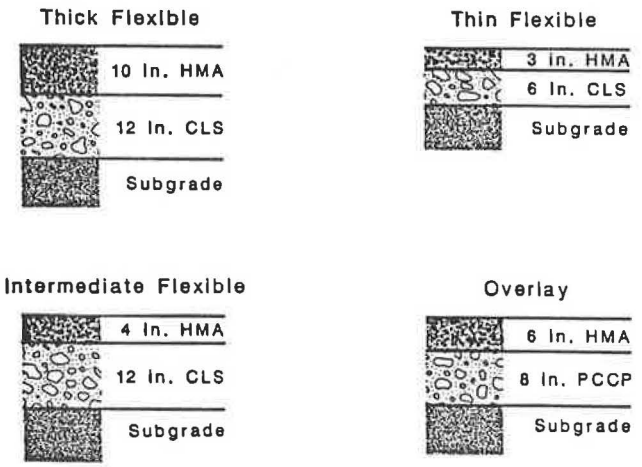

FIGURE 2 Four distinct pavement structural categories.

evaluated diametrally, over a range of temperatures and at a slow rate of loading to simulate the slow thermal contraction and fracture process in the pavement.

The most important aspect of this improved mixture design approach lies in its direct link to pavement structural design. The rationale is that the material properties that determine the success or failure of a pavement structure cannot be adequately assessed without full consideration of the pavement structural conditions.

A system of pavement structural categories was arranged to identify four distinctive categories of pavement structure commonly encountered in the field. The four pavement structures listed in the following paragraph represent the pavement types used in the development of mixture acceptance criteria. Therefore, asphalt mixtures can be evaluated on the basis of mechanical conditions present under a selected set of pavement structural arrangements.

The structural categories and their representative pavement cross sections (Figure 2) were as follows:

- Thick flexible pavement: 10-in. HMA, 12-in. crushed limestone base (CLS), and subgrade (weak, moderate, or soft).
- Thin flexible pavement: 3-in. HMA, 6-in. CLS, and subgrade (weak, moderate, or soft).
- Intermediate flexible pavement: 4-in. HMA, 6-in. CLS, and subgrade (weak, moderate, or soft).
- HMA overlaying a portland cement concrete pavement (HMA/PCCP): 6-in. AC, 8-in. PCCP, and subgrade (weak, moderate, soft).

OVERVIEW OF METHODOLOGY

The methodology is based on a series of mechanistic material characterization procedures that relate directly to the pavement distress modes. The hierarchy of this design and analysis approach may be expressed as the following:

1. Mixture design in accordance with a standard procedure (e.g., Texas method);
2. Mixture stiffness characterization related to threshold resilient modulus for subgrade protection and stiffness and flexibility analysis for flexural fatigue evaluation;
3. Permanent deformation potential analysis; and
4. Thermal cracking analysis.

An overview of this mechanistic methodology is presented in the following sections.

Stiffness Characterization

In flexible pavements, the HMA is normally the stiffest layer and thus the layer that contributes most effectively to distribution of vertical compressive stresses. A high level of subgrade protection can be achieved through the use of a stiff HMA layer. However, a life cycle cost penalty is associated with this simplistic approach; that is, the stiffest HMA layer may not be desirable from a flexural fatigue point of view. The tradeoff situation that exists between subgrade rutting and fatigue cracking will be discussed in the following sections.

Subgrade Rutting

Flexible pavements are usually designed with the stiffest and highest-quality material on the top layer, and with a gradual transition to softer and lower-quality material in the layers below. A methodology was developed for selecting the proper level of HMA stiffness (the HMA threshold resilient modulus) to protect the subgrade from excessive rutting. The criterion was based on earlier work (*8*) synthesized by Monismith and Finn:

$$N_{18} = (6.15 \times 10^{-7})\, \varepsilon_3^{-4} \quad (1)$$

where

N_{18} = number of 18-kip axle passes to cause a ¾-in. subgrade deformation, and
ε_3 = vertical compressive strain (in./in.) at the top of the subgrade.

There are other subgrade rutting models similar to this criterion (Figure 3). All of these models are empirical; however, they are performance based, and input parameters are mechanistic. Therefore, the approach may be regarded as mechanistic-empirical. Figure 4 shows a schematic representation of a subgrade protection criteria chart. A flow chart illustration of the subgrade protection criterion is shown in Figure 5.

Flexural Fatigue

Once a minimum level of HMA stiffness is determined through the subgrade protection criterion, the fatigue resistance of the mixture is analyzed to ensure a proper balance between stiffness and flexibility. The term "fatigue life" is defined as the magnitude of traffic, expressed in terms of the number of 18-kip equivalent single-axle loads (ESALs), that a pavement structure can handle before a certain amount of distress, usually defined as a percentage of cracking in the wheel path area, is observed.

Finn et al. (*9*) developed a fatigue model on the basis of laboratory and field data from the AASHO Road Test (*10*) to predict up to 10 percent cracking in the wheel path area.

$$\log N_f = 15.947 - 3.291 \log(\varepsilon_t) - 0.845 \log\left(\frac{E^*}{10^3}\right) \quad (2)$$

where

N_f = number of cycles (18-kip ESALs) to failure,
ε_t = repeated tensile strain (in./in. $\times 10^{-6}$), and
E^* = complex modulus (psi) of HMA, approximated by the resilient modulus.

Monismith et al. (*11*) stated that stiffness moduli determined from the ratio of applied stress and the recoverable strain (commonly known as the resilient modulus) should provide essentially the same moduli as that determined from creep and sinusoidal loading (commonly known as the com-

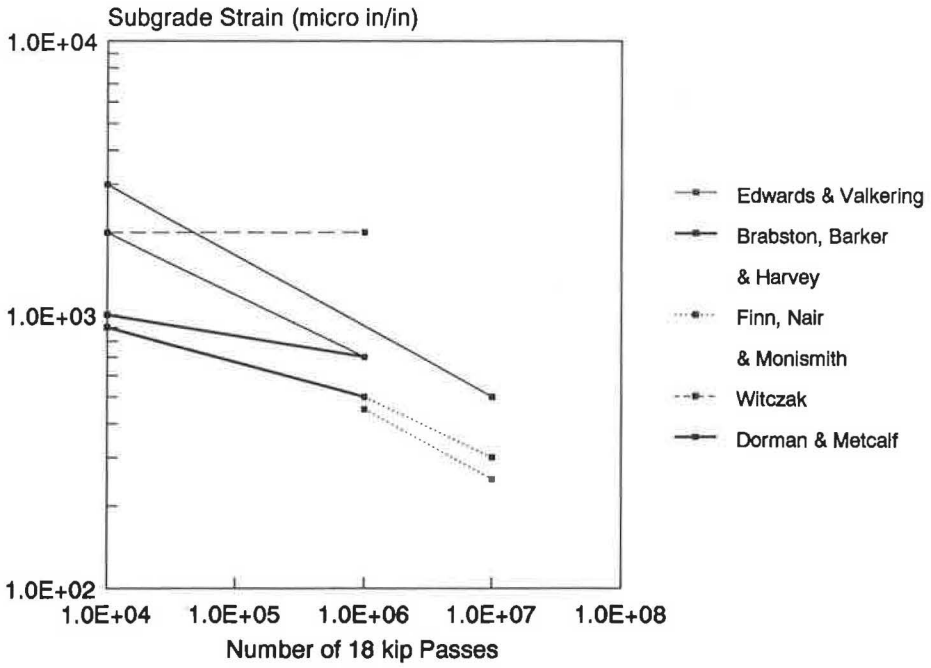

FIGURE 3 Excessive subgrade deformation criteria (*8*).

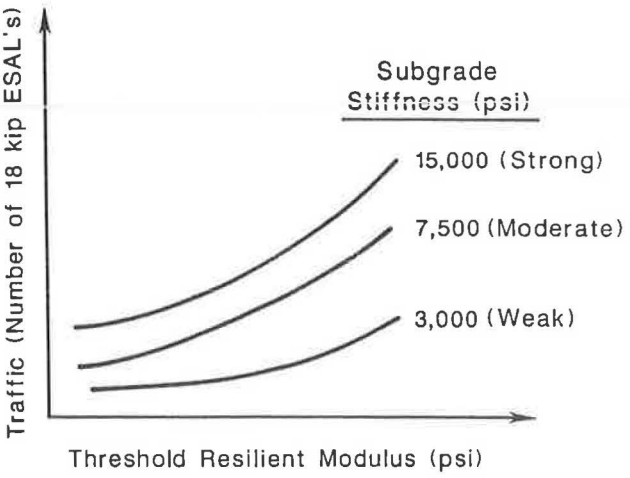

FIGURE 4 Schematic of the threshold resilient modulus of asphalt layer determined on the basis of subgrade excessive deformation criteria.

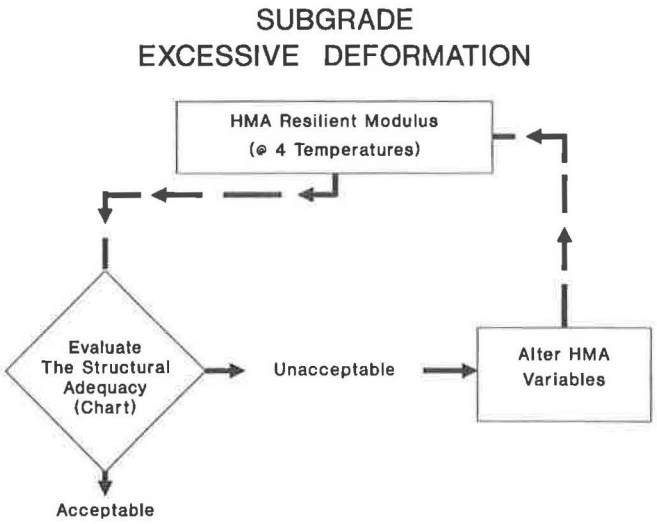

FIGURE 5 Flow chart describing subgrade rutting analysis subsystem.

plex modulus). Hence, the substitution of resilient modulus for complex modulus in Equation 2 is assumed to be valid.

Equation 2 was obtained through laboratory testing followed by shifting of the laboratory data to match the AASHO Road Test (*10*) observations. The resulting shift was about 1,300 percent, which suggests that the actual fatigue life of the pavement in the field was approximately 13 times greater than the laboratory-based predictions. The following explanations could explain this interesting phenomenon:

- Rest periods between traffic loadings, viscoelastic relaxation, and chemical rebonding and healing of asphalt;
- Kneading and surface-crack closing actions of tires; or
- Buildup of residual compressive stresses.

The first step in this rational fatigue analysis approach calls for the evaluation of HMA stiffness at the mean annual pavement temperature (Figure 6). On the basis of this selected value of HMA stiffness, measured in terms of resilient modulus, the induced tensile strain at the underside of the HMA layer is evaluated. Repeated load-induced tensile strain, the primary cause of fatigue cracking, is evaluated from a series of charts developed for each category of pavement structure (Figure 7a). These charts used the results of over 100 computer runs of layered-elastic pavement. The final step in fatigue life evaluation is shown schematically in Figure 7b, which was developed from solutions of layered-elastic pavement runs and Equation 2. Figure 8 is a flow chart representation of the fatigue analysis procedure.

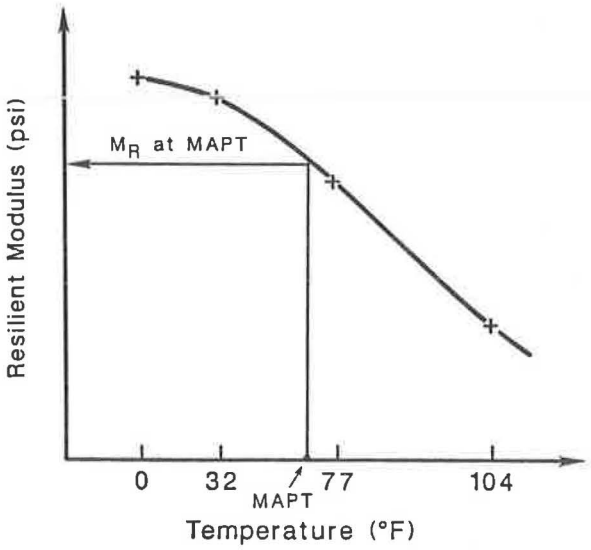

FIGURE 6 Determination of the resilient modulus at the mean annual pavement temperature.

Permanent Deformation

The proposed methodology calls for a static creep-recovery test for evaluation of resistance to permanent deformation potential. The data from this simple test are collected in terms of deformations, both recoverable and irrecoverable, as a function of time. The irrecoverable portion of deformation is responsible for rutting.

A rutting model using the information obtained from the creep-recovery test was developed. This model was based on some earlier work on creep and rutting by Shell researchers (*12,13*). The original Shell rutting model assumes that a linear-elastic relationship (Hooke's Law) is capable of characterizing deformation processes that are by nature not only inelastic but are also viscoelastic, viscoplastic, and plastic. Because of this serious invalid assumption (i.e., using Hooke's Law for characterization of permanent deformation), Shell researchers had to incorporate a composite correction factor into their model.

The relationship between stress level and permanent deformation is not linear (*14–18*). These observations led to the development of a refined version of the original Shell equation. The modified version of the Shell rutting equation does not depend on empirical correction factors; it accounts for

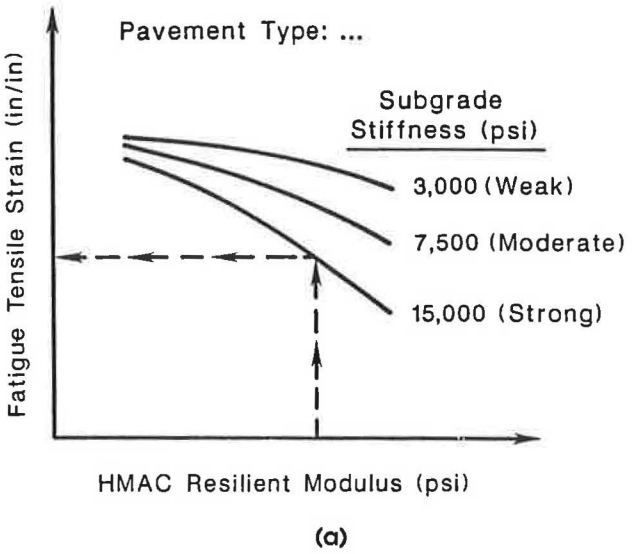

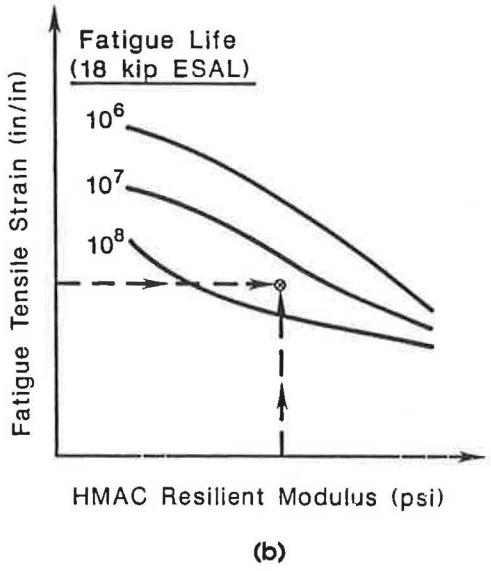

FIGURE 7 Schematic diagrams representing a, the evaluation of fatigue tensile strain, and b, fatigue life.

plasticity trends and nonlinearity of such deformations in the following format:

$$h = H\left(\frac{Z\sigma_{tire}}{\sigma_{lab}}\right)^{1.61}\varepsilon_{vp}(t) \quad (3)$$

where

h = calculated rut depth (in.),
H = asphaltic layer thickness (in.),
Z = vertical stress distribution factor derived from layered-elastic solutions (*13*),
σ_{tire} = average tire contact pressure (psi),
σ_{lab} = stress level (psi) at which the creep test is conducted in the laboratory, and
$\varepsilon_{vp}(t)$ = viscoplastic trend (in./in.) of the mixture measured by the creep test.

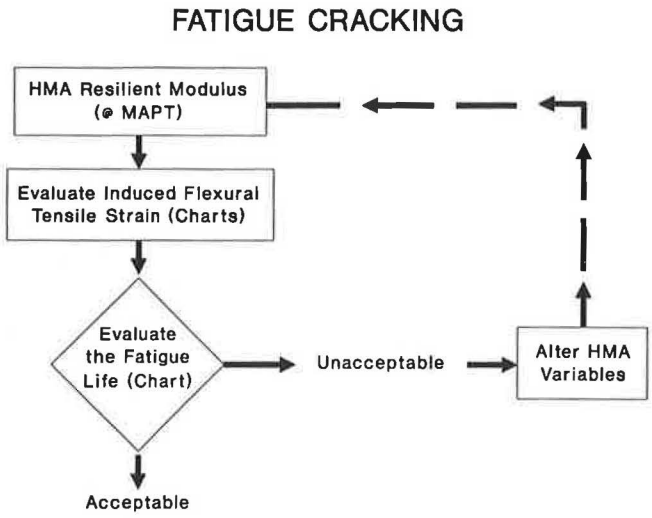

FIGURE 8 Flow chart describing fatigue analysis subsystem.

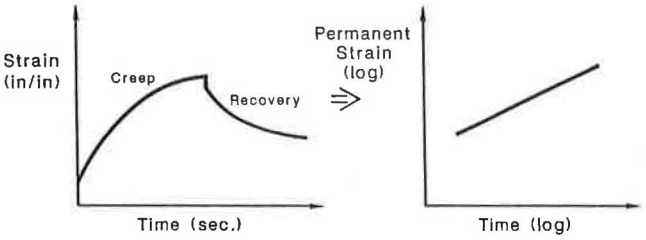

FIGURE 9 Schematic diagrams describing procedures for characterization of permanent deformation.

In Equation 3, the ratio of field to laboratory compressive stresses is raised to the exponent 1.61 to account for deformation processes that are nonlinear (i.e., doubling of stress level will triple the rutting). The magnitude of this exponent was determined from several high- and low-stress creep tests and other sources (*14,15,18*).

Rutting criteria charts were developed on the basis of this new rutting model and a stiffness parameter called the "viscoplastic stiffness." The new stiffness parameter is a stress-normalized viscoplastic strain function. Figure 9 shows schematically the procedure by which nonrecoverable strains are characterized as a function of time. Similar to creep stiffness, viscoplastic stiffness has a power-law decay exponent, measured by many researchers (*15,17,18*) to be in the range of -0.25 to -0.27. A set of rutting severity limits (*19*) and assumed power-law–type rutting accumulation rates of 0.25 to 0.27 (the sign change is due to the inverse relationship between strain and stiffness) were the basis for developing a set of rutting criteria charts for specific pavement categories, and layer moduli. Figure 10 shows a schematic of a rutting criteria chart. A flow chart representation of the rutting analysis procedure is shown in Figure 11.

Thermal Cracking

This mode of distress occurs as the result of thermally induced tensile stresses developing in pavement layers. Most methods

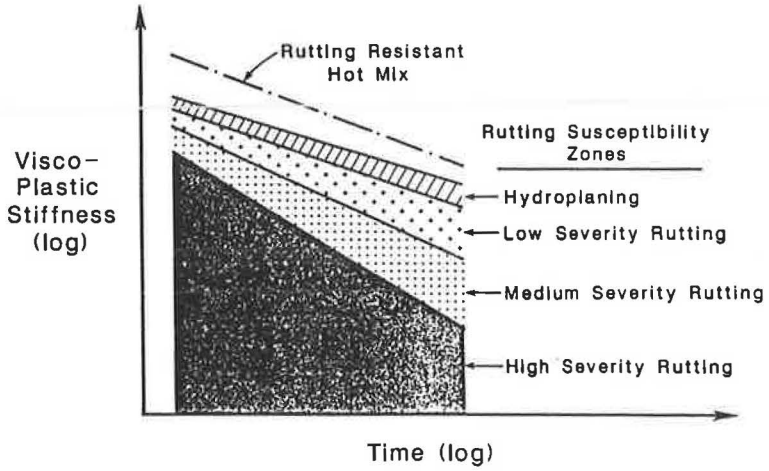

FIGURE 10 Schematic rutting criteria chart.

for calculation of thermally induced stresses are based on algorithms similar to those used in the computer program COLD (*20*). This program was originally developed by Christison (*21*) at the University of Alberta. On the basis of thermal properties of the pavement, solar radiation, and air temperature, the program COLD generates a series of temperature profiles through a one-dimensional finite element routine.

The temperature drop with time induces thermal stresses that could potentially exceed the tensile strength of HMA and induce cracking. Induced tensile stresses are calculated as follows:

$$\sigma_x(t) = \int_{t_0}^{t_1} S(\Delta t,T)\cdot\alpha\cdot dT(t) \quad (4)$$

where

t = time;
T = temperature;
$\sigma_x(t)$ = induced thermal stress;
$S(\Delta t,T)$ = mix stiffness, time- and temperature-dependent;
$\Delta t = t_1 - t_0$; and
α = coefficient of thermal expansion.

The current version of the COLD program characterizes the HMA stiffness in terms of resilient modulus input over a range of temperatures. On the basis of the relationship between resilient modulus and temperature, the HMA is classified as being within a certain response zone (Figure 12). The response zones were established using an extensive body of existing resilient moduli versus temperature (*22*). Thermally induced stresses are then calculated on the basis of the resilient modulus response zone classification and climatic conditions (e.g., temperature drop rate or solar radiation). These induced conditions are shown schematically as a set of tensile stress boundary curves (Figure 13).

Finally, the thermally induced stresses and the tensile strength of the HMA are compared over a range of temperatures in a failure envelope format (Figure 14). A flow chart representation of the low-temperature cracking characterization is shown in Figure 15.

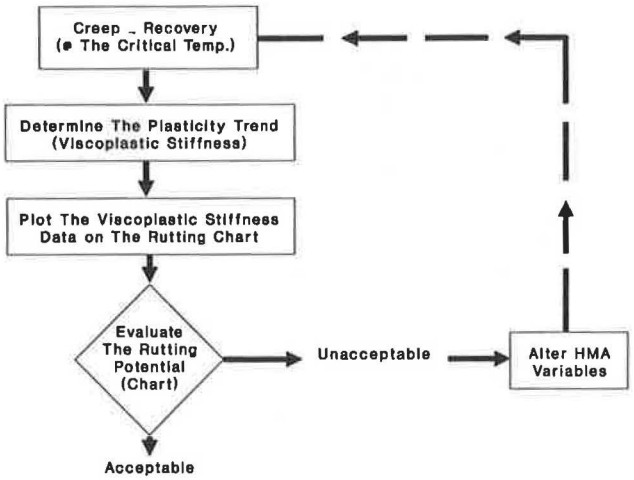

FIGURE 11 Flow chart describing rutting analysis subsystem.

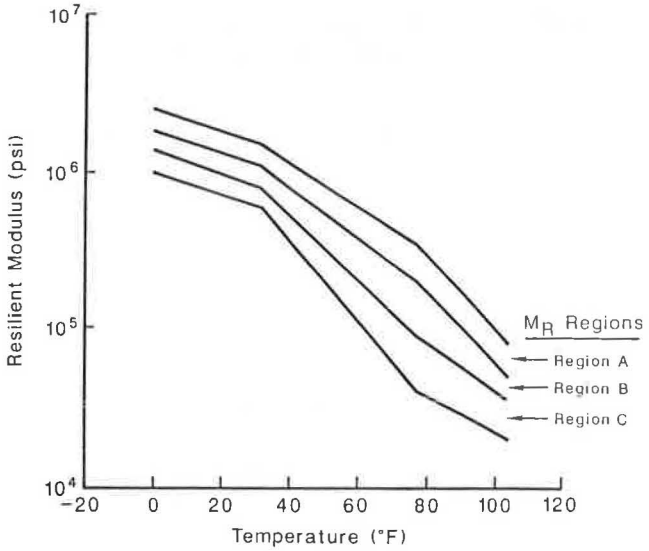

FIGURE 12 Schematic distribution of resilient modulus regions.

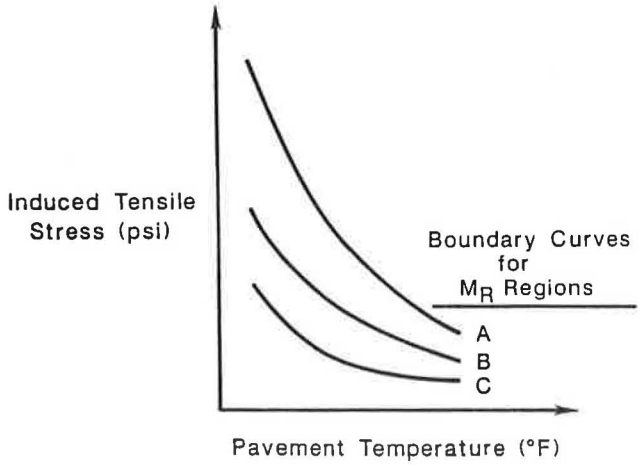

FIGURE 13 Schematic distribution of thermal stress versus pavement temperature for a given cooling rate.

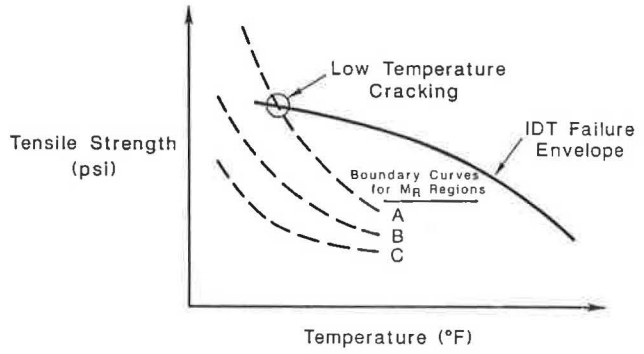

FIGURE 14 Procedure for evaluating thermal cracking potential using the indirect tensile failure envelope concept.

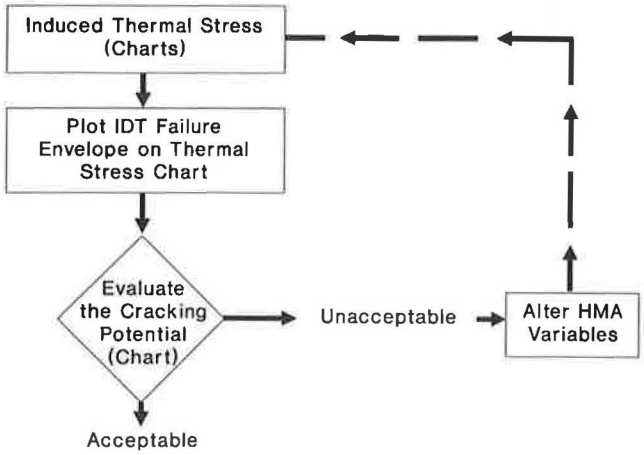

FIGURE 15 Flow chart describing thermal cracking analysis subsystem.

CONCLUSIONS AND RECOMMENDATIONS

HMA can be designed and analyzed using a rational approach. The methodology accounts for different modes of pavement distress (subgrade rutting, fatigue cracking, rutting, and low-temperature cracking) using fundamental engineering parameters. By using these mechanistic parameters in the mix design,

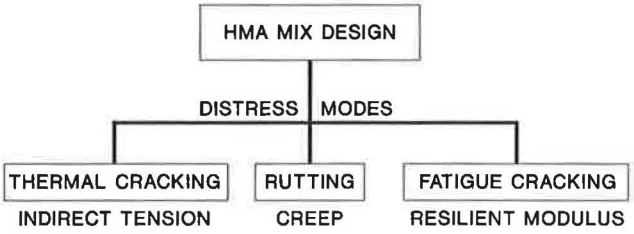

FIGURE 16 Integration of mix design and pavement design by using rational mixture characterization methodologies.

structural pavement design may be integrated with the HMA mixture design (Figure 16).

This procedure should be implemented on an interim basis, and the success or failure rates should be monitored. Standard procedures are needed for resilient modulus characterization of flexible pavement materials. Also, standards should be developed for a creep and permanent deformation test. Whenever possible, the creep test should be conducted at temperatures representative of field conditions. Shift factors should also be developed and used.

ACKNOWLEDGMENTS

This work was funded by Texas SDHPT and FHWA, U.S. Department of Transportation. Typing of the manuscript was done by Dale Hall of the University of Kentucky.

REFERENCES

1. P. S. Kandhal and W. S. Koehler. *Marshall Mix Design, Current Practices*. Association of Asphalt Paving Technologists, Vol. 54, St. Paul, Minn., 1985.
2. *Manual of Testing Procedures, 200-F Series*. Texas State Department of Highways and Public Transportation, Austin, 1985.
3. *Mix Design Methods for Asphalt Concrete and Other Hot-Mix Types*. Report MS-2. The Asphalt Institute, College Park, Md., 1979.
4. D. N. Little, J. W. Button, R. M. White, E. K. Ensley, Y. Kim, and S. J. Ahmed. *Investigation of Asphalt Additives*. Report DTFH-61-84-C-00066. Texas Transportation Institute, College Station, 1986.
5. K. Mahboub and D. L. Allen. Characterization of Rutting Potential of Large-Stone Asphalt Mixes in Kentucky. In *Transporta-*

tion Research Record 1259, TRB, National Research Council, Washington, D.C., 1990.
6. F. L. Roberts, J. T. Tielking, D. Middleton, R. L. Lytton, and K. H. Tseng. *Effects of Tire Pressure on Flexible Pavement*. Report 372–1f. Texas Transportation Institute, College Station, 1986.
7. H. Consuegra, D. N. Little, and H. von Quintas. Comparative Evaluation of Laboratory Compaction Devices Based on Their Ability to Produce Mixtures with Engineering Properties Similar to Those Produced in the Field. In *Transportation Research Record 1228*, TRB, National Research Council, Washington, D.C., 1989.
8. A. M. Claessen, J. M. Edwards, P. Sommer, and P. Uge. Asphalt Pavement Design, The Shell Method. *Proc., 4th International Conference on Structural Design of Asphalt Pavements, Vol. 1*, University of Michigan, Ann Arbor, 1977.
9. F. N. Finn, C. Saraf, R. Kulkarni, W. Smith, and A. Abdullah. The Use of Distress Prediction Subsystems for the Design of Pavement Structures. *Proc., 4th International Conference on Structural Design of Asphalt Pavements, Vol. 1*, University of Michigan, Ann Arbor, 1977.
10. *Special Report 73: The AASHO Road Test*. HRB, National Research Council, Washington, D.C., 1962.
11. C. L. Monismith, J. A. Epps, and F. N. Finn. Improved Asphalt Mix Design. *Proc., Association of Asphalt Paving Technologists*, Vol. 54, St. Paul, Minn., 1985.
12. P. J. Van de Loo. Creep Testing: A Simple Tool to Judge Asphalt Mix Stability. *Proc., Association of Asphalt Paving Technologists*, Vol. 43, St. Paul, Minn., 1974.
13. P. J. Van de Loo. The Creep Test, A Key Tool in Asphalt Mix Design and in the Prediction of Pavement Rutting. *Proc., Association of Asphalt Paving Technologists*, Vol. 47, St. Paul, Minn., 1978.
14. S. A. Khedr. Deformation Mechanism in Asphalt Concrete. *Journal of Transportation, ASCE*, Vol. 112, No. 1, New York, 1986.
15. K. Mahboub and D. N. Little. *Improved Asphalt Concrete Mixture Design Procedure*. Report 474-1F. Texas Transportation Institute, College Station, 1988.
16. J. S. Lai and D. Anderson. Irrecoverable and Recoverable Nonlinear Viscoelastic Properties of Asphalt Concrete. In *Highway Research Record 468*, HRB, National Research Council, Washington, D.C., 1973.
17. D. F. Kinder. *A Study of Both the Viscoelastic and Permanent Deformation Properties of a New South Wales Asphalt*. Australian Road Research Board, New South Wales, 1986.
18. M. Perl, J. Uzan, and A. Sides. Visco-Elastic-Plastic Constitutive Law for a Bituminous Mixture Under Repeated Loading. In *Transportation Research Record 911*, TRB, National Research Council, Washington, D.C., 1983.
19. *Highway Distress Identification Manual for Highway Conditions and Quality of Highway Construction Survey*. DOT-HFH-11-9175/NCHRP 1-19. U.S. Department of Transportation, Washington, D.C., 1979.
20. F. Finn, C. L. Saraf, R. Kulkarni, K. Nair, W. Smith, and A. Abdullah. *NCHRP Report 291: Development of Pavement Structural Subsystems*. TRB, National Research Council, Washington, D.C., 1986.
21. J. J. Christison and K. O. Anderson. The Response of Asphalt Pavements to Low Temperature Climatic Environments. *Proc., 3rd International Conference on Structural Design of Asphalt Pavements*, London, 1972.
22. J. A. Epps, D. N. Little, R. J. Holmgreen, and R. L. Terrel. *NCHRP Report 224: Guidelines for Recycling Pavement Materials*. TRB, National Research Council, Washington, D.C., 1980.

Publication of this paper sponsored by Committee on Characteristics of Bituminous Paving Mixtures To Meet Structural Requirements.

Evaluation of Surface Mixtures of Steel Slag and Asphalt

A. SAMY NOURELDIN AND REBECCA S. MCDANIEL

The demand for good-quality highway materials continues to increase whereas economical sources are becoming more limited. This demand may become more critical, especially with the policy (adopted by some state highway departments) of banning some aggregate types that have been frequently used in the past for producing paving mixtures. Steel slag aggregates have not yet been used extensively in pavement layers, even though they have been used successfully in the past. Steel slag has performed well in a number of surface-course applications subject to high traffic volumes (when such mixtures have been properly designed and constructed). Research, development, and demonstration work are still required to ensure the full exploitation of steel slag. The suitability of steel slag aggregates in combination with natural sand was evaluated for use in bituminous pavement surface layers constructed to serve high-volume, high-speed, and heavy-load traffic. This evaluation was made through a literature search, a field investigation, and a laboratory characterization of bituminous mixtures prepared with various gradations and proportions of steel slag aggregate. Marshall-sized specimens were tested in the laboratory for tensile characteristics, expansive properties after freeze-thaw cycling, and Marshall stability. The field investigation included a surface condition survey and skid resistance measurements. Use of steel slag in asphaltic mixes is still highly localized in steel production areas. Some highway agencies do not permit its use, although the performance record of steel slag mixtures is reported to be excellent. Some inputs should be considered in further evaluation of steel slag asphaltic mixtures. This process may lead to the development of technical specifications and recommendations for more extensive use of steel slag aggregates in pavement layers.

Many highway departments in the United States and Canada are taking actions to reduce and possibly prevent asphaltic pavement rutting on their highway systems. These actions are warranted because of the increased occurrence of rutting in pavements that have performed satisfactorily for several years. These increases are the results of ever-increasing truck volumes, gross weights, and tire contact pressures. Truck gross weights of over 500,000 lb and tire pressures of over 120 psi have been frequently reported.

Major changes in materials, together with some changes in mix design and construction procedures for asphalt pavement resurfacing and overlays, are currently recommended and applied. The use of some aggregate materials has been severely limited, if not prohibited. Natural sand, for example, is often prohibited from being used as a fine aggregate material in producing bituminous surface mixtures.

A. S. Noureldin, Public Works Department, Cairo University, Cairo, Egypt. Current affiliation: Ministry of Communications, King Abdel Aziz Road, Riyadh 11178, Saudi Arabia. R. S. McDaniel, Indiana Department of Transportation, Division of Research, West Lafayette, Ind. 47906.

The policy of banning the use of various aggregates to obtain higher-quality asphaltic mixtures has its drawbacks, because it usually results in higher construction, maintenance, overlay, and resurfacing costs. Asphalt pavement mix design, thickness design, and construction procedures have to be developed to adapt to the use of poor-quality as well as good-quality aggregates.

Quality assurance specifications of most state highway departments (including Indiana) are getting tighter and tighter. Minimum Marshall stability (as an example) for accepting an asphalt mix is 1,200 lb in Indiana. Other state highway departments are using 1,500 lb as a minimum acceptable value. Minimum values of 2,000 lb are used in Canada and are currently recommended for use by some state highway departments. However, no well-known criteria have tied the Marshall mix design (or any other mix design procedure) to pavement thickness design of asphaltic surface mixtures. If a specific thickness was designed for a mixture with a Marshall stability of 2,000 lb, a greater thickness could be designed for a mixture with a 1,200-lb Marshall stability value and, similarly, a lower thickness could be designed for a mix with a 2,800-lb stability value.

Asphaltic mixtures composed of steel slag as coarse aggregate, natural sand as fine aggregate, and AC–20 asphalt cement were evaluated. Natural sand is considered a poor-quality aggregate and can produce tender asphaltic mixtures subject to rutting. Steel furnace slag is considered an acceptable aggregate type by the Indiana Department of Transportation's *Standard Specifications* (*1*). However, most contractors tend not to use it because of its relatively high cost. The cost per unit weight of steel furnace slag is almost the same as that of any other coarse aggregate type used in Indiana. However, the pavement thickness produced by a ton of steel slag is considerably smaller than that produced by any other coarse aggregate type, because of the high specific gravity (3.4) of the steel slag.

Asphaltic mixtures containing different proportions of steel slag and natural sand were produced and evaluated using Marshall stability and indirect tensile tests (indirect tensile strength, stiffness, and deformation). Other Marshall mix design parameters (air voids, voids in mineral aggregate, and voids filled with bitumen and density) were also investigated.

The combination of natural sand and steel slag produced an asphaltic paving mixture (in the laboratory) with good stability and stiffness. In addition, high stiffness values of laboratory-compacted cores containing steel slags suggest that its relatively high cost could be compensated for by either using it with inexpensive, low-quality fine aggregate or reducing the thickness of asphaltic paving surface layers in which steel slag is used.

REVIEW OF LITERATURE

Ferrous Slags Production

Ferrous slags are by-products of the iron- or steel-making process. Formation begins when iron ore, coke, and a flux (either limestone or dolomite) are melted together in huge furnaces. When the metallurgical smelting process is complete, the lime in the flux has been chemically combined with the aluminates and silicates of the ore and coke ash to form a nonmetallic product called slag.

During the period of cooling and hardening from the molten state, the slag can be treated to form several specific types, which can in turn be crushed or screened to isolate diverse grades and sizes. The various types of ferrous slag can be classified under four basic headings (*2*,*3*):

1. Air-Cooled Blast Furnace Slag is produced by pouring molten slag into pits or banks and permitting it to cool and solidify slowly under atmospheric conditions. It can be processed, crushed, and screened into sizes. It is a relatively light-weight type of aggregate.
2. Expanded Blast Furnace Slag is produced by applying a controlled amount of water, steam, or compressed air to molten slag. It is also a light-weight type of aggregate.
3. Granulated Blast Furnace Slag is produced by sudden quenching of molten slag in water. It is a noncrystalline, light-weight, granular material.
4. Steel Slag, a by-product of the steel-making process (using open hearth, electric, or oxygen steel furnaces), has a higher specific gravity (3.2 to 3.6) than blast furnace slags because of its high iron content. Steel slag may be recycled to produce more iron products and one of the three iron blast furnace slags. However, this recycling procedure is usually not economical.

Table 1 presents the chemical composition of steel slag together with that of iron blast furnace slags for comparison purposes (*3*).

General Characteristics of Steel Slag Aggregates

Steel slag consists of crushed angular particles with rough, irregular surfaces. It has essentially no flat or elongated pieces and has a rougher surface texture than gravels and crushed stones. Steel slag is highly resistant to weathering, as are the iron blast furnace slags. Freezing and thawing effects and sulfate soundness losses are reported to be exceptionally low (*3*,*4*).

Rough-surfaced, angular particles of steel slag develop high internal friction and good particle interlock, which contribute to high stability when used as aggregate for bituminous mixes. Crushed steel slag typically has an angle of internal friction in the range of 45 to 50 degrees (*2*).

The hardness of steel slag, as measured by Moh's mineralogic scale, is usually 7, compared with values of 6 for air-cooled blast furnace slags and 3 to 4 for dolomite and limestone (*2*,*3*).

The abrasion characteristics of steel slag aggregate are also distinctive. Typical Los Angeles abrasion values (ASTM C131) are in the range of 20 to 25 percent, compared with 35 to 40 percent for air-cooled blast furnace slag and natural dolomite (*2*,*3*). Therefore, the change in gradation (degradation) under traffic would be negligible if steel slag was used for surface paving layers. Table 2 presents a comparison of some properties of steel slag aggregate and air-cooled blast furnace slag.

The weight per unit volume of slag is significantly higher than that of iron blast furnace slags and all natural aggregates. Bituminous paving mixtures produced using steel slag aggregates will display high density values and generally greater stability and stiffness values than bituminous mixes using any other type of aggregate material.

The distinctive color and texture of steel slag paving mixtures may also be useful in distinguishing traffic lanes from shoulders and keeping highway users alert to impending stops and highway width changes. Rumble strips can be constructed with steel slag to warn drivers of approaching intersections. These may help reduce accident rates at intersections with a high accident frequency and may prevent rutting.

TABLE 1 COMPOSITION OF IRON BLAST FURNACE SLAGS AND STEEL SLAG (*3*)

Compound	Iron Blast Furnace Slag (%)	Steel Slag (%)
Calcium oxide	36–45	25–42
Silicon dioxide	33–42	15–17
Aluminum oxide	8–16	2–3
Magnesium oxide	3–16	6–10
Iron (FeO and Fe_2O_3)	0.3–2	20–26
Calcium sulfate	1–3	–
Manganese oxide	0.2–1.5	8–12
Titanium dioxide	0–1	0–1
Free lime	0–1	2–4

TABLE 2 TYPICAL CHARACTERISTICS OF STEEL SLAG AND AIR-COOLED BLAST FURNACE SLAG (*2*,*3*)

Parameter	Air-Cooled Blast Furnace	Steel Slag
Bulk specific gravity	2.1–2.5	3.2–3.6
Porosity (%)	Up to 5	Up to 3
Rodded unit weight (lb/ft³) (ASTM C28)	75–90	100–120
Los Angeles abrasion (%) (ASTM C131)	35–45	20–25
Sodium sulfate losses (%) (ASTM C88)	<12	<12
Angle of internal friction (degrees)	40–45	40–50
Hardness (Moh's scale of mineral hardness)[a]	5–6	6–7
California bearing ratio[b] (%)	Up to 250	Up to 300
Unit weight of Marshall compacted bituminous mix (lb/ft³)	125–145	160–190
Polarity	Alkaline (pH 8–10)	Alkaline (pH 8–10)
Asphalt content requirements in dense graded mixes (%)	Up to 8	Up to 6.5

[a]Hardness of dolomite measured on same scale is 3 to 4.
[b]Top size ¾ in. Typical CBR value for crushed limestone is 100 percent.

Steel Slag Use in Asphaltic Paving Mixtures

Steel slag aggregates have been used successfully in asphaltic surface mixtures in Europe, Canada, Australia, and parts of the United States (*4,16*). No major problems with the quality and durability of steel slag asphaltic concrete (AC) pavements have been reported. Steel slag has also been used in hot mixes for winter patching. It retains heat very well, and its high unit weight and stability tend to hold patches in place.

Bituminous test sections were constructed in 1974 on Highway 401, Toronto By-Pass, Canada, as part of a program to determine the most suitable material to improve driving quality (*5,7,16*). Highway 401 is considered one of the busiest freeways north of Toronto. Sections constructed with steel slag gave the highest skid numbers during the 4-year study period. In addition, steel slag asphaltic mixtures displayed higher Marshall stability values (3,500 lb from laboratory-compacted specimens and 3,650 lb from field cores) than all other asphalt mixtures used in 18 different test sections. Steel slag asphaltic mixtures provide superior skid resistance. The wet-road accident rate did not significantly exceed the dry-road accident rate for steel slag AC surfacings, whereas the opposite was generally true for all other surfacings.

Highway trials using a blend of air-cooled blast furnace slag (coarser portion) and steel slag (finer portion) in AC surface courses have proven most satisfactory; excellent skid resistance was developed. This type of mix would allow a much fuller use of the finer steel slags (*3*).

Steel slag aggregates have also been used for pavement bases and subbases, shoulders, fills, and berm stabilization. Its use for pavement layers in parking lots and high-speed turns is currently being considered (*3,4,9–12*).

There has been interest in Europe and Australia concerning the use of steel slag in stabilized bases. Stabilized bases consisting of 60 percent blast furnace slag (0 to 60 mm), 25 percent steel slag (0 to 15 mm), and 15 percent granulated blast furnace slag have been placed and compacted with standard highway equipment (at approximately 10 percent water content); the results were reported to be excellent.

Factors To Be Considered When Employing Steel Slag Aggregates

When using steel slag aggregate materials for road construction the following factors should be considered.

Variations in Characteristics

Variations in the characteristics of steel slag and iron blast furnace slags may be expected, because both types are by-products of the iron- and steel-making process, not a slag aggregate-making process. The economic worth of steel slag for return to blast furnace, burden for recycling, and potential application of steel slag as a fertilizer may help cause these variations between plants and even within the same plant and furnace (open hearth, basic oxygen, and electric arc). Although not much variation in aggregate gradation may be expected because of processing and screening procedures, variations in specific gravity and other characteristics may be expected (*3,6*).

Unit Weight

The weight per unit volume of steel slag is significantly higher than that of blast furnace slag and of most natural aggregates. As a result, a larger tonnage of steel slag is required to produce a given volume of bituminous mix or to cover a given area of pavement with a specific thickness. This factor becomes important where long shipping distances are involved in obtaining sufficient materials for construction.

Expansive Nature

Although blast furnace slags are stable, steel slags have a potentially expansive nature (volume changes of up to 10 percent). This expansion can be attributed to the hydration of calcium and magnesium oxides (*2*). Because serious damage may result from the indiscriminate use of steel slags in confined applications, potential long-term volume changes must be checked before such use. Obviously, steel slags should not be used in portland cement concretes (unless shown otherwise by a detailed evaluation), because expansion will result in rapid destruction of the concrete. However, the expansion can be tolerable when controlled by suitable aging or treatment of aggregates with spent acids, or when the steel slag particles are properly coated with an asphaltic binder (*2,5*).

The expansive nature of steel slags can be traced back to the steel-making process, in which the conversion of pig iron to steel involves the controlled adjustment of various impurities and the addition of small quantities of constituents that give special properties to the steel. Although the steel slag constituents are similar to those of blast furnace slag, the proportions are different (Table 1). The calcium and magnesium oxides are not completely combined in steel slags, and there is general agreement in the literature that the hydration of unslaked lime (free CaO) and magnesium oxide (MgO) in contact with moisture is largely responsible for the expansive nature of most steel slags. The unslaked lime hydrates rapidly and can cause large volume changes in a few weeks. MgO hydrates more slowly and contributes to long-term expansion that may take several years to develop in the field. Because steel-making slags are reduced in size and water is involved during processing, CaO hydration may occur and the aging process may be accelerated, thus decreasing short- or long-term expansion.

Steel slags must be checked for potential expansion, because even aging for long periods in large dumps does not guarantee the elimination of expansive behavior (particularly if the slag is unprocessed and large lumps are involved).

A simple, economical, and rapid test procedure for evaluating the expansion potential of steel slags was reported by Emery (*3,16*). The procedure involved preparing steel slag specimens and a nonexpansive control using the standard proctor test. Stainless steel molds with perforated base plates allowed for moisture movement during an immersion period. The specimens were totally immersed in a water bath at 82°C ± 1°C and the amount of vertical expansion was monitored over time. The 82°C test temperature was selected on the basis of the initial expansion test series at 60°C. Expansion levels of 5 to 9 percent observed at 82°C (about three times that at 60°C) were similar to the levels of long-term expansion

often observed in the field. A short monitoring period of 1 to 7 days appeared adequate to predict potential expansive behavior in the field. Surcharge weights can be used to simulate overburden conditions. Adoption of the laboratory-accelerated expansion tests at 82°C was given support by a series of long-term expansion tests at 20°C ± 1°C. After 475 days at 20°C, expansion was about half of that observed in 7 days at 82°C.

This test series indicated that aging in stockpiles (preferably after processing and in small quantities), spent acid treatments, and the use of coarser sizes all tend to limit the potential expansion of steel slags. These results are in qualitative agreement with field observations. Aging steel slag in large heaps or pieces is not very effective, because steel slag remains expansive for extremely long periods if not directly exposed to weathering (*3,16*).

The discussion in this section has been concerned with the potential expansion of steel slag that has not been coated with asphaltic cement. The use of steel slag in AC generally results in an acceptable product, because the asphaltic cement film coating the steel slag limits potential expansion. However, the question often arises concerning the need for aging steel slag before use in AC. If the finer sizes are used (<13 mm), prior aging is not critical, because the watering and screen processing during travel through the asphalt plant dryer and screens allow for any immediate expansion. However, a minimum aging period of 30 days is still recommended by many authorities, particularly for the coarser (>19 mm) asphalt mixes (*3,16*).

Steel slag may continue to be put mainly to such uses as railway ballast, pavement bases for shoulders, fills, and ice control grits. However, the economics of handling and using a heavy aggregate, the virtual elimination of any expansion-related problems by the asphaltic cement coating, and the potentially excellent performance of steel slag AC mixes make the use of steel slag aggregate more practical.

FIELD CONDITION SURVEY OF STEEL SLAG BITUMINOUS SURFACE LAYERS IN INDIANA

Steel slag and asphalt mixtures were used to provide a 1- to 1.25-in.-thick surface layer for a number of roadways in Indiana between 1979 and 1981. Tables 3 and 4 present the pavement performance history of these layers (discussed later in detail) together with traffic information.

Skid Resistance Measurements

Skid resistance numbers (friction numbers) measured using ASTM E-274 are presented in Table 3. Initial friction numbers, obtained in the year of construction, were exceptionally high (between 50 and 70). In addition, four out of five roadway sections displayed a reduction of only 0 to 3 percent/year. The roadway section on US-231 (Table 3) was the only section to display a large reduction in friction numbers (12 percent/year). This section was overlayed in 1985 (before the beginning of this study), and the cause of the drop in friction number could not be determined (Table 3).

Friction numbers obtained from the roadway sections presented in Table 3 also match those superior values obtained for steel slags used in other states and countries (*5,15*) and could be attributed to the low abrasion and high hardness characteristics of the steel slag (Table 2).

Visual Inspections

Sections of Indiana's SR-55, US-6, and I-80/90, which were constructed using steel slag aggregates in the surface layers, were visually inspected for surface deficiencies during August 1988. Pavement surface deficiencies on the three sections were similar and followed identical patterns (Figure 1).

TABLE 3 SKID RESISTANCE AND LIFE CYCLE INFORMATION OF STEEL SLAG ASPHALT SURFACE LAYERS IN INDIANA

Indiana Highway	Contract Number	Section Length	Construction Date	Overlay Date	Life Cycle	Initial Friction Number	Updated Friction Number
US-231	RS-12551	7.40 mi.	1980	1986	6 years	59.0	23.9 (1985)
SR-55	RS-13065	6.63 mi.	1981	----	_ 7 years	50.4	50.4 (1984)
US-6	RS-11898	11.70 mi.	1979	----	_ 9 years	69.9	55.6 (1986)
US-20	RS-12422	7.70 mi.	1980	1986	6 years	64.4	59.9 (1984)
US-35	RS-12337	5.97	1980	1986	6 years	67.2	59.6 (1984)
US-12	RS-13062	2.80 mi.	1981	1987	6 years	----	----
I-80/90	Toll Road	17.80 mi.	1980	----	_ 8 years	----	----

NOTES: 1. Type of overlay was sand seal.

2. Friction Numbers (Skid Resistance Numbers) are measured using ASTM E-274, Brake Force Trailer.

TABLE 4 FIELD INFORMATION OF STEEL SLAG ASPHALT SURFACE LAYERS IN INDIANA

Indiana Highway	Contract Number	Directional No of Lanes	Directional ADT*	Surface Thickness, Inch	Crack Intensity
US-231	RS-12551	1	3110	1.00	overlaid
SR-55	RS-13065	1	7238	1.00	high
US-6	RS-11898	1	2425	1.00	high
US-20	RS-12422	2	4765	1.25	overlaid
US-35	RS-12337	1	3460	1.25	overlaid
US-12	RS-13062	3	7500	1.00	overlaid
I-80/90	Toll Road	2	7000	1.25	high

*ADT is the average daily traffic in equivalent passenger cars (1983 information).

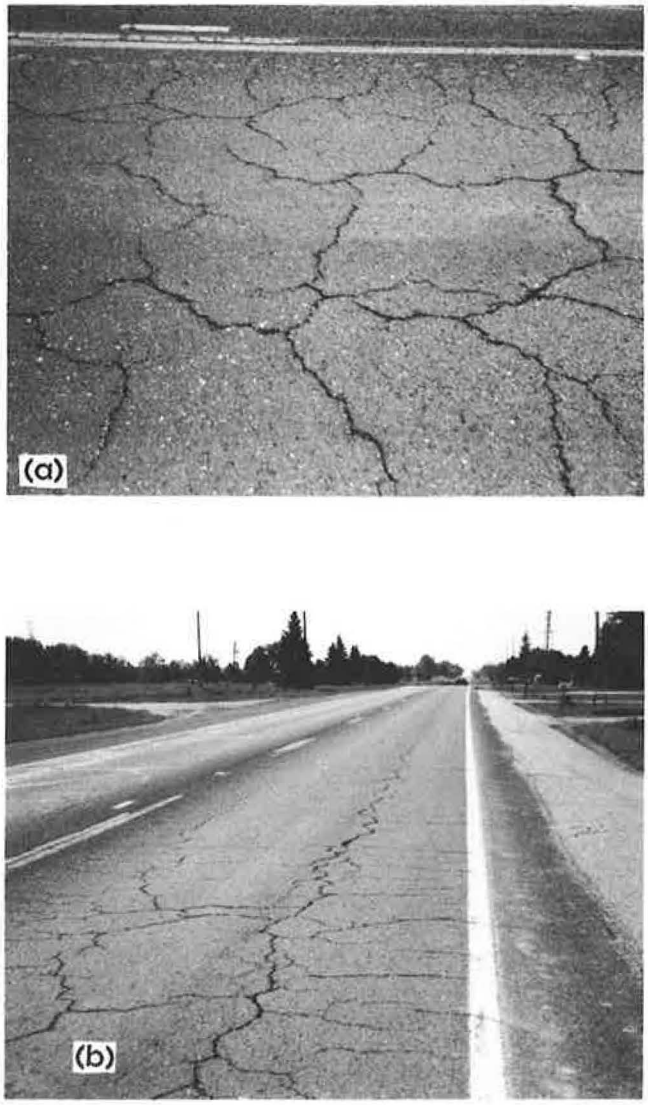

FIGURE 1 Cracking pattern observed on US-6, SR-55, and I-80/90: a, top view; b, longitudinal view.

Interconnected cracks forming a series of large polygons with sharp corners or angles and extending along the entire roadway portion were observed (typical map cracking). No indications of base failure or reduction in resilience of the underlying pavement layers were observed, and only cracks associated with the pavement surface were present. In addition, the pavement surface displayed some white-to-gray discolorations (Figure 2) at or near these cracks (similar to those obtained in the laboratory after successive freezing and thawing). However, absolutely no raveling, rutting, or shoving was observed at any location on those three roadway sections, and the pavement surface appeared to maintain its resilience after 8 years of traffic.

The map cracking could be attributed to age hardening (the pavement was 8 years old), weathering, and shrinkage of the asphaltic surface under climatic conditions. These conditions may have been complicated by the possible insufficiency of asphalt content and pavement thickness for the surface layer. The pavement surface thickness ranged between 1 and 1.25 in. The design asphalt content was 5.5 percent, and some cores displayed an extracted asphalt content of only 4.7 percent.

Another important factor is the possible accelerated hardening of the asphalt binder caused by the ferric and ferrous oxides present in steel slag particles (20 to 26 percent, Table 1). Ferric and ferrous components are typically used as catalysts to accelerate oxidation of asphalt in the production of air-blown asphalts. Air-blown asphalts have higher viscosity and softening point, and lower penetration, ductility, and adhesiveness than regular, straight-run distillation asphalts. Their use in paving mixtures is limited because of their potential for causing cracking.

Pavement Surface Temperature

Surface temperatures were recorded on portions of Indiana US-6, paved with a steel slag asphaltic surface on the westbound side and a natural aggregate (crushed limestone and natural sand) asphaltic surface on the eastbound side. The

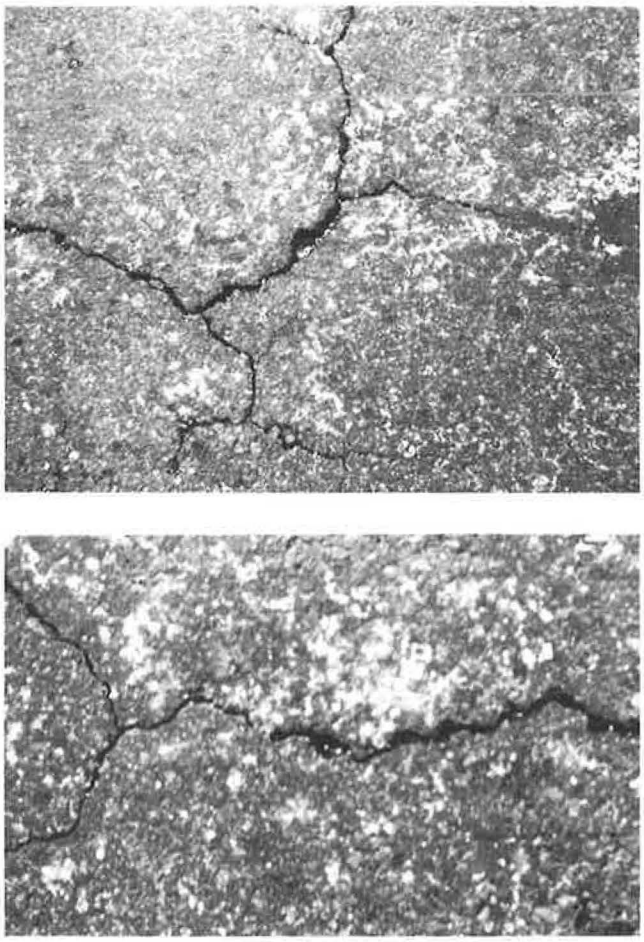

FIGURE 2 Surface discoloration, probably caused by hydration of free lime present in steel slag aggregates.

main objective was to investigate the effect of the large amounts of iron (ferric and ferrous oxide) present in steel slag aggregates and the dark black color of paving surfaces constructed with steel slags on the resulting pavement surface temperature.

An infrared noncontact-type field thermometer was used to measure and record temperature along the cross section of the eastbound side (natural aggregate) and the westbound side (steel slag). A simple statistical analysis of variance (ANOVA) indicated that no significant difference in temperature existed between points within the cross section of the eastbound side. The same result was obtained along the westbound side. Significant differences, however, were obtained between the two sides. The surface constructed using steel slag displayed a surface temperature 5°F to 10°F higher than the other surface. This could be attributed, in part, to the very low specific heat of the ferric and ferrous components in steel slag aggregate, resulting in a greater increase in pavement surface temperature (at the same amount of heat) than other aggregate types.

This factor becomes important when considering the age-hardening rate of asphalt binder, which may be accelerated because of this phenomenon, especially during hot weather. On the other hand, because of the low specific heat of steel slag, the low amount of heat available during winter may be enough to keep pavement surfaces warmer and hence decelerate ice formation during cold weather.

MATERIALS USED AND LABORATORY EVALUATION PROCEDURES

The materials used in the laboratory evaluation were (a) steel slag coarse aggregates (meeting the Indiana specified gradation requirements for No. 11 coarse aggregate), provided by Heckett Slag Products, Harsco Corporation, (b) Hanna natural sand (meeting the Indiana specifications for 23 sand), and (c) ASTM-designated AC–20 (Amoco Oil Company, Inc.). Table 5 presents the gradations of the steel slag coarse aggregate and Hanna sand, and Table 6 presents the characteristics of the AC–20.

Six combinations of coarse and fine aggregate were selected to produce mixtures with a wide range of gradations and proportions of steel slag coarse aggregates:

- Mix 1: 100 percent coarse aggregate (steel slag) and 0.0 percent natural sand (Hanna sand). This mix met the Indiana specifications for No. 11 bituminous-coated aggregate.
- Mix 2: 87 percent steel slag coarse aggregates and 13 percent sand. The amount of sand was the maximum percentage to keep the mix within specification of No. 11 bituminous-coated aggregate.
- Mix 3: 73 percent steel slag coarse aggregate and 27 percent natural sand. This mix contained the minimum amount of sand required to keep the mix within Indiana specifications for No. 11 binder mix.
- Mix 4: 59 percent steel slag coarse aggregate and 41 percent natural sand. This mix contained the largest amount of sand required to keep the mix within Indiana specifications for No. 11 binder mix.
- Mix 5: 47 percent steel slag coarse aggregate and 53 percent natural sand. This mix met the Indiana specification for No. 11 surface mix using the minimum amount of sand.
- Mix 6: 40 percent steel slag coarse aggregate and 60 percent natural sand. This mix met the Indiana specification for No. 11 surface mix using the maximum amount of natural sand.

Table 7 presents the gradations of Mixes 1 through 6, and Table 8 presents the Indiana specifications for No. 11 surface, No. 11 binder, and No. 11 bituminous-coated aggregate.

Marshall mix design procedures were conducted on each of the six mixes using 75 blows per face for specimen compaction. Each specimen's unit weight, percentage of air voids (AV), percentage of voids in aggregate mass (VMA), and percentage of voids in aggregate mass that are filled with bitumen (VFB) were determined in addition to Marshall stability and flow values.

Six specimens were used to represent each asphalt content. Three of those specimens were used for the Marshall mix design procedures. The indirect tensile test (split tension) was conducted at 75°F on the other three specimens to obtain tensile characteristics of Mixes 1 through 6 at different asphalt contents.

The average height of the specimens tested for Marshall stability was measured, and those specimens were exposed to

TABLE 5 GRADATION OF STEEL SLAG COARSE AGGREGATES AND HANNA SAND

Sieve Size	% Passing Steel Slag	Specification Limits*	% Passing Hanna Sand	Specification Limits*
1/2"	100	100	----	----
3/8"	83	75 - 95	100	100
#4	12	10 - 30	98	95 - 100
#8	3	0 - 10	91	80 - 100
#16	2	----	82	50 - 85
#30	2	----	60	25 - 60
#50	2	----	11	5 - 30
#100	2	----	1	0 - 10
#200	1	----	0	0 - 3

*Specification limits are for #11 coarse aggregate and #23 sand, IDOH Standard Specifications (16).

TABLE 6 CHARACTERISTICS OF AC-20

Test	Value
Penetration, 100 gm, 5 sec., 77°F, 0.1 mm	65
Absolute Viscosity, 140°F, Poise	1890
Softening Point, °F	122
Ductility, 77°F, 5 cm/min., Cm	150+

30 successive cycles of freezing and thawing (17 hr of freezing at −10°F and 7 hr of thawing by soaking in a water bath at 75°F). Average heights were remeasured after the freeze-thaw cycling.

LABORATORY TEST RESULTS AND DISCUSSION

Marshall Mix Design Data

Tables 9–14 present the asphalt mix properties for the six designed mixtures. The amounts of natural sand and steel slag coarse aggregate used are given for comparison purposes.

Asphalt Content

Mixes 3 through 6 displayed maximum density and stability at asphalt contents of 5.0 percent, 5.5 percent, 6.5 percent, and 7.5 percent, respectively. The increase in the amount of natural sand (27 percent for Mix 3, 41 percent for Mix 4, 53 percent for Mix 5, and 60 percent for Mix 6) increased the surface area of the mix and consequently increased the amount of asphalt required for proper coating. However, this was not true for Mixes 2 and 1, consisting of 13 and 0.0 percent natural sand, respectively. Mixes 2 and 1 displayed maximum density and stability at asphalt contents of 5.5 and 6.0 percent, respectively, although they contained less than Mix 3. The use of high percentages of rough-surfaced steel slag apparently increased the asphalt requirement.

Asphalt mixes containing 100 percent steel slag coarse aggregate may require relatively high asphalt contents to peak

TABLE 7 GRADATION OF MIXES 1 THROUGH 6

Sieve Size	Percent Passing					
	Mix 1[a]	Mix 2[a]	Mix 3[b]	Mix 4[b]	Mix 5[c]	Mix 6[c]
½-in.	100	100	100	100	100	100
⅜-in.	83	85	88	90	92	93
#4	12	23	35	47	58	64
#8	3	14	27	39	50	56
#16	2	12	24	35	44	50
#30	2	10	18	26	33	37
#50	2	3	4	6	7	7
#100	2	2	2	2	1	1
#200	1	1	1	1	0	0

[a]#11 bituminous coated aggregate.
[b]#11 binder.
[c]#11 surface.

TABLE 8 INDOT SPECIFICATIONS FOR #11 SURFACE, #11 BINDER, AND #11 BITUMINOUS-COATED AGGREGATES

Sieve Size	#11 Bit. Coated Aggregate	#11 Binder	#11 Surface
1/2"	100	100	100
3/8"	75 - 100	78 - 98	85 - 98
#4	10 - 35	35 - 50	57 - 67
#8	0 - 15	20 - 45	31 - 62
#16	-----	11 - 36	17 - 50
#30	-----	6 - 26	8 - 37
#50	-----	2 - 18	3 - 25
#100	-----	0 - 11	0 - 14
#200	0 - 6	0 - 3	0 - 3

TABLE 9 CHARACTERISTICS OF MIX 1—100 PERCENT STEEL SLAG COARSE AGGREGATE, 0 PERCENT NATURAL SAND

	AC (%)				
	4.5	5.0	5.5	6.0	6.5
Unit Weight, PCF	150.5	151.1	151.5	152.0	151.8
% Air Voids	21.6	20.5	19.41	18.3	17.5
% VMA	34.0	33.3	32.7	31.9	32.0
% VFB	36.5	38.4	40.7	42.6	45.3
Max.th.Density, PCF	192.0	190.0	188.0	186.0	184.0
Marshall Stability, Lbs.	1400	1550	1600	2100	1750
Flow, 1/100 inch	8.0	8.0	9.0	10	10
S_T, Psi	112	124	126	133	126
e_T	0.004	0.005	0.006	0.007	0.008
E, 10^4 psi	7.0	7.0	7.0	8.0	8.0
Freeze-Thaw Cycling Effect	6.7	5.5	5.0	0.1	0.0

NOTE: 1. Effect of successive freezing and thawing cycles was measured by the percent increase in average specimen height before and after exposure to 30 cycles.

2. S_T, e_T and E are tensile strength, strain and stiffness modulus respectively.

TABLE 10 CHARACTERISTICS OF MIX 2—87 PERCENT STEEL SLAG COARSE AGGREGATE, 13 PERCENT NATURAL SAND

	AC (%)			
	4.5	5.0	5.5	6.0
Unit Weight, PCF	156.2	156.5	157.0	156.9
% Air Voids	16.5	15.5	14.4	13.6
% VMA	29.5	29.2	28.3	29.0
% VFB	44.1	46.9	49.1	53.1
Max.th.Density, PCF	187.1	185.2	183.4	181.6
Marshall Stability, Lbs.	1800	2500	2600	2200
Flow, 1/100 inch	10	11	12	15
S_T, Psi	121	144	146	137
e_T	0.006	0.006	0.007	0.008
E, 10^4 psi	7.0	8.0	10.0	8.0
Freeze-Thaw Cycling Effect	5.5	4.0	2.6	0.1

TABLE 11 CHARACTERISTICS OF MIX 3—73 PERCENT SLAG STEEL COARSE AGGREGATE, 27 PERCENT NATURAL SAND

	AC (%)			
	4.5	5.0	5.5	6.0
Unit Weight, PCF	159.5	162.0	158.4	157.8
% Air Voids	10.0	9.2	8.9	8.5
% VMA	23.4	23.0	22.9	23.3
% VFB	57.3	60.0	61.1	63.7
Max.th.Density, PCF	177.2	175.6	173.9	172.4
Marshall Stability, Lbs.	2000	2850	2650	2250
Flow, 1/100 inch	9.0	9.0	10.0	11.0
S_T, Psi	148	160	158	156
e_T	0.007	0.007	0.007	0.008
E, 10^4 psi	8.0	11.0	10.0	9.0
Freeze-Thaw Cycling Effect	5.4	3.6	0.9	0.1

TABLE 12 CHARACTERISTICS OF MIX 4—59 PERCENT STEEL SLAG COARSE AGGREGATE, 41 PERCENT NATURAL SAND

	AC (%)			
	4.5	5.0	5.5	6.0
Unit Weight, PCF	152.2	152.3	154.0	153.6
% Air Voids	11.6	10.7	9.1	8.4
% VMA	23.6	23.2	22.8	22.9
% VFB	50.8	53.9	60.1	63.4
Max.th.Density, PCF	172.2	170.6	169.2	167.7
Marshall Stability, Lbs.	1400	1800	2100	1900
Flow, 1/100 inch	6.0	6.0	8.0	8.0
S_T, Psi	148	156	158	156
e_T	0.007	0.007	0.007	0.007
E, 10^4 psi	8.0	9.0	10.0	10.0
Freeze-Thaw Cycling Effect	4.2	3.6	0.8	0.0

TABLE 13 CHARACTERISTICS OF MIX 5—47 PERCENT STEEL SLAG COARSE AGGREGATE, 53 PERCENT NATURAL SAND

	AC (%)			
	5.5	6.0	6.5	7.0
Unit Weight, PCF	145.0	145.7	148.0	147.7
% Air Voids	11.7	10.6	8.5	7.9
% VMA	24.4	24.3	24.0	24.1
% VFB	52.0	56.5	64.6	67.4
Max.th.Density, PCF	164.2	162.9	161.7	160.4
Marshall Stability, Lbs.	1350	1450	1500	1400
Flow, 1/100 inch	6.0	6.0	8.0	8.0
S_T, Psi	140	147	155	140
e_T	0.006	0.007	0.007	0.008
E, 10^4 psi	6.0	6.0	8.0	7.0
Freeze-Thaw Cycling Effect	0.5	0.1	0.0	0.0

TABLE 14 CHARACTERISTICS OF MIX 6—40 PERCENT STEEL SLAG COARSE AGGREGATE, 60 PERCENT NATURAL SAND

	AC (%)				
	6.0	6.5	7.0	7.5	8.0
Unit Weight, PCF	145.0	145.4	145.6	146.0	145.4
% Air Voids	8.8	8.0	7.2	6.3	6.0
% VMA	22.2	22.0	21.8	21.8	21.9
% VFB	60.4	63.6	67.0	71.1	72.6
Max.th.Density, PCF	159.0	158.0	156.9	155.8	154.7
Marshall Stability, Lbs.	1200	1200	1200	1250	1200
Flow, 1/100 inch	7.0	7.0	7.0	8.0	8.0
S_T, Psi	140	144	146	150	147
e_T	0.007	0.008	0.008	0.008	0.009
E, 10^4 psi	6.0	6.0	6.0	7.0	6.0
Freeze-Thaw Cycling Effect	0.1	0.0	0.0	0.0	0.0

in density and stability. The addition of natural sand (to a certain extent) may reduce the required amount of asphalt for maximum density and stability, as shown in Figure 3.

Unit Weight

Natural sand was used with steel slag coarse aggregate to produce asphalt mixtures with unit weights lower than those obtained when using steel slag sand. Use of steel slag sand can also result in high shipping costs. The steel slag surface mixture (containing steel slag coarse and fine aggregates) used on US-6 displayed a unit weight of 186 lb/ft^3, which is at least 30 percent higher than any other No. 11 surface mixes produced using natural aggregates. Mixes 1 through 6 (Tables 9–14) displayed unit weights of 145 to 162 lb/ft^3, only 5 to 15 percent higher than No. 11 surface mixtures produced without steel slag aggregates. The use of more open graded mixes when using smaller amounts of natural sand is another alternative to avoid the high-density disadvantage of steel slag.

Marshall Stability

Although the high specific gravity of steel slag aggregates is a disadvantage when considering shipping cost, it helps create the superior stability that may be expected from steel slag asphaltic mixtures. Marshall stabilities of 3,500 to 4,000 lb have been frequently reported for steel slag mixtures containing both coarse and fine steel slag aggregates (*3*,*5*,*7*).

Natural sand use in asphaltic surface mixtures is generally limited and is banned by some state highway departments. Natural sand combined with dolomite (coarse aggregate) produced asphalt mixes (with different gradations and asphalt contents) with Marshall stabilities of no more than 1,250 lb at optimum asphalt content. Minimum acceptable Marshall stability, by Indiana Department of Transportation specification, is 1,200 lb.

Tables 9–14 present Marshall stability values for Mixes 1 through 6. A stability of at least 1,200 lb was obtained for all mixes at any asphalt content. The use of natural sand (known to produce tender mixes) not only compensated for the high specific gravity of the steel slag coarse aggregate but maintained good stability in combination with steel slag. Mix 3 displayed the largest stability (2,850 lb) and density at an asphalt content of 5 percent (Figures 4 and 5).

Aggregate Gradation Curves

Figure 6 shows the aggregate gradation curves for Mixes 1 through 6, together with the curve for maximum density. Higher Marshall stability values were obtained (at optimum asphalt content) as the mix gradation got closer to the Fuller's maximum density curve, for Mixes 1, 2, and 3. However, lower stability values were obtained for Mixes 4, 5, and 6, which crossed the maximum density curve; these mixes may have been too densely graded. Mixes 4, 5, and 6 had more material passing No. 16 and No. 30 sieves (i.e., they may also have been over sanded).

The gradation curve for Mix 3 suggests that this mix may have had more materials passing the No. 8, No. 16, and No. 30 sieves than were needed, as indicated by the hump in the gradation curve in that region. The same observation can be made for Mix 2, but this mix may have had insufficient amounts of material passing the No. 50, No. 100, and No. 200 sieves.

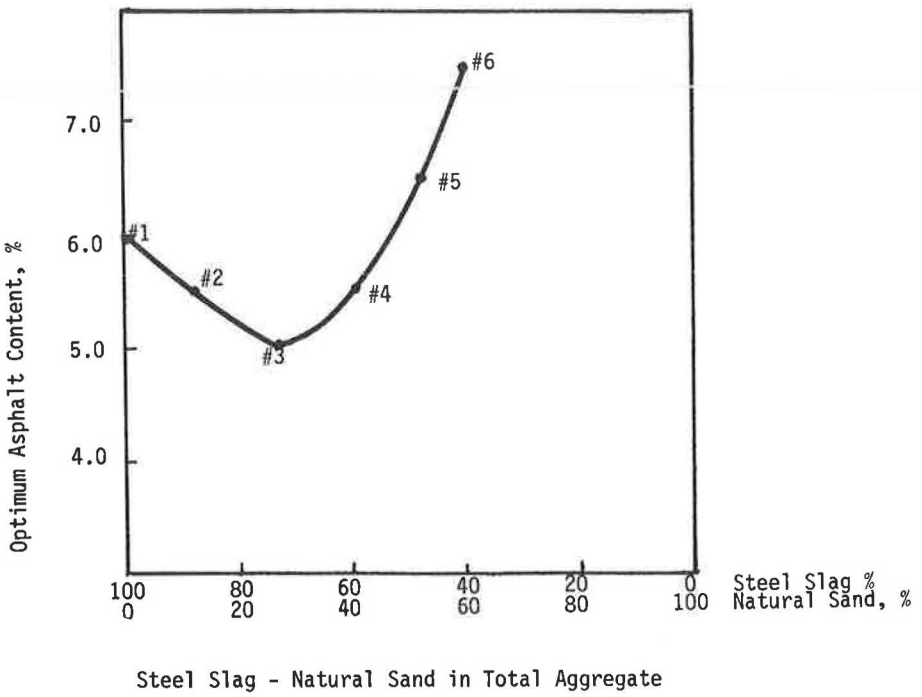

FIGURE 3 Asphalt content requirements for maximum density and stability for six mixes.

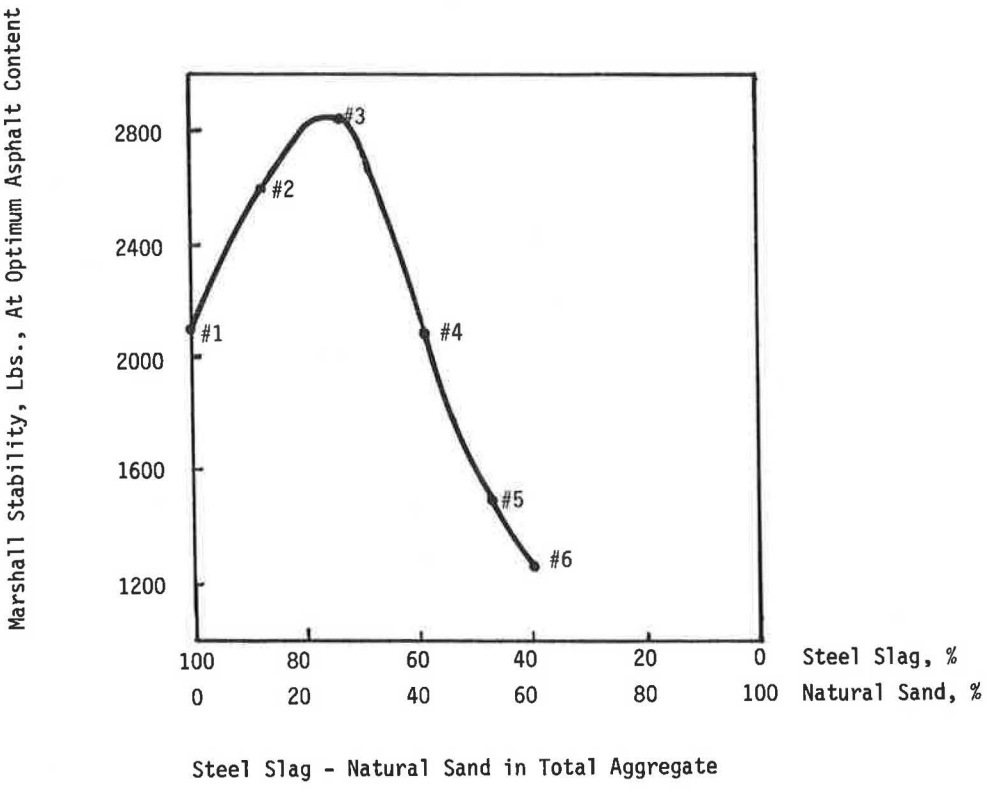

FIGURE 4 Marshall stability at optimum asphalt content for six mixes.

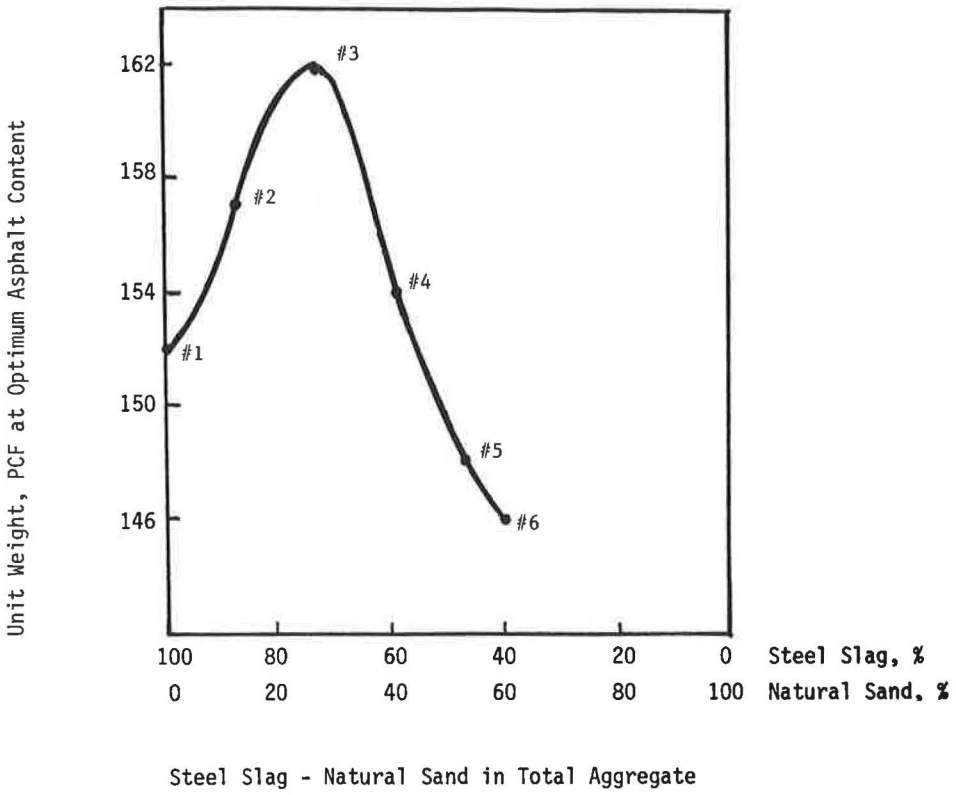

FIGURE 5 Unit weight at optimum asphalt content for six mixes.

Indirect Tensile Characteristics

The indirect tensile test was conducted at 75°F. The following indirect tensile test parameters were used to characterize steel slag asphalt mixtures in the compacted state (*17–23*):

$$S_T = 0.1556\frac{P_{max}}{H} \quad (1)$$

where

S_T = tensile strength (psi),
H = specimen height (in.), and
P_{max} = load at failure (lb).

$$e_T = KX_v \quad (2)$$

where

e_T = total tensile horizontal strain at failure,
X_v = recorded vertical deformation at failure (in.), and
K = 0.09 at test temperature of 75°F.

$$E = \frac{3.56\,S}{H} \quad (3)$$

where

E = stiffness modulus (psi),
S = slope of initial tangent of the load-deformation plot (lb/in.), see Figure 7, and
H = specimen height (in.).

Paving mixtures with low tensile strength values have a tendency to develop low-temperature cracking problems in the field, especially when used for surface mixtures. An indirect tensile strength of 150 psi at 75°F is usually considered an average value for asphaltic surface mixtures (*23*). Values of more than 150 psi generally reflect good crack resistance, whereas values of less than 150 psi may be considered low. Paving mixtures with low tensile strain values also tend to be less resistant to cracking, whereas those with high strain values may tend to develop rutting distress. A strain value of 0.008 at 75°F can be considered an average value for asphalt surface mixtures.

The stiffness modulus E measured using the indirect tensile test generally averages 60,000 psi for asphalt surface mixtures. Conceptually, pavement thickness for paving surface mixtures can be reduced when using mixes with a large stiffness modulus or increased when using mixes with a small stiffness modulus.

Tables 9–14 present indirect tensile characteristics for Mixes 1 through 6. Indirect tensile strength values peaked with the same asphalt contents that provided maximum density and stability (Figure 8). They followed almost the same trend as the Marshall stability values, displaying a peak strength at a natural sand content of 27 percent (Mix 3). Except for Mixes 3, 4, and 5, all other mixtures indicated average or below-average tensile strengths for a bituminous surface mix (with 150 psi generally considered average). In addition, the tensile strength values of Mixes 3, 4, and 5 did not exceed the previously specified average value by a significant margin.

Failure tensile strains for all six mixtures (Tables 9–14) displayed average or below-average values for a surface mix-

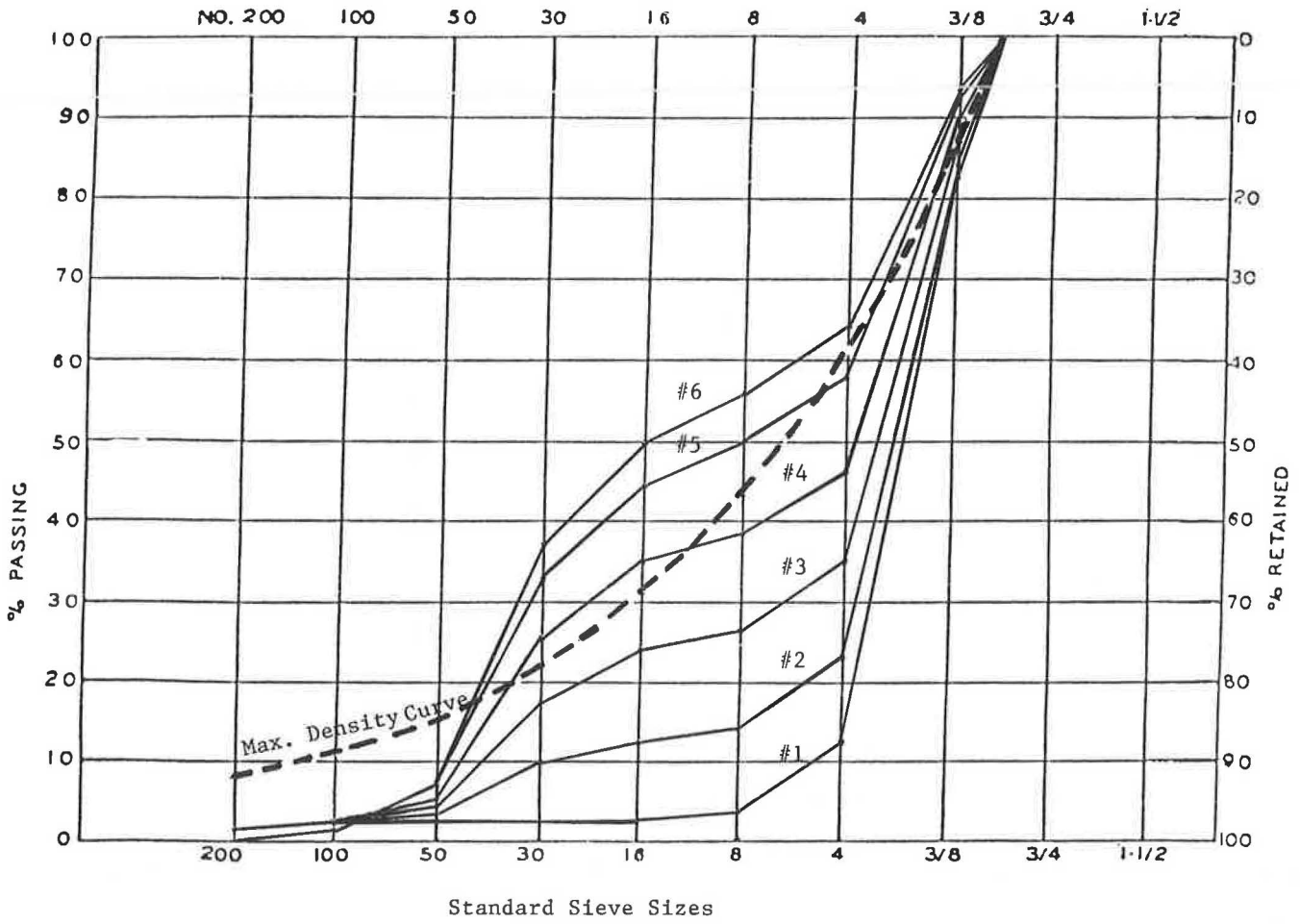

FIGURE 6 Aggregate gradation curves for six mixes.

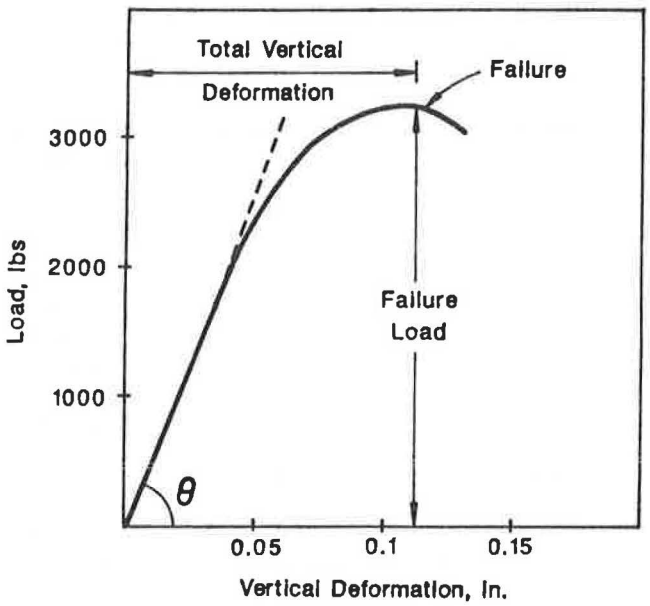

FIGURE 7 Typical load versus vertical deformation trace during indirect tensile test.

ture (with 0.008 generally considered average). Low tensile strength and failure tensile strain could be attributed to the lack of dust (materials passing No. 200 sieve) in the six mixtures and the resulting lack of total binder (asphalt plus filler) content.

Stiffness modulus values (Tables 9–14) for the six mixtures, unlike tensile strength and strain characteristics, were up to 80 percent higher than a typical average value obtained from natural-aggregate AC surface mixes (60,000 psi). The largest values were obtained at the asphalt contents corresponding to maximum density and stability. Mix 3 displayed the largest modulus value followed by Mixes 4, 2, 1, 5, and 6 (Figure 9). Elastic analysis techniques for pavement thickness design indicate the use of an at least 15-percent thinner asphalt surface layer containing steel slag and natural sand. This thinner layer could play an important role in compensating for the high-density disadvantage of steel slag asphalt mixtures.

Freezing and Thawing Effect

All specimens tested for Marshall stability were exposed to 30 successive cycles of freezing and thawing (17 hr of freezing

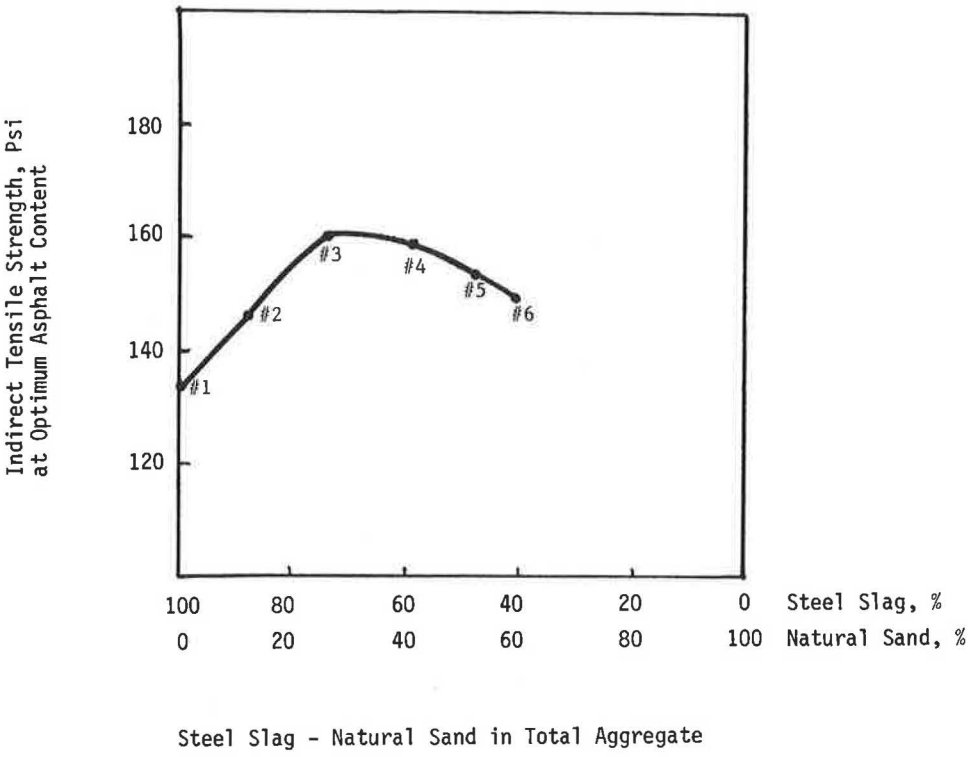

FIGURE 8 Indirect tensile strength at optimum asphalt content for six mixes.

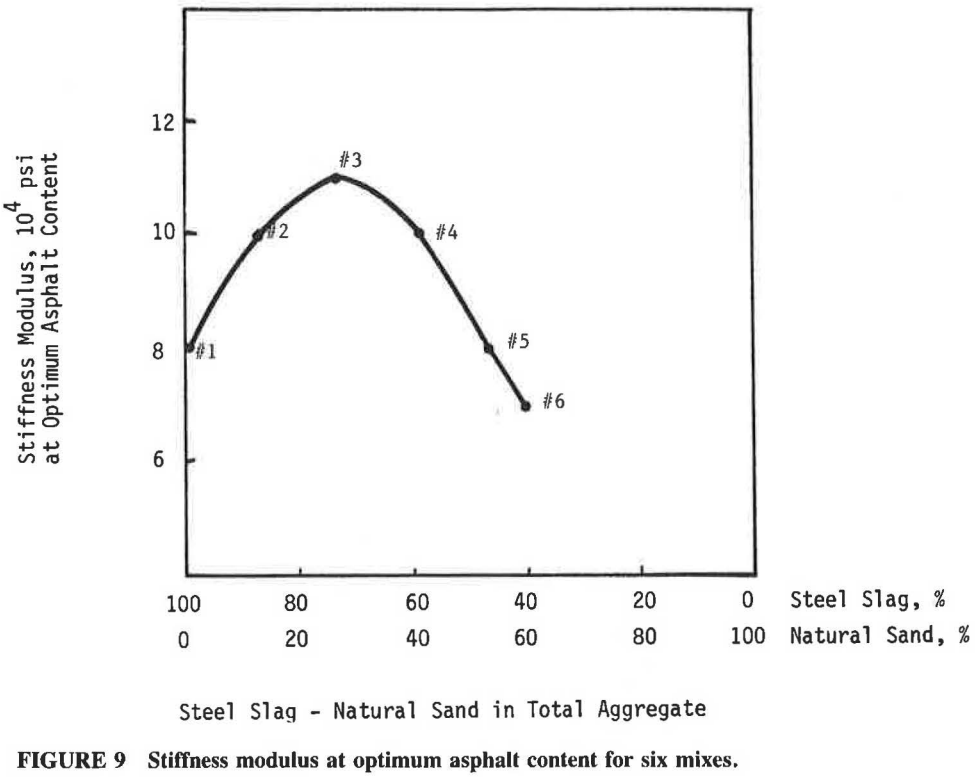

FIGURE 9 Stiffness modulus at optimum asphalt content for six mixes.

at −10°F and 7 hr of thawing by soaking in a water bath at 75°F). Average specimen height was measured for each specimen before and after exposure to freeze-thaw cycling.

Tables 9–14 also present the percentage of change in specimen height caused by freezing and thawing at different asphalt contents for the six steel slag and natural sand mixtures. Values given are the average of three replications. Statistical analysis of variance (ANOVA) for the complete data indicated a significant percentage increase in specimen height after freezing and thawing (up to 6.7 percent increase).

Larger increases were found to be associated with specimens displaying lower asphalt contents formed by using larger percentages of steel slag. In addition, randomly positioned, white-to-gray, powderlike veins were observed on the surface of specimens exposed to freezing and thawing. These veins were probably caused by the hydration of free lime in steel slag aggregates. Veins were also observed in the field at or near surface cracking in the steel slag paving surface mixes.

SUMMARY OF RESULTS

Analysis and evaluation of the laboratory test data combined with the literature search and field investigation provided insight into the characteristics of steel slag and asphalt surface mixtures containing steel slag and natural sand. The test results, however, may be limited to the materials used and test conditions applied in this study.

The main findings can be summarized as follows:

1. The use of steel slag aggregate in asphalt surface mixtures provides pavement surfaces with good skid resistance.
2. Asphaltic paving mixtures using steel slag aggregates display exceptionally high stability, which may prove to be rut resistant when used in pavement surface layers.
3. The potential expansive characteristics of steel slag aggregate may be controlled by using a relatively large asphalt content to provide a thick coating of asphalt around the steel slag particles, thus reducing or possibly preventing direct exposure to moisture. Another alternative is to replace steel slag sand with natural sand. The stability reduction caused by the addition of more asphalt, more natural sand, or both, is tolerable.
4. The use of natural sand with steel slag coarse aggregate not only compensates for the high specific gravity and expansive potential of steel slag aggregate but also maintains good stability for the mixture.
5. The presence of ferrous and ferric oxides in steel slag aggregates may accelerate the hardening of the asphalt binder in the paving mixture and hence aggravate low-temperature cracking of the pavement surface. The use of softer asphalts (AC–10 or Indiana designated asphalt emulsion AE–90, instead of AC–20 and AE–60) is a possible alternative to counteract the accelerated hardening rate.
6. The high unit weight of steel slag mixtures can be significantly reduced by using more open pavement surface mixtures and by replacing steel slag fine aggregate with natural sand.
7. Asphalt paving mixtures produced in this study from steel slag and natural sand displayed average or below-average tensile strengths and failure strain.
8. Asphalt paving mixtures produced in this study from steel slag and natural sand displayed exceptionally large stiffness modulus values. A large stiffness value is an indicator of the possibility of using a reduced pavement thickness.
9. The effect of successive freezing and thawing on laboratory-compacted mixtures of steel slag and natural sand was generally marginal.
10. As a net result, the replacement of steel slag sand by natural sand, designing the asphalt mix slightly opened, using a slightly larger asphalt content than the optimum value, using softer grades of asphalts, and probably using reduced-design thickness may be recommended for steel slag asphalt surface mixtures to compensate for their large unit weight, expansive nature, tendency to accelerate the hardening of the asphalt binder, and relatively large cost. Performance of paving mixtures using these recommendations should be verified under actual field conditions.

ACKNOWLEDGMENTS

This research was carried out at the Indiana Department of Transportation, Division of Research. The authors are grateful to Harold Pettigrew for his efforts in running the necessary laboratory tests and Keith J. Kercher and Joseph J. Sudol for their technical guidance during the course of the study.

REFERENCES

1. *Standard Specifications*. Indiana Department of Highways, West Lafayette, 1988.
2. *Slag; The All-Purpose Construction Aggregate*. National Slag Association, 1986.
3. J. J. Emery. Slag Utilization in Pavement Construction. In *Extending Aggregate Resources*, Report STP 774. ASTM, Philadelphia, Pa., 1982, pp. 95–118.
4. A. R. Lee. *Blast Furnace and Steel Slag: Production, Properties and Uses*. Halsted Press, New York, 1975.
5. J. Ryell, J. Corkhill, and G. Musgrove. Skid Resistance of Bituminous-Pavement Test Sections: Toronto By-Pass Project. In *Transportation Research Record 712*, TRB, National Research Council, Washington, D.C., 1979.
6. D. A. Anderson and J. J. Henry. Synthetic Aggregates for Skid-Resistant Surface Courses. In *Transportation Research Record 712*, TRB, National Research Council, Washington, D.C., 1979.
7. J. T. Corkhill. Construction of 17 Test Sections of Special Bituminous Mixes. *Proc., Canadian Technical Asphalt Association*, 1975.
8. S. H. Dahir. *Alternatives for Optimization of Aggregate and Pavement Properties Related to Friction and Wear Resistance*. Pennsylvania Transportation Institute, FHWA, U.S. Department of Transportation, 1978.
9. B. S. Heaton. Steel Furnace Slag As an Aggregate in Asphaltic Concrete. In *Utilization of Steel Plant Slags Symposium*, Transportation and Road Research Laboratory, Woolongong, Australia, 1979.
10. A. Panis. Steel-Plant Slag Cinders. Presented at the International Symposium on Slags, Cinders and By-Products, Mons, Belgium, 1975.
11. J. J. Emery. Waste and By-Product Utilization in Highway Construction. *Resource Recovery and Conservation*, Vol. 1, Elsevier Scientific Publishing Company, Canada, 1975, pp. 24–43.
12. Uses of Low-Cost Construction Materials Outlined. *Chemical and Engineering News*, Vol. 54, No. 48, Nov. 1976.
13. J. E. Shoenberger. *Cost-Effective Surfacing for Tracked Vehicle Traffic*. Report GL-87-18. Waterways Experiment Station, Geotechnical Laboratory, 1987.

14. J. J. Emery, M. A. Lee, and N. Kamel. *Skid Resistance Predictive Models for Asphaltic Concrete Surface Courses*. Report STP 763, ASTM, Philadelphia, Pa., 1982, pp. 61–72.
15. *An Investigation of Skid Resistant Asphaltic Mix Designs*. Report FHWA-RD-MO-79-74-4. Missouri State Highway Department, FHWA, U.S. Department of Transportation, 1978.
16. J. J. Emery, R. G. Drysdale, and P. S. Nicholson. Steel Slag Asphalt Mixes. *Proc., Canadian Technical Asphalt Association*, 1973.
17. F. L. L. B. Carniero and A. Barcellus. *Union of Testing and Research Laboratory for Materials and Structures*. No. 13, 1953.
18. G. W. Maupin. Results of Indirect Tensile Tests Related to Asphalt Fatigue. In *Highway Research Record 404*, HRB, National Research Council, Washington, D.C., 1972, pp. 1–7.
19. M. S. Mamlouk. *Characterization of Cold Mixed Asphalt Emulsion Treated Bases*. Report JHRP-79-19. Purdue University, West Lafayette, Ind., 1979.
20. T. W. Kennedy. Characterization of Asphalt Pavement Materials Using the Indirect Tensile Test. *Proc., Association of Asphalt Paving Technologists*, Vol. 46, St. Paul, Minn., 1977.
21. G. W. Maupin. The Use of Antistripping Additive in Virginia. *Proc., Association of Asphalt Paving Technologists*, Vol. 51, 1982, p. 343.
22. W. O. Handley et al. *A Method of Estimating Tensile Properties of Materials Tested in Indirect Tension*. Research Report 98-7. Center for Highway Research, The University of Texas at Austin, 1970.
23. A. S. Noureldin. *Material Characterization of Hot-Mix Recycled Bituminous Pavements*. Ph.D. dissertation. Purdue University, West Lafayette, Ind., 1987.

Publication of this paper sponsored by Committee on Characteristics of Bituminous Paving Mixtures To Meet Structural Requirements.

Monitoring Asphalt Concrete Performance at High Altitudes in the Peruvian Andes

JACOB GREENSTEIN, Y. HERRERA, AND ALBERTO GARCIA

Thermal cracking in Peru usually occurs in roads with elevations higher than 3,700 meters above sea level (MASL). Asphalt pavements at elevations between 3,700 and 4,300 MASL usually develop thermal cracking, but this type of distress is more severe at even higher altitudes, especially with the combined effects of the large amount of solar radiation, daily temperature cycle, and relatively large amounts of precipitation. The asphalt concrete (AC) thickness of 8 to 12 cm in the La Oroya-Cerro de Pasco Road was designed to carry traffic of approximately 1,000 trucks per day. When the asphalt mixture was designed and constructed according to standard practice and specifications, severe longitudinal cracking appeared 5 to 8 months after completion of construction. In order to reduce this thermal cracking, the following material characteristics and construction procedures were analyzed: (a) engineering properties of the top crude and the asphalt cement; (b) engineering properties of aggregates, particularly those used for fines and filler materials; (c) optimum heating temperature of the asphalt aggregates before mixing; (d) minimum air temperature at which AC can be laid and compacted; (e) measures taken to protect the prime coat and base course; (f) types of asphalt cements used and their respective engineering properties; (g) tensile strength and workability characteristics of the AC mixture; and (h) types and quantities of additives. Preliminary conclusions of specification modification have been adopted by the Peruvian road authorities to improve asphalt performance at high altitudes.

Thermal cracking is the major cause of distress in asphalt concrete (AC) in the higher altitudes of the Peruvian Andes. The main factor causing such cracking is the daily extreme temperature variation that results in repeated tensile stresses and strains, causing rapid thermal fatigue. The Andes cross Peru in a north-south direction at elevations between 2,000 and 5,000 meters above sea level (MASL).

Daily variation in air temperature at altitudes of over 3,700 MASL is between −5°C and +30°C and is accompanied by strong solar radiation. The 120-km asphalt road that connects La Oroya and Cerro de Pasco is located at elevations between 4,100 and 4,350 MASL. Typical hourly and daily air temperature changes at 4,100 MASL are shown in Figures 1 and 2. Figure 1 shows the hourly temperature changes recorded from April 26 to 28, 1982, and indicates that the daily air temperature is above the freezing point for only about 8 to 10 hr, resulting in alternate freezing and thawing.

The AC in the La Oroya-Cerro de Pasco Road was 8 to 12 cm thick. The 12 cm of AC was designed to carry traffic of approximately 1,000 (mostly overloaded) trucks per day. Although the pavement structure and material properties for the road conformed to AASHTO and ASTM standard design procedures and specifications (*1–3*), severe cracking appeared 5 to 8 months after construction. This cracking usually occurs in the form of longitudinal cracks, combined with some transverse cracking. Longitudinal cracks usually appeared after 5 to 6 months, and usually in the lane or road center as shown in Figure 3. This thermal cracking was not associated with traffic stresses. After 3 to 5 months, transverse cracking appeared on the road surface, as shown in Figure 4. Two years after construction, the road surface was severely cracked, as shown in Figure 5. With no modification of the specifications or construction procedures, pavement that was designed for 15 to 20 years was completely cracked after approximately 3 years, as shown in Figure 6. In order to reduce this thermal cracking, the following material characteristics and construction procedures were analyzed:

- Engineering properties of the top crude and asphalt cement;
- Engineering properties of aggregates, particularly those used for fines and filler;
- Optimum heating temperature of the asphalt aggregates before mixing;
- Minimum air temperature at which AC can be laid and compacted;
- Measures taken to protect the prime coat and base course;
- Types of asphalt cements used and their respective engineering properties;
- Tensile strength and workability characteristic of the AC mixture; and
- Types and quantities of additives.

ENGINEERING PROPERTIES OF TOP CRUDE OIL AND ASPHALT CEMENT

The original design of the AC specifies the use of an 85 to 100 penetration (in 0.1 mm) of asphalt cement. The asphalt cement actually used in the road has a penetration of 90, 2.5 percent of wax, and fulfills the specification requirements of AASHTO M20–70. The AC produced with this cement developed 3- to 4-mm widths of longitudinal and 1- to 2-mm widths of transverse cracking 5 to 8 months after the completion of construction. In order to better understand and identify the reasons for such cracking, the chemical properties of the crude oil were analyzed.

The asphalt cement in Peru is produced by the government's national petroleum company, Petro Peru. A mix of crude oil produced by Petro Peru comes mainly from the Peruvian Amazonian region and is used to produce the asphalt cement. The crude obtained from the primary distillation used for

Louis Berger Inc., 100 Halsted St., East Orange, N.J. 07019.

the asphalt production for high altitudes has the properties presented in Table 1.

The American Petroleum Institute (API) crude density value of 18.7° presented in Table 1 indicates that the crude is chemically classified as Naftanic (*4*). Because the crude API is less than 35°, it is adequate for production of asphalt cement for normal environmental conditions (*5,6*). Petro Peru also produces crude oil with an API density of over 35° (*7*) that was not used to produce asphalt cement for high altitudes.

The Watson characterization factor K_W (*4,5*) is used to analyze the adequacy of the topped crude to produce the appropriate asphalt cement.

$$K_W = \frac{T_B^{1/3}}{G} \tag{1}$$

where

K_W = Watson characterization factor,
T_B = crude fermenting temperature in °R, and
G = crude specific gravity at 60°F.

Tests by Petro Peru show that T_B = 1,304°R and G = 0.9421 (Table 1); therefore, according to Equation 1, K_W = 11.6, which is less than 11.8, the permissible upper limit (*5,6*). Therefore, the two Peruvian topped crude quality indicators, API < 35° and K_W < 11.8, indicate that this crude is adequate for asphalt cement production (*5,6*). This conclusion was verified in Peru only for asphalt pavement constructed below 3,700 MASL. The asphalt thermal cracking is far less severe at altitudes below 3,700 MASL. Because of the extensive thermal cracking at altitudes higher than 4,100 MASL with this asphalt cement, the Peruvian Road Authority decided to

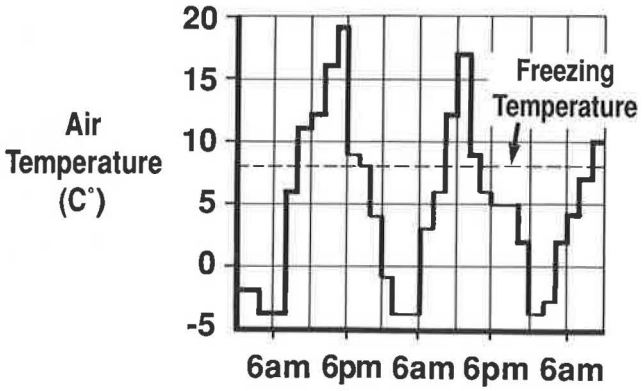

FIGURE 1 Changes of hourly air temperature, Oroya-Cerro de Pasco Road at 4,100 MASL, April 26–28, 1982.

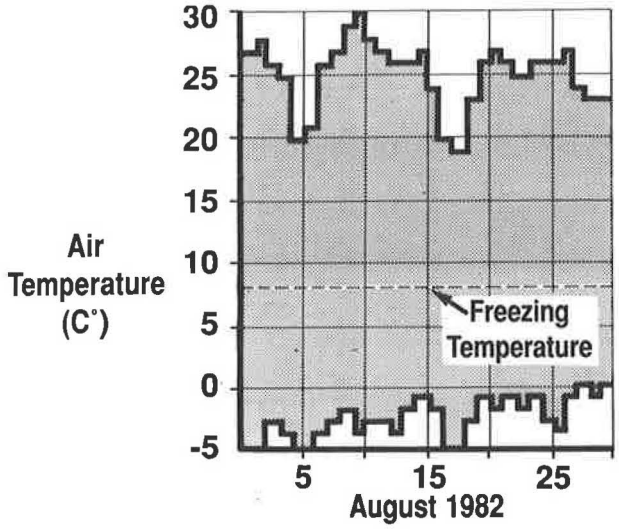

FIGURE 2 Typical changes of daily air temperature, Oroya-Cerro de Pasco Road at 4,100 MASL.

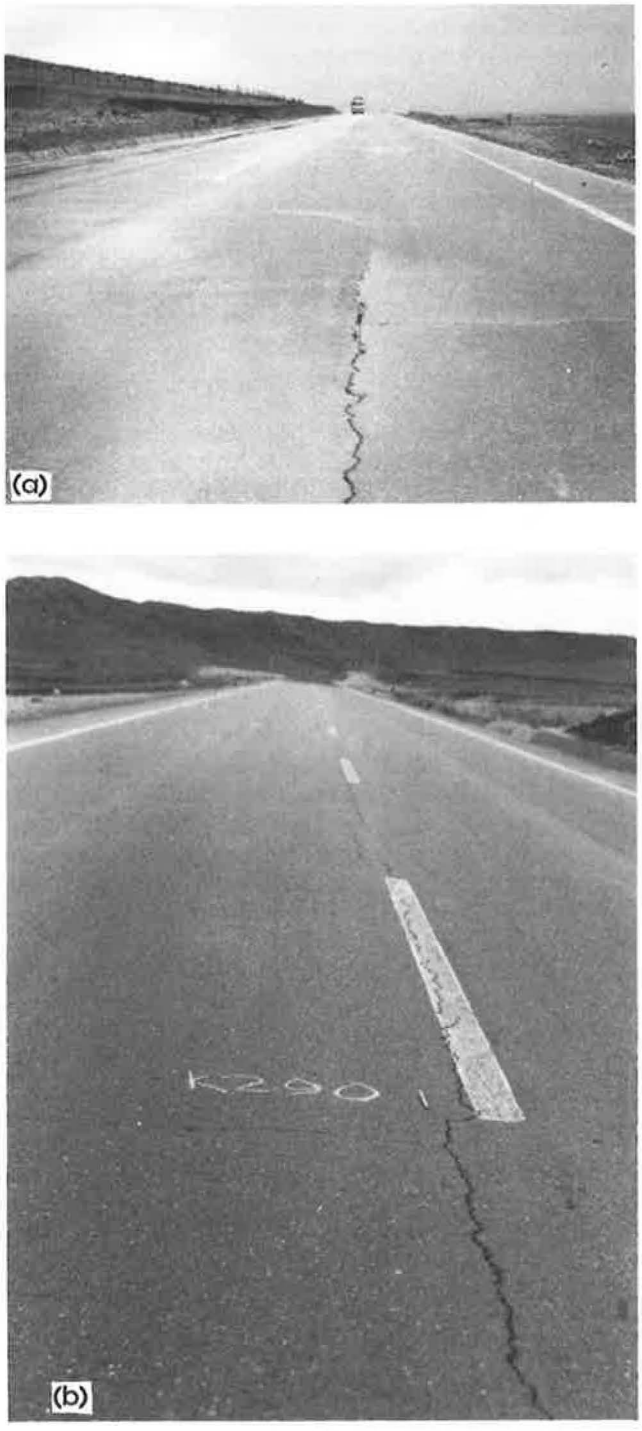

FIGURE 3 a, Typical longitudinal cracking; b, typical longitudinal joint cracking.

FIGURE 4 Typical transverse cracking.

FIGURE 5 Typical pavement cracking, 2 years after completion of construction.

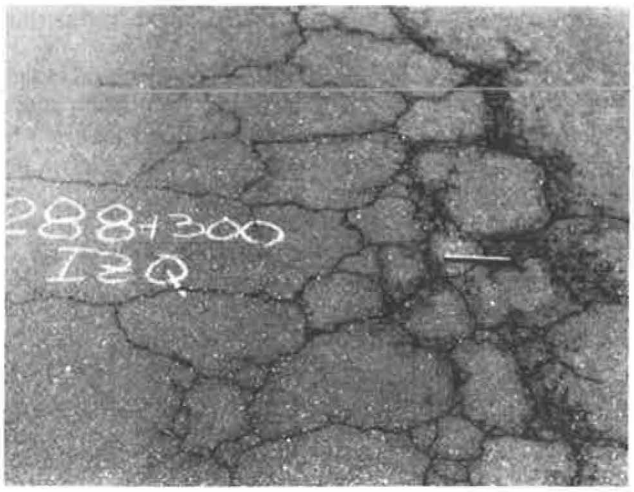

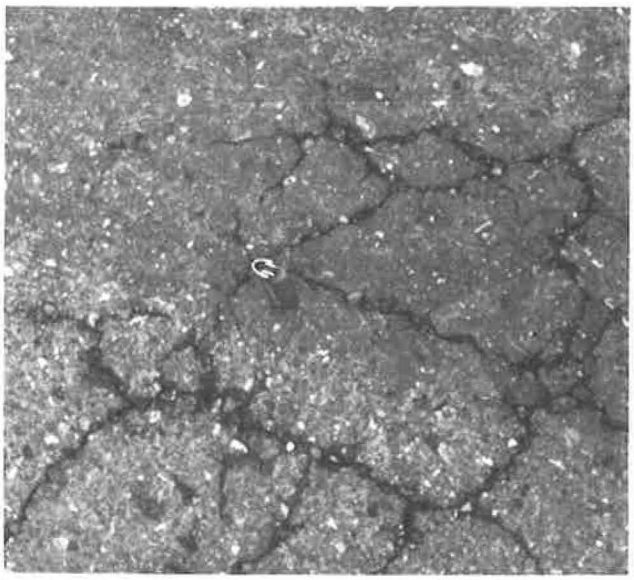

FIGURE 6 Typical pavement cracking, 3 years after completion of construction.

use a combination of mix crude with $K_w < 11$, and preferably $K_w = 10.0$ to 10.5. This crude contains mainly pure aromatic ($K_w = 10$) or Naftanic ($K_w = 10.5$). The road authority also decided that although trucks in Peru are usually overloaded, 120–150 penetration (in 0.1 mm) asphalt was more appropriate than 85–100 AC for reducing thermal cracking with no significant increases in surface rutting. Implementation and monitoring of these conclusions are scheduled after new asphalt road and highway projects are completed in the Peruvian high-altitude region.

ANALYSIS OF THERMAL CRACKING

Severe temperature variations that cause stiffness changes in the asphalt layers are known to develop thermal cracking (*8–12*). In order to analyze the relationship between thermal cracking occurring after the completion of some road sections and asphalt properties, the relationship between the asphalt stiffness changes in the road and its penetration index were investigated. The penetration index (PI) is used as an indicator

of the asphalt cement's elastic viscous properties. The investigation in Peru was carried out with three 85–100 penetration (in 0.1 mm) asphalt cements with penetration index values of −0.15, −0.50, and +0.90. The extreme asphalt stiffness changes occurring in high altitudes were calculated using the extreme representative temperatures of −5°C and +20°C for maximum and minimum asphalt stiffness in the La Oroya-Cerro de Pasco Road. The stiffnesses of both the original asphalt cement and the residue after the thin-film oven test (TFOT) were determined (*8–10*). For all three asphalts, the maximum and minimum stiffnesses were determined for loading periods of 0.01 and 0.1 sec, respectively. Table 2 presents the relationship between the asphalt penetration index, asphalt stiffness changes, and actual road surface cracking.

Table 2 indicates that surface cracking in high altitudes occurs earlier and more severely when (a) the value of the penetration index is 0.9, and (b) the calculated stiffness changes after TFOT are greater than 4,000 kg/cm². Significantly less cracking occurred when the stiffness changes after TFOT were less than 3,000 kg/cm². This conclusion was verified in mountainous areas, below 3,700 MASL. In these lower altitudes, stiffness changes in residue from TFOT were less than 3,000 kg/cm². No thermal cracking occurred at altitudes below 3,700 MASL.

The relative inferiority of asphalt with the higher penetration index of 0.9 was also determined by testing asphalt samples extracted from the La Oroya-Cerro de Pasco Road pavement at an elevation of 4,100 MASL after 11 months of service. The asphalt properties are presented in Table 3. The conclusion from this study adopted by the Peruvian Road Authority was that for high altitudes the asphalt stiffness changes and the penetration index should be limited. The absolute value of the penetration index was limited to 0.5 or less. The Peruvian findings and conclusions are equivalent to the finding of Marks et al. (*11*) that the use of a highly temperature-susceptible asphalt cement produced severe transverse cracking. Marks et al. analyzed the relationship between temperature susceptibility of asphalt, its stiffness, and the frequency of transverse cracking, by using the Pen-Vis number (PVN) developed by McLeod (*12*). PVN values represent the rela-

TABLE 1 PROPERTIES OF THE PERUVIAN TOPPED CRUDE

Test Description	Crude Test Result	ASTM		
		Designation	Specification	
			Minimum	Maximum
API Gravity (°API)	+18.7	D 287	15	35
Specific Gravity (60°F)	+0.9421	D3142	0.865	0.996
Viscosity, Saybolt Furol (210° F)	+99	E 102	-	-
Kinematic Viscosity (210° F)	+25	D2170	-	-
Universal Saybolt Viscosity (210° F)	+122	D2161	-	-
Draining Point (°F)	+70	D 97	14	-
Salts (lb/1,000 barrels)	50	D 3220	5	150
n-Heptane Insoluble (%)	0.96	D 3279	0.9	16
Solubility in Trichloroethylene (%)	99.7	D2042	99	-
Index of Acidity (mg KOH/yr)	0.175	D 664	-	1.0

TABLE 2 RELATIONSHIP BETWEEN ASPHALT STIFFNESS CHANGES, PENETRATION INDEX, AND SURFACE CRACKING (AC: 85–100)

Asphalt Penetration Index	Stiffness Changes (kg/cm) −5° C, 0.01 sec +20° C, 0.1 sec	Period After Completion of Construction with Minor or No Cracking
-0.15, -0.50	1. Original AC: less than 2,000 2. AC After TFOT: less than 3,000	3 years
+0.9	1. Original AC: over 3,000 2. AC After TFOT: over 4,000	5-8 months

TABLE 3 ASPHALT PROPERTIES BEFORE AND AFTER USE IN THE ROAD AFTER 11 MONTHS ON THE ROAD

Asphalt Property	Original Value (Before Use)	Penetration Index +0.9	Penetration Index -0.15-0.5
Penetration	90	28-41	50-60
Softening Point	49°C	75-100°C	-
Penetration Index	+0.90 -0.15-0.50	5.2-6.6 -	- 2.0-2.5

tionship between the asphalt viscosity at 140°F and the penetration at 77°F. McLeod established that PVN = 0 represents an excellent AC with low temperature susceptibility. PVN = 0 is equivalent to the penetration index's being zero; PVN = 1.5 represents an AC with high temperature susceptibility.

AGGREGATE AND MATERIAL PROPERTIES

The aggregates commonly used both for base course and AC are partially crushed gravel that meets AASHTO and ASTM standard specifications for road construction. The aggregate chemical analysis had the following composition: $CaCO_3$ (60 percent), $MgCO_3$ (6 percent), SiO_2 (29 percent), and other materials (5 percent). The aggregate absorption to water and asphalt was 1.0 to 1.6 percent and 0.3 to 0.5 percent, respectively. When thermal cracking commenced 5 to 8 months after construction, the road authorities started to monitor and compare the asphalt surface conditions with the construction and quality control records. These records indicated that less thermal cracking occurs when the base course and AC materials have the following two properties:

1. The base course is open-graded nonplastic that was prime coated immediately after compaction. Proper coating was defined when the prime coat penetrated 20 mm or more into the base course materials. With good pavement drainage and proper surface sealing, less humidity was present in the base course and the daily freeze and thaw were reduced. Because it is almost economically impossible in the Peruvian mountain area to construct an open base course that meets a minimum California bearing ratio (CBR) of 80, zero plastic index, and zero passing sieve 200, the road authority decided to limit the plastic index and the percentage passing sieve 200 to 2 and 5 percent, respectively.
2. The AC fine aggregate material passing sieves 40 and 200 is nonplastic. The construction record shows that this conclusion is less significant if an additive in the form of hydrated lime is added to the AC mix.

CONSTRUCTION CONSIDERATIONS

Heating Temperature

The temperature range for heating the AC in Peru followed standard practice that specifies Sabolt Furol viscosity of 75 to 150 SSF to achieve proper coating. This criterion has been appropriate for achieving adequate aggregate coating at altitudes below 3,700 MASL. At altitudes above 4,100 MASL, where the air pressure is about 0.6 atmospheres, relatively poor coating was achieved when asphalt viscosity during standard mixing procedures in the asphalt plant was 120 SSF or more. Better aggregate coating was achieved when the asphalt viscosity range during mixing was narrowed to 75 to 100 SSF. These viscosity limits occur at temperatures of 145°C and 140°C, respectively. Because reducing the heating temperature in the high altitude also reduces asphalt oxidation, for better control the asphalt heating temperature should be established at 140°C to achieve adequate coating at viscosity of 100 SSF.

Compaction of AC

The standard practice in Peru of compacting AC mixtures permits breakdown at 100°C to 110°C, and compaction is completed before the mix temperature drops to 70°C. This compaction temperature control permits the achievement of adequate density. The air voids in the compacted mixture range between 3 and 6 percent. Implementation of this temperature compaction control in high altitudes resulted in lower density and significantly higher air voids in the compacted mix, mainly between 8 and 11 percent. Only a slight reduction in air voids in the compacted mix, with no significant reduction in stability, was obtained when the amount of asphalt cement in the mixture was increased beyond the optimum determined according to the Marshall design procedure. From the experience obtained on the La Oroya-Cerro de Pasco road project, it was concluded that proper density and air voids can be achieved only if the compaction breakdown is done when the mix temperature is 115°C to 130°C and compaction is completed before the asphalt mixture temperature in the road drops to 90°C or 85°C. Difficulties in obtaining the proper density and percentage of air voids were recorded when the ambient air temperature dropped to 15°C or less. Road sections where the AC mixture was laid when the ambient air temperature was between 12°C and 15°C show relatively lower densities or higher air voids of approximately 5 to 8 percent and were associated with accelerated surface cracking. Severe surface cracking occurred when compaction was carried out in an ambient air temperature below 12°C. On the basis of this experience, the Peruvian Road Authority specified that in high altitudes the AC can be laid when the ambient air

temperature is above 12°C as it rises and above 15°C as it drops. This severe requirement significantly limits the daily AC construction period to about 5 to 6 hr, which naturally increases construction costs.

Longitudinal Joint Construction

Standard construction procedures such as sawing, tack coating, or heating, failed to prevent joint cracking along the La Oroya-Cerro de Pasco Road, as shown in Figure 3b. This type of distress can be reduced when the full asphalt road width is constructed simultaneously.

In the Juliaca Airport asphalt pavement project constructed at an elevation of 3,890 MASL, thermal cracking had not developed 2 years after construction. In this project (see Figure 7), the conclusions obtained from the La Oroya-Cerro de Pasco highway were implemented.

AC MIXTURE ADDITIVES

In order to improve asphalt pavement performance, the Peruvian Road Authority studied the use of different additives for asphalt mixes. For Peru, the most practical and easy-to-use asphalt additives are portland cement and hydrated lime. These additives are usually used when the quantity of mineral filler is insufficient or when the fine material or AC does not meet standard specifications. Usually 1.0 to 1.5 percent of the mix of hydrated lime, or 2 to 3 percent of portland cement, is sufficient to improve the AC mix and to fulfill Marshall design procedures and immersion compression strength criteria. Using hydrated lime was especially successful and was in accordance with the findings of the National Lime Association (*13*) and Plancher et al. (*14*). The conclusions of the Peruvian experience in using lime in asphalt mixtures are as follows:

- Lime, which reduces stripping of asphalt from aggregates, absorption of water, and swell, makes the pavement more waterproof.

FIGURE 7 AC surface condition—Juliaca Airport at 3,890 MASL.

- Lime increases strength, stability, and resistance to water immersion; improves durability; raises the asphalt viscosity; eliminates tender mixes; and helps to achieve specified densities.
- Lime neutralizes acid aggregates and permits the use of local submarginal aggregates.
- Lime improves surface conditions and reduces oxidation and surface aging.

Lime treatment removes polar viscosity-building components and reduces the susceptibility of the asphalt to laboratory oxidative hardening. The benefits of lime treatment in reducing asphalt oxidative hardening are attributed to two synergistic effects: (a) lime reduces the formation of oxidation products by removing oxidation catalysts or promoters, and (b) lime reduces the sensitivity of the asphalt to these oxidation products by removing polar molecules that would otherwise interact with the oxidation products to cause an increase in viscosity.

The first road section between La Oroya and Cerro de Pasco was constructed without any lime in the AC mix because the local filler was nonplastic with 60 percent of $CaCO_3$ and both the aggregate and the AC mixture fulfill the AASHTO and ASTM standard specifications (*2,3*). When surface thermal cracking developed only 5 to 8 months after construction, authorities studied the use of hydrated lime in the asphalt mix. They decided to use hydrated lime as 2 percent of the total weight of the filler, even though the materials met the specifications. Use of lime in the AC mixture and the other implementations mentioned significantly improved the performance of asphalt pavement at 4,160 MASL. Figure 8 shows a typical improved pavement section 2 years after construction. After this performance period, the width of a typical thermal crack was 1 mm (Figure 8b). A typical road condition 5 years after construction is shown in Figure 9. After this period, the typical crack width is about 2 mm.

A visual survey of the road in the spring of 1986 showed that after 5 years of service the thermal cracking reached stable conditions. In the last year or so, no significant deterioration or new thermal cracking has occurred and the typical crack width is still 2 mm, as shown in Figure 9. Riding quality is good and in the first approximation the existing 1 to 2 mm of thermal cracking does not affect the pavement riding quality along the La Oroya-Cerro de Pasco Road at altitudes of 4,100 to 4,300 MASL.

Other additives that might reduce thermal cracking at high altitudes are amine and latex. Adding about 0.5 percent of amine or 5 percent of latex by weight of asphalt cement reduces the penetration index by slightly increasing the asphalt penetration, reducing the softening point ring-and-ball temperature, and increasing ductility after TFOT. The calculated stiffness changes in residue after the TFOT were 2,500 kg/cm^2 or less, which, according to Table 2, indicates an improvement in reducing thermal cracking. Nevertheless, because of the relatively high cost of amine and latex additives, their use in Peru is still limited.

SUMMARY AND CONCLUSIONS

The following preliminary conclusions were reached after 5 years of asphalt surface performance monitoring of the La

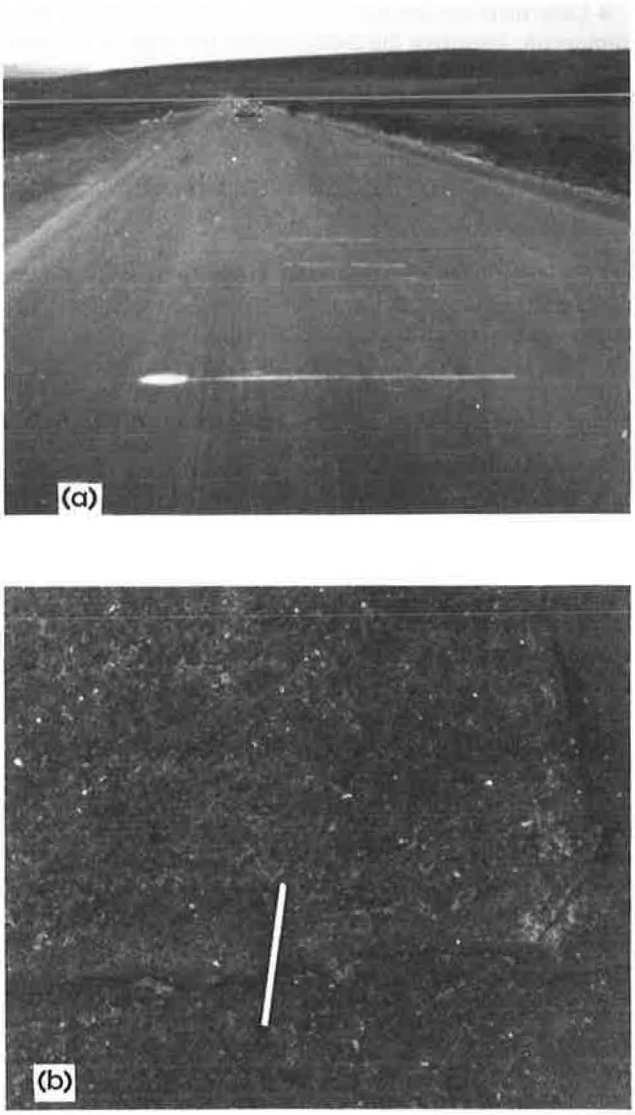

FIGURE 8 a, Road surface 2 years after completion of construction (with 2 percent hydrated lime); b, typical 1-mm thermal crack, 2 years after completion of construction (with 2 percent hydrated lime).

Oroya-Cerro de Pasco highway located at altitudes of 4,100 to 4,300 MASL in Peru's mountainous region.

1. The preferable topped crude used for asphalt production for high altitudes should contain mainly pure aromatic or Naftanic with the Watson characterization factor K_w value between 10.0 and 10.5.

2. Road sections in which the asphalt cement absolute penetration index (PI) is equal to or less than 0.5 show less cracking than other sections, in which the asphalt cement had a PI value of 0.9. A 120 to 150 penetration (in 0.1 mm) grade asphalt cement with a PI value of less than 0.5 is recommended for use in high altitudes, even for extremely overloaded trucks.

3. The asphalt stiffness changes in residue of the TFOT reflect the resistance of the asphalt mixture to thermal cracking. When the calculated stiffness changes after the TFOT are greater than 4,000 kg/cm², severe thermal cracking is expected. Significantly less cracking occurred when the stiffness changes were less than 3,000 kg/cm². The stiffness changes were calculated for the representative extreme conditions (a) temperature of −5°C and loading period of 0.01 sec, and (b) temperature of +20°C and loading period of 0.1 sec. Another indicator that reflects the resistance of the asphalt mixture to thermal cracking is the ductility of the residue of the TFOT. The use of additives is required when the ductility of the residue is less than 75 percent of the original ductility. The use of 0.5 percent of amine or 5 percent of latex by weight of asphalt cement is effective in increasing ductility and reducing thermal stiffness changes and surface cracking.

4. To reduce thermal cracking in the Peruvian high-altitude region, the following engineering properties and construction procedures of the base course materials were specified:

- Open grading with less than 55 percent passing sieve 200, PI < 2, and generally good drainage conditions.
- Asphalt prime coat laid immediately after the completion of the base course and with penetration into the base course of 20 mm or more.
- Coated base course carefully maintained to limit rainfall penetration.

5. Natural and crushed gravel were adequate for the asphalt mixture when the material passing sieves 40 and 200 was nonplastic.

6. When the asphalt cement and AC mixture produced in the high altitudes of Peru were heated to 140°C, better aggregate coating and less oxidation and thermal cracking occurred in the road. These conclusions were compared to the road sections in which the heating temperature was about 160°C. The 140°C temperature corresponds to the Sabolt Fural viscosity of 100 SSF and is found to be the optimum asphalt heating temperature in road projects at such high altitudes.

7. Compaction of the dense AC mixture was better achieved when breakdown temperatures were 115°C to 130°C and the required degree of compaction was obtained before the mix temperature in the road was reduced to 85°C or 90°C.

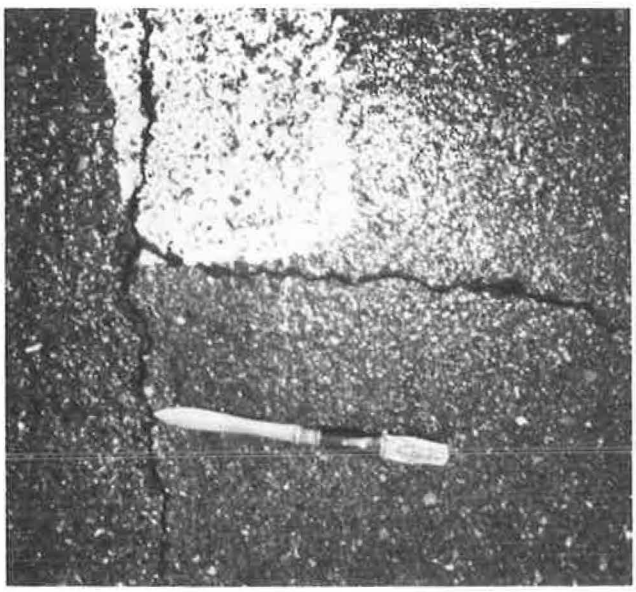

FIGURE 9 Typical 2-mm thermal crack, 5 years after completion of construction (with 2 percent hydrated lime).

8. When the ambient air temperature drops to 15°C, construction should stop. Road sections in which AC was laid at an ambient air temperature of 12°C to 15°C show relatively poor performance, and severe cracking occurred when the ambient temperature had dropped to 12°C or less.

9. Road sections constructed in full width show less longitudinal cracking than when each lane is constructed separately.

10. Road sections with 1 to 2 percent of hydrated lime enriched with CaO or 3 percent of portland cement show less thermal cracking. Also, the hydrated lime improved workability, reduced stripping of asphalt from aggregate, reduced absorption of water, and increased stability and resistance to immersion. In general, use of hydrated lime contributed to performance of the AC in the road.

REFERENCES

1. *AASHTO Interim Guide for Design of Pavement Structures.* AASHTO, Washington, D.C., 1972.
2. *Standard Specification for Transportation Materials and Methods of Sampling and Testing: Part 1—Specifications.* AASHTO, Washington, D.C., 1986.
3. *Annual Book of ASTM Standards: Part 15—Road, Paving, Bituminous Materials, Skid Resistance.* ASTM, Philadelphia, Pa., 1975.
4. J. H. Gary and G. E. Handwerk. *Refino de Petroleo—Tecnologia y Economia.* Capitulo 3—Materiales Primas de Una Refineria, *Editorial Reverte*, Madrid, 1980, pp. 17–27.
5. D. Wuithier and A. Diraoud. El Petroleo: Refino y Tratamiento Quimico. *Editorial Blume*, Madrid, 1971, pp. 48–52.
6. W. L. Nelson. *Oil and Gas Journal*, Vol. 68, No. 44, 1970, pp. 92–96.
7. H. A. Illichi, F. R. Haney, and T. J. Jackson. Hydrocarbon Geochemistry of Oils from Maranon Vasin, Peru. *Bulletin V*, No. 12, American Association of Petroleum Geologists, Tulsa, Oklahoma, 1977, p. 61.
8. *Design Techniques to Minimize Low-Temperature Asphalt Pavement Transverse Cracking: A State-of-the-Art Report*, RR-81-1. The Asphalt Institute, Lexington, Ky., 1981.
9. W. Heukelon. *Observations on the Rheology and Fracture of Bituminens and Asphalt Mixes.* Shell International Petroleum Co., Ltd., Amsterdam, Holland, Feb. 1966.
10. L. Francken. Modile Complexe des Melandes Bitumineux. *L.C.P.C. Especial*, No. 5, Dec. 1977.
11. J. V. Marks and L. C. Huisman. Reducing the Adverse Effects of Transverse Cracking. In *Transportation Research Record 1034*, TRB, National Research Council, Washington, D.C., 1985, pp. 80–86.
12. N. W. McLeod. Asphalt Cement: Pen-Vis Number and Its Application to Moduli of Stiffness. *ASTM Journal of Testing and Evaluation*, Vol. 4, No. 4, July 1976.
13. Hydrated Lime in Asphalt Paving, *Bulletin Number 325*, The National Lime Association, Washington, D.C.
14. H. Plancher, E. L. Green, and J. C. Peterson. *Paving Asphalts: Reduction of Oxidative Hardening of Asphalt by Treatment with Hydrated Lime: A Mechanistic Study.* Report FHWA-RD-77–147, FHWA, U.S. Department of Transportation, Apr. 1977.

Publication of this paper sponsored by Committee on Characteristics of Bituminous Paving Mixtures To Meet Structural Requirements.

Relating Hot-Mix Properties to Properties of Conventional or Polymer-Modified Binders

DAVID F. ROGGE, CHARLES IFFT, AND LEWIS G. SCHOLL

Increasing use of asphalt binders altered with elastomeric or plastic modifiers makes the specification of binders a difficult task. Ideally, a generic specification would allow various suppliers and additives to compete on the basis of expected performance differences in the hot-mix pavements resulting from the use of these binders. Unique characteristics of polymer-modified hot mix were investigated, and binder tests and properties that could be used to predict mix performance whether conventional or modified binders are used were determined. Two mix designs incorporating three conventional asphalts and six different modified asphalts were tested in two phases. The objective was to determine which binder tests had promising correlations with important mix properties. Fraass point and Pen-Vis number showed the most promise for controlling temperature susceptibility of the hot mix at low temperatures. Penetration at 25°C and force ductility areas, particularly peak area, showed the most promise for predicting strength properties of mixes. The best prediction of fatigue life and permanent deformation, as measured by diametral testing, resulted from a combination of penetration at 25°C and force ductility area values as independent variables in multiple regression analysis.

Highway agencies have the opportunity to improve asphalt pavement performance through the addition of various polymer additives to conventional asphalts. Polymer additives to asphalt materials are being advocated as having high potential for improving long-term pavement performance through their ability to improve the properties of the asphalt binder and the resulting asphalt concrete mix. Claims have been made that polymer additives to asphalt can improve adhesion and cohesion, temperature susceptibility, modulus, resistance to fatigue, resistance to rutting, and durability (*1*). Improvements to these qualities in hot-mix pavements have the potential to lengthen pavement service life. Because these additives are relatively new to hot-mix pavement construction in the United States, it was necessary to determine their effect on asphalt pavements, identify appropriate properties that relate to performance, select testing procedures to aid in design and construction of these pavements, and investigate tests to predict the long-term behavior of the pavements.

Ideally, binder tests and properties would be identified that could predict mix performance, regardless of whether binders were conventional or modified with polymers. Goodrich (*2*) correlated binder properties with important properties of hot mix prepared with the binders. Three conventional and two polymer-modified binders were used. In many respects, the present research replicated Goodrich's work, expanding the number of binder and mix tests and properties as well as the number of binders and design mixes.

The objectives of this research were to

1. Conduct a literature review on the use of, test procedures for, and specifications used in the design of polymer-modified asphalt hot mixes;
2. Identify the important properties required for polymer-modified hot mixes and determine the best measuring method; and
3. Recommend interim specifications and test methods for polymer-modified asphalt and polymer-modified hot mixes.

RESEARCH METHODOLOGY

The literature search was conducted using the Transportation Research Information Service (TRIS) data base, as well as from reference lists of various publications and reports dealing with polymer-modified asphalts. Promising documents were obtained and reviewed. A synthesis on polymer types, polymer-modified asphalt hot-mix properties, and testing procedures was formulated and presented in an interim report (*3*).

The laboratory investigation was conducted in two phases. The preliminary testing program focused on using tests that were identified in the literature as likely to predict field performance of polymer-modified asphalts. The initial testing included all promising binder tests and the mix tests required for the validation process. After the initial testing, the most promising binder tests were selected for further examination in a program using fewer tests, but more binders. Different aggregate sources and gradations were used for the two testing programs.

During the laboratory testing program, three conventional binders and six binders using elastomeric and plastic modifiers were tested. At the conclusion of the final laboratory testing program, correlations of various binder test properties with mix-test results were made for both the preliminary and final testing programs. Binder properties were sought that correlated well with important mix properties for the two different mix designs represented by the preliminary and final testing programs.

More detailed reports of this research were provided by Ifft (*4*) and Rogge et al. (*5*).

D. F. Rogge and C. Ifft, Department of Civil Engineering, Oregon State University, Corvallis, Oreg. 97331. L. G. Scholl, Materials and Research Section, Oregon Department of Transportation, 800 Airport Road, S.E., Salem, Oreg. 97310.

TESTING PROGRAM

The laboratory testing program was conducted in two phases: preliminary and final. Table 1 presents the mix-testing procedures used to evaluate mix performance. Table 2 presents the binder test procedures used to develop binder properties to relate to the mix-test results.

The preliminary testing program was conducted with a broad range of mixture and binder tests using one conventional and four modified binders. One aggregate source and mix design was used. The dense-graded mix used lime-treated sand and gravel from eastern Oregon, with a 5 percent binder content. The tests selected for inclusion in the preliminary testing program were chosen on the basis of the extensive literature review; a questionnaire completed by experts on polymer asphalt; and a survey of practical limitations of equipment, funding, and staffing.

The final testing program presented a narrower focus for testing procedures, but expanded the number of binders to two conventional and eight modified binders. The larger number of binders allowed for more data points for correlation between binder properties and mix properties. A different aggregate source and design mix was used. Sand and gravel from a Willamette Valley pit were used without lime treatment. The asphalt content of this dense-graded mix was 5 percent.

All conventional and modified binders for both testing phases were intended to approximate an AC–20 grading. All modified binders were blended and furnished by the suppliers. In reality, several of the binders did not meet an AC–20 specification. Table 3 presents the binders used in preliminary and final testing.

RESULTS OF THE TESTING PROGRAM

Ideally, using binder tests that predict mix performance in the field is preferable. Because the scope and duration of this project did not allow for field testing, the best mix performance indicators that could be obtained were mix test results from laboratory testing. The combination of the preliminary and final testing programs provided the opportunity for one or more binder tests to illustrate their ability to predict important mix properties for two different aggregates and mix designs, regardless of the conventional or modified binder used. The preliminary testing employed five different binders and therefore generated a maximum of five data points for correlation of binder and mix properties. Some correlations only involved four data points. The final testing, which employed 10 different binders, produced a maximum of 10 data points for correlation.

Variations in Polymer-Modified Binders

The binders modified with styrene-butadiene (SB), styrene-butadiene rubber (SBR), and styrene-butadiene-styrene (SBS) were each supplied for the preliminary and final testing programs by the same suppliers to the same specifications. For example, the SB specification and supplier were the same for both the preliminary and final testing programs. Nevertheless, large variations in properties occurred for the SB- and SBS-modified binders between materials supplied for the preliminary and final testing. Possible explanations are that the blending of small quantities of these materials makes it difficult to develop uniformity, or that the modifiers were not completely compatible with the base asphalts.

Problems with Conventional Viscosity Tests

Problems occurred when conventional viscosity measurements were made with polymer-modified binders at 60°C and possibly at 135°C. In some cases, absolute viscosity measurements resulted in clogging of tubes. As discussed by

TABLE 1 PRELIMINARY AND FINAL MIX-TESTING PROGRAMS

Performance	Mix Tests	Prel.	Final
Fatigue Life	Diametral Fatigue	X	X
Rutting Resistance	Uniaxial Creep	X	
	Permanent Deformation	X	X
Low-Temperature Crack Resistance	Ind. Tens. @ 0°C, .05 in./min.	X	
	Ind. Tens. @ -10°C, .05 in./min.	X	X
	Modulus @ 0°C	X	X
	Modulus @ -10°C	X	X
Temperature Susceptibility	Modulus vs Temp., -10°C, 0°C, 25°C	X	X
Long-Term Durability: Moisture Resistance	Modified Lottman Conditioning	X	
Heat/Oxygen Resistance	Pressure Oxygen Bomb	X	
	Forced Draft Oven for 14 Days @ 60°C	X	
Modulus @ 25°C	Diametral Resilient Modulus	X	X
Tensile Strength @ 25°C	Indirect Tensile Test @ 25°C, 2in/min.	X	X

TABLE 2 PRELIMINARY AND FINAL BINDER-TESTING PROGRAMS

Performance	Binder Tests	Prel.	Final
Consistency	Fraass Brittle Point	X	X
	Penetration @ 4°C	X	X
	Penetration @ 25°C	X	X
	Softening Point		X
	Viscosity at 60°C	X	X
	Viscosity at 135°C	X	X
Load Resistance	Force Ductility @ 4°C	X	X
	Force Ductility @ 25°C	X	
	Toughness and Tenacity (25°C)	X	X
	Dynamic Mechanical Analysis	X	
Durability:			
Mix Prep. Aging	RTFO	X	X
Long-Term Aging	POB	X	

TABLE 3 BINDERS USED IN PRELIMINARY AND FINAL TESTING

Preliminary Testing:

Code	Binder Type	Comments
A1	AC-20 (conventional)	
B1	EVA modified	
C1	SBS modified	
D1	SBR modified	
E1	SB modified	

Final Testing:

Code	Binder Type	Comments
A2	AC-15 (conventional)	
B2	AR-2000 (conventional)	
C2	polyethylene fiber modified	
D2	EVA modified	
E2	SBR modified	Same supplier as D1
F2	SB modified	Same supplier as E1
G2	SBS modified	Same supplier as C1
H2	neoprene modified	
I2	EVA modified	Same supplier as B1
J2	SBS modified	Same supplier as C1 & G2

Shuler and Pavlovich (*6*), this difficulty is caused by the shear-thinning properties of polymers. One solution is to move away from conventional viscosity testing toward constant-power viscosity (*7*) or another method of constant-stress viscosity measurement when polymers are used.

Binder Strength Tests

The question of whether tests such as force ductility and toughness and tenacity are required was to be answered by the testing programs. On the basis of preliminary and final testing, the answer was maybe—the tests did show promise for predicting mix properties and provided the best predictive ability for mixture strength and modulus properties.

Although the preliminary test program ran both of these tests at the same temperature (25°C) to see if similar results could be obtained, they could not. A temperature of 25°C is not good for force ductility testing. Most binders cannot be taken to failure at this temperature in force ductility testing because of extension limits of the testing equipment. Different strain rates may also confuse the issue. Toughness and tenacity testing uses 20 cm/min, whereas force ductility testing uses 5 cm/min.

Toughness and tenacity testing splits the total area under the load deformation curve into two areas (see Figure 1). Toughness is defined as the total area, and tenacity is defined as the tail of the curve. The best correlations for toughness and tenacity properties were not for toughness or for tenacity, but rather for the area that represented the difference of these two areas, herein called "peak area." Developing areas analogous to toughness, tenacity, and peak area for the force ductility stress-strain curves also produces good correlations for peak area. However, peak area is strongly related to engi-

neering stress, which is easier to compute. Because the two properties showed relationship to each other with $R^2 > 0.95$, computing peak area may not be worth the extra effort.

Long-Term Aging

Another question that the testing programs attempted to answer was whether tests of long-term aging effects are required when polymers are used. Time and budget constraints permitted the inclusion of only a small-scale aging test in the preliminary testing program. Because of a combination of procedural errors and some values that looked questionable, it is uncertain whether the results of this testing are reliable. The polymer-modified binders seemed to be affected more adversely by pressure oxygen bomb (POB) conditioning than was the conventional binder. This testing, therefore, does nothing to alleviate concerns regarding the long-term durability of polymers raised by Goodrich (*2*), Button and Little (*8*), and Krivohlavek (*9*). If polymer binders degrade more quickly than conventional binders, perceived present benefits could quickly disappear. Some type of specification binder test should be developed that can be used to reject binders that may be subject to accelerated aging. The POB, long-term durability (LTD) test (*2*), and tanning booth described by Krivohlavek (*9*) are possibilities. More research is needed.

Predicting Mix Properties From Binder Tests

Using results of binder and mix testing from both the preliminary and final testing programs, attempts were made to correlate all binder properties with all mix properties. Promising correlations were identified. A relationship was considered promising when the coefficient of determination (R^2) was ≥ 0.70.

Because of the larger number of data points in the final testing, the analysis was focused on promising relationships from this testing. Because preliminary testing only resulted in four or five data points, those results were not given much weight. Preliminary testing served primarily to aid in planning final testing. The approach taken is that a high R^2 value on preliminary testing can serve as supporting evidence for high R^2 on final testing, but that low R^2 on preliminary testing does not necessarily rule out a relationship or negate high R^2 values for final testing. This result follows from the dramatic volatility of R^2 when only four or five data points are involved (see Figure 2). The R^2 value for the final test data shown in Figure 2 is 0.75 and the relationship is positive or direct. If only *A2*, *C2*, *D2*, and *E2* had been selected for testing, the

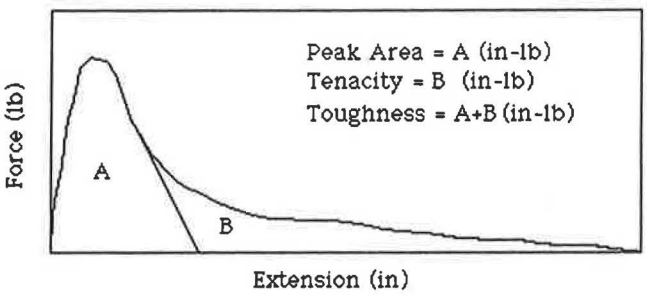

FIGURE 1 Typical toughness and tenacity curves.

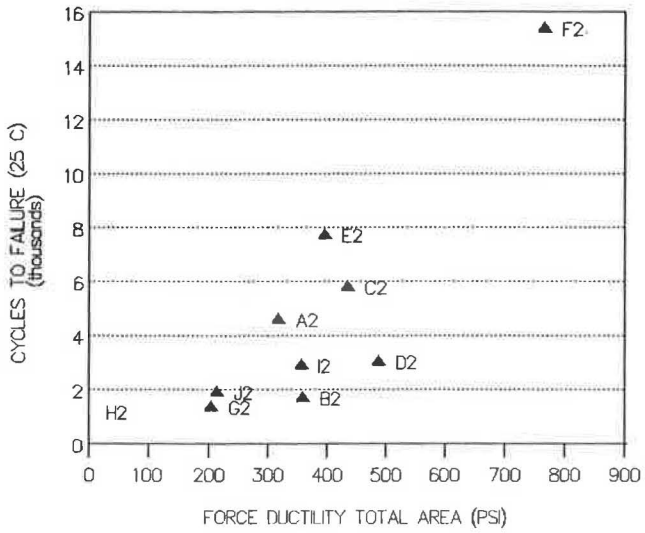

FIGURE 2 Fatigue life versus original force ductility total area—final testing.

R^2 value would have been 0.10 and the relationship would have been inverse. If only these four data points had been generated, a slight shift of *A2* upward and to the right could even result in a high R^2 value for an inverse relationship.

The individual binder properties, which appear to be the best predictors of mix performance on the basis of simple linear regression, are presented in Table 4 and discussed in the following paragraphs. Multiple regression results are discussed later.

Predicting Fatigue Life

The only single-binder properties that showed promise for predictive ability in the final testing were the original force ductility total area ($R^2 = 0.75$) and its component area force ductility tenacity ($R^2 = 0.73$). The scattergram for fatigue cycles to failure versus original force ductility total area for final testing is shown in Figure 2.

Predicting Rutting Resistance

The two mix tests aimed at predicting rutting resistance were 40°C uniaxial compression creep (preliminary) and permanent deformation data from 25°C diametral fatigue testing (preliminary and final). No promising correlations were obtained for uniaxial compression creep testing in the preliminary testing. This test was dropped from the final testing program. No promising correlations were obtained for permanent deformation data in the final testing.

Predicting Resistance to Thermal Cracking

Low-temperature, low-strain-rate indirect tensile testing was the mix-testing procedure chosen to provide an indication of the ability of a mix to resist thermal cracking. Probably the

TABLE 4 PROMISING CORRELATIONS FROM FINAL TESTING—R^2 VALUES

Performance	Mix/Binder Properties	Final
Fatigue Life	Diametral Fatigue	
	Orig FD Total Area	.75
	Orig FD "Tenacity"	.73
Rutting Resistance	Uniaxial Creep	N/T
	Permanent Deformation	<.70
Low-Temperature Crack Resistance	Ind. Tens. Stress @ -10°C, .05 in/min	
	Orig. Penetration (25°C)	.88
	Orig. FD Engr Stress (4°C)	.71
	Orig. FD Peak Area (4°C)	.78*
	Orig. PI	.83
	RTFO Penetration (25°C)	.81
	Modulus @ 0°C	
	Orig. FD Engr Stress (4°C)	.80
	Orig. FD Peak Area (4°C)	.82*
	Orig. T&T Peak Area	.70
	Orig. Fraass Pt	.78*
	RTFO FD Engr Stress (4°C)	.76*
	RTFO FD Peak Area (4°C)	.71*
	Modulus @ -10°C	
	Orig. T&T Peak Area	.70
	Orig. FD Engr Stress (4°C)	.83
	Orig. FD Peak Area (4°C)	.91
	Orig. PVN	.72
	Orig. Fraass Pt.	.80
	RTFO FD Engr Stress	.89
	RTFO FD Peak Area	.84
Temperature Susceptibility at Low Temperature	Modulus Difference, -10°C, 25°C	
	Orig. FD Engr Stress (4°C)	.76
	Orig. FD Peak Area (4°C)	.84
	Orig. PVN	.74
	Orig. Fraass Pt.	.82
	RTFO FD Engr Stress (4°C)	.89
	RTFO FD Peak Area	.83
Modulus at 25°C	Diametral Resilient Modulus	
	Original Penetration (25°C)	.87
	Orig. T&T Peak Area	.70
	Orig. FD Engr Stress (4°C)	.74
	Orig. FD Peak Area (4°C)	.79
	Orig. PI	.78
	RTFO Penetration (25°C)	.82
	RTFO T&T Peak Area	.77*
Tensile Strength at 25°C	Indirect Tens. Stress @ 25°C, 2in/min	
	Orig. Penetration (25°C)	.86
	Orig. FD Engr Stress (4°C)	.74
	Orig. FD Peak Area (4°C)	.80
	Orig. PI	.82
	RTFO Penetration (25°C)	.84

N/T = Not Tested
* = > 0.70 in preliminary testing

best indicator that could be obtained from this test would be tensile strain at failure. Laboratory equipment restraints made it impractical to measure this property. Instead, maximum tensile stress, maximum compressive strain, and work to failure were determined.

Final testing produced no promising predictors for compressive strain or work to failure. However, many promising predictors of tensile stress at −10°C were found. These are original (R^2 = 0.88) and rolling thin-film oven (RTFO) (R^2 = 0.81) penetration at 25°C, original penetration index (PI) (R^2 = 0.83), and the original force ductility (4°C) engineering stress (R^2 = 0.71) and peak area (R^2 = 0.78). Considering results from preliminary testing, original and RTFO penetration at 25°C, and original force ductility peak area look most promising. Figures 3 and 4 show scattergrams for the relationships between penetration at 25°C and force ductility peak area with indirect tensile stress at −10°C.

Modulus values at 0°C and −10°C could also be considered indicators of resistance to low-temperature thermal cracking. Low modulus at low temperature is preferred. Force ductility (4°C) properties were found that predicted these properties in final testing. These properties were original and RTFO peak area and maximum engineering stress. These properties also served as reasonable predictors of strength and modulus at 25°C. In these relationships, larger force ductility values imply larger mix property values. At cold temperatures, because low modulus is desired, lower force ductility values are better. Therefore, it would be preferable to find a different predictor of low-temperature modulus. Original PVN showed some promise at −10°C, but Fraass brittle point of original binders

was a promising predictor of modulus at both 0°C and −10°C. Hence, the use of Fraass point to predict cold-temperature properties is preferred over force ductility properties. Figure 5 shows a scattergram for Fraass point versus mix modulus at 0°C.

Fraass point for RTFO residues, POB Fraass point, loss tangent at 40°C, and force ductility true stress at 25°C had promising predictions of low-temperature properties in the preliminary testing, but, for various reasons, were not part of the final testing program.

Predicting Low-Temperature Temperature Susceptibility

To further evaluate potential for thermal cracking, an evaluation of the sensitivity of mix modulus to changes in temperature at low temperatures was made. To accomplish this, change in modulus values between −10°C and 25°C was computed for each mixture. Binder properties were then correlated against these mixture values. Three binder properties warrant discussion: PI, PVN, and Fraass brittle point.

The two most accepted measures of temperature susceptibility of asphalts are PI and PVN. These measures concentrate on binder consistency at temperatures of 25°C and above. They do not use measures of consistency below 25°C. Nonetheless, if the plot of consistency on a bitumen test data chart (BTDC) is linear, PI and PVN values should also predict low-temperature temperature susceptibility of mixtures. When correlations were made with mixture modulus change, PVN correlated better than PI. Original PVN had an R^2 value of 0.73 for the final test program and favorable correlation in the preliminary program. Because significant problems were encountered in measuring viscosity by conventional means for some of the polymers, PVN correlations would be better if a more accurate means of determining viscosity is used. PVN, with both original binders and residues, correctly identified the two most low-temperature-sensitive mixes from both the preliminary and the final testing programs.

Fraass brittle point for original binders (RTFO residues were not tested in either phase) was a better predictor of the low-temperature sensitivity of the resulting mix as predicted by modulus-versus-temperature curves. Final test R^2 value was 0.82 with favorable preliminary correlation. A scattergram of this relationship is shown in Figure 6. Until routine viscosity testing for polymer-modified asphalts can be improved, Fraass brittle point appears to be an acceptable method for predicting rate of change of mix modulus at low temperatures.

Original RTFO force ductility engineering stress and peak area also showed promise for predicting modulus change. PVN and Fraass point are of more interest because they provide indicators separate from strength properties.

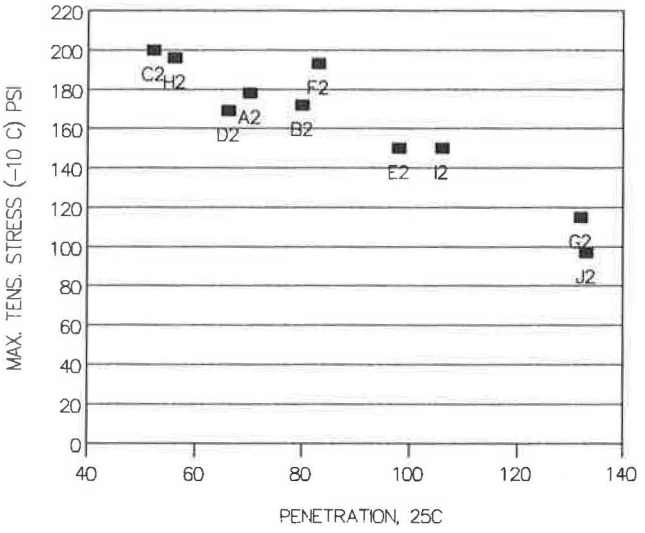

FIGURE 3 Tensile strength (−10°C) versus penetration at 25°C—final testing.

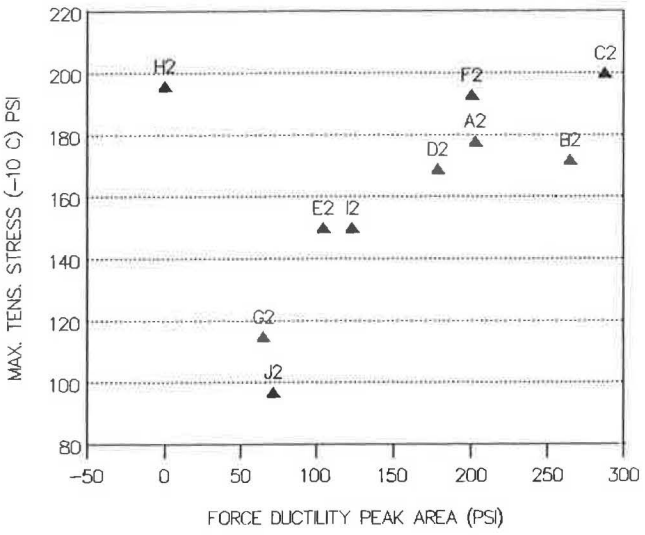

FIGURE 4 Tensile strength (−10°C) versus original force ductility peak area—final testing.

Predicting Stiffness at 25°C

Modulus at 25°C, which is used in mechanistic pavement design, is considered a measure of quality of asphalt concrete pave-

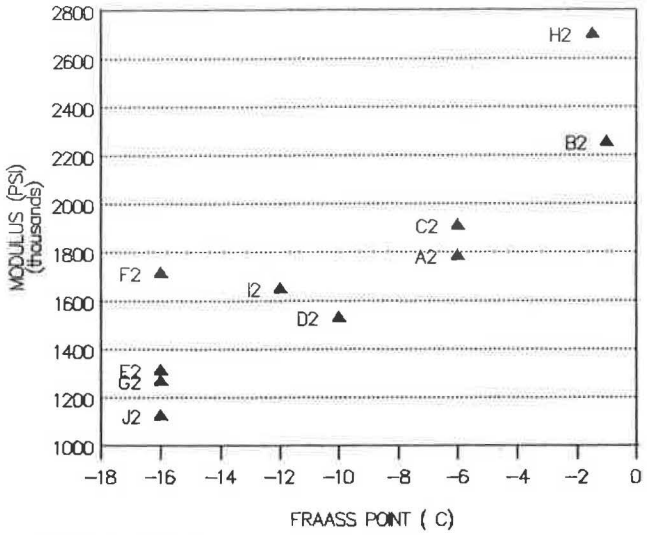

FIGURE 5 Modulus (0°C) versus original Fraass point—final testing.

ment, and is used to predict other mixture properties. Correlations of all binder properties were made with modulus values at 25°C. The most promising binder properties (and their final R^2 values) were original penetration at 25°C (R^2 = 0.87), RTFO penetration at 25°C (R^2 = 0.82), original force ductility peak area at 4°C (R^2 = 0.79), and RTFO toughness and tenacity peak area (R^2 = 0.77).

Predicting Tensile Strength at 25°C

Tensile strength at 25°C, which is considered an important measure of quality of asphalt concrete, is used to predict fatigue life. Correlations of all binder properties were made with tensile strength values at 25°C. The most promising predictors were original and RTFO penetration at 25°C with final R^2 values of 0.86 and 0.84.

Predicting Mix Properties by Multiple Regression

The five data points of the preliminary testing program were clearly inadequate for multiple regression analysis. The maximum 10 data points provided by the final testing are marginal for multiple regression; 20 points would be preferred. Nevertheless, analysis was attempted for the final testing program selecting pairs of binder tests as predictor variables.

Penetration at 25°C was the most helpful variable in explaining variability when paired with other binder properties in multiple regression analysis. Two results are worthy of discussion.

The combination of penetration at 25°C and force ductility total area showed promise for predicting fatigue life (original R^2 = 0.79; RTFO R^2 = 0.82). However, the plot of force ductility area versus penetration at 25°C for RTFO residues (see Figure 7) shows the problems in writing a specification on the basis of this relationship. On the plot, 100 percent represents the binder with the longest fatigue life in the final testing program and the remaining percentages show the relative fatigue lives of the other binders. The two best performers can easily be isolated with a maximum-penetration, minimum-area requirement, but separating moderate performers from poor performers is not as straightforward. When the preliminary test data are normalized and added to the plot, the usefulness of the relationship breaks down further. The 10 and 20 percent performers become intermingled with 50 and 100 percent performers.

The combination of penetration at 25°C and force ductility tenacity or tail area showed promise for predicting resistance to permanent deformation (RTFO R^2 = 0.90). Figure 8 shows a plot of force ductility tenacity versus penetration at 25°C for RTFO residues. Again, the top two performers may easily be separated with a maximum-penetration, minimum-area requirement. The midrange performers even show some separation from the poorest performers. However, when preliminary test data are added to the plot, the relationship breaks down, with a 12 percent performer intermingled with 100 and 50 percent performers.

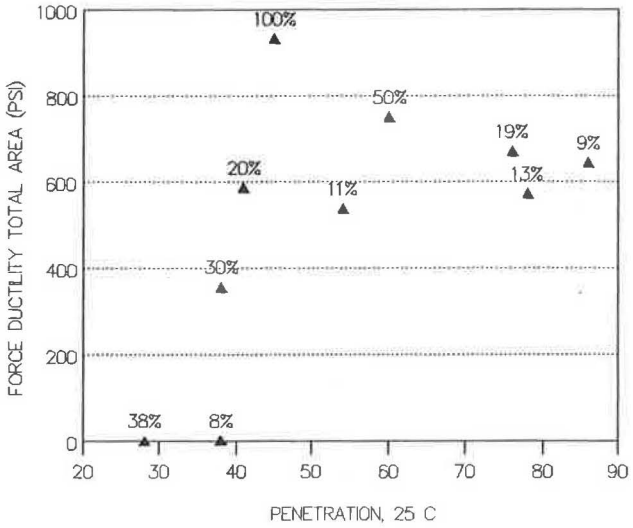

FIGURE 7 RTFO force ductility total area versus RTFO penetration at 25°C—final testing.

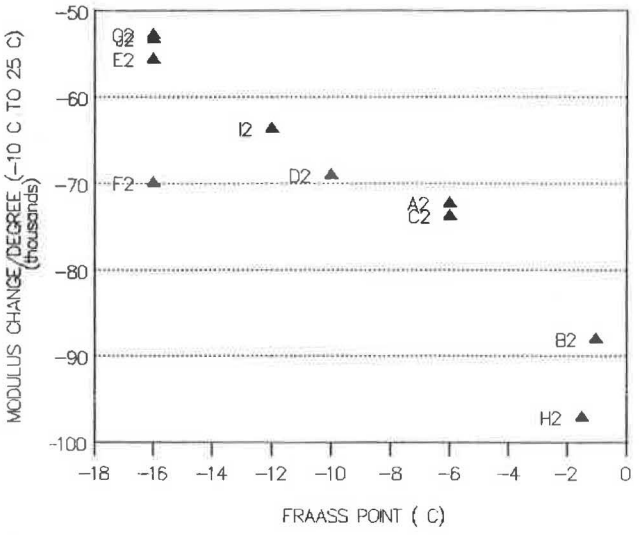

FIGURE 6 Modulus change versus original Fraass point—final testing.

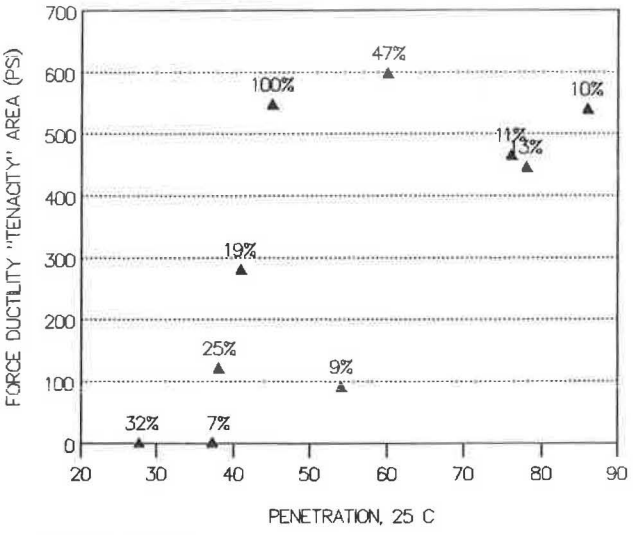

FIGURE 8 RTFO force ductility tenacity versus RTFO penetration at 25°C—final testing.

A word of caution is in order. Permanent deformation data were generated from the diametral fatigue test. Permanent deformation results are closely correlated with fatigue lives. Therefore, predicting diametral fatigue life is equivalent to predicting permanent deformation.

Only in the area of fatigue and permanent deformation does multiple regression analysis indicate that force ductility testing contributes more to predicting mix properties than does simple binder tests already in common usage. Combinations of RTFO penetration at 25°C, viscosities at 60°C and 135°C, and ring-and-ball softening point produced R^2 values approximating 0.89 or better for modulus at all temperatures (−10°C, 0°C, 25°C) and maximum indirect tensile stress at −10°C and 25°C.

Correlation Summary

Penetration at 25°C and force ductility peak area and maximum engineering stress appear to be the best predictors of strength and stiffness at all temperatures. In addition, Fraass point and PVN show promise for predicting low-temperature temperature susceptibility and low-temperature stiffness. Force ductility total area (toughness) and tenacity or tail area show some promise for predicting fatigue life, particularly when paired with penetration at 25°C. Force ductility tenacity shows some promise for predicting permanent deformation at 25°C when paired with penetration at 25°C.

Another way to evaluate relationships is to determine which individual correlations showed promising R^2 relationships both in preliminary and final testing. When done, the only binder properties producing R^2 values >0.70 in simple linear regression in both testing programs were as follows:

1. Original force ductility (4°C) peak area's predicting indirect tensile stress at −10°C,
2. Original force ductility (4°C) peak area's predicting modulus at 0°C,
3. RTFO force ductility (4°C) peak area's predicting modulus at 0°C,
4. RTFO force ductility (4°C) maximum engineering stress' predicting modulus at 0°C,
5. Original Fraass point's predicting modulus at 0°C, and
6. RTFO toughness and tenacity peak area's predicting modulus at 25°C.

Of these, Relations 2 and 6 showed the strongest correlations. Five out of six of these predictions are for low-temperature mixture properties. Four of these same five predictors use low-temperature binder tests. Four of the predictors used force ductility testing.

In addition, RTFO loss tangent at 40°C might have been promising in both preliminary and final testing, had it been included in final testing. However, the equipment required for dynamic mechanical analysis on which the computation of loss tangent is based is not commonly available for highway agency use.

Although force ductility peak area showed better correlations than maximum engineering stress, the two are closely related. In fact, simple linear regression of these two properties produced R^2 values that were >0.95. Because maximum engineering stress is easier to compute, it is questionable whether the extra effort of obtaining peak area is worthwhile.

Recommendations for Specification Testing Based on This Research

On the basis of the laboratory testing performed for this research project, the following binder properties show promise for inclusion in a generic premium binder specification:

- Consistency:
  —Fraass brittle point,
  —Penetration at 25°C, and
  —PVN.
- Strength characteristics:
  —Force ductility testing at 4°C for peak area, total area, tenacity area, and maximum engineering stress.

The results of this research are consistent with the preponderance of literature in concluding that polymer modification can improve the temperature susceptibility of asphalts. This study was only interested in temperature susceptibility at low temperatures. PI and PVN, the two most accepted methods of measuring temperature susceptibility, are based on consistency measurements only at temperatures ≥25°C and present problems when polymer-modified asphalts are encountered. Some of these binders have nonlinear curves when consistency data are plotted on BTDCs (see Figure 9). Conventional viscosity measurements produce misleading results because of the shear susceptibility of polymers. Nevertheless, even with questionable viscosity values, the use of PVN correctly identified the binders that were most temperature susceptible at low temperatures.

Fraass brittle point showed better correlations with mix low-temperature temperature susceptibility than did PVN. Fraass brittle point offers an alternative to the use of PVN for control of low-temperature temperature susceptibility—an alternate that avoids the problem of viscosity measurement for polymer-modified asphalts and concentrates on the low-temperature end of the temperature consistency curve. Use of Fraass brittle point in conjunction with penetration grading would completely eliminate the need for viscosity testing in binder specifications. Proper use of PVN or Fraass point in binder specifications should ensure the use of either a conventional or modified asphalt with low-temperature susceptibility at low temperatures.

From a strength standpoint, force ductility testing appears to offer the most potential for predicting mix performance. This statement is based on limited test data, and is not universally agreed on in the literature. For the laboratory testing in this research, however, it does show promise for predicting strength and stiffness of mixtures, particularly at low temperatures and particularly if binders with very low values (brittle materials) are rejected. Penetration at 25°C, a much simpler test, showed promise for predicting strength at both low and moderate temperatures.

In summary, PVN and Fraass point may be used to control low-temperature temperature susceptibility of hot mix. Force ductility areas may be used to eliminate brittle binders, and show promise for controlling strength and stiffness properties

of hot mix (given a specific aggregate source and gradation). Penetration at 25°C was a good overall indicator of strength and stiffness and, when combined with force ductility area values, showed promise of predicting fatigue life and permanent deformation as measured by diametral testing.

CONCLUSIONS AND RECOMMENDATIONS

The recommendations that follow are based on limited testing involving three conventional and six polymer-modified binders with two different aggregates and design mixes. For the binders and mixes tested, the following conclusions are warranted:

1. Force ductility total area and tenacity area for original binders show some promise for predicting fatigue life as determined by diametral testing. The combination of penetration at 25°C and force ductility total area for RTFO residues show the most promise for predicting fatigue life.

2. Mix permanent deformation resistance, as defined in this study, cannot be predicted with any single binder test studied. The most promising basis for predicting permanent deformation resistance of the mix is the combination of force ductility tenacity or tail area with penetration at 25°C.

3. Improvements in low-temperature temperature susceptibility can be predicted with either Fraass brittle point or PVN.

4. The area under the primary peak of the force ductility stress-strain curve or the toughness and tenacity force-extension curve has better predictive ability of mixture properties than either the total area (toughness) or tail area (tenacity). However, this peak is only a marginally better predictor than maximum engineering stress, which is easier to compute.

5. With the exception of low-temperature modulus prediction, more force ductility peak area is better.

6. Force ductility (4°C) testing of RTFO residues clearly identifies the more brittle binders.

7. Penetration at 25°C shows promise for predicting modulus at 25°C and indirect tensile strength at 25°C.

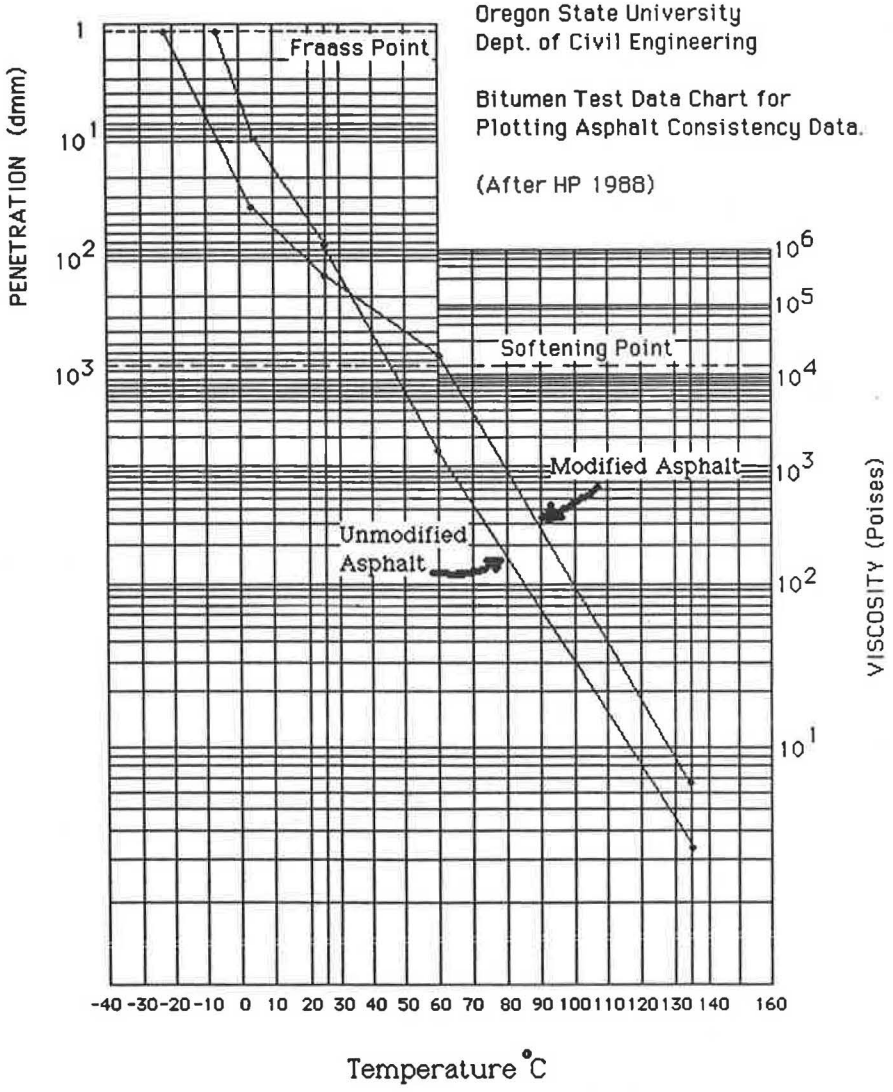

FIGURE 9 Nonlinearity of temperature-consistency curve for modified binder.

8. Only for diametral fatigue and permanent deformation, multiple regression analysis indicates that force ductility testing contributes more to predicting mix properties than do simple binder tests already in common usage. Pairings of RTFO penetration at 25°C, viscosities at 60°C and 135°C, and ring-and-ball softening point produce R^2 values of 0.89 or higher for modulus at all temperatures (−10°C, 0°C, 25°C) and maximum indirect tensile stress at −10°C and 25°C.

9. The shear susceptibility of polymer modifiers creates problems when conventional viscosity measurements are made. Other types of viscosity measurement should be explored.

10. Testing of long-term aging effects on polymer-modified binders is needed.

11. The limited dynamic mechanical testing of binders performed in this research project showed promise for predicting mix properties.

12. Properties of the same modified binders supplied at different times for preliminary and final testing showed wide variations in physical properties.

13. The diametral fatigue testing results for SBS-modified binders in this research project showed much poorer performance than the generally outstanding beam fatigue results reported for these binders in the literature.

ACKNOWLEDGMENTS

The authors gratefully acknowledge the funding provided by FHWA through the Oregon Department of Transportation (ODOT) and the laboratory testing work performed by ODOT's materials laboratory, particularly by Glenn Boyle, Hector Morales, and Pat Turpen. They are also appreciative of the dynamic mechanical binder testing donated to the research project by Joe Goodrich of Chevron Research. The response of all the polymer asphalt experts to the initial questionnaire is also appreciated. In addition, guidance provided by R. G. Hicks and R. L. Terrel proved most beneficial.

REFERENCES

1. R. L. Terrel and J. L. Walter. Modified Asphalt Pavement Materials: The European Experience. *Proc., Association of Asphalt Paving Technologists*, St. Paul, Minn., Feb. 1986, pp. 482–518.
2. J. L. Goodrich. Asphalt and Polymer Modified Asphalt Properties Related to the Performance of Asphalt Concrete Mixes. *Proc., Association of Asphalt Paving Technologists*, St. Paul, Minn., Feb. 1988.
3. D. F. Rogge, C. Ifft, R. G. Hicks, and L. G. Scholl. *Evaluation of Polymer Modified Asphalt in Hot Mix Pavement.* Transportation Research Report 88-27, TRI, Oregon State University, Corvallis, 1988.
4. C. Ifft. *Evaluation of Polymer Modified Asphalt in Hot Mix Pavement.* M.S. thesis. Oregon State University, Corvallis, 1989.
5. D. F. Rogge, C. Ifft, L. G. Scholl, and R. G. Hicks. *Laboratory Study of Test Methods for Polymer Modified Asphalt in Hot Mix Pavement.* Research Report, Oregon Department of Transportation, Salem, Nov. 1989.
6. T. S. Shuler and R. D. Pavlovich. *Characterization of Polymer Modified Binders.* Research Report 52001-1f, New Mexico Research Institute, University of New Mexico, Albuquerque, Jan. 1987.
7. R. Roque, M. Tia, and B. E. Ruth. Asphalt Rheology to Define the Properties of Asphalt Concrete Mixtures and the Performance of Pavements. In *Asphalt Rheology*, ASTM STP 941, Philadelphia, Pa., 1987.
8. J. W. Button and D. N. Little. Asphalt Additives for Increased Pavement Flexibility. Texas Transportation Institute, College Station, Nov. 1987.
9. D. D. Krivohlavek. The Use of High Molecular Weight Radial S–B Block Copolymers in Highway Overlay Construction. *Proc., Association of Asphalt Paving Technologists*, St. Paul, Minn., Feb. 1988.

Publication of this paper sponsored by Committee on Characteristics of Bituminous Paving Mixtures To Meet Structural Requirements.

Fatigue Characteristics of Alaskan Pavement Mixes

NICK F. COETZEE AND BILLY G. CONNOR

Mechanistic analysis procedures for pavement evaluation have been simplified with recent development in microcomputers. These procedures require pavement fatigue models to make them useful for evaluation of pavement life. Although numerous models exist, their applicability to cold climates requires further investigation. The purpose of this study was to determine the applicability of existing fatigue models in Alaska, determine if different asphalt concrete mixes used in Alaska differed in performance, and determine whether laboratory-prepared samples perform differently than field-compacted samples. Testing consisted of three-point bending tests with temperatures ranging from 80°F to −15°F. A materials testing system modified for the test procedure was used with computerized data acquisition systems. All tests were displacement controlled. None of the existing fatigue relationships were adequate. As a result, a new equation was developed that better fits AC-2.5 and AC-5 at temperatures below 45°F. This equation is much more sensitive to strain than the Asphalt Institute equations. AC-2.5 and AC-5 performed similarly at temperatures below 20°F. At temperatures as low as −15°F, no difference in performance was noted. Laboratory-prepared samples and field samples showed equivalent performance. The data indicated a difference between the time at which the maximum load occurred and the time at which the maximum strain occurred. This difference, or phase lag, was greatest at the beginning of the test and almost in phase at the end of the test. This phenomenon should be explored further, because it may provide a method of determining remaining life.

Application of state-of-the-art mechanistic analysis procedures to pavement design and evaluation have been simplified with developments in microcomputers. These procedures are based on fundamental engineering principles that require a knowledge of material response parameters. The approach is often used for estimating remaining life for existing pavements and expected life of new pavements, based on fatigue concepts. A number of sources of fatigue relationships for asphalt concrete (AC) are available (*1–6*). However, it is not clear if these relationships are applicable in Alaska during low-temperature periods. This project investigated the applicability of typical fatigue relationships to the pavement design process in Alaska. The project also investigated whether laboratory-compacted samples provided similar fatigue results to field-compacted samples. The generated fatigue equations have been compared with the relationship developed by the Asphalt Institute (AI) because this relationship is widely used.

Preliminary analyses were performed on the generated data in terms of simplistic energy or work approaches to fatigue in asphalt concrete. On the basis of limited data from these initial analyses, this approach holds promise for future development.

N. F. Coetzee, Dynatest Consulting, Inc., P.O. Box 71, Ojai, Calif. 93024. B. G. Connor, Alaska Department of Transportation and Public Facilities, 2301 Peger Road, Fairbanks, Alaska 09709–5316.

TESTING EQUIPMENT AND PROGRAM

A modified material testing system (MTS) universal testing machine was used to perform the cyclic loading tests. A load application system was developed to use with the MTS load frame to apply third-point bending to beam specimens. Environmental control chamber dimensions restricted specimen size to 2 × 2 × 15 in.

The basic equipment consisted of a model 810 MTS system, with a model 413 master control panel, 442 controller, and 410 digital function generator. A trigger generator acting as gate to the MTS function generator produced the load pulse—a 0.1-sec haversine load cycle with a 0.9-sec rest period. The relaxation period of 0.9 sec was chosen to ensure that full recovery was achieved by the material between applied loads. Loads were applied in the typical third-point loading used for this type of test, ensuring a constant bending moment over the middle third of the beam. Tests were run in a displacement control mode using a displacement gauge to monitor center deflections of the beam. This information provided feedback for the MTS load system control. Loads were measured using a 5,000-lb load cell. Strains were measured directly using an extensometer attached to the beam with adhesive. Stresses were calculated from load, deflection, and beam dimensions using beam theory. Modulus was calculated from computed stress and measured strain.

During testing, strain was measured only in the tension region of the beam. Initial tests using two extensometers to measure strains on both sides of the beam confirmed that the system was functioning adequately. Stresses based on these measurements were compared with theoretical calculations, as plotted in Figure 1, and show good agreement, with minor errors developing mainly in the failure zone at approximately 375 psi. Additional assumptions were checked during this phase. Calculated modulus, plotted against stress level, remained relatively insensitive to stress level for most of the stress range. As expected, major deviations occurred during failure. Variations also occurred in the calculated modulus at the low end of the stress scale because of a number of factors, including load system friction.

Load, deflection, and strain measurements were monitored and recorded using a Hewlett-Packard HP85 microcomputer and HP7090A measurement plotting system, or recording plotter. This plotter can monitor three channels at one time

and has the ability to record, digitize, and store approximately 1,000 data points per channel per scan. The computer was programmed to scan and record a 4-sec window, covering the 0.1-sec load pulse plus 0.9-sec rest period, at specified load strokes throughout a test sequence.

Strokes for recording were closely spaced initially, but the intervals increased as the test progressed. The HP85 recorded a complete digitized record for each specified stroke on magnetic tape. The data were then transferred to a microcomputer diskette. Data can be plotted directly by the recording plotter or computer. Resolution as shown in Figure 2 is excellent, but is affected by the base length of the record, because the points sampled remain constant at 1,000.

The time lag between load and response peaks, shown in Figure 2, is an interesting feature of the test record. A lag is not unexpected because of the viscoelastic nature of the AC being tested, a factor observed by other researchers. The time lag decreases as damage accumulates until load and response are in phase at failure. This finding may be useful for determining condition of in-service pavement materials in terms of total accumulated damage, and for estimating remaining life.

Testing included two grades of asphalt cement, AC-5.0 and AC-2.5, which are commonly used in Alaska. The range of temperatures focused on lower temperatures to provide information for the Alaskan pavement design process. The program involved tests under the conditions presented in Table 1.

The intent of this program was to

- Determine if typical existing fatigue equations are applicable at low temperatures, and if not, to develop such equations.
- Determine if typical AC mixes used in Alaska perform significantly differently at low temperatures.
- Determine if laboratory prepared samples perform differently than field-compacted samples.

Originally, the intended minimum temperature was −40°F for the project. The maximum that could be achieved within the project budget was −15°F. However, the −15°F appears to be adequate, because the data collected seemed to indicate that both AC-5.0 and AC-2.5 mixes behave similarly below about 20°F.

An axial extensometer, a displacement gauge, and a thermocouple were used with test specimens. The extensometer,

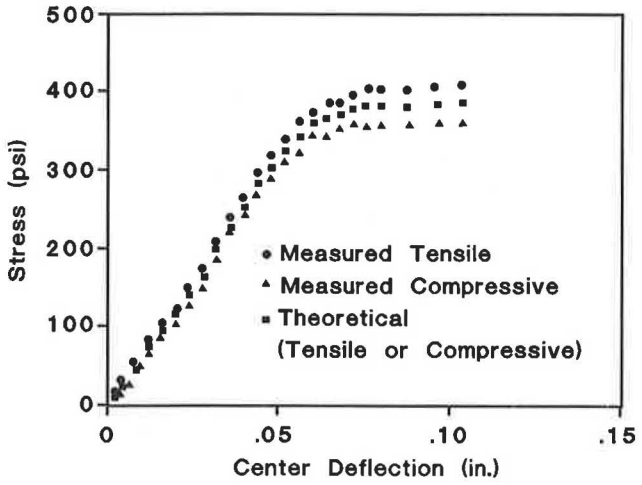

FIGURE 1 Comparison of measured (computed) and theoretical stresses.

TABLE 1 TEST PROGRAM

Temperature (°F)	Asphalt Grade AC 5.0	AC 2.5
80	Field samples	Field samples
40	Field and lab samples	Field samples
20	Field samples	Field and lab samples
10	Field samples	Field samples
-15	Field samples	Field samples

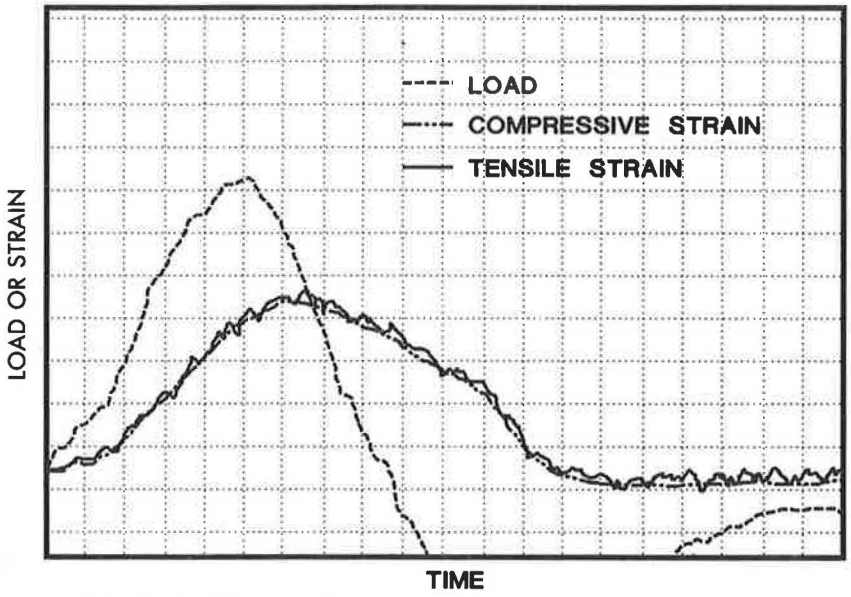

FIGURE 2 Typical data record.

used to measure tensile strain, was affixed with contact cement to the top surface of the specimen. The displacement gauge was used to measure and control the center deflection. Specimen and load frame temperatures were monitored using thermocouples. The cooling equipment was activated, and sufficient time was allowed for the sample and load system to reach thermal equilibrium. At low temperatures, monitoring loads induced by thermal contraction of the steel testing fixture and adjusting the position of the center clamps were necessary. Testing began after the load assembly had reached thermal equilibrium. The system was preprogrammed to deliver a predetermined deflection at the center of the AC once every second.

TEST PROCEDURE

Typical AC samples and materials were collected from Fairbanks and Anchorage. Testing focused on AC-5.0 hot-mix material using Fairbanks Sand and Gravel (FSG) aggregate, and AC-2.5 material using EarthMovers (EM) aggregate. Both field- and laboratory-compacted specimens were tested. Field compaction involved the use of forms at the paving site, into which the job-mix was placed and compacted using rollers. Laboratory compaction involved the use of a Cox kneading compactor and a laboratory duplication of the job-mix specifications, following the ASTM D3202 test procedure. Both laboratory and field samples were sawed into 2- × 2- × 16-in. nominal samples for testing.

Equipment was programmed to record all information in the stroke sequence 1, 11, 30, 62, 126, 254, 510, 1022, 2046, 4094, 8190, 16382, etc. Test data are shown in Figure 3. The load-deflection curves are not produced, but the energy values are listed. These energy or work values are the areas under the load-deflection curves shown, in in.-lb, and are a measure of the work done on the sample during a load pulse. The first curve in Figure 3, or Energy Input (1), is a measure of the work done by the load from the undeflected position to the

```
SUMMARY OF RECORD # 7
RECORDED 13 JUN 88
FROM MASTER FILE: A2170A
RECORD BEGINS W/ STROKE# 510

  BEAM DEPTH =   1.948
  BEAM WIDTH =   2.025

  CH# 1 = LOAD
  CH# 2 = STRAIN
  CH# 3 = DEFL

VALUES FOR MAX. ON CH# 1
  CH# 1 =    347.370000
  CH# 2 =        .000356
  CH# 3 =        .007353
  MOD E =   1979000

VALUES FOR MAX. ON CH# 2
  CH# 1 =    343.070000
  CH# 2 =        .000363
  CH# 3 =        .007150
  MOD E =   1916800
```

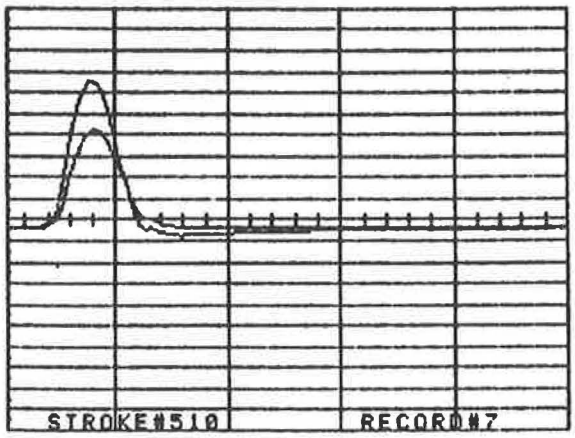

PHASE ANGLE IS 14.400 DEGREES

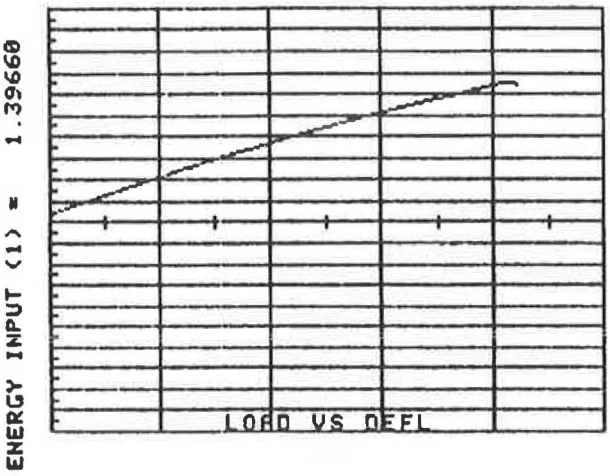

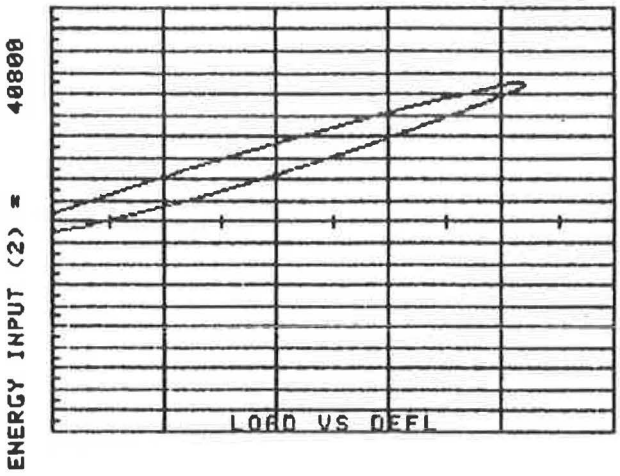

FIGURE 3 Typical reduced load, strain, and deflection data.

point of maximum deflection. Energy Input (2) in Figure 3 is the area within the hysteresis loop, which assumes that the machine provides Energy Input (1). However, the elastic rebound of the sample uses up stored energy to return to its original position. Therefore, only the net work represented by the hysteresis loop area is imparted to the sample during the load cycle. This net work contributes to accumulated damage. This may be the case for AC at low temperatures where the viscous component of the viscoelastic response is minor. A third energy, now shown in Figure 3, was also calculated. The loading arrangement is such that the MTS loading ram applies the desired deflection, and then performs a positive return to the undeflected position. A load cycle of 0.1 sec can allow a significant viscous strain to occur in AC at higher temperatures. As a result, the sample has work performed on it again by the machine positive return stroke in restoring it to the undeflected position. Energy Input (3) is considered to be representative of this situation, and is calculated from the equation Energy 3 = 2 * (Energy 1) − Energy 2. This energy relates to the work done in deforming the beam plus the additional work required to return it to the undeformed shape. For any AC sample, not one of these work estimates would reflect exactly the sample and system interaction. However, they do provide a beginning point to consider the material behavior. Some preliminary analyses indicated good correlation between energy, strain, and the number of cycles to failure.

All essential fatigue data are available, as shown in Figure 3, including measured loads, strains and deflections, and calculated moduli. Two sets of maximum values for load, strain, and deflection are recorded, and these are related to the phase angle.

Because there is a time lag between applied load and resulting strain response, load and strain peaks occur at different times. The two sets of recorded values correspond to these two times. On the basis of behavior of the specimens tested, this time lag, quantified by the phase angle, reduces as damage accumulates. The tests were performed under deflection control, and the required load monitored. Fatigue failure was chosen as the point where the applied load dropped to 50 percent of the initial load required to generate a given strain level. At this point, the phase angle, or time lag, was typically zero (i.e., the load and response peaks occurred at the same time).

This phenomenon warrants additional study to determine if it is possible to estimate the amount of accumulated damage for in-service materials by measuring the time lag between load and response. The data from individual tests provide some insight into material behavior during testing. Figure 4 shows data from an AC-5 mix tested at 20°F. This test illustrates, for instance, that the choice of 50 percent of original load as a failure criterion is reasonable, because rapid damage appears to occur in that region. All three measures of work or energy are shown in Figure 4, and all exhibit similar characteristics to the load curve. Although these tests are referred to as strain control, the control variable is deflection, and some strain variation is typical. The large strain variation in Figure 4, however, is atypical.

DATA ANALYSIS

The experimental data were used to develop fatigue relationships as a function of the number of repetitions, the initial applied strain, and modulus. Figures 5–7 show typical log of initial strain versus log of load repetitions plots developed from the test data. As expected, the plots show relatively consistent linear relationships between log strain and log repetitions for specific temperature ranges. The correlation coefficients for Equations 1–6 (Table 3) support this. Actual data analysis sequence is indicated by the regression equation number sequence shown in Tables 2 and 3. Analysis involved use of a statistics software package for microcomputers to perform multiple linear regression analyses (*7*).

For instance, each of Equations 1–6 (Table 3) considered a set of AC-5 test data at a specific temperature, while Equation 7 (Table 3) combined AC-5 field and laboratory samples with AC-2.5 samples, all at 40°F. This sequential analysis allowed combination of the data sets while determining whether obvious differences exist between data sets. In some cases, decisions were based on visual inspection of plotted data. As an example, a combined plot of the data for Equations 4

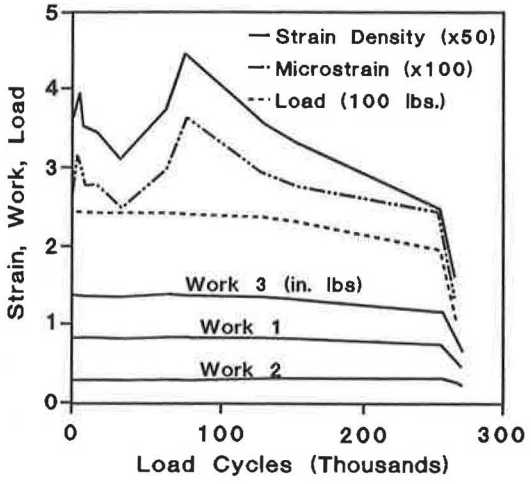

FIGURE 4 Typical data available from specific tests.

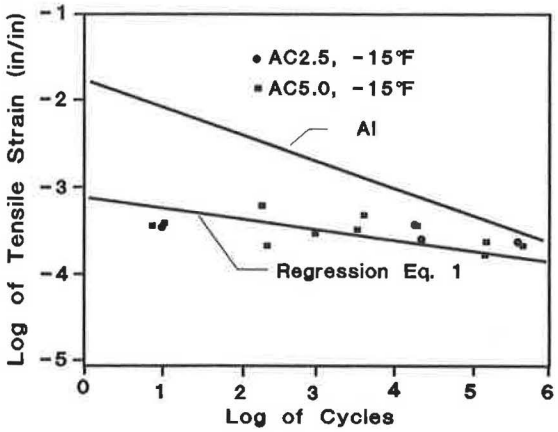

FIGURE 5 Test data for −15°F, showing Regression Equation 1 (Equation 1, Table 3) and the Asphalt Institute equation.

and 5 revealed little or no difference between field- and laboratory-compacted AC-5 samples at 40°F. Further, inclusion of AC-2.5 data at 40°F (i.e., the data used for regression Equation 7, Table 3) indicates that these mixes respond similarly at this temperature, with a correlation coefficient of 0.922 for Equation 7 (Table 3).

The complete analysis sequence provided the following general conclusions:

1. Laboratory- and field-compacted samples responded similarly.
2. Below about 20°F, the AC-5 and AC-2.5 mixes responded similarly.
3. Fatigue behavior below about 20°F is not significantly affected by temperature, which is consistent with the work reported by Salam (*8*).

Two basic relationships are available as current common approaches in the literature (*1–3*):

$$N = a\varepsilon^b \quad (1)$$

$$N = a\varepsilon^b E^c \quad (2)$$

where

N = load repetitions to failure,
ε = tensile horizontal strain resulting from each load application, and
a,b,c = material constants found by regression analysis.

Fifteen combinations of the data were considered. The results are shown in Tables 2 and 3 for Equations 1 and 2, respectively, while the relevant relationships are also plotted on Figures 5–7. The AI equation, which is commonly used for design purposes, has also been plotted for comparison purposes. This equation takes the form

$$N = 18.4C\,(4.32 \times 10^{-3})\,\varepsilon^{-3.29}(E^*)^{-0.854} \quad (3)$$

where

$$C = 10^M,$$

$$M = 4.84\left(\frac{V_b}{V_v + V_b} - 0.69\right),$$

N = number of load repetitions to failure,
ε = tensile strain (in./in.),
E^* = dynamic modulus (psi),
V_v = volume of air voids in mix (%), and
V_b = volume of asphalt cement in mix (%).

For this project, V_v and V_b came from the mix design information. The plots in Figures 5–7 show that, generally, the equations developed for this project tend to have a significantly flatter slope than the comparable AI relationship, and that the estimates are more conservative for low repetitions (less than approximately 1 million) and less conservative at high repetitions. The derived slopes decrease to some extent with temperature and the match with the AI relationship is better at higher temperatures than at lower temperatures. Table 3 indicates generally higher correlation coefficients than Table 2. This is not surprising because Equation 2 includes a modulus term E that is highly correlated with temperature and can thus deal effectively with data sets containing data from tests with widely varying temperature conditions, whereas Equation 1 does not. On the basis of these findings, the equations in Table 2 should be discarded and those in Table 3 retained. Typically, Equations 1 through 15 (Table 3) match the experimental data as shown in Figures 5–7, and from the correlation coefficients in Table 3.

DISCUSSION OF RESULTS

Testing Capabilities

The fatigue testing equipment developed and used for this project hampered, to some extent, the process of data collection. However, at this point, the system is functional, reliable, and capable of producing high-quality data that can provide useful information for application in mechanistic design procedures. A continuing fatigue testing program should be initiated. Of particular interest would be tests on samples from in-service pavements that would allow investigation of aging

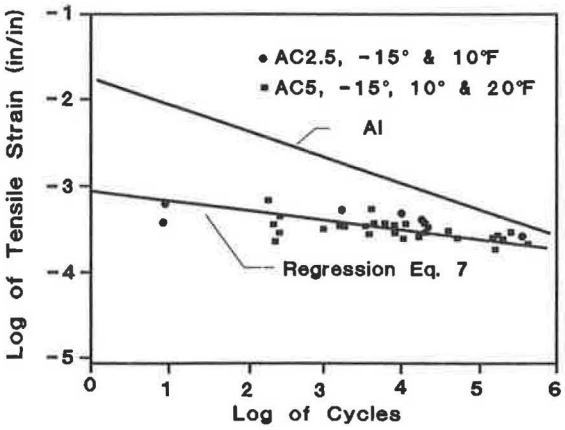

FIGURE 6 Test data for 40°F, showing Regression Equation 7 (Equation 7, Table 3) and the Asphalt Institute equation.

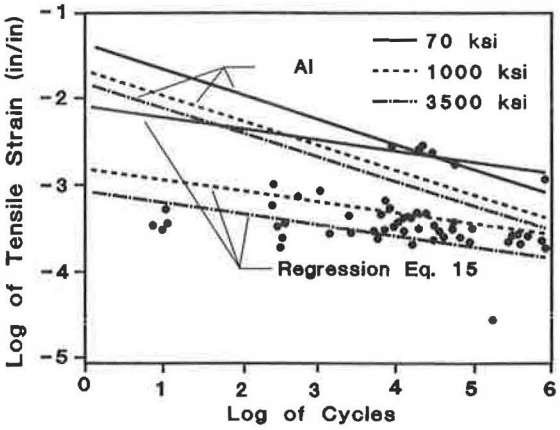

FIGURE 7 All test data, showing Regression Equation 15 (Equation 15, Table 3) and the Asphalt Institute equation.

effects, including the effect of freeze-thaw cycles on pavement materials, as well as those of damage accumulation during service.

Fatigue Analyses

Data were analyzed using statistical regression methods, and a series of regression equations was developed that are presented in Tables 2 and 3. It is recommended that only Table 3 be considered for use in design applications. The simplest approach would be to use Equation 15 (Table 3) as a general equation, i.e.,

$$N = (3.364 \times 10^6)\, \varepsilon^{-7.370}\, E^{-4.470} \quad (4)$$

where

ε = tensile strain, and
E = modulus (psi).

Equation 4 has the advantage of being based on the largest data sample, but it should be noted that additional verification testing is desirable. There is a difference between the measured data and typical fatigue equations, such as the AI equation, particularly at lower temperatures. A number of factors could contribute to this difference, such as the effect of air voids. The AI equation takes this effect into account, but the values assumed in the AI equation for comparison purposes were design air voids at optimum asphalt content, because no air void measurements were made during the project. Typical measured densities were close to design densities so that the assumption appears reasonable. Inclusion of measured void data could have a significant effect. Also, the fatigue data measured during the project were predominantly at lower temperatures, which is not the case for the AI equation. Further, the project data base of approximately 65 tests was smaller than that for the AI equation, which should thus be generally more reliable than the developed equations. However, for low-temperature analysis, the developed equations may be more applicable, but field verification is necessary. In particular, the shift factor between laboratory and field response needs to be determined and verification at a higher number of load cycles, i.e., in excess of one million cycles or more, would be desirable. It is recommended that Equation 15 be applied only in cases where the resilient modulus of the asphalt concrete exceeds 1,500,000 psi.

Energy or Work Approaches

A few preliminary analyses were performed considering total energy input to (or work done on) the sample. The approach

TABLE 2 REGRESSION EQUATION COEFFICIENTS FOR EQUATION 1

Data	Equation #	a	b	Correlation coefficient	Asphalt Institute a	Asphalt Institute b
AC 5(-15°F)	16	5.741×10^{-16}	-5.333	.555		
AC 5(10°F)	17	7.396×10^{-30}	-9.303	.682	1.480×10^{-6}	-3.29
AC 5(20°F)	18	4.315×10^{-29}	-9.261	.622	1.848×10^{-6}	-3.29
AC 5(40°F)	19	7.367×10^{-10}	-4.004	.890	3.330×10^{-6}	-3.29
AC 5(40°F) (lab)	20	4.909×10^{-12}	-4.623	.951	3.330×10^{-6}	-3.29
AC 5(80°F) AC 5 (40°F - field & lab)	21	5.741×10^{-8}	-4.462	.959	1.585×10^{-5}	-3.29
AC 2.5(40°F) AC 5 (10°F)	22	6.933×10^{-15}	-5.487	.922	3.330×10^{-6}	-3.29
AC 2.5(10°F) AC 5(10°F,20°F)	23	6.353×10^{-18}	-5.977	.679	1.480×10^{-6}	-3.29
AC 5(10°F,20°F)	24	3.508×10^{-23}	-7.507	.576	Varies	-3.29
AC 2.5(10°F) AC 5(-15°F,20°F)	25	1.875×10^{-19}	-6.461	.656	Varies	-3.29
AC 5 (-15°F,10°F,20°F)	26	4.477×10^{-17}	-5.742	.545	Varies	-3.29
AC 2.5(10°F) AC 5(40°F,80°F)	27	1.945×10^{-17}	-5.843	.593	Varies	-3.29
AC 2.5(40°F) AC 5 (20°F,40°F,80°F)	28	1.542×10^{2}	-0.600	.213	Varies	-3.29
AC 2.5 (20°F,40°F)	29	1.535×10^{2}	-0.544	.175	Varies	-3.29
ALL DATA	30	1.271×10^{2}	-0.491	.120	Varies	-3.29

is simple, shows significant promise, and is conceptually appealing from a fundamental material behavior standpoint. It is possible that the idea can be related to bond energy and fracture considerations. From an application point of view, use of work or energy per unit strain in a mechanistic design procedure is no more difficult than the use of strain alone. A correlation between this work or energy approach and some of the existing empirical pavement deflection basin parameter approaches would not be surprising, but is pure conjecture.

SUMMARY AND RECOMMENDATIONS

Flexural fatigue tests were performed at various temperatures on AC beams manufactured from typical Alaskan paving mixtures. Both AC-5 and AC-2.5 mixes were tested at temperatures ranging from −15°F to 80°F. Laboratory- and field-compacted specimens were used.

On the basis of the test data, it was concluded that

1. Laboratory- and field-compacted samples responded similarly in the tests,
2. The AC-5 and AC-2.5 mixes responded similarly below approximately 20°F,
3. Fatigue behavior below approximately 20°F does not appear to be significantly affected by temperature, and
4. The measured fatigue data are different from behavior predicted by typical fatigue equations such as the Asphalt Institute relationship.

A number of fatigue relationships developed from the test data are presented in Tables 2 and 3. It is recommended that Equation 15 in Table 3 be used for low-temperature applications in Alaska, but field verification needs to be carried out. A shift factor may be necessary to calibrate laboratory data to field conditions.

TABLE 3 REGRESSION EQUATION COEFFICIENTS FOR EQUATION 2

Data	Eq. #	a	b	c	Correlation coefficient	The Asphalt Institute a	b	c
AC 5(-15°F)	1	0.7513	-8.215	-3.720	.672	.5893	-3.29	-.854
AC 5(10°F)	2	2.897×10^{12}	-11.343	-7.620	.776			
AC 5(20°F)	3	1.324×10^{17}	-8.085	-6.501	.799			
AC 5(40°F)	4	3.292×10^{3}	-4.577	-2.411	.954			
AC 5(40°F) (lab)	5	9.528×10^{-52}	-5.201	6.324	.951			
AC 5(80°F) AC 5(40°F - field & lab)	6	6.368×10^{-5}	-4.739	-0.783	.961			
AC 2.5(40°F) AC 5(10°F)	7	1.241×10^{-15}	-5.464	0.137	.922			
AC 2.5(10°F) AC 5 (10°F,20°F)	8	6.040×10^{20}	-12.926	-9.792	.825			
AC 5 (10°F,20°F)	9	1.245×10^{19}	-9.131	-7.405	.757			
AC 2.5(10°F) AC 5 (-15°F,20°F)	10	3.006×10^{11}	-10.840	-7.156	.795			
AC 5 (-15°F, 10°F,20°F)	11	11.53	-8.673	-4.312	.714			
AC 2.5(10°F) AC 5 (40°F,80°F)	12	12.71	-9.015	-4.520	.730			
AC 2.5(40°F) AC 5 (20°F,40°F, 80°F)	13	6.565×10^{6}	-5.764	-3.640	.905			
AC 2.5 (20°F,40°F)	14	2.152×10^{6}	-6.047	-3.700	.866			
ALL DATA	15	3.364×10^{6}	-7.370	-4.470	.703			

REFERENCES

1. *Research and Development of the Asphalt Institute's Thickness Design Manual (MS-1)*, 9th ed. Research Report No. 82.2 The Asphalt Institute, College Park, Md., Aug. 1982.
2. E. J. Yoder and M. W. Witczak. *Principles of Pavement Design*, 2nd ed. John Wiley, N.Y., 1975.
3. J. A. Epps, F. N. Finn, and C. L. Monismith. *Pavement Management Including Recycling*. ITS Extension Programs, University of California, Berkeley, Calif., March 1982.
4. Y. M. Salam. *Characterization of Deformation and Fracture of Asphalt Concrete*. Ph.D. dissertation, University of California, Berkeley, Calif., 1971.
5. M. DiFazio. *Statistics Software for Microcomputers*. Kern International Inc., Duxbury, Mass., 1984.
6. H. V. Southgate, R. C. Deen, and J. G. Mayes. Strain Energy Analysis of Pavement Designs for Heavy Trucks. In *Transportation Research Record 949*, TRB, National Research Council, Washington, D.C., 1983.
7. F. N. Finn. *NCHRP Report 39: Factors Involved in the Design of Asphaltic Pavement Surfaces*. HRB, National Research Council, Washington, D.C., 1967.
8. F. N. Finn and C. L. Monismith. *NCHRP Synthesis of Highway Practice 116: Asphalt Overlay Design Procedures*. TRB, National Research Council, Washington, D.C., Dec. 1984.

Publication of this paper sponsored by Committee on Frost Action.

Evaluation of Dune Sand and Asphalt Mixes Containing Different Amounts of Crusher Waste Dust

JAMAL A. ALMUDAIHEEM

An attempt was made to characterize the dune sand and asphalt mixes containing crusher waste dust. Dune sand and asphalt mixes were found to be weak, easily deformable, and to contain a considerable amount of air voids. The optimum asphalt content from results of Marshall stability and split tensile strength tests was about 12 percent by weight of sand. The properties of such mixes were improved to a great extent by introducing crusher waste dust into the blend. Five percentages of dust by weight of dune sand were used; namely, 10, 20, 30, 40, and 50 percent. Not only the content of air voids and the optimum asphalt content were reduced by the dust, but also the stability, split tensile strength, and resilient modulus were significantly increased. The modified sand mixes that were developed have a great potential for being used in low- or medium-volume roads, particularly in areas where good-quality aggregate is scarce and dune sands are abundant.

In the last decade and a half, the Kingdom of Saudi Arabia has passed through a period of extremely rapid rate of infrastructural developments. Construction of hundreds of kilometers of freeways, urban arterials, and agricultural roads is an important sector of such development. Growth in socioeconomic and industrial sectors has also generated a great deal of intra- and intercity vehicle transportation.

The Kingdom of Saudi Arabia has nearly completed the construction of principal highways and expressways that link main cities. The development of paved highways (primary, secondary, and feeder) over the period 1970 to 1987 is shown in Figure 1 (*1*). The length of paved highways has tremendously increased over this period. The increase in the length of agricultural roads for the same period is shown in Figure 2 (*1*). The majority of existing low-volume roads are dirt tracks (unpaved) that are hazardous and require continuous maintenance. One suggestion for improving and upgrading the quality of these roads was to cover them with asphalt concrete layers. The high percentages of these low-volume roads that run through sand dune areas, coupled with the high cost of scarce good-quality aggregate that is imported from other localities, necessitate the upgrading of the locally available dune sands for such construction purposes.

The primary objective of this research was to evolve suitable techniques for using locally available marginal aggregates for construction of low-volume roads.

Sand and asphalt mixes made with wind-blown sands are characterized by high content of voids and low strength. One approach for improving the strength of such mixes is to alter the gradation and hence modify the voids ratio by introducing crusher waste dust into the dune sand and asphalt mixes.

King Saud University, College of Engineering, Civil Engineering Department, P.O. Box 800, Riyadh, Saudi Arabia, 11421.

MATERIALS USED

Dune Sand

Dune sand is available in abundant quantities in Saudi Arabia. The dune sand selected was obtained from the Al-Thumamah area northeast of Riyadh. The sand consists of rounded, subrounded, and subangular grains with a hard, smooth surface texture. The sand is essentially a single-sized material with a nominal maximum size of Sieve #30 and almost no materials finer than Sieve #200. The sand has a uniformity coefficient of about 2. The grain size distribution for this sand is shown in Figure 3. The physical properties of the dune sand used are presented in Table 1.

Crusher Waste Dust

The crusher waste dust materials were collected from a crusher site in Al-Dariyah, north of Riyadh. This material is a by-product of aggregate scalping and crushing of limestone boulders, which are weak. This material is produced in vast quantities, creating a disposal problem. The gradation of the crusher waste dust and results of the tests conducted on such materials are presented in Tables 2 and 3.

Asphalt

Asphalt cement of grade 60/70 penetration, which is widely used for hot mixes in Saudi Arabia, was used throughout this study. Results of various tests performed on the asphalt are presented in Table 4. When the test results were compared to ASTM specifications, the results indicated that the asphalt used was within the specified limits.

SAMPLE PREPARATION

Six different percentages of crusher waste dusts were blended with dune sand: 0, 10, 20, 30, 40, and 50 percent of crusher waste dusts by weight of sand. These blends are hereafter

designated as blends SF–0, SF–10, SF–20, SF–30, SF–40, and SF–50, respectively.

The precalculated weight of combined aggregate was adjusted to produce a compacted Marshall specimen that was heated in an oven at 180°C ± 2°C for at least 4 hr. The asphalt was heated in small containers to 155°C ± 3°C in an electric oven for not more than 1 hr. These two temperature values were used to ensure that the mixing and compaction temperatures were 155°C ± 4°C and 144°C ± 4°C, respectively. The mixing and compaction temperatures were established from the viscosity versus temperature chart for the asphalt cements used, which corresponded to viscosities of 170 ± 20 and 280 ± 30 centistokes, respectively (*2*). The hot-aggregate mix (sand and desired portion of crusher waste dust) was dumped into a preheated mixing bowl and mixed thoroughly by hand. The required amount of heated asphalt was then added to the aggregate mix. Mixing was performed with a mechanical kitchen mixer type Hobart N–50 mixer at medium speed for about 1.5 min to ensure a uniform dispersion of asphalt. The hot mixture was then compacted in Marshall molds using a Marshall electric compactor consisting of a 10-lb hammer falling through a height of 18 in. Fifty blows on each side were applied. This number of blows was appropriate for the traffic category (i.e., for roads of low traffic volume).

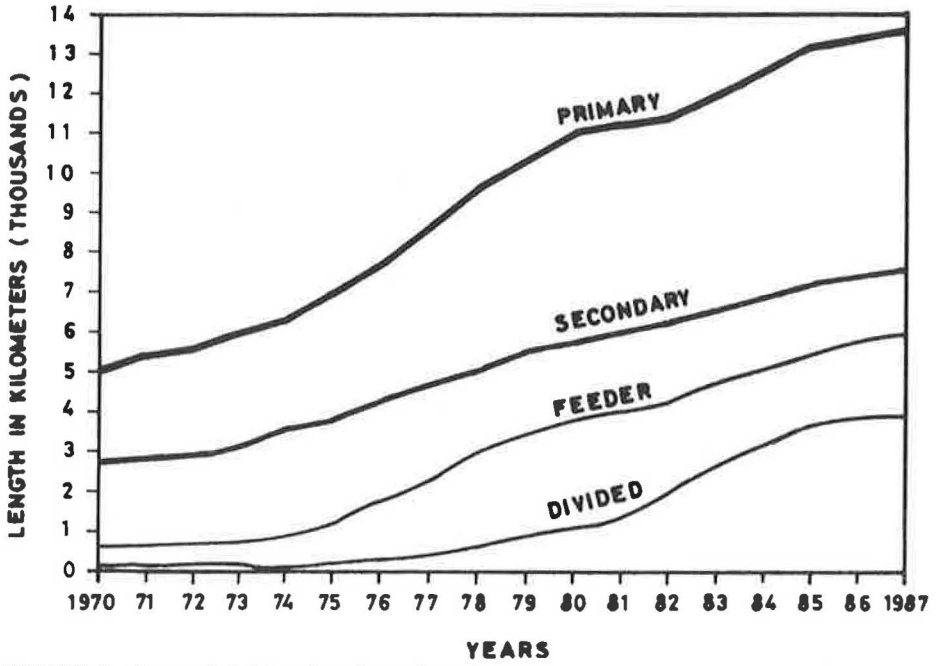

FIGURE 1 Accumulated lengths of paved roads.

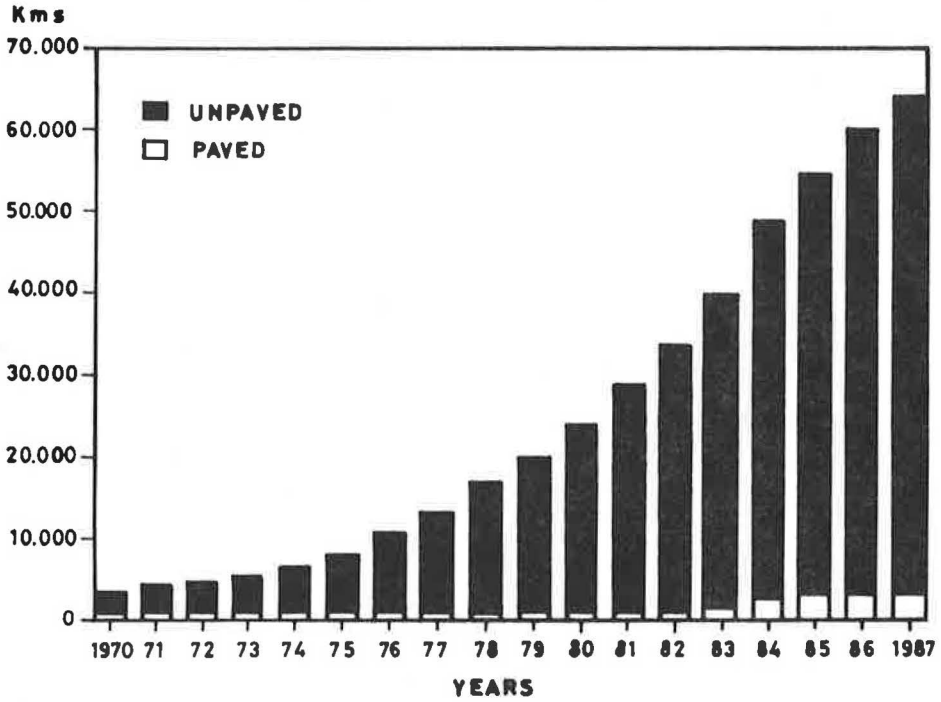

FIGURE 2 Accumulated lengths of agricultural roads.

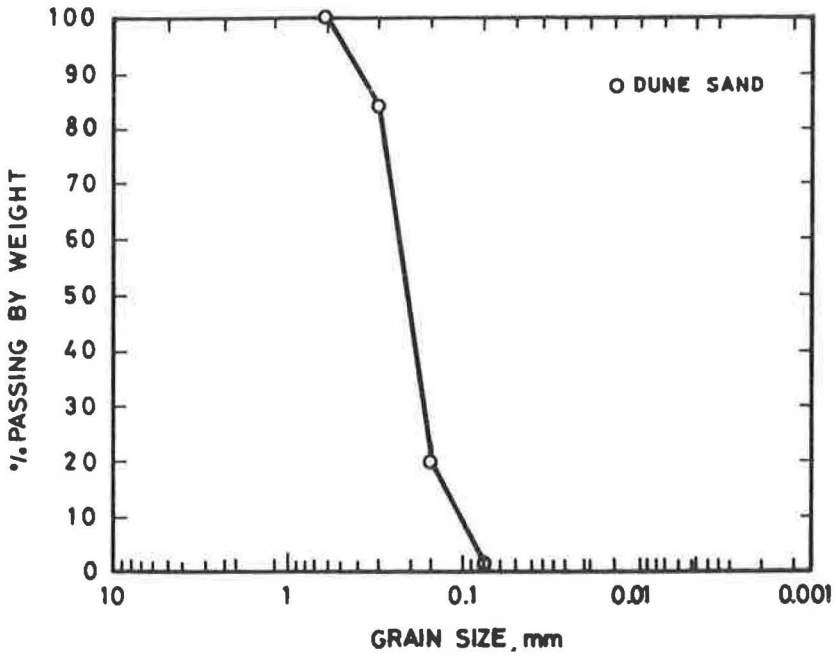

FIGURE 3 Gradation of dune sand (ASTM C-136).

TABLE 1 PHYSICAL PROPERTIES OF DUNE SAND USED

Property	ASTM Designation	Value
Bulk specific gravity:		
- Oven dry condition	C-128	2.653
- Saturated surface dry condition	C-128	2.663
Apparent specific gravity	C-128	2.680
Water absorption (%)	C-128	0.370
Sand Equivalent value (%)	D-2419	77
Centrifugal kerosene equivalent (CKE)		4.5

LABORATORY TESTS

The prepared specimens of the entire mixes were evaluated using Marshall stability, unit weight and voids analysis, static testing to determine the indirect tensile strength, and dynamic testing to determine resilient modulus. Tests for all mixes were run on Marshall-sized specimens, 4 in. in diameter and 2.5 in. in height, fabricated at different ratios of asphalt contents and filler to sand. Two duplicates of each sample were used throughout this study.

Samples to be tested for indirect tensile strength were prepared and maintained at 25°C for at least 2 hr to ensure constant temperature through the sample. The samples were then tested at a stroke rate of 2 in./min until failure. The ultimate load was recorded to determine the indirect tensile strength from the following equation (*3–5*):

$$\sigma_t = 2P/\pi dt \quad (1)$$

where

σ_t = split tensile strength (psi),
P = total applied load at failure (lb),
t = specimen thickness (in.), and
d = specimen diameter (in.).

For each mix, the average σ_t value for each set of two samples was calculated.

The diametral resilient modulus is obtained from a dynamic test response by which the elastic modulus of asphalt mixes can be determined. The test consists of applying a repetitive dynamic load diametrally on the specimen and measuring the corresponding horizontal resilient strain by use of linear variable differential transformers (LVDTs) at various numbers of load repetitions. The system used to test the specimens was that for the repeated diametral test described in ASTM D4123. Loads and strains were recorded with a two-channel oscillographic recorder. The specimens were tested using a

pulse load duration of 0.1 sec applied at a frequency of 0.5 Hz. A seating load of 10 lb was used to prevent hammering action and to hold the specimen in place. Four levels of pulse loads, 50, 100, 150, and 200 lb, were selected. These loads were selected to ensure that the applied load could engage 10 to 50 percent of the tensile strength of the specimen, as recommended by ASTM D4123. Room temperature was maintained at 25°C throughout the test period by conducting the test inside a controlled-temperature chamber.

The resilient modulus M_r was calculated using the following equation (*6*):

$$M_r = \frac{P_r(\mu + 0.2734)}{t \cdot \Delta H} \quad (2)$$

where

P_r = applied dynamic pulse load (lb),
μ = Poisson ratio (= 0.35 for asphaltic materials),
t = specimen thickness (in.), and
ΔH = total horizontal elastic strain (in.).

Before taking any reading, 50 or more load applications were applied to properly seat the loading strips on the specimen (*7*), and to allow the deformation to stabilize.

TEST RESULTS AND DISCUSSION

A presentation of the entire results for the mixes investigated would be lengthy. The shapes of the curves found for the different types of mixes were identical and in general agreement with the normal shape of the curves for Marshall stability, density, voids ratio, voids in mineral aggregate (VMA), tensile strength, and resilient modulus. Typical mix design results for mix SF–30 are shown in Figures 4–6. A summary of the properties of the sand and asphalt mixes at optimum bitumen content, as a function of filler content, is indicated in Table 5 and Figure 7. The optimum asphalt content values were obtained from results of the Marshall stability, split tensile, and resilient modulus tests.

TABLE 2 HYDROMETER ANALYSIS FOR CRUSHER WASTE DUST

Particle diameter (D), mm	% Finer
0.075	100.00
0.0488	96.7
0.0356	90.8
0.0260	84.9
0.0189	78.9
0.0137	73.1
0.0100	67.1
0.0072	59.8
0.0048	49.7
0.0035	38.5
0.0013	21.1

TABLE 3 CHARACTERISTICS OF CRUSHER WASTE DUST

Property	Result
Apparent Specific Gravity	2.715
Atterberg Limits:	
Liquid Limit (%)	22.80
Plastic Limit (%)	17.20
Shrinkage Limit (%)	15.82
Plasticity Index	5.60

The following trends summarize the basic properties of the mixtures:

1. Marshall Stability. The results generally indicated that stability tends to increase when the crusher waste dust content is increased. The stability values of dune sand and asphalt mixes did not exceed 73 lb at an asphalt content of 12 percent. This low stability at such high and uneconomic asphalt content has been increased by more than 4- and 40-fold by the addition of 10 and 50 percent by sand weight, respectively, of crusher waste dust at even lower optimum asphalt contents. However, the optimum asphalt content monotonically increases with increasing percentage of dust in the range investigated. This increase is explained by the increase in surface area contributed by dust particles with the increase of dust percentage.

The addition of 10 percent crusher waste dust does not improve the stability value to a satisfactory level to sustain traffic loading [specified by the Asphalt Institute to be a minimum of 500 lb for conventional mixes (2)] even under low-traffic conditions. This mix is still weak and does not satisfy the minimum criteria of stability. Hence, no further tests were conducted on this mix.

High stability values were possible by increasing the dust content beyond 10 percent. As indicated in Table 5 and Figure 7, stability values greater than 800 lb were obtained by the addition of 20, 30, 40, and 50 percent by sand weight of crusher waste dust. The stability is linearly proportional to the dust content as shown in Figure 7.

The addition of crusher waste dust does not affect the flow values appreciably in the range of asphalt contents investigated. This fact indicates that the stiffness of mixes is not affected by introducing dust.

2. Density. The density of a compacted mix depends on the density of its constituent materials and the percentage of air voids. Because the percentage of air voids is reduced with increasing dust percentage, the density of mixes increases, as

TABLE 4 CHARACTERISTICS OF ASPHALT CEMENT USED

Property	ASTM Designation	Result	MOC* Specification Min.	Max.
Original Asphalt				
Penetration (0.1 mm) @ 25°C (100 g, 5 second)	D5	60	60	70
Kinematic viscosity, cst (135°C)	D2170	403	200	-
Absolute viscosity by vacuum capillary viscometer, poises (60°C)	D2171-85	2459	-	-
Ductility, cm (25°C, 5 cm/min)	D113	100+	100	-
Flash point (°C)	D92	340	232.2	-
Fire point (°C)	D92	370	-	-
Specific gravity	D70	1.035	-	-
Softening point (°C)	D36-86	50.2	-	-
Loss on heating (%)	D6	0.016	-	0.8
Residue from TFOT				
Penetration (0.1 mm) @ 25°C (100 gm, 5 sec)	D5	41	-	-
Retained penetration, % of original	-	68.3	52	-
Kinematic viscosity, cst (135°C)	D2170	553	-	-
Ductility, cm (25°C, 5 cm/min)	D113	65	50	-

*MOC = Ministry of Communications, Kingdom of Saudi Arabia

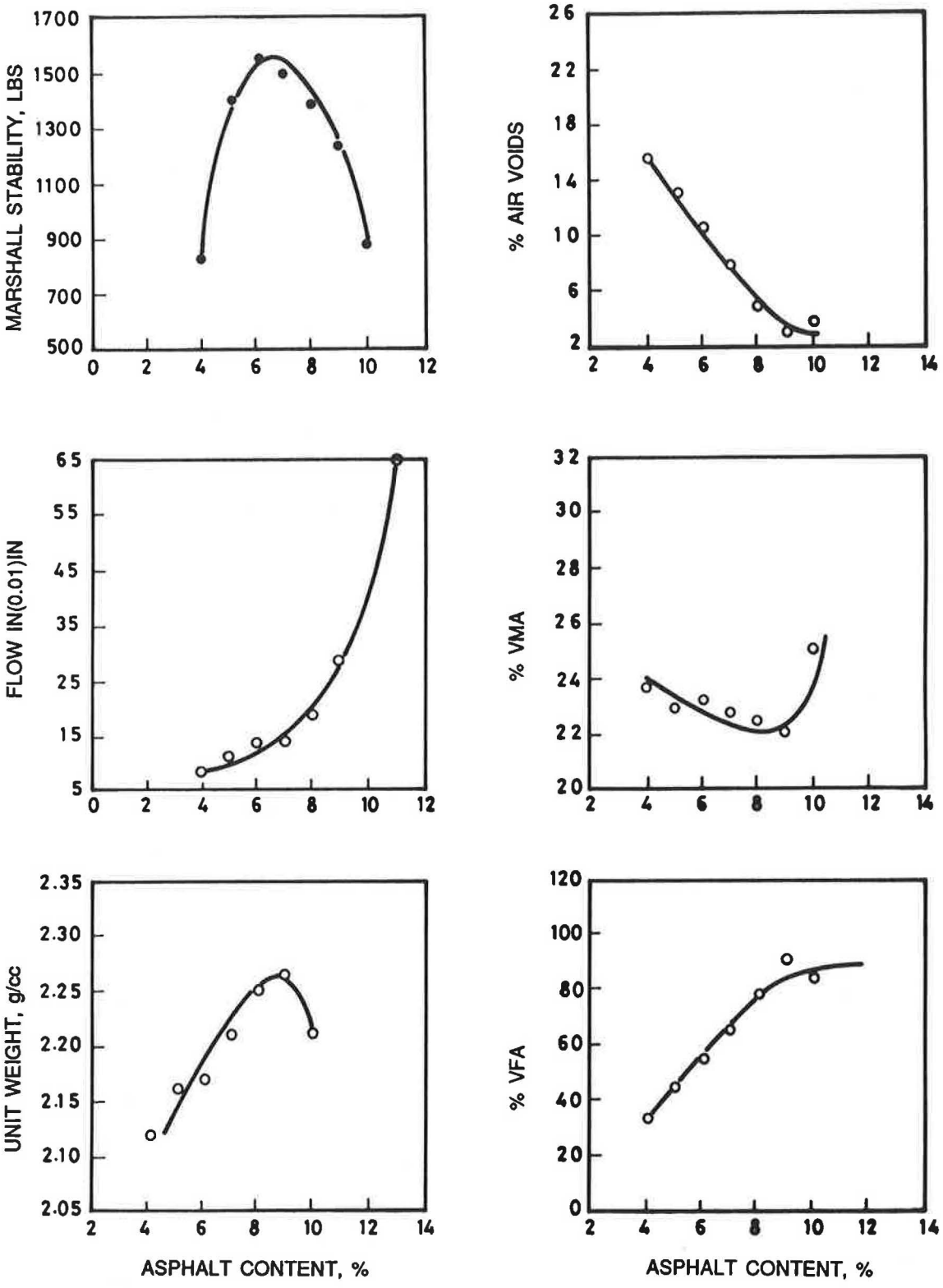

FIGURE 4 Results of Marshall mix design for SF–30 mixes.

shown in Figure 7. The addition of 50 percent dust causes about a 15 percent increase in the density. The curve tends to peak at 50 percent dust content because there is no more air to be replaced by dust. This behavior is clear from the curve of percentage air voids versus dust content where the curve starts to level off beyond 40 percent dust content.

3. Air Voids and VMA. Air voids content in dune sand and asphalt mixes is extremely high, ranging from 23.5 percent at 5 percent asphalt content to 9 percent at 15 percent asphalt content because the mixes are single-size aggregates having uniform textures. The low percentage of air voids content at optimum asphalt content indicated in Table 5 is attributed to the high optimum asphalt content value of 12 percent. The dust decreases the percentage of air voids by filling the void spaces between the sand particles, hence producing denser mixes.

The addition of 40 percent dust or more produces mixes with percentage of air voids that is below the specified percentage. Therefore, using such high dust percentages should be avoided.

VMA also decreases with increasing dust percentages. The VMA curve shows the same trend as the air voids curve in the sense that it starts to level off when air voids replacement becomes impossible.

4. Split Tensile Strength. From Figure 7, the tensile strength increases as the dust content increases. The dune sand and asphalt mix without any improvement of crusher waste dust had low strength. The strength was improved many times by adding dust.

Mixes with 30 percent or more crusher waste dust had strength values comparable with the strength of conventional mixes. Figure 7 also shows that there might be an optimum dust content for tensile strength because the curve tends to level off, suggesting that the dust in excess of the optimum reduces the free binding agent. Huschek and Angst (*8*) found that the maximum split tensile strength for a pavement mix showed a tendency to peak at an effective filler concentration of approximately 0.6.

5. Resilient Modulus. Results of resilient modulus values for the designated mixes SF–20, SF–30, SF–40, and SF–50 are shown in Figure 7 at their optimum asphalt content values. As the dust content increases, the resilient modulus increases because the increase in stiffness of asphalt mixes is directly proportional to the stiffness of the binder (*9*).

TABLE 5 PROPERTIES OF SAND AND ASPHALT MIXTURES AT OPTIMUM ASPHALT CONTENT FOR VARIOUS AMOUNTS OF FILLER

Filler Content	Optimum AC, %	Stability (lbs)	Density (g/cc)	% Air Voids	% VMA	ITS (psi)	MR x10^3 psi
0	12	73	2.009	10.10	33.40	41.40	-
10	4	358	1.962	21.58	29.16	-	-
20	6	805	2.127	12.58	24.92	86.20	125.70
30	7	1037	2.217	7.70	22.70	115.74	170.00
40	7.5	2350	2.270	3.30	21.00	107.00	215.00
50	8	2960	2.320	2.10	20.10	122.00	220.00

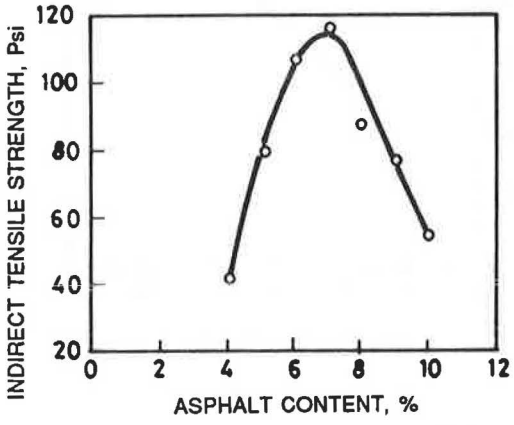

FIGURE 5 Split tensile strength versus asphalt content for SF–30 mixes.

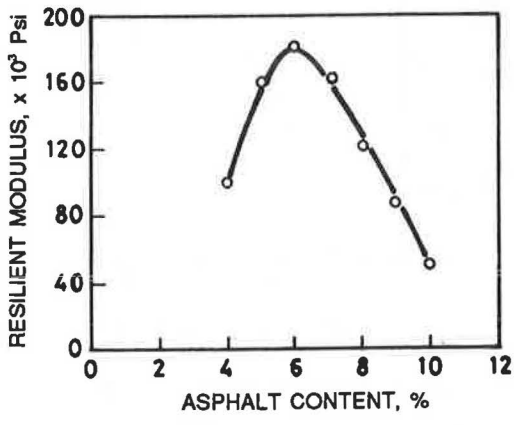

FIGURE 6 Resilient modulus versus asphalt content for SF–30 mixes.

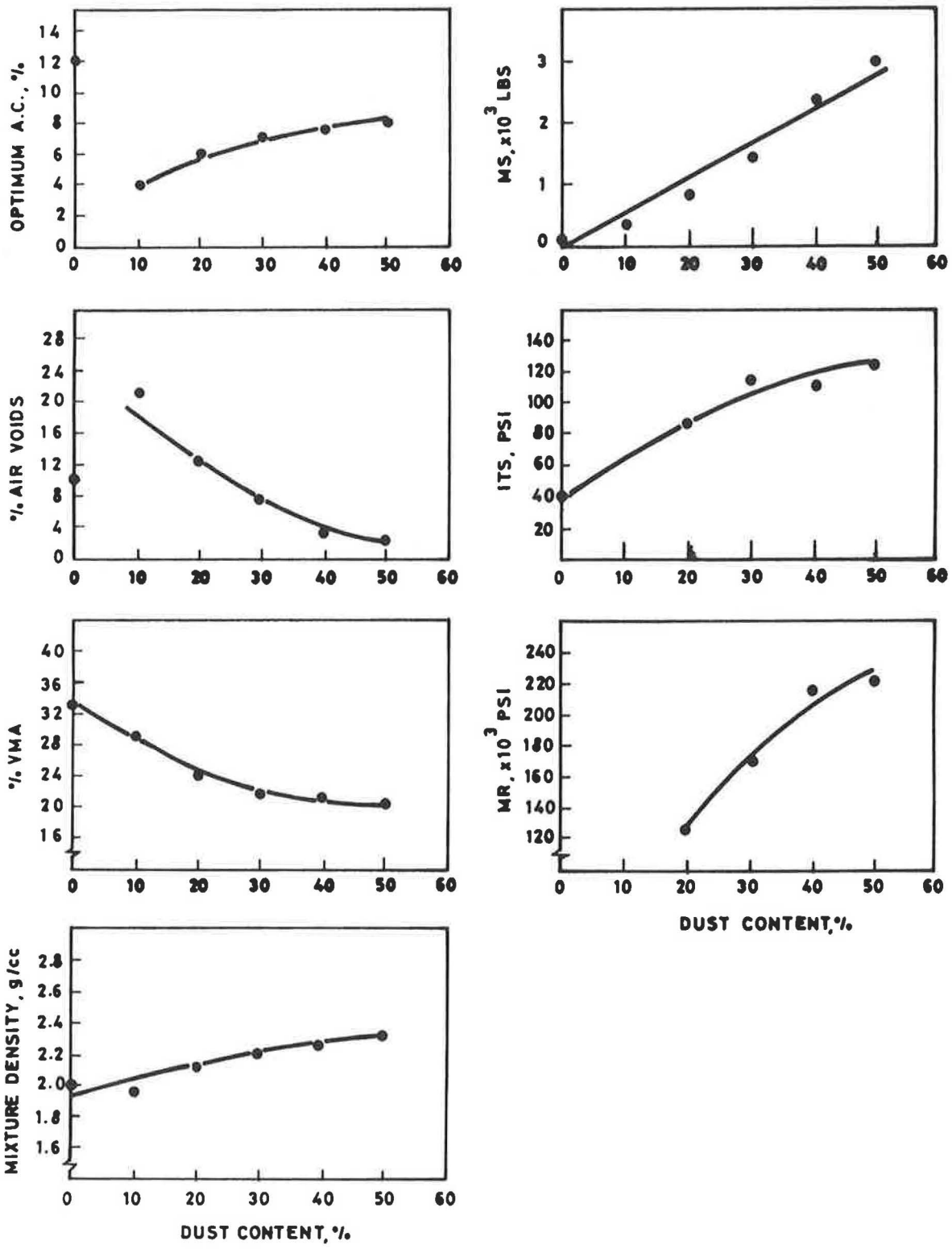

FIGURE 7 Basic properties of sand and asphalt mixes at their optimum asphalt content, as a function of dust content, and percent by weight of sand.

CONCLUSIONS

1. Dune sand and asphalt mixes are weak, unstable, and easily deformed under light loads. The mixes are characterized by a considerable amount of air voids content.

2. The dune sand used in this study had an optimum asphalt content of 12 percent by weight of sand. This value was obtained from results of Marshall stability and split tensile strength.

3. The introduction of crusher waste dust to the dune sand and asphalt mixes at different ratios improved the mix properties. The modified sand mixes that were developed have a great potential for use in low- or medium-volume roads, especially in desert-like areas where the dune sands are available in abundant quantities and hot-asphalt concrete mixes are uneconomical.

4. The air voids content of the dune sand and asphalt mixes was reduced by introducing crusher waste dust. The percentage decrease in air voids is directly proportional to the amount of dust added.

5. The optimum asphalt content of sand and asphalt mix was substantially decreased by the introduction of crusher waste dust.

REFERENCES

1. *General Public Relations and Information Publication*. Ministry of Communications, Kingdom of Saudi Arabia, Riyadh, 1988.
2. *Mix Design Methods for Asphalt Concrete and Other Hot-Mix Types*. Manual Series No. 2, The Asphalt Institute, Lexington, Ky., 1984.
3. J. N. Anagnos and T. W. Kennedy. *Practical Method of Conducting the Indirect Tensile Test*. Research Report 98-10, Center for Highway Research, University of Texas at Austin, Aug. 1972.
4. T. W. Kennedy and W. R. Hudson. Application of the Indirect Tensile Test to Stabilized Materials. In *Highway Research Record 235*, HRB, National Research Council, Washington, D.C., 1968.
5. R. Hass and W. R. Hudson. *Pavement Management Systems*. Krieger Publishing Co., Malabar, Fla., 1982.
6. E. J. Yoder and M. W. Witczak. *Principles of Pavement Design*. John Wiley, New York, 1978.
7. J. Walter, A. M. Brickman, R. G. Hicks, and T. S. Vinson. *Installation, Operation and Maintenance Procedures for Repeated Load Triaxial and Diametral Test Equipment*. Transportation Research Report 84-1. Transportation Research Institute, Oregon State University, Corvallis, 1984.
8. S. Huschek and C. Angst. Mechanical Properties of Filler-Bitumen Mixes at High and Low Services Temperature. *Proc., Association of Asphalt Paving Technologists*, Vol. 49, St. Paul, Minn., 1980, pp. 440–458.
9. R. T. Schmidt and P. E. Graf. The Effect of Water on the Resilient Modulus of Asphalt in Treated Mixes. *Proc., Association of Asphalt Paving Technologists*, Vol. 41, St. Paul, Minn., 1972, pp. 118–162.

Publication of this paper sponsored by Committee on Characteristics of Bituminous Paving Mixtures To Meet Structural Requirements.